UNIVERSIDAD AUTÓNOMA DE MADRID
Programa de Doctorado en Biociencias Moleculares

Temporal dynamics and pathophysiology of the edematous response after acute myocardial infarction: a translational journey

RODRIGO FERNÁNDEZ JIMÉNEZ

Madrid, 2017

Department of Biochemistry
School of Medicine
UNIVERSIDAD AUTÓNOMA DE MADRID

Temporal dynamics and pathophysiology of the edematous response after acute myocardial infarction: a translational journey

Doctoral thesis presented to earn the Doctor of Philosophy degree with International distinction by:

Rodrigo Fernández Jiménez
Bachelor of Medicine and Surgery

Under the guidance of:

Dr. Borja Ibáñez Cabeza

Conducted in the Spanish National Center for Cardiovascular Research (CNIC)

Madrid, 2017

Departamento de Bioquímica
Facultad de Medicina
UNIVERSIDAD AUTÓNOMA DE MADRID

Temporal dynamics and pathophysiology of the edematous response after acute myocardial infarction: a translational journey

Memoria presentada para optar al grado de Doctor con Mención Internacional por:

Rodrigo Fernández Jiménez
Licenciado en Medicina y Cirugía

Bajo la dirección de:

Dr. Borja Ibáñez Cabeza

Realizada en el Centro Nacional de Investigaciones Cardiovasculares Carlos III (CNIC)

Madrid, 2017

Dedication

To Raquel and Lore, for their unconditional love.

“Much of the difficulties facing the world is because
the ignorant are completely safe, and
the intelligent are full of doubt”
Bertrand A. W. Russel

Acknowledgements

I would like to thank Borja Ibáñez and Valentín Fuster for giving me the opportunity to initiate my research career in a unique environment at the *Centro Nacional de Investigaciones Cardiovasculares Carlos III* (CNIC), and for all their support and mentorship during these years. I would like to thank my thesis supervisor, Teresa González, for all her help.

I would like to thank all the staff from CNIC I interacted with and made the daily work easier, from the animal care facility staff to the personnel at the cafeteria. Special thanks to my colleagues and friends Javier Sánchez, Jaime García-Prieto, Carlos Galán, Jaume Agüero, Gonzalo López, Gonzalo Pizarro, Ana García, José Manuel García, Leticia Fernández, Xavier Rosselló, David Sanz-Rosa, Eeva Soininen and many others from the *Translational Laboratory for Cardiovascular Imaging and Therapy* for their invaluable teaching process and help for achieving the work contained in this dissertation. The studies presented here are definitively the consequence of a resilience team effort. I would also like to give thanks to Simon Bartlett from CNIC, whose work was far beyond English editing, contributing with critical input from the scientific point of view.

I would also like to thank my friends and colleagues from *Universidad de Zaragoza* and *Hospital Clínico Universitario San Carlos* in Madrid for giving me the clinical skills and perspective which have been crucial to orientate my preclinical research.

Finally, I would like to very special thank my parents, Rosa and Carlos, and my sister, Laura, for their always support and care.

SUMMARY

Post-myocardial infarction tissue composition is highly dynamic and can be characterized by cardiac magnetic resonance, which has been used to assess surrogate outcomes and efficacy endpoints in many experimental and clinical studies. However, there is a paucity of studies tracking the temporal dynamics of these processes and analyzing their pathophysiology in a comprehensive manner. The experimental and clinical work contained in this dissertation shows that the degree and extent of post-myocardial infarction tissue composition changes (mainly edema; but also necrosis, hemorrhage and microvascular obstruction) as assessed by cardiac magnetic resonance are variable according to the time from infarction, duration of ischemia, cardioprotective strategies, and the interplay between them. These dynamic changes should be taken into consideration when performing image acquisition. Comparative studies should be performed at similar timings to avoid the bias of these dynamic changes.

Thus, and in contrast to the accepted view, it is shown for the first time that myocardial edema in the week after ischemia/reperfusion is a bimodal phenomenon, both in pigs and humans. The initial wave of edema, appearing abruptly upon reperfusion and which is significantly attenuated at 24 hours, is due to the reperfusion process itself. The deferred wave of edema, appearing progressively days after ischemia/reperfusion and reaching a plateau between days 4 to 7, is mainly caused by the tissue healing processes.

These findings highlight the need for standardizing experimental and clinical protocols for post-myocardial infarction tissue characterization aiming to quantify edema, myocardial area at risk, infarct size, myocardial salvage, intramyocardial hemorrhage and microvascular obstruction. The timeframe between day 4 and 7 post-infarction seems a good compromise solution according to translational data here presented. However, further studies and expert consensus are needed to stablish more precise recommendations.

RESUMEN

La evolución de la composición del tejido miocárdico post-infarto es un proceso muy dinámico que se puede caracterizar mediante resonancia magnética cardíaca. Ello se ha utilizado para evaluar parámetros de eficacia terapéutica y pronósticos en multitud de estudios experimentales y clínicos. Sin embargo, existe una escasez de trabajos longitudinales que hayan estudiado de forma detallada la evolución de esta dinámica tisular y su fisiopatología. El trabajo experimental y clínico presentado en esta tesis demuestra que la severidad y la magnitud de los cambios en la composición tisular del miocardio post-infarto (fundamentalmente edema; pero también necrosis, hemorragia y obstrucción microvascular) evaluados mediante resonancia magnética cardíaca están muy influenciados por el momento temporal en que se evalúa al individuo, el tiempo de isquemia, la utilización de estrategias cardioprotectoras, y la interacción entre estos factores.

Así, y contrariamente a la visión establecida, se demuestra por primera vez que el edema miocárdico en la semana posterior al proceso de isquemia/reperfusión es un fenómeno bimodal, tanto en el modelo porcino como en el ser humano. La onda de edema inicial, que aparece abruptamente tras la reperfusión y que se disipa alrededor de las 24 horas, está directamente relacionada con el propio proceso de reperfusión. La onda de edema posterior, que aparece progresivamente días después del proceso de isquemia/reperfusión y alcanza una meseta entre el día 4 al 7, está originada fundamentalmente por los procesos de cicatrización del tejido.

Estos hallazgos ponen de relieve la necesidad de estandarizar los protocolos experimentales y clínicos de caracterización tisular post-infarto mediante técnicas de imagen que tenga por objeto cuantificar el edema miocárdico, el área en riesgo, el tamaño del infarto, el área salvada, la hemorragia intramiocárdica, y la obstrucción microvascular. En base a los resultados translacionales que aquí se presentan, el período de tiempo comprendido entre el día 4 y el 7 después del infarto pudiera ser un buen momento para este fin. Sin embargo, se necesitan estudios adicionales y un consenso de expertos para establecer recomendaciones más precisas.

TABLE OF CONTENTS

ABBREVIATIONS

CNIC: Centro Nacional de Investigaciones Cardiovasculares Carlos III

MI: myocardial infarction

PCI: percutaneous coronary intervention

HF: heart failure

I/R: ischemia/reperfusion

MaR: myocardium at risk

CMR: cardiac magnetic resonance

T2W: T2 weighted

STIR: short-tau inversion recovery

IMH: intramyocardial hemorrhage

MVO: microvascular obstruction

GraSE: gradient-spin-echo

ROI: region of interest

1 INTRODUCTION

1.1 Myocardial infarction: scope of the problem

1.1.1 Trends in mortality

Myocardial infarction (MI), presented as ST-segment elevation due to complete coronary occlusion of an epicardial coronary artery, is the most severe manifestation of ischemic heart disease. Timely reperfusion (blood flow restoration) via percutaneous coronary intervention (PCI) and the increased use of adjuvant evidence-based pharmacological therapies have been demonstrated as the most effective means to reduce the mortality associated with MI.[1] Despite a widespread implementation of such early invasive strategies, secular trends of mortality reduction associated with MI have reached a plateau over the last decade,[2] most likely due to the changing population of patients undergoing PCI who suffer now from additional comorbidities.[3] Consequently, MI persists as a major contributor of mortality worldwide causing more than a third of deaths in developed nations annually,[4] suggesting that additional strategies are needed to further reduce mortality in this population.

1.1.2 Trends in morbidity

Paradoxically, the improvement on care delivery systems for patients presenting with acute MI has significantly increased the incidence of chronic heart failure (HF):[5] patients with poor post-MI left ventricular function would not have survived to the acute phase in the past, but with the advent of reperfusion now survive the index episode and continue to live with a significantly damaged heart. Chronic treatment of HF represents a huge social and economic burden on individuals and healthcare systems.[6] Intense research effort has led to interventions (drugs and devices) that reduce long-term mortality in survivors with depressed post-MI ventricular function.[7]

However, the implementation of these strategies comes at a high cost, precluding their universal implementation.[8] Therefore, the possibility of preventing (rather than treating) post-MI HF by using therapies able to reduce cardiac damage, which will eventually result in better heart performance, is of significant clinical and socioeconomic value.

1.2 Ischemia/reperfusion injury and cardioprotection

1.2.1 Concept

As mentioned before, reperfusion, i.e. blood flow restoration into the ischemic territory, is the main available treatment to stop the progression of ischemic damage during an acute MI. However, a large body of experimental and clinical literature supports the notion that reperfusion induces additional harm to the myocardium, known as reperfusion injury.[9, 10] Thus, the damage inflicted on the myocardium during an MI is better defined as ischemia/reperfusion (I/R) injury, and reperfusion injury is nowadays considered “a necessary evil” being responsible for up to 50% of the final damage extent.[11]

Among others, the main determinants of infarct size are (1) the size of the hypoperfused myocardial zone previously perfused by the occluded coronary artery (i.e. myocardium at risk, [MaR]); (2) the duration of myocardial ischemia; and (3) the implementation of an effective therapy capable of targeting I/R injury and therefore reducing cardiac damage. Among the two first determinants, the former is not modifiable by definition while the latter has been remarkably reduced and optimized over the last decades.[2] Consequently, the field of cardioprotection constitutes a window of opportunity, and has generated a huge amount of human and economic efforts being of scientific and clinical relevance.

1.2.2 Pathophysiology of ischemia/reperfusion injury

Understanding the pathophysiology and the temporal evolution of events underlying myocardial I/R is likely one of the most important first steps before any attempt of testing any potential cardioprotective strategy. From a simplistic point of view, the typical morphological features of reperfused MI are contraction band necrosis, mitochondrial and cardiomyocyte swelling and disruption, accompanied by microvascular destruction, interstitial hemorrhage, and inflammation.[10] Thus, it has

been classically described that the infract healing process involves a sequential infiltration of neutrophils and macrophages, removal of necrotic myocytes, formation of granulation tissue, and collagen deposition intermingled with groups of cardiomyocytes.[12] The coronary microcirculation plays a critical role in the complex processes happening after I/R given that the microcirculatory network is the interface between the epicardial coronary artery and the cardiomyocyte.[10, 13] Thus, no matter how rapidly the blood flow is restored to the culprit epicardial artery; if there is microvascular injury, the myocardial tissue will remain without efficient perfusion. One of the main contributors to dysfunctional coronary microcirculation is the edema that quickly develops in the myocardium within minutes of acute MI. Edema induces and external compression to the microcirculation contributing to poor perfusion despite patency of the main coronary artery.

1.2.3 Myocardial edema after ischemia/reperfusion

As with most organs, water is a major component of healthy cardiac tissue. In steady-state conditions, myocardial water content is stable and mostly intracellular, with only a very small interstitial component. Cardiac edema occurs in numerous pathological conditions in which this homeostasis is disrupted, and affects both fluid accumulation within cardiomyocytes (intracellular edema) and outside cells (interstitial edema).[14-16] In the context of I/R, edema appears initially in the form of cardiomyocyte swelling during the early stages of ischemia.[14] Myocardial edema is then significantly exacerbated upon restoration of blood flow to the ischemic area. This increase is due to increased cell swelling and, more importantly, to interstitial edema secondary to reactive hyperemia and leakage from damaged capillaries when the hydrostatic and osmotic pressure is restored upon reperfusion.[13]

Finally, the generation of tissue edema following reperfusion can result in external compression of the microcirculation, and might be one of the principal causes of reduced perfusion capacity of the capillary network after I/R.[10] Thus, a profound study of the post-MI edematous reaction seems to be crucial in the understanding of the complex phenomenon of myocardial I/R and the discovery of effective cardioprotective therapies. Likely equally important is the possibility of having translational tools able to precisely characterize post-MI tissue composition;

therefore able to monitor these processes in vivo, quantify the extent of cardiac damage and cardioprotection, and predict functional recovery after MI.

1.3 Tissue characterization by cardiac magnetic resonance

1.3.1 The possibility of performing in vivo pathology

Histologic evaluation has been classically considered the reference standard for the evaluation of myocardial tissue. However, it is poorly suited for serial (or even single) measurements into the required follow-up clinical field. Conversely, several non-invasive imaging modalities have been developed for the characterization of the heart, including positron emission tomography, single-photon emission computed tomography, and computed tomography. However, it is cardiac magnetic resonance (CMR) the tool that probably has captured more attention over the last decades for such a purpose given that offers a unique combination of versatility, high spatial resolution and high soft tissue contrast with no ionizing radiation.[17] Thus, CMR is nowadays considered to be able to perform a comprehensive analysis of the post-MI heart, including in vivo tissue characterization which is considered a surrogate for histologic evaluation.

1.3.2 Readouts of ischemia/reperfusion injury and cardioprotection

Testing the effect of cardioprotective therapies benefits from measuring of MaR and infarct size in the same CMR examination session to quantify the amount of salvaged myocardium, i.e. % of MaR with no infarction, a theoretical better (normalized) surrogate of their effect;[18, 19] therefore reducing the sample size needed in trials.[20] Thus, on the basis of the biological assumptions that (1) an intense edematous reaction confined to the post-I/R region appears early after MI and persists in stable form for at least 1 week;[21, 22] that (2) the entire jeopardized myocardium shows a detectable (and homogeneous) edematous reaction, regardless of the outcome (death or salvage); and that (3) CMR is able to unequivocally detect this edematous reaction retrospectively,[23] the use of edema-sensitive T2-weighted (T2W) CMR sequences to delineate the spatial extent of post-MI edema was rapidly incorporated as an index of the original occluded coronary artery perfusion territory (or MaR).[24, 25] Among T2W sequences, dark-blood short-tau inversion recovery (STIR) methods are well studied and widely used for clinical

and research purposes.[19, 24, 26] Thus, hyperintense areas on T2W-STIR CMR imaging have been classically proposed as having a good correlation with post-MI edema and, thus, with MaR.[25]

On the other hand, and also based on the biological assumption that the necrotic tissue extent persists in stable form for at least 1 week, the use of T1-weighted CMR sequence with an inversion recovery pre-pulse after the administration of gadolinium contrast is an in vivo well stablished reference to measure infarct size,[27] with its size and distribution being well correlated with remodeling and prognosis.[26] Consequently, CMR-based extent of edema, infarct size and myocardial salvage have been and continue to be used as main endpoint in multiple clinical and experimental studies at a variety of post-MI time points.[28] Finally, there is growing evidence that the extent of microvascular injury, i.e. intramyocardial hemorrhage (IMH) and microvascular obstruction (MVO), provide important information for predicting adverse left ventricular remodeling and clinical events after MI.[29-31] Notably, the degree of IMH and MVO can be quantified as well with CMR, by delineating hypointense areas on T2W-STIR and late gadolinium enhancement sequences, respectively;[32] and are being incorporated progressively in experimental research and clinical studies.

1.4 Translational preclinical models of myocardial infarction

Most of the studies validating CMR against reference histology for in vivo myocardial tissue characterization are derived from experimental (preclinical) studies, as it is most of the knowledge in regards to the pathophysiology underlying MI and cardioprotection.

Small animal models may help to identify potential mechanisms, but their significant anatomic/physiological differences from humans make it challenging to extrapolate results to the clinical setting.[33] Large animal models exhibit a much closer match to human anatomy and physiology making feasible the use of clinically applicable imaging technology and methodology; thus, they become a mandatory step before initiating human trials.[34, 35] For the latter, it is important to select the patients who have been shown to derive the most benefit from a cardioprotective strategy applied as an adjunct to PCI to reduce MI size; this includes those patients presenting with relatively short ischemic time, large MaR, fully occluded coronary artery prior PCI,

and no significant coronary collaterals.[36] Among the larger mammals, pigs and primates have little collateral blood flow, whereas cats and especially dogs have a sizeable innate collateral circulation; therefore, different species develop myocardial necrosis during acute MI at significantly different rates.[37] Based on these premises, the reperfused acute MI model induced in the swine by closed-chest I/R, via mid left anterior descending coronary artery balloon complete occlusion followed by balloon deflation and reestablishment of blood flow, has become one of the most translational preclinical models of MI.[38-41] Nevertheless, tolerance to I/R varies notably across different strains or concomitant medication, among others;[33] consequently, it is fair to acknowledge that any preclinical model may have many limitations.

1.5 Controversy and research gaps on post-myocardial infarction edema

1.5.1 CMR methods to detect myocardial edema

As mentioned before, there is particular interest on using T2W CMR to detect and track edema since this is a common pathological feature of many cardiovascular conditions.[14-16] However, it is fair to recognize that dark-blood STIR methods are qualitative in nature and present inherent limitations which include variations in surface coil sensitivity, motion artifacts, incomplete blood suppression, and the subjectivity of image interpretation.[42] Adequate slice thickness and some technical advances (surface-coil intensity correction algorithms or the use of body coils) may help to overcome some of the cons of T2W-STIR imaging.[43] However, efforts over the last decade have been directed at implementing more robust methods for CMR edema imaging.

In this regard, quantitative T2 mapping methods, which provide direct measurement of intrinsic tissue properties in the form of T2 relaxation time that can be compared among studies, are less dependent on confounders affecting signal intensity and might overthrow some of T2W imaging limitations.[44] However, it is noteworthy that the relationship between T2 relaxation time and true myocardial water content directly quantified in the tissue has been explored in only a few studies conducted more than two decades ago.[45-49] These studies were performed in low magnetic fields or with excised hearts, factors well known to affect T2 relaxation time;[50]

therefore the evidence supporting the validity of T2 mapping for the precise quantification (degree and spatial extent) of myocardial edema is scarce. In addition, some newer mapping methods are either time consuming or require specialized software for data acquisition and/or post-processing, factors which limit their routine clinical use.

Based on previous assumptions, we here identified an important gap in knowledge: the possibility of validating a CMR T2 mapping method for fast and accurate quantification of T2 relaxation time, and consequently myocardial water content, which could be easily integrated in daily clinical and research imaging protocols would be of great value.

1.5.2 Myocardial edema as marker of the jeopardized myocardium

As previously mentioned, experimental and clinical studies have relied on the pathophysiological assumption that myocardial edema appears early after I/R and persists in a stable form for at least 1 week for the use of T2 CMR sequences to retrospectively quantify MaR and myocardial salvage.[21, 22] Thus, the time chosen for the CMR examination varies significantly among studies,[28] from several hours or days[21, 22, 51] to several weeks[52] after reperfusion.

Notably, it is well known that reperfusion, a pre-requisite for myocardial protection during infarction, alters post-MI tissue composition and dynamics compared with the nonreperfused setting.[12] Nonetheless, most current knowledge of the pathophysiology and tissue modifications in the post-infarcted myocardium is based on observations in nonreperfused hearts. In addition, T2 in the post-ischemic area might be affected by the presence of IMH and/or MVO,[30, 53] and the implementation of cardioprotective therapies able to reduce infarct size like post-conditioning[54] and remote conditioning.[55, 56] Consequently, it is remarkably that despite T2 CMR is increasingly used for the detection of myocardial edema, its capacity to retrospectively depict the true MaR is a matter of debate.[23, 24, 57]

Based on background described before, here we identified another important gap in knowledge: the dynamics and pathophysiology of myocardial edema after I/R are poorly understood, as they will be the implications of related novel findings for the retrospective quantification of MaR and salvage based on edema-based T2 CMR. There is therefore a need for a comprehensive myocardial tissue characterization

study in the context of I/R, comprising both translational CMR imaging methods and reference standard measurements.

The work described in this dissertation is focused on the understanding of the above mentioned gaps in knowledge, which otherwise we think are essential to make a successful translation from the preclinical laboratory to the clinical setting.

2 OBJECTIVES

Under the global hypothesis that myocardial edema after I/R is a dynamic phenomenon modulated by multiple factors, the main objectives of the present work thesis are as follows:

Objective 1. To provide a validation of a CMR method for fast and accurate quantification of myocardial edema which could be easily integrated in daily protocols.

Objective 2. To study the temporal evolution of myocardial edema, and other myocardial tissue components, after I/R in the preclinical setting.

Objective 3. To decipher into the pathophysiology underlying the dynamics of myocardial edema after I/R in the preclinical setting.

Objective 4. To study the impact of ischemia duration and protective strategies in the temporal dynamics of tissue composition after I/R, and their implications for assessing MaR and salvage, in the preclinical setting.

Objective 5. To characterize the temporal evolution of myocardial edema, and its implications for assessing MaR and salvage, by CMR in ST-segment elevation MI patients undergoing primary PCI.

3 MATERIALS, METHODS AND RESULTS

The doctoral student was first exposed to translational approaches related to I/R, cardioprotection and imaging of the post-MI heart by the host institution. This capacitation included the opportunity of reviewing literature and writing scientific documents, being crucial for a successful achievement of the thesis objectives. Outcomes derived from this training phase are reflected as well in this dissertation as a key step in the learning process of the scientific research method. Thus, the present thesis work has been organized in three chapters as mentioned below. For each of the chapters, a brief introduction to the published scientific documents and contribution performed by the doctoral student are indicated.

Chapter I. Myocardial infarction: scope, opportunities and challenges.

Chapter II. Translational implementation of cardiac magnetic resonance to the post-myocardial infarction heart.

Chapter III. Temporal dynamics and pathophysiology of the edematous response after myocardial infarction.

3.1 Chapter I. Myocardial infarction: scope, opportunities and challenges

As an initial step of this research work, a profound review of available literature related to the pathophysiology of MI, non-invasive imaging methods for myocardial tissue characterization (mainly CMR methods), and translational preclinical models of I/R injury and cardioprotection was performed.

As a result, we have contributed to the literature with 1 review article and 2 editorial articles for which I am the first author. For each of the scientific documents, I was responsible for reviewing the literature, drafting the manuscript, and elaborating and making critical input in the peer review process.

Editorial #1. "*Health and cost benefits associated with the use of metoprolol in heart attack patients*".[58] In this editorial work, a brief overview on the magnitude of the MI disease, and current and future socioeconomic challenges are discussed in the context of the results from the METOCARD-CNIC trial.[51, 59, 60] This proof-of-concept trial demonstrated that the administration of intravenous metoprolol before reperfusion reduces infarct size and the cases of post-MI chronic HF, being a promising low-cost an safe therapy likely to have a major health and socioeconomic positive impact. The results from this clinical study lead by the director of this thesis, Dr Borja Ibanez, constitutes a paradigmatic translational success story. Thus, the clinical trial was launched after encouraging preclinical results;[61] whereas a subsequent journey back to the bench was performed after to decipher into the mechanisms behind this protective effect.[40, 62] As it will be shown later, this translational process was replicated in several occasions by the doctoral student as part of his research work contained in this thesis.

Review article #1. "*Animal models of tissue characterization of area at risk, edema and fibrosis*".[63] This article aims at concisely reviewing recent and significant developments in the field of imaging techniques, mainly CMR, in relevant animal models of tissue characterization of area at risk, edema, and fibrosis.

Ex vivo histologic analyses of tissue samples have been classically considered the gold standard in the study of tissue properties and its composition. However, over the past decade, there has been a growing interest in the in vivo myocardial characterization with different imaging techniques, which can be potentially translated into the clinic in order to make an early diagnosis and evaluate serial changes, opening the possibility of dynamic evaluation. Animal models have become an essential tool to achieve this goal. Myocardial in vivo tissue characterization is of great importance because it can provide translational meaningful information to understand pathophysiological processes underlying different cardiac diseases.

Editorial #2. "*CAESAR: one step beyond in the construction of a translational bridge for cardioprotection*".[64] Most promising cardioprotective agents have failed to replicate the positive results in experimental models in the clinical arena over the last decades. In this editorial, a critical discussion on the challenges and reasons of such failure are discussed in the context of the initial outcomes from the CAESAR initiative.[34] Several Working Groups of experts have deeply discussed the reasons for the failure to effectively translate potential therapies for protecting the heart from I/R, making recommendations to try solving this unmet research need.[35, 65] The United States of America initiative included the creation of a national network of research laboratories with expertise in small and large animal models of I/R injury to systematically test a particular cardioprotective therapy using a multicenter randomized controlled study approach as a checkpoint before jumping into the clinical setting: the CAESAR (Consortium for preclinicAl assESsment of cARdioprotective therapies).[34] A movement for the establishment of a European network of research centers to test cardioprotective interventions in an attempt to mimic the pioneer endeavor of the CAESAR's enterprise is ongoing.[65]

Editorial #1. “*Health and cost benefits associated with the use of metoprolol in heart attack patients*”.[58]

Health and cost benefits associated with the use of metoprolol in heart attack patients

Expert Rev. Clin. Pharmacol. 7(6), 687–689 (2014)

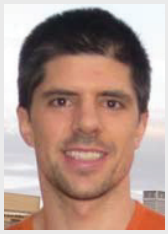

Rodrigo Fernández-Jiménez

Department of "Atherothrombosis, Imaging and Epidemiology", Centro Nacional de Investigaciones Cardiovasculares Carlos III (CNIC), Melchor Fernández Almagro, 3. 28029, Madrid, Spain
and
Hospital Clínico San Carlos, Madrid, Spain

Borja Ibanez

Author for correspondence: Department of "Atherothrombosis, Imaging and Epidemiology", Centro Nacional de Investigaciones Cardiovasculares Carlos III (CNIC), Melchor Fernández Almagro, 3. 28029, Madrid, Spain
and
Hospital Clínico San Carlos, Madrid, Spain
Tel.: +34 914 531 200
Fax: +34 914 531 245
bibanez@cnic.es

Heart attack (myocardial infarction) is a highly prevalent entity worldwide. Widespread implementation of reperfusion strategies has dramatically reduced the mortality associated with infarction. Paradoxically, the mortality reduction has significantly increased the incidence of chronic heart failure (HF). Treatment of HF, once present, represents a huge socioeconomic burden on individuals and healthcare systems. The possibility of preventing rather than treating post-infarction HF would be of paramount importance. Given that infarct size is the main determinant of adverse post-infarction outcomes (including chronic HF), therapies able to reduce infarct size are needed. The single administration of intravenous metoprolol before reperfusion has been recently shown to reduce infarct size and reduce the cases of chronic HF in a proof-of-concept trial. If confirmed in larger trials, this low-cost therapy is expected to have a major health and socioeconomic impact.

Heart attack, mainly presented as ST-segment elevation myocardial infarction (STEMI) due to complete occlusion of an epicardial coronary artery, is a leading cause of mortality and morbidity worldwide [1]. Timely reperfusion and aggressive invasive management (percutaneous coronary interventions [PCI]) have been demonstrated as the most effective therapy to reduce the mortality associated with STEMI. Risk-adjusted in-hospital mortality had decreased from ≈30% in 1985 to ≈5.5% among STEMI patients treated in routine practice in 2008 [2], reaching a plateau thereafter [3]. The latter suggests that additional strategies beyond reperfusion are needed to further reduce mortality in this population.

Paradoxically, the significant reduction in acute mortality during a STEMI, resulting from the universal implementation of timely reperfusion, has significantly increased the incidence of chronic heart failure (HF): patients with poor left ventricular function previously have died in the acute phase, but with the advent of reperfusion now survive the acute episode and continue to live with a significantly damaged heart [2]. Indeed, STEMI is a major cause of chronic HF, with reduced left ventricular ejection fraction (LVEF) post-infarction being one of the single principal causes of chronic HF, both in developed and other low- to middle-income countries [4,5]. Because mortality rates for STEMI patients have declined, attention has shifted toward reducing post-infarction HF because this outcome is thought to reflect the downstream impact of acute therapies for STEMI.

Immense research efforts have led to chronic HF interventions (pharmacological and device-based) that reduce long-term mortality in STEMI survivors with low LVEF [6]. Nonetheless, the implementation of these strategies comes at a high cost, which precludes its universal application [7,8]. Chronic treatment of HF once present represents a huge social and economic burden on individuals and healthcare systems. Moreover, for chronic HF, frequent hospital readmissions are the main contributors to the

Keywords: β-blocker • cost–effectiveness • heart failure • implantable cardioverter-defibrillator • infarct size • left ventricular ejection fraction • metoprolol • mortality • myocardial infarction

EXPERT REVIEWS

 10.1586/17512433.2014.960847 ISSN 1751-2433

escalating long-term healthcare costs [9,10]. The possibility of preventing (rather than treating) post-infarction HF would therefore be of significant clinical and socioeconomic importance.

The size of the infarct after a STEMI has been demonstrated as the main determinant of adverse post-infarction outcomes (including chronic HF). Patients with larger infarcts are at the highest risk since they have chronic severely depressed LVEF and associated HF [11]. Therefore, cost–effective therapies able to reduce infarct size are urgently needed since smaller infarctions will result in better heart performance and translate into fewer short- and long-term adverse clinical outcomes, helping to alleviate the huge socioeconomic burden of post-infarction HF.

Early intravenous (iv.) β-blocker initiation during a STEMI was proposed long ago as a therapy to limit infarct, but its real cardioprotective capacity during STEMI has been controversial [12]. Metoprolol tartrate was one of the first β-blockers released for clinical use and second iv. β-blocker agent clinically approved in the USA in 1978 [13]. Metoprolol is a β1-selective blocker. In spite of the availability of other drugs from the same family, metoprolol offers some potential advantages, like short half-life, easy administration in bolus injection and potential pleiotropic effects. These advantages, in addition to the clinical benefits here described, makes metoprolol the leading drug of its class. Surprisingly, in the current era of primary PCI as the treatment of choice for STEMI, no randomized trials assessing the beneficial effects of pre-reperfusion β-blocker administration had been reported until the advent of the METOCARD-CNIC trial [14,15].

In this trial, patients (mean age ≈ 58 years, ≈ 85% males) with anterior STEMI, Killip I or II, revascularized by PCI within 6 h from symptom onset with no obvious contraindication for the administration of β-blockers were randomized to receive up to three 5-mg iv. boluses of metoprolol tartrate [16] or control. In this context, early iv. metoprolol administration before reperfusion reduced infarct size (adjusted treatment effect, –6.5 g; 95% CI, –11.4 to –1.8; p = 0.012) and increased LVEF (adjusted treatment effect 2.7%; 95% CI, 0.1–5.2; p = 0.045) with no increase in adverse events in the acute phase (7.1% in the pre-reperfusion iv. metoprolol group, vs 16 events (12.3%) in the control group; p = 0.21). Patients receiving iv. metoprolol tartrate before reperfusion had a reduced incidence of HF readmissions over a median 2 years follow-up (2.2 vs 7% in iv. metoprolol and control groups, respectively, p = 0.04) [15]. Of note, the occurrence of severely depressed LVEF at 6 months was significantly lower in patients treated with iv. metoprolol (11 and 27% of patients in the iv. metoprolol and control groups, respectively, had an LVEF ≤35%, p = 0.006). Consequently, the proportion of patients fulfilling class-I indications for implantable cardioverter defibrillator (ICD) was significantly lower in the metoprolol group [15,17]. Early β-blockage before reperfusion is not encouraged in clinical guidelines, mainly due to the results of the COMMIT trial, which demonstrated no short-term net clinical benefit of early metoprolol in STEMI patients undergoing thrombolysis [18]. This trial recruited all comers with almost no restriction. Subgroup analyses suggested that patients fitting the inclusion criteria of the METOCARD-CNIC benefited from early iv. metoprolol in terms of mortality reduction. In addition, the clinical benefits associated with infarct size reduction (and post-infarction LVEF improvement) are expected to occur late (months to years) after STEMI. In the COMMIT trial, clinical follow-up was less than 1 month. It is plausible that longer follow-up of the COMMIT trial would show additional benefit of early metoprolol administration in survivors. Thus, an important lesson from the COMMIT trial is that not all STEMI patients benefit from very early β-blockage, a deduction supported by the results observed in the METOCARD-CNIC trial [15], following the personalized medicine principle.

ICD devices are of great value in reducing long-term mortality rates of STEMI patients. However, the enormous economic burden for health services precludes its universal implementation [19]. Even in advanced economies, cost considerations preclude universal implementation of ICD therapy in all patients who fulfill class-I indication [8]. Of note, mean initial implantation costs including procedure and single-chamber ICD device have been estimated to be around €30,000 ($40,000 in the USA or £23,000 in the UK) [20]. This initial estimation does not include post-discharge costs (tests, follow-up exams), potential related complications or device replacement. Some studies addressing cost–effectiveness of ICD therapy for post-infarction primary prevention have suggested unfavorable results for device implantation, even for class-I indication patients [21]. Moreover, there are many intangible impacts on psychological aspects. Fear of death, shock and public embarrassment are commonly experienced by recipients. The possibility of reducing the number of patients fulfilling criteria for primary prevention ICD implant would have an impact in the reduction of costs and also in the increased accessibility of those with a clinical indication. The cost of iv. metoprolol is less than €2 (<$3 in the USA or<£4 in the UK), and thus it appears a highly cost–effective therapy to tackle the huge socioeconomic burden associated with post-infarction HF.

It is important to highlight that the METOCARD-CNIC trial was powered to detect differences in infarct size; therefore, all other promising findings described here should be taken as hypothesis generating. The 'Impact of pre-reperfusion Metoprolol On clinical eVEnts after myocardial infarctiON' (MOVE ON!) trial is a European endeavor that will recruit more than 3000 patients in seven countries. The MOVE ON! trial will prospectively test the hypothesis that a single administration of iv. metoprolol in STEMI patients transferred to PCI will reduce the incidence of hard clinical endpoints, including chronic HF and cardiac mortality, and will specifically evaluate the savings to the healthcare systems by this low-cost therapy.

The cost of chronic HF treatment is estimated to represent 2% of the total healthcare budgets across Europe [5]. This represents approximately €48 billion for the European member states. STEMI is the most common cause of chronic HF, accounting for approximately 35% of all chronic HF cases. Thus, the cost of treating STEMI and its consequences is approximately €20 billion/year in Europe. The potential cost savings associated with early metoprolol administration are speculative at this stage,

but a plausible scenario can be proposed: assuming that half of the at-risk population might be able to receive the new therapy proposed in this application, the 25% reduction in cases of post-infarction chronic HF might represent a saving of around €5 billion/year across Europe. The MOVE ON! trial will tell whether these projections are real. If positive, it may have a major health and socioeconomic impact on infarcted patients.

Financial & competing interests disclosure

The authors have no relevant affiliations or financial involvement with any organization or entity with a financial interest in or financial conflict with the subject matter or materials discussed in the manuscript. This includes employment, consultancies, honoraria, stock ownership or options, expert testimony, grants or patents received or pending, or royalties.

No writing assistance was utilized in the production of this manuscript.

References

1. O'Gara PT, Kushner FG, Ascheim DD, et al. 2013 accf/aha guideline for the management of st-elevation myocardial infarction: a report of the american college of cardiology foundation/american heart association task force on practice guidelines. J Am Coll Cardiol 2013;61:e78-140
2. Eapen ZJ, Tang WH, Felker GM, et al. Defining heart failure end points in ST-segment elevation myocardial infarction trials: integrating past experiences to chart a path forward. Circ Cardiovasc Qual Outcomes 2012;5:594-600
3. Menees DS, Peterson ED, Wang Y, et al. Door-to-balloon time and mortality among patients undergoing primary pci. N Engl J Med 2013;369:901-9
4. Callender T, Woodward M, Roth G, et al. Heart failure care in low- and middle-income countries: a systematic review and meta-analysis. PLoS Med 2014;11:e1001699
5. Chronic heart failure: National clinical guideline for diagnosis and management in primary and secondary care: Partial update. London: 2010
6. Yancy CW, Jessup M, Bozkurt B, et al. 2013 ACCF/AHA guideline for the management of heart failure: a report of the American College of Cardiology Foundation/American Heart Association task force on practice guidelines. J Am Coll Cardiol 2013;62:e147-239
7. Hlatky MA, Mark DB. The high cost of implantable defibrillators. Eur Heart J 2007;28:388-91
8. LaPointe NM, Al-Khatib SM, Piccini JP, et al. Extent of and reasons for nonuse of implantable cardioverter defibrillator devices in clinical practice among eligible patients with left ventricular systolic dysfunction. Circ Cardiovasc Qual Outcomes 2011;4:146-51
9. NICE G. National Clinical Guideline Centre. The Management of Chronic Heart Failure in Adults in Primary and Secondary Care. 2010. Available from: http://guidance.nice.org.uk/CG108/Guidance/pdf/English
10. Braunschweig F, Cowie MR, Auricchio A. What are the costs of heart failure? Europace 2011;13(Suppl 2):ii13-17
11. Larose E, Rodes-Cabau J, Pibarot P, et al. Predicting late myocardial recovery and outcomes in the early hours of ST-segment elevation myocardial infarction traditional measures compared with microvascular obstruction, salvaged myocardium, and necrosis characteristics by cardiovascular magnetic resonance. J Am Coll Cardiol 2010;55:2459-69
12. Gerczuk PZ, Kloner RA. An update on cardioprotection: a review of the latest adjunctive therapies to limit myocardial infarction size in clinical trials. J Am Coll Cardiol 2012;59:969-78
13. Koch-Weser J. Drug therapy: Metoprolol. N Engl J Med 1979;301:698-703
14. Ibanez B, Macaya C, Sanchez-Brunete V, et al. Effect of early metoprolol on infarct size in ST-segment-elevation myocardial infarction patients undergoing primary percutaneous coronary intervention: the effect of metoprolol in cardioprotection during an acute myocardial infarction (METOCARD-CNIC) trial. Circulation 2013;128:1495-503
15. Pizarro G, Fernandez-Friera L, Fuster V, et al. Long-term benefit of early pre-reperfusion metoprolol administration in patients with acute myocardial infarction: results from the METOCARD-CNIC trial (effect of metoprolol in cardioprotection during an acute myocardial infarction). J Am Coll Cardiol 2014;63:2356-62
16. Ibanez B, Fuster V, Macaya C, et al. Study design for the "effect of metoprolol in cardioprotection during an acute myocardial infarction" (metocard-cnic): a randomized, controlled parallel-group, observer-blinded clinical trial of early pre-reperfusion metoprolol administration in ST-segment elevation myocardial infarction. Am Heart J 2012;164:473-80.e475
17. Antoniucci D. Block the ischemia and reperfusion damage: an old adjunctive drug for a new reperfusion strategy. J Am Coll Cardiol 2014;63:2363-4
18. Chen ZM, Pan HC, Chen YP, et al. Early intravenous then oral metoprolol in 45,852 patients with acute myocardial infarction: Randomised placebo-controlled trial. Lancet 2005;366:1622-32
19. Abegunde DO, Mathers CD, Adam T, et al. The burden and costs of chronic diseases in low-income and middle-income countries. Lancet 2007;370:1929-38
20. Cowie MR, Marshall D, Drummond M, et al. Lifetime cost-effectiveness of prophylactic implantation of a cardioverter defibrillator in patients with reduced left ventricular systolic function: results of Markov modelling in a European population. Europace 2009;11:716-26
21. Tung R, Zimetbaum P, Josephson ME. A critical appraisal of implantable cardioverter-defibrillator therapy for the prevention of sudden cardiac death. J Am Coll Cardiol 2008;52:1111-21

Review article #1. “*Animal models of tissue characterization of area at risk, edema and fibrosis*”.[63]

Curr Cardiovasc Imaging Rep (2014) 7:9259
DOI 10.1007/s12410-014-9259-z

CARDIAC MAGNETIC RESONANCE (E NAGEL AND V PUNTMANN, SECTION EDITORS)

Animal Models of Tissue Characterization of Area at Risk, Edema and Fibrosis

Rodrigo Fernández-Jiménez · Leticia Fernández-Friera · Javier Sánchez-González · Borja Ibáñez

Published online: 13 February 2014

Abstract Myocardial in vivo tissue characterization is of great importance because it can provide meaningful information to understand pathophysiological processes underlying different cardiac diseases. Ex vivo histologic analyses of tissue samples have been classically considered the gold standard in the study of tissue properties and its composition. However, over the past decade, there has been a growing interest in the in vivo myocardial characterization with different imaging techniques, which can potentially be translated into the clinics in order to make an early diagnosis and evaluate serial changes, opening the possibility of dynamic evaluation. Animal models have become an essential tool to achieve this goal. This article aims at concisely reviewing recent and significant developments in the field of imaging techniques—mostly cardiac magnetic resonance—in relevant animal models of tissue characterization of area at risk, edema, and fibrosis.

This article is part of the Topical Collection on *Cardiac Magnetic Resonance*

R. Fernández-Jiménez · L. Fernández-Friera · J. Sánchez-González · B. Ibáñez
Centro Nacional de Investigaciones Cardiovasculares Carlos III (CNIC), Madrid, Spain

R. Fernández-Jiménez · B. Ibáñez
Hospital Universitario Clínico San Carlos, Madrid, Spain

L. Fernández-Friera
Hospital Universitario Montepríncipe, Madrid, Spain

J. Sánchez-González
Philips Healthcare, Madrid, Spain

B. Ibáñez (✉)
Department of Epidemiology, Atherothrombosis and Imaging, Centro Nacional de Investigaciones Cardiovasculares Carlos III (CNIC), Melchor Fernández Almagro, 3, 28029 Madrid, Spain
e-mail: bibanez@cnic.es

Keywords Magnetic resonance · Animal model · Area at risk · Edema · Fibrosis

Introduction

In vitro tissue characterization techniques have been classically considered as the gold standard for assessment of cardiac diseases and treatments. Although these methods are very useful for a profound analysis of tissue composition, they have limitations such as changes in tissue composition because of manipulation, poorly suited for serial measurements and inability to translate it into the required follow-up clinical field. Conversely, several imaging modalities have been developed for the in vivo characterization of cardiac tissue properties such as positron emission tomography (PET) [1] or computed tomography (CT) [2]. However, cardiac magnetic resonance (CMR) is the technique that has captured most of the attention in preclinical and clinical research, since it offers a combination of high spatial resolution and high soft tissue contrast with no ionizing radiation. These features entitle CMR as an ideal tool for imaging the heart in terms of myocardial structure and function, becoming a reference standard modality for the tissue characterization in general, and for evaluation of the heart in particular, in preclinical and clinical research, including small/large animals and humans [3].

Myocardial tissue characterization in the context of a myocardial infarction or a suspected cardiomyopathy is one of the most frequent clinical indications to perform a CMR. Specific MR sequences addressing a comprehensive evaluation of heart structure and function are currently implemented in most clinical protocols [4], including late gadolinium enhancement sequences, which allow visualization and quantification of macroscopic areas of scar tissue [5]. However, an intense clinical and research interest is found today in the development of CMR sequences, which are dependent on native

myocardial signal characteristics—because of change in its composition—rather than in exogenous contrast-based images, to demonstrate pathophysiology and tissue characterization in cardiac disease [6].

Special attention has been focused in distinguishing and quantifying several main components of myocardial tissue (water, collagen, fat) that can be altered in different clinical scenarios, mostly in myocardial infarction and cardiomyopathies. In fact, changes in water content have been demonstrated after an ischemic event and other myocardial forms of inflammation such as myocarditis or sepsis, making possible the identification and delineation of the area of a myocardial insult [7]. Conversely, increased amounts of fibrosis, mainly—but not restricted to—collagen, has been also extensively shown after myocardial infarction and in other cardiomyopathies in the form of macroscopic areas of fibrosis (scar), as well as more recently in several cardiac diseases in the form of diffuse microscopic fibrosis, the former being associated with poor prognosis and mortality [8-12] and to be better correlated with actual infarct size than other biomarkers [13]. Finally, changes in the amount of myocardial, epicardial, or pericardial fat have been also shown in a wide spectrum of heart and systemic diseases, being a marker as well of adverse outcomes [14-16].

Some ex vivo models have been proposed as valid tools for the development of novel MR sequences in this regard [17]. However, beyond its value in the development of new imaging algorithms, relevant animal models can further provide, with a human, closer profound understanding of disease-related mechanisms and pathophysiology, important information before experimental-to-clinical leap, and histologic validation of new imaging methods and sequences. The purpose of the present review is to bring an updated overview of the most recent works involving small and large animal models using imaging technology—mainly CMR—for the in vivo tissue characterization of myocardial area at risk, edema, and fibrosis.

Animal Models of Tissue Characterization of Area at Risk

The myocardial territory, which becomes ischemic after occlusion of its supplying coronary artery, defines the region potentially at risk for necrosis, named as area at risk (thereafter, AAR). Modern percutaneous revascularization techniques and pharmacologic interventions aim to salvage areas of reversibly acute injured myocardium, thus, limiting infarct size and improving prognosis [18-21]. Testing the efficacy of cardioprotective therapies benefits from measuring both infarct size and AAR to calculate the normalized amount of myocardial salvage, which is probably a better measure of therapeutic efficacy than the absolute infarct size (Fig. 1) [22, 23]. Thus, there is considerable interest in finding a reproducible in vivo imaging method, which accurately reflects the AAR. CMR has become a paradigm of this research being one of the imaging techniques that have generated more published articles and controversies over recent past years on this topic.

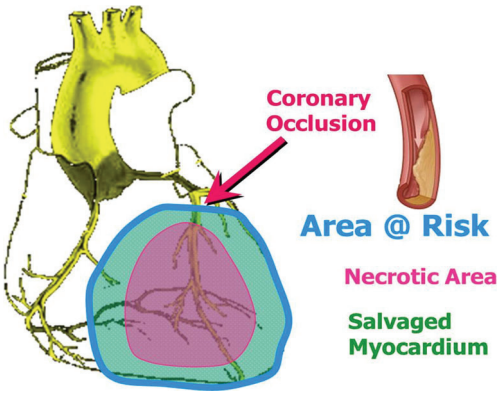

Fig. 1 Diagram representing both the AAR (blue delimited region), defined as the hypoperfused myocardial distal to a coronary occlusion; and the salvaged myocardium (green area), defined as the difference between the myocardial AAR and the necrotic area (pink area)

Hyperintense areas on T2-weighted MR imaging have been classically proposed as having good correlation with AAR in animal models [24••, 26], being among the most popular sequences used in humans to retrospectively delineate the ischemic myocardium (ie, to delineate area of former ischemia after the acute episode). Signal intensity on T2-weighted MR sequences appears to be linearly related to myocardial water content, which seems to be increased over the ischemic territory in the form of myocardial edema [27-29]. However, all these assumptions come from wide experimental studies and fewer human studies [30], most of them with small sample sizes and mixed patient population. As a result of this great heterogeneity, if these hyperintense areas accurately track the AAR or just the infarcted region, or merely something related to it, is still a matter of controversy [31••, 32••]. Moreover, T2-weighted imaging is often limited by a low signal-to-noise ratio, motion artifacts, incomplete blood suppression, and coil sensitivity related-issues of surface coils [33]. On top, no consensus exists in regards to how this data has to be optimally acquired and quantitatively analyzed.

Newer quantitative MR methods as T1 and T2 mapping, which allow direct measurement of intrinsic tissue properties in the form of T1 and T2 relaxation times, respectively, are less dependent on confounders affecting signal intensity and could overcome some of T2-weighted imaging limitations [34, 35] (Fig. 2). In this way, in a recent animal research in a dog model of ischemia/reperfusion injury [36], the accuracy for quantifying AAR with clinically available T1- and T2-mapping sequences, compared with microsphere blood flow analysis as a reference standard was demonstrated. However, pre-reperfusion delineation of AAR is likely the most accurate approach to delineate the anatomic myocardium at risk in the

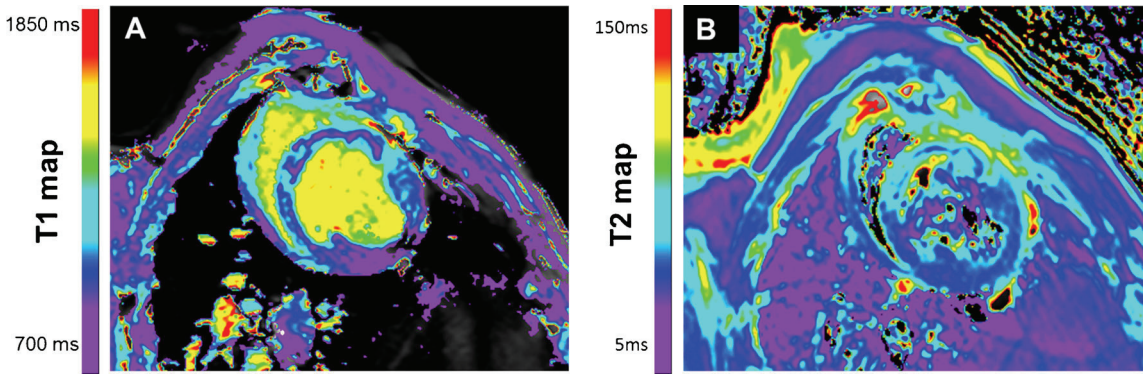

Fig. 2 Direct measurement of intrinsic tissue properties in the form of T1 mapping (Panel A) and T2 mapping (Panel B) in a pig model of ischemia/reperfusion injury. Note abnormal T1 and T2 relaxation times over anterior ventricular wall

experimental setting since reperfusion induces tissue changes after reperfusion that can modify the extension of former ischemic insult. Pathophysiological responses after acute myocardial infarction include edema, hemorrhage, and microvascular obstruction along with cellular damage, which probably have counter-acting effects on T2 and T1 relaxation times, as recently demonstrated in a porcine model of myocardial infarction [37].

Thus, in a recent experimental work it compared the accuracy of early postreperfusion CMR and prereperfusion multidetector computed tomography (MDCT) imaging to measure the size of the AAR, using pathology as a reference technique in a porcine acute myocardial infarction model [38]. It was shown that pathology best correlated with measurements made by MDCT. However, AAR measurements obtained by several T2-weigthed sequences (T2-STIR and T2-ACUTE) resulted in a modest correlation with pathology overestimating the anatomic extension of AAR. In our laboratory, we have been able to reproduce prereperfusion MDCT to measure AAR (Fig. 3, unpublished data) with similar results. However, this approach is hardly expected to be translated into humans, and available information suggests that postreperfusion T2-weighted imaging (or any other postreperfusion sequence or technique) aimed to measure AAR may have some limitations depending on the timing of image acquisition after ischemic insult.

On top, novel CMR methods have been recently added to the AAR identification and characterization repertoire. MR spectroscopy (MRS) and MR-based molecular imaging methods have shown promise for evaluating cardiac metabolism in the setting of ischemia/reperfusion. For example, phosphorus-31 MRS can assess high-energy phosphate content and energy reserve in the heart in animal and human subjects [39]. In a rat model of myocardial infarction, whole heart PCr content was inversely correlated with infarct size, whereas ATP distribution provided a profile of viable myocardium around the infarction reflecting remodeling of the heart [40]. In rats undergoing ligation of the left anterior descending coronary artery, 1H-MRS proved lower creatine myocardium content compared with controls [41]. In addition, dynamic nuclear polarization has been recently shown to allow a signal increase of more than 10,000-fold, opening the door to new understanding of the metabolic processes in the heart [42]. Experiments performed in the globally ischemic, isolated rat heart have demonstrated that hyperpolarized 13C-pyruvate can show the glycolytic switch characteristic of myocardial ischemia [43, 44]. In addition, hyperpolarized experiments in pig model of ischemia/reperfusion showed the potential of 13C-bicarbonate and (1-13C) alanine maps to distinguish between stunned myocardium and not viable tissue [45]. Modified blood oxygen level-dependent (BOLD) sequence, which signal intensity changes primarily from

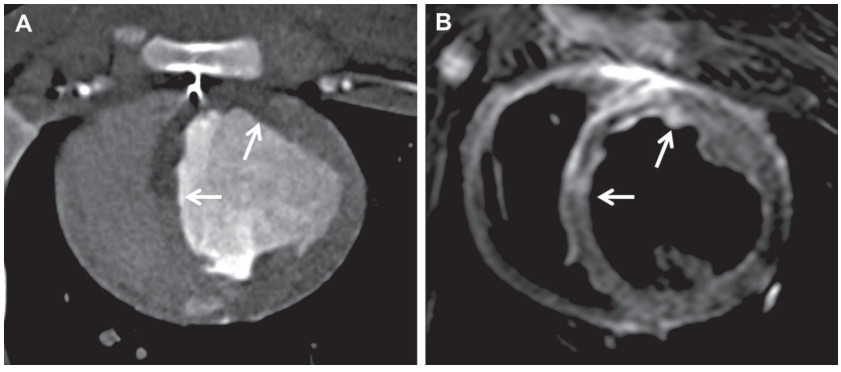

Fig. 3 In vivo delineation of area at risk at the mid-ventricular level using prereperfusion multidetector computed tomography (Panel A, white arrows) and postreperfusion T2-weighted STIR magnetic resonance sequence (Panel B, white arrows) in the same pig submitted to transient percutaneous occlusion of the left anterior descending coronary artery

alterations in blood oxygen saturation (and so, from changes in myocardial perfusion) has been just proposed as able to detect ischemic myocardium in a dog model of severe coronary stenosis, even earlier in time than the appearance of edema [46]. Tracking of upregulated vascular cell and intercellular adhesion molecules (VCAM and ICAM, respectively) following ischemia using targeted microparticles of iron oxide, which shorten T2 and T2* relaxation times, have also shown promise for the detection and localization of recent ischemia. Thus, they have been reported as suitable for the early identification of ischemic/damage organs [47, 48] as well as myocardial AAR [49] in small animal models, although its translation into the clinic does not seem to be around the corner. Finally, re-invented balanced steady-state free precession (bSSFP) sequence with T2 preparation, has been also recently described as potentially able to detect myocardial edema in both porcine model and patients with reperfused acute myocardial infarction, due to its sensitivity to T1, T2, and magnetization transfer effects [50-52].

Despite all these experiments and some clinical studies [30], important questions remain unclear. As previously mentioned, comprehensive study of the time course of myocardial edema and its visualization by CMR from the just early reperfusion is of critical importance and not fully addressed at the moment. Knowing the optimal time to accurately measure AAR would allow standardization of experimental and clinical protocols, avoiding conflicting data published over the literature. Large animal models of ischemia/reperfusion involving CMR studies become an ideal platform to go in depth into this phenomenon. Among them, pig is one of the most translational and reliable model to study ischemia/reperfusion-related issues since shows, unlike other mammals but similar to humans, analogous coronary artery anatomy and distribution [53, 54], and minimal pre-existing coronary collateral flow [55••, 56].

Animal Models of Tissue Characterization of Infarction-Unrelated Myocardial Edema

Experimental myocardial edema is mostly generated through a surgical (small and large animal models) or percutaneous (only large animal models) ischemia/reperfusion procedure involving transient occlusion of a coronary artery. This procedure has been described elsewhere [23], and its edema-related consequences have been briefly reviewed along previous section.

Different procedures inducing infarct-independent increase of myocardial water content in animal models have been also described, trying to reproduce other forms of myocardial edema. Sepsis triggered by sublethal injection of lipopolysaccharide [57, 58] or mechanical-induced peritonitis [59] has been shown to augment water content in the myocardium due to increased vascular permeability in mice. Global acute myocardial edema has been induced in a canine model by transient elevation of coronary sinus pressure [60]; whereas local myocardial edema has been described in the setting of experimental autoimmune myocarditis in CD69-defficient mice, which is characterized by an infiltration of inflammatory cells into the myocardium, fibrosis, edema, and necrosis, leading to ventricular wall dysfunction and heart failure [61].

Same CMR sequences described in previous section for AAR identification have been investigated for tissue characterization of noninfarct models of myocardial edema since share identical target; that is myocardial edema and so, changes in water tissue content. However, some imaging techniques are briefly pointed in this section since are specifically focused in tracking changes in the amount and conformation properties of the tissue water content itself, beyond the ischemic view.

Diffusion imaging provides information of water molecules displacement using motion sensitive gradients [62] adding complementary information to T2 weighted for edema definition (Fig. 4). Although limited experiments have been reported in animal models, different publications in human subjects have proposed this technique as a valuable tool for edema identification mostly using this diffusion information as a black-blood technique obtaining better blood suppression than conventional T2-weighted images [63].

Sodium chemical shift imaging (^{23}Na-CSI) has been reported as able to assess the sodium gradient and cell membrane integrity in order to visualize areas of myocardial edema in isolated rat hearts [64]. Because of expansion of the extracellular space in interstitial edema, imaging intra- and extracellular sodium separately may provide an alternative approach to assess myocardial edema. In this way, an elevated total sodium signal has been observed after myocardial infarction both in small and large animals [65, 66], and humans [67]. In a very recent research, using a noninfarcted isolated heart model of extracellular edema and ^{23}Na-CSI, it has been shown that viable edematous myocardium with cell membranes still intact is characterized by increased extracellular sodium but normal intracellular sodium since viable cells are able to maintain a normal sodium gradient [68]. Although promising, translation into clinically feasible seems to be again further away.

Animal Models of Tissue Characterization of Myocardial Fibrosis

Myocardial fibrosis is a common phenomenon that is observed in different stages in a wide variety of heart diseases. Collagen accumulation and increase in extracellular volume is basically shown in the myocardium in 2 ways: macroscopic fibrosis in the form of a visible based scar and microscopic

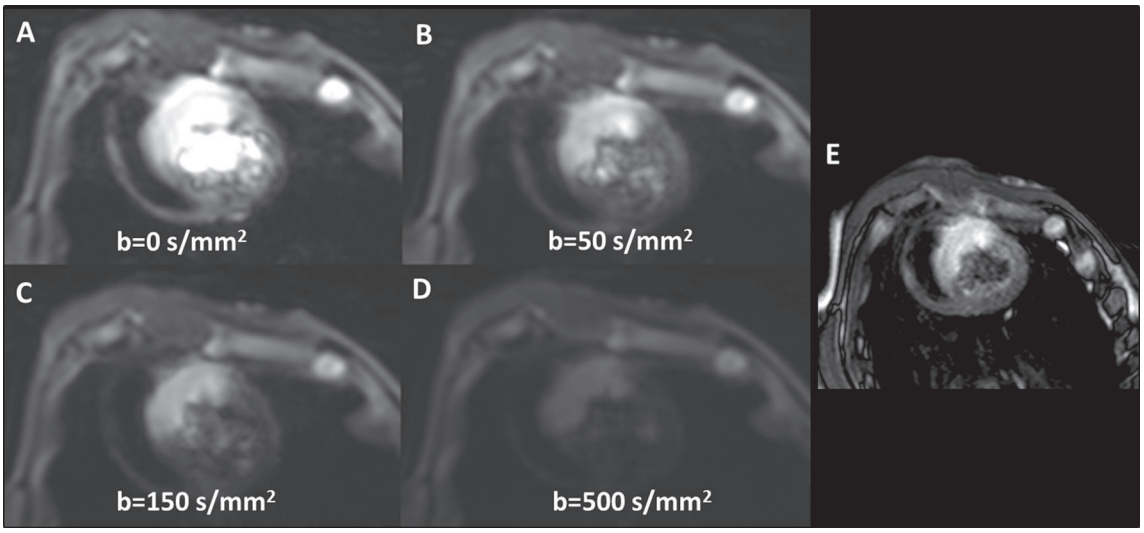

Fig. 4 In vivo diffusion-weighted images (Panels A, B, C and D) from a pig submitted to myocardial infarction. All images show a very bright region corresponding to edema within the area at risk, with different diffusion weighted b values (0, 50, 150, 500 s/mm2). Image of the ventricle at same level using a T2W-STIR sequence for comparison between both techniques (Panel E)

fibrosis in the form of diffuse global fibrosis. Myocardial fibrosis has become one of the hot topics at the moment, generating a huge amount of publications in animal models and humans over the last recent years.

Macroscopic fibrosis in the form of a scar (Fig. 5) has been classically and extensively described after myocardial infarction, and in other cardiomyopathies [69, 70], based on delayed enhancement sequences both in CMR and CT [71], being its size and distribution intimately associated with heart remodeling, prognosis, and mortality of patients [69, 71-75]. Small and large animal models of myocardial infarction are now being frequently used for preclinical testing of cardioprotective therapies [23], development, and progress in imaging techniques [76], and study of scarring-related arrhythmias [77, 78]. Moreover, animal models closely reproducing human atrial arrhythmias are becoming a nice platform

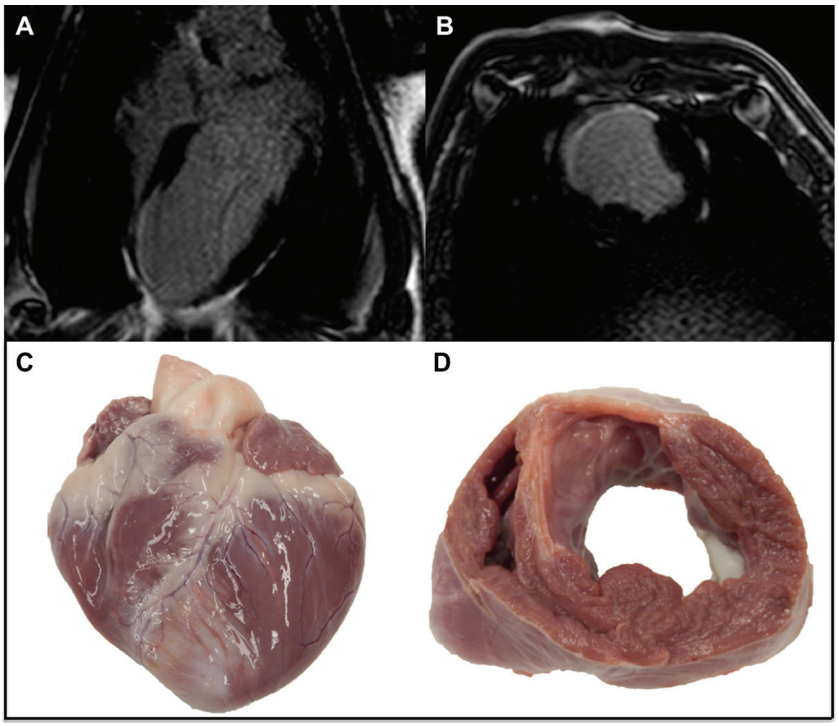

Fig. 5 Macroscopic fibrosis in the form of scar localized at the mid-ventricular anterior wall on magnetic resonance images using late gadolinium enhancement (Panels A and B), which is also demonstrated on pathological specimen (Panels C and D)

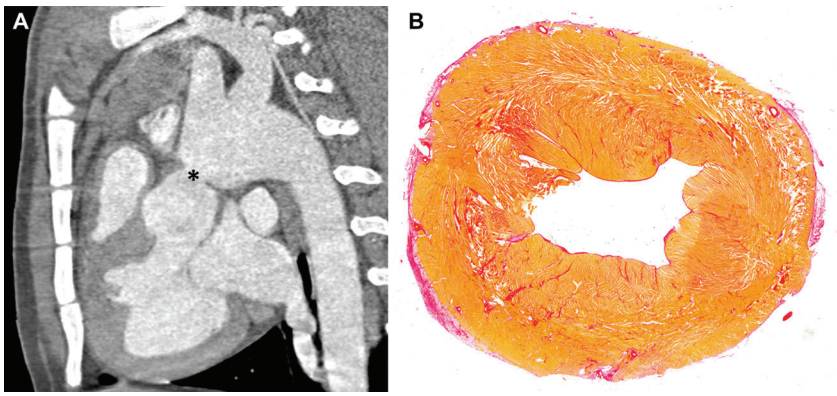

Fig. 6 Cardiac contrast computed tomography - sagittal view showing surgical placement of a banding at the ascending aorta (black asterisk) of a pig (Panel A). Histologic mid-ventricular short axis slice of the same animal with Picrosirius red staining demonstrating left ventricular hypertrophy and diffuse interstitial fibrosis (Panel B, red fibers; courtesy of Damian Sanchez-Quintana)

to develop and improve new and classic ablation techniques, which can potentially be translated to clinical trials, along with going in depth with arrhythmia-related imaging, mechanisms, and pathophysiology [79-81].

Although conventional late gadolinium enhancement CMR sequences are able to identify macroscopic fibrosis in conditions such as myocardial infarction and other cardiomyopathies as previously described, they are less suitable for in vivo detection of microscopic diffuse myocardial fibrosis since the myocardium is globally affected by smaller collagen deposits and there may be little normal myocardium to compare with. However, relying on quantification of the T1 relaxation times after contrast enhancement equilibrium, the myocardial extracellular volume fraction has been proposed as having a good correlation with the amount of diffuse fibrosis [82, 83]. Fibrosis shortens the postcontrast longitudinal relaxation time (and so, T1) properties of the myocardium and this feature may be tracked by specific pulse sequences. Thus, a shorter myocardial T1 after administration of gadolinium-based contrast agent indicates extracellular matrix expansion and is associated with accumulation of connective tissue in the myocardium. Promising noncontrast CMR methods for the discrimination of normal and diffusely diseased myocardium are emerging as the recently described T1 native [84].

Animal models have become critical for validation of newer CMR methods, and research in fibrosis imaging is not an exception. Diffuse myocardial fibrosis over the left ventricle has been generated in small and large animals mostly based on different approaches such as placement of aortic constrictive banding [85] or drug administration [86, 87],

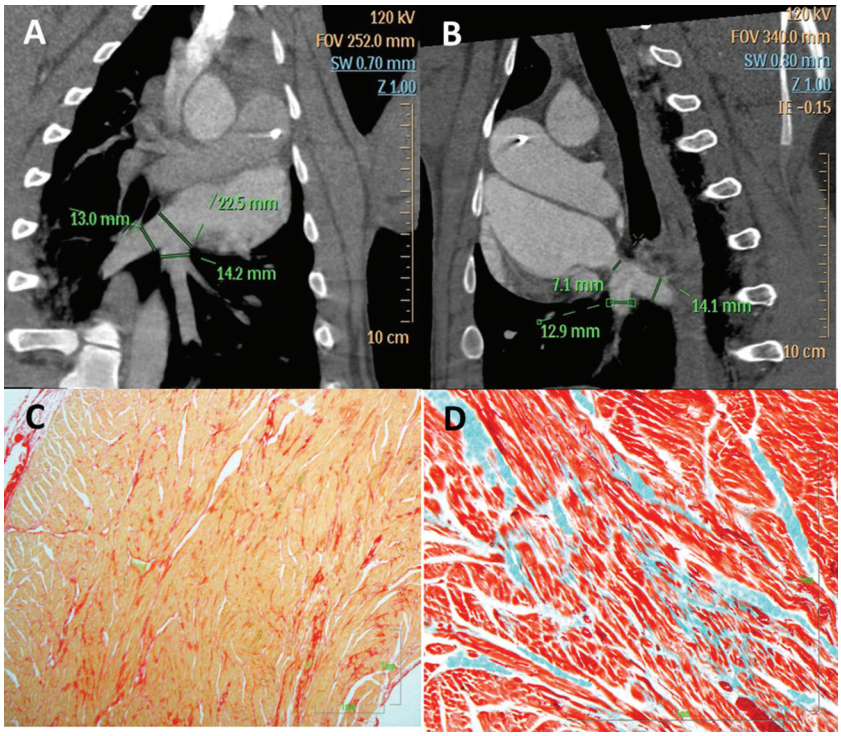

Fig. 7 Contrast computed tomography images showing normal pulmonary vein anatomy (Panel A) and a significant stenosis of the inferior pulmonary vein (Panel B) in a pig model of pulmonary hypertension. Histologic images of the right ventricle of the same pig using Picrosirius red (Panel C) and Masson trichrome (Panel D) stainings showing myofiber disarray and diffuse myocardial fibrosis over the right ventricle (courtesy of Damian Sanchez-Quintana)

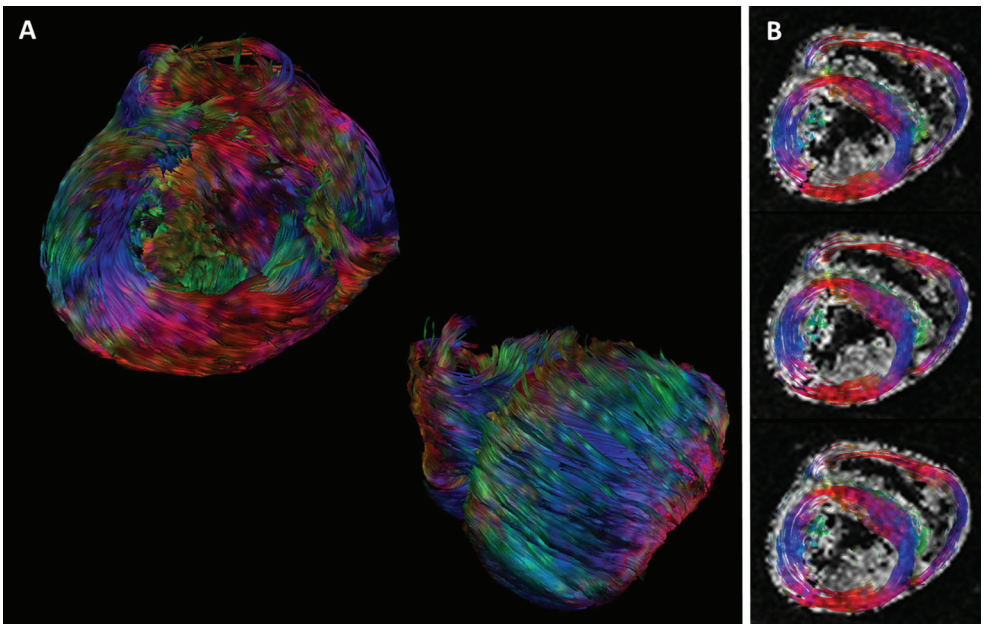

Fig. 8 Diffusion tensor 3D reconstruction imaging of an ex vivo pig heart showing the myofiber tracks form a long axis and short axis view (Panel A). Two-dimensional cross sections of the same ventricle at 3 different levels. Note circumferential organization of the myofibers (courtesy of Prof Jesús Ruíz-Cabello)

overall inducing pressure-overload left ventricular hypertrophy (Fig. 6); although other animal models reproducing specific cardiomyopathies have been also reported [88]. Particular modified sequences for generating T1 maps, and so detecting diffuse fibrosis, have been developed and are needed in small animals due to their high heart rates [89]. Although not so well studied, generation of animal models with diffuse myocardial fibrosis in the right ventricle (Fig. 7) is an interesting and promising approach for investigating its forgotten diseases and for achieving new treatments for pulmonary hypertension [90, 91].

Novel imaging techniques have been recently described adding new information about myocardial fibrosis. Diffusion tensor magnetic resonance imaging (DT-MRI) is a diffusion-weighted technique that uses the directionality information of water diffusion to track myofibers orientation and organization [92] (Fig. 8). This myofiber organization can be measured with a DTI parameter called fractional anisotropy that represents the capability of water molecules to move more easily in 1 direction compared with the others. Thus, DT-MRI has demonstrated a reduction of fractional anisotropy values in the infarcted and border zones compared with the remote myocardium showing good agreement with histology findings in a pig model [93, 94]. New approaches using molecular imaging have emerged to in vivo visualize and quantify inflammatory molecules involved in the formation of scar tissue in the postinfarction myocardium [95]. For example, targeting myofibroblasts or metalloproteinases using specific ligands have been proposed for imaging left ventricular remodeling in a murine model of myocardial infarction [96]. Thus, the possibility to identify early stages of postinfarction healing may allow the development of new therapies focused in preventing irreversible changes.

Conclusions

Characterization of myocardial tissue changes with CMR represents a valuable tool to define the presence and stage of a particular heart disease, and to serially and noninvasively monitor both animal models and patients for progression of disease or therapeutic efficacy. However, despite great development in the last years, this topic is far from been closed, remaining important questions to be answered. Early detection as well as timing and mechanistics of these tissue changes are of great importance and interest, although little and controversial information only is published at present. Full animal models become the ideal tool for the in vivo development of newer imaging methods, which would potentially allow answering these questions since ability for follow-up acquisitions and feasibility of validation and translation to the clinic.

Compliance with Ethics Guidelines

Conflict of Interest Rodrigo Fernández-Jiménez declares that he has no conflict of interest. Leticia Fernández-Friera declares that he has no conflict of interest. Javier Sánchez-González declares that he has no conflict of interest. Borja Ibáñez declares that he has no conflict of interest.

Human and Animal Rights and Informed Consent This article does not contain any studies with human or animal subjects performed by any of the authors.

References

Papers of particular interest, published recently, have been highlighted as:
•• Of major importance

1. Dobrucki LW, Sinusas AJ. PET and SPECT in cardiovascular molecular imaging. Nat Rev Cardiol. 2010;7:38–47.
2. Nacif MS, Kawel N, Lee JJ, et al. Interstitial myocardial fibrosis assessed as extracellular volume fraction with low-radiation-dose cardiac CT. Radiology. 2012;264:876–83.
3. Pennell DJ. Cardiovascular magnetic resonance. Circulation. 2010;121:692–705.
4. Kramer CM, Barkhausen J, Flamm SD, et al. Standardized cardiovascular magnetic resonance (CMR) protocols 2013 update. J Cardiovasc Magn Reson. 2013;15:91.
5. Ordovas KG, Higgins CB. Delayed contrast enhancement on MR images of myocardium: past, present, future. Radiology. 2011;261:358–74.
6. Kramer CM, Narula J. CMR imaging: creating contrast without cosmetics. JACC Cardiovasc Imaging. 2011;4:1326–7.
7. Garcia-Dorado D, Andres-Villarreal M, Ruiz-Meana M, et al. Myocardial edema: a translational view. J Mol Cell Cardiol. 2012;52:931–9.
8. Azevedo CF, Nigri M, Higuchi ML, et al. Prognostic significance of myocardial fibrosis quantification by histopathology and magnetic resonance imaging in patients with severe aortic valve disease. J Am Coll Cardiol. 2010;56:278–87.
9. Gulati A, Jabbour A, Ismail TF, et al. Association of fibrosis with mortality and sudden cardiac death in patients with nonischemic dilated cardiomyopathy. JAMA. 2013;309:896–908.
10. Klem I, Weinsaft JW, Bahnson TD, et al. Assessment of myocardial scarring improves risk stratification in patients evaluated for cardiac defibrillator implantation. J Am Coll Cardiol. 2012;60:408–20.
11. O'Hanlon R, Grasso A, Roughton M, et al. Prognostic significance of myocardial fibrosis in hypertrophic cardiomyopathy. J Am Coll Cardiol. 2010;56:867–74.
12. Shiozaki AA, Senra T, Arteaga E, et al. Myocardial fibrosis detected by cardiac CT predicts ventricular fibrillation/ventricular tachycardia events in patients with hypertrophic cardiomyopathy. J Cardiovasc Comput Tomogr. 2013;7:173–81.
13. Fernandez-Jimenez R, Lopez-Romero P, Suarez-Barrientos A, et al. Troponin release overestimates infarct size in presence of left ventricular hypertrophy. J Am Coll Cardiol. 2012;60:640–1.
14. Holloway CJ, Ntusi N, Suttie J, et al. Comprehensive cardiac magnetic resonance imaging and spectroscopy reveal a high burden of myocardial disease in HIV patients. Circulation. 2013;128:814–22.
15. Rijzewijk LJ, van der Meer RW, Smit JW, et al. Myocardial steatosis is an independent predictor of diastolic dysfunction in type 2 diabetes mellitus. J Am Coll Cardiol. 2008;52:1793–9.
16. Wong CX, Abed HS, Molaee P, et al. Pericardial fat is associated with atrial fibrillation severity and ablation outcome. J Am Coll Cardiol. 2011;57:1745–51.
17. Schuster A, Grunwald I, Chiribiri A, et al. An isolated perfused pig heart model for the development, validation and translation of novel cardiovascular magnetic resonance techniques. J Cardiovasc Magn Reson. 2010;12:53.
18. Ibanez B, Macaya C, Sanchez-Brunete V, et al. Effect of early metoprolol on infarct size in st-segment-elevation myocardial infarction patients undergoing primary percutaneous coronary intervention: the effect of metoprolol in cardioprotection during an acute myocardial infarction (METOCARD-CNIC) Trial. Circulation. 2013;128:1495–503.
19. Botker HE, Kharbanda R, Schmidt MR, et al. Remote ischaemic conditioning before hospital admission, as a complement to angioplasty, and effect on myocardial salvage in patients with acute myocardial infarction: a randomized trial. Lancet. 2010;375:727–34.
20. Heusch G. Cardioprotection: chances and challenges of its translation to the clinic. Lancet. 2013;381:166–75.
21. Piot C, Croisille P, Staat P, et al. Effect of cyclosporine on reperfusion injury in acute myocardial infarction. N Engl J Med. 2008;359:473–81.
22. Friedrich MG, Abdel-Aty H, Taylor A, et al. The salvaged area at risk in reperfused acute myocardial infarction as visualized by cardiovascular magnetic resonance. J Am Coll Cardiol. 2008;51:1581–7.
23. Ibanez B, Prat-Gonzalez S, Speidl WS, et al. Early metoprolol administration before coronary reperfusion results in increased myocardial salvage: analysis of ischemic myocardium at risk using cardiac magnetic resonance. Circulation. 2007;115:2909–16.
24.•• Aletras AH, Tilak GS, Natanzon A, et al. Retrospective determination of the area at risk for reperfused acute myocardial infarction with T2-weighted cardiac magnetic resonance imaging: histopathological and displacement encoding with stimulated echoes (DENSE) functional validations. Circulation. 2006;113:1865–70. *Pioneer study in dogs demonstrating that edema imaging by T2-weighted cardiac magnetic resonance is a useful tool for retrospectively delineating the area at risk in reperfused myocardial infarction.*
25. Garcia-Dorado D, Oliveras J, Gili J, et al. Analysis of myocardial oedema by magnetic resonance imaging early after coronary artery occlusion with or without reperfusion. Cardiovasc Res. 1993;27:1462–9.
26. Tilak GS, Hsu LY, Hoyt Jr RF, et al. In vivo T2-weighted magnetic resonance imaging can accurately determine the ischemic area at risk for 2-day-old nonreperfused myocardial infarction. Invest Radiol. 2008;43:7–15.
27. Boxt LM, Hsu D, Katz J, et al. Estimation of myocardial water content using transverse relaxation time from dual spin-echo magnetic resonance imaging. Magn Reson Imaging. 1993;11:375–83.
28. Higgins CB, Herfkens R, Lipton MJ, et al. Nuclear magnetic resonance imaging of acute myocardial infarction in dogs: alterations in magnetic relaxation times. Am J Cardiol. 1983;52:184–8.
29. Jennings RB, Schaper J, Hill ML, et al. Effect of reperfusion late in the phase of reversible ischemic injury. Changes in cell volume, electrolytes, metabolites, and ultrastructure. Circ Res. 1985;56:262–78.
30. Carlsson M, Ubachs JF, Hedstrom E, et al. Myocardium at risk after acute infarction in humans on cardiac magnetic resonance: quantitative assessment during follow-up and validation with single-photon emission computed tomography. JACC Cardiovasc Imaging. 2009;2:569–76.
31.•• Arai AE, Leung S, Kellman P. Controversies in cardiovascular MR imaging: reasons why imaging myocardial T2 has clinical and pathophysiologic value in acute myocardial infarction. Radiology. 2012;265:23–32. *Excellent controversy showing arguments in favor of the used of T2-weighted imaging for delineating the area at risk in ischemic myocardial injury.*
32.•• Croisille P, Kim HW, Kim RJ. Controversies in cardiovascular MR imaging: T2-weighted imaging should not be used to delineate the area at risk in ischemic myocardial injury. Radiology. 2012;265:12–22. *Excellent controversy showing arguments against the used of T2-weighted imaging for delineating the area at risk in ischemic myocardial injury.*
33. Friedrich MG, Kim HW, Kim RJ. T2-weighted imaging to assess post-infarct myocardium at risk. JACC Cardiovasc Imaging. 2011;4:1014–21.
34. Ferreira VM, Piechnik SK, Dall'Armellina E, et al. Non-contrast T1-mapping detects acute myocardial edema with high diagnostic accuracy: a comparison to T2-weighted cardiovascular magnetic resonance. J Cardiovasc Magn Reson. 2012;14:42.

35. Verhaert D, Thavendiranathan P, Giri S, et al. Direct T2 quantification of myocardial edema in acute ischemic injury. JACC Cardiovasc Imaging. 2011;4:269–78.
36. Ugander M, Bagi PS, Oki AJ, et al. Myocardial edema as detected by pre-contrast T1 and T2 CMR delineates area at risk associated with acute myocardial infarction. JACC Cardiovasc Imaging. 2012;5:596–603.
37. Ghugre NR, Ramanan V, Pop M, et al. Quantitative tracking of edema, hemorrhage, and microvascular obstruction in subacute myocardial infarction in a porcine model by MRI. Magn Reson Med. 2011;66:1129–41.
38. Mewton N, Rapacchi S, Augeul L, et al. Determination of the myocardial area at risk with pre- versus post-reperfusion imaging techniques in the pig model. Basic Res Cardiol. 2011;106:1247–57.
39. Neubauer S. The failing heart—an engine out of fuel. N Engl J Med. 2007;356:1140–51.
40. Friedrich J, Apstein CS, Ingwall JS. 31P nuclear magnetic resonance spectroscopic imaging of regions of remodeled myocardium in the infarcted rat heart. Circulation. 1995;92:3527–38.
41. Bottomley PA, Weiss RG. Noninvasive localized MR quantification of creatine kinase metabolites in normal and infarcted canine myocardium. Radiology. 2001;219:411–8.
42. Schroeder MA, Clarke K, Neubauer S, et al. Hyperpolarized magnetic resonance: a novel technique for the in vivo assessment of cardiovascular disease. Circulation. 2011;124:1580–94.
43. Merritt ME, Harrison C, Storey C, et al. Inhibition of carbohydrate oxidation during the first minute of reperfusion after brief ischemia: NMR detection of hyperpolarized 13CO2 and H13CO3. Magn Reson Med. 2008;60:1029–36.
44. Schroeder MA, Swietach P, Atherton HJ, et al. Measuring intracellular pH in the heart using hyperpolarized carbon dioxide and bicarbonate: a 13C and 31P magnetic resonance spectroscopy study. Cardiovasc Res. 2010;86:82–91.
45. Golman K, Petersson JS, Magnusson P, et al. Cardiac metabolism measured noninvasively by hyperpolarized 13C MRI. Magn Reson Med. 2008;59:1005–13.
46. Tsaftaris SA, Zhou X, Tang R, et al. Detecting myocardial ischemia at rest with cardiac phase-resolved blood oxygen level-dependent cardiovascular magnetic resonance. Circ Cardiovasc Imaging. 2013;6:311–9.
47. Akhtar AM, Schneider JE, Chapman SJ, et al. In vivo quantification of VCAM-1 expression in renal ischemia reperfusion injury using non-invasive magnetic resonance molecular imaging. PLoS One. 2010;5:e12800.
48. McAteer MA, Sibson NR, von Zur MC, et al. In vivo magnetic resonance imaging of acute brain inflammation using microparticles of iron oxide. Nat Med. 2007;13:1253–8.
49. Grieve SM, Lonborg J, Mazhar J, et al. Cardiac magnetic resonance imaging of rapid VCAM-1 up-regulation in myocardial ischemia-reperfusion injury. Eur Biophys J. 2013;42:61–70.
50. Kellman P, Aletras AH, Mancini C, et al. T2-prepared SSFP improves diagnostic confidence in edema imaging in acute myocardial infarction compared with turbo spin echo. Magn Reson Med. 2007;57:891–7.
51. Kumar A, Beohar N, Arumana JM, et al. CMR imaging of edema in myocardial infarction using cine balanced steady-state free precession. JACC Cardiovasc Imaging. 2011;4:1265–73.
52. Zhou X, Rundell V, Liu Y, et al. On the mechanisms enabling myocardial edema contrast in bSSFP-based imaging approaches. Magn Reson Med. 2011;66:187–91.
53. Crick SJ, Sheppard MN, Ho SY, et al. Anatomy of the pig heart: comparisons with normal human cardiac structure. J Anat. 1998;193(Pt 1):105–19.
54. Weaver ME, Pantely GA, Bristow JD, et al. A quantitative study of the anatomy and distribution of coronary arteries in swine in comparison with other animals and man. Cardiovasc Res. 1986;20:907–17.
55.•• Maxwell MP, Hearse DJ, Yellon DM. Species variation in the coronary collateral circulation during regional myocardial ischaemia: a critical determinant of the rate of evolution and extent of myocardial infarction. Cardiovasc Res. 1987;21:737–46. *In vivo evaluation of the coronary collateral circulation in eight animal species (dog, cat, rat, guinea pig, ferret, baboon, rabbit, pig), a critical determinant of the rate of myocardial necrosis progression resulting from experimental coronary artery occlusion*.
56. White FC, Carroll SM, Magnet A, et al. Coronary collateral development in swine after coronary artery occlusion. Circ Res. 1992;71:1490–500.
57. Castanares-Zapatero D, Bouleti C, Sommereyns C, et al. Connection between cardiac vascular permeability, myocardial edema, and inflammation during sepsis: role of the alpha1AMP-activated protein kinase isoform. Crit Care Med. 2013;41(12):e411–22. doi:10.1097/CCM.0b013e31829866dc.
58. Smeding L, Plotz FB, Lamberts RR, et al. Mechanical ventilation with high tidal volumes attenuates myocardial dysfunction by decreasing cardiac edema in a rat model of LPS-induced peritonitis. Respir Res. 2012;13:23.
59. Smeding L, Leong-Poi H, Hu P, et al. Salutary effect of resveratrol on sepsis-induced myocardial depression. Crit Care Med. 2012;40:1896–907.
60. Dongaonkar RM, Stewart RH, Quick CM, et al. Award article: Microcirculatory Society Award for Excellence in Lymphatic Research: time course of myocardial interstitial edema resolution and associated left ventricular dysfunction. Microcirculation. 2012;19:714–22.
61. Cruz-Adalia A, Jimenez-Borreguero LJ, Ramirez-Huesca M, et al. CD69 limits the severity of cardiomyopathy after autoimmune myocarditis. Circulation. 2010;122:1396–404.
62. Luna A, Sánchez-González J, Caro P. Diffusion-weighted imaging of the chest. Magn Reson Imaging Clin N Am. 2011;19:69–94.
63. Okayama S, Uemura S, Watanabe M, et al. Novel application of black-blood echo-planar imaging to the assessment of myocardial infarction. Heart Vessels. 2010;25:104–12.
64. Jansen MA, Van Emous JG, Nederhoff MG, et al. Assessment of myocardial viability by intracellular 23Na magnetic resonance imaging. Circulation. 2004;110:3457–64.
65. Constantinides CD, Kraitchman DL, O'Brien KO, et al. Noninvasive quantification of total sodium concentrations in acute reperfused myocardial infarction using 23Na MRI. Magn Reson Med. 2001;46:1144–51.
66. Kim RJ, Judd RM, Chen EL, et al. Relationship of elevated 23Na magnetic resonance image intensity to infarct size after acute reperfused myocardial infarction. Circulation. 1999;100:185–92.
67. Ouwerkerk R, Bottomley PA, Solaiyappan M, et al. Tissue sodium concentration in myocardial infarction in humans: a quantitative 23Na MR imaging study. Radiology. 2008;248:88–96.
68. Aguor EN, van de Kolk CW, Arslan F, et al. 23Na chemical shift imaging and Gd enhancement of myocardial edema. Int J Cardiovasc Imaging. 2013;29:343–54.
69. Green JJ, Berger JS, Kramer CM, et al. Prognostic value of late gadolinium enhancement in clinical outcomes for hypertrophic cardiomyopathy. JACC Cardiovasc Imaging. 2012;5:370–7.
70. Rathod RH, Prakash A, Powell AJ, et al. Myocardial fibrosis identified by cardiac magnetic resonance late gadolinium enhancement is associated with adverse ventricular mechanics and ventricular tachycardia late after Fontan operation. J Am Coll Cardiol. 2010;55:1721–8.
71. Sato A, Nozato T, Hikita H, et al. Prognostic value of myocardial contrast delayed enhancement with 64-slice multidetector computed tomography after acute myocardial infarction. J Am Coll Cardiol. 2012;59:730–8.
72. Beek AM, Kuhl HP, Bondarenko O, et al. Delayed contrast-enhanced magnetic resonance imaging for the prediction of regional functional improvement after acute myocardial infarction. J Am Coll Cardiol. 2003;42:895–901.

73. Gerber BL, Garot J, Bluemke DA, et al. Accuracy of contrast-enhanced magnetic resonance imaging in predicting improvement of regional myocardial function in patients after acute myocardial infarction. Circulation. 2002;106:1083–9.
74. Ingkanisorn WP, Rhoads KL, Aletras AH, et al. Gadolinium delayed enhancement cardiovascular magnetic resonance correlates with clinical measures of myocardial infarction. J Am Coll Cardiol. 2004;43:2253–9.
75. Dweck MR, Joshi S, Murigu T, et al. Midwall fibrosis is an independent predictor of mortality in patients with aortic stenosis. J Am Coll Cardiol. 2011;58:1271–9.
76. Schelbert EB, Hsu LY, Anderson SA, et al. Late gadolinium-enhancement cardiac magnetic resonance identifies postinfarction myocardial fibrosis and the border zone at the near cellular level in ex vivo rat heart. Circ Cardiovasc Imaging. 2010;3:743–52.
77. McDowell KS, Arevalo HJ, Maleckar MM, et al. Susceptibility to arrhythmia in the infarcted heart depends on myofibroblast density. Biophys J. 2011;101:1307–15.
78. Ng J, Jacobson JT, Ng JK, et al. Virtual electrophysiological study in a 3-dimensional cardiac magnetic resonance imaging model of porcine myocardial infarction. J Am Coll Cardiol. 2012;60:423–30.
79. Filgueiras-Rama D, Price NF, Martins RP, et al. Long-term frequency gradients during persistent atrial fibrillation in sheep are associated with stable sources in the left atrium. Circ Arrhythm Electrophysiol. 2012;5:1160–7.
80. McGann CJ, Kholmovski EG, Oakes RS, et al. New magnetic resonance imaging-based method for defining the extent of left atrial wall injury after the ablation of atrial fibrillation. J Am Coll Cardiol. 2008;52:1263–71.
81. Cooper LL, Odening KE, Hwang MS, et al. Electromechanical and structural alterations in the aging rabbit heart and aorta. Am J Physiol Heart Circ Physiol. 2012;302:H1625–35.
82. Iles L, Pfluger H, Phrommintikul A, et al. Evaluation of diffuse myocardial fibrosis in heart failure with cardiac magnetic resonance contrast-enhanced T1 mapping. J Am Coll Cardiol. 2008;52:1574–80.
83. Flett AS, Hayward MP, Ashworth MT, et al. Equilibrium contrast cardiovascular magnetic resonance for the measurement of diffuse myocardial fibrosis: preliminary validation in humans. Circulation. 2010;122:138–44.
84. Puntmann VO, Voigt T, Chen Z, et al. Native T1 mapping in differentiation of normal myocardium from diffuse disease in hypertrophic and dilated cardiomyopathy. JACC Cardiovasc Imaging. 2013;6:475–84.
85. Zhang M, Takimoto E, Hsu S, et al. Myocardial remodeling is controlled by myocyte-targeted gene regulation of phosphodiesterase type 5. J Am Coll Cardiol. 2010;56:2021–30.
86. Coelho-Filho OR, Mongeon FP, Mitchell R, et al. Role of transcytolemmal water-exchange in magnetic resonance measurements of diffuse myocardial fibrosis in hypertensive heart disease. Circ Cardiovasc Imaging. 2013;6:134–41.
87. Messroghli DR, Nordmeyer S, Dietrich T, et al. Assessment of diffuse myocardial fibrosis in rats using small-animal Look-Locker inversion recovery T1 mapping. Circ Cardiovasc Imaging. 2011;4:636–40.
88. Stedman HH, Sweeney HL, Shrager JB, et al. The mdx mouse diaphragm reproduces the degenerative changes of Duchenne muscular dystrophy. Nature. 1991;352:536–9.
89. Messroghli DR, Nordmeyer S, Buehrer M, et al. Small animal Look-Locker inversion recovery (SALLI) for simultaneous generation of cardiac T1 maps and cine and inversion recovery-prepared images at high heart rates: initial experience. Radiology. 2011;261:258–65.
90. Garcia-Alvarez A, Fernandez-Friera L, Garcia-Ruiz JM, et al. Noninvasive monitoring of serial changes in pulmonary vascular resistance and acute vasodilator testing using cardiac magnetic resonance. J Am Coll Cardiol. 2013;62:1621–31.
91. Hadri L, Kratlian RG, Benard L, et al. Therapeutic efficacy of AAV1.SERCA2a in monocrotaline-induced pulmonary arterial hypertension. Circulation. 2013;128:512–23.
92. Holmes AA, Scollan DF, Winslow RL. Direct histologic validation of diffusion tensor MRI in formaldehyde-fixed myocardium. Magn Reson Med. 2000;44:157–61.
93. Pop M, Ghugre NR, Ramanan V, et al. Quantification of fibrosis in infarcted swine hearts by ex vivo late gadolinium-enhancement and diffusion-weighted MRI methods. Phys Med Biol. 2013;58:5009–28.
94. Wu EX, Wu Y, Nicholls JM, et al. MR diffusion tensor imaging study of postinfarct myocardium structural remodeling in a porcine model. Magn Reson Med. 2007;58:687–95.
95. Jaffer FA, Libby P, Weissleder R. Molecular imaging of cardiovascular disease. Circulation. 2007;116:1052–61.
96. Su H, Spinale FG, Dobrucki LW, et al. Noninvasive targeted imaging of matrix metalloproteinase activation in a murine model of postinfarction remodeling. Circulation. 2005;112:3157–67.

Editorial #2. “*CAESAR: one step beyond in the construction of a translational bridge for cardioprotection*”.[64]

Editorial

CAESAR

One Step Beyond in the Construction of a Translational Bridge for Cardioprotection

Rodrigo Fernández-Jiménez, Borja Ibanez

Timely reperfusion is known as the best therapeutic strategy for limiting the extent of myocardial damage during an ST-segment–elevation myocardial infarction (STEMI).[1,2] The concept of reperfusion as a means to limit necrosis during an STEMI was established in an experimental large animal (dog) model 4 decades ago.[3,4] Noteworthy, the translation of the reperfusion concept in STEMI is one of the most successful stories of therapies ever. This example highlights the critical relevance of using preclinical models similar to humans for efficient translational research. Further research in the field identified that reperfusion is not a free lunch, and it can come at the price of inducing additional damage to the myocardium, a phenomenon known as reperfusion injury.[5] The final extent of myocardial necrosis after a STEMI, resulting from both ischemic and reperfusion injuries, is a major determinant of mortality and morbidity after infarction.[6] Therefore, huge efforts have been dedicated for exploring cardioprotective therapies that might limit ischemia/reperfusion injury beyond timely reperfusion. Opposed to what occurred with the reperfusion concept, the translation of therapies aiming to ameliorate reperfusion injury has been more disappointing than the former. With the exception of a few therapies succeeding in translating experimental results into positive proof of concept clinical trials demonstrating reduction in infarct size and increase in myocardial salvage,[7–11] most promising cardioprotectives agents/interventions have failed to replicate the positive results in experimental models in the clinical arena over the last decades.[8,12] It is important to note that failure in translation is not restricted to the cardioprotection field, and similar frustrating findings have been observed in other areas.[13,14]

Article, see p 572

What are the reasons responsible for this loss in translation? Inadequate experimental data and overoptimistic erroneous conclusions resulting from methodological flaws in animal studies might be one of the main reasons accounting for this scientific inconsistency.[15] Like in any formal clinical trial, animal studies testing the efficacy of a given (cardioprotective) therapy/intervention should be based on a well-designed prespecified protocol paying rigorous attention to design (including expected effect size), conduct, statistical, and reporting-style aspects. Unfortunately, critical methodological elements such as blinding, randomization, or a priori sample size calculation are too frequently neglected in the experimental setting, increasing the chances of biased and hyped positive results.[16] In the case of cardioprotective therapies, specific aspects directly related to the ultimate myocardial damage, such as animal species, strain differences, anesthetic agents, duration of ischemia, drug administration, manner and duration of reperfusion, and methodology and timing of end point (myocardial damage/salvage) evaluation,[17–19] may be decisive in the outcome of the study as well. Having all these variables as potential sources of variability, it is not so surprising that the replication and reproducibility of experimental results among different laboratories are alarmingly low.[20] Several Working Groups of experts have deeply discussed the reasons for the failure to effectively translate potential therapies for protecting the heart from ischemia/reperfusion, making recommendations to try solving this unmet research need.[17,19,21] The US initiative further included the creation of a national network of research laboratories with expertise in small and large animal models of ischemia/reperfusion injury to systematically test a particular cardioprotective therapy using a multicenter randomized controlled study approach as a checkpoint before jumping into the clinical setting: the CAESAR (Consortium for preclinicAl assESsment of cARdioprotective therapies) Cardioprotection Consortium[22] (http://www.nihcaesar.org/). Recently, the European Society of Cardiology Group in Cellular Biology of the Heart have proposed the establishment of a European network of research centers to test cardioprotective interventions[17] in an attempt to mimic the pioneer endeavor of the CAESAR's enterprise.

Two highly relevant papers on the topic of translating preclinical results into clinics in the field of cardioprotection during STEMI appear in this issue of the Journal. Jones et al[23] report the initial validation of the CAESAR initiative by testing the protection afforded by preconditioning, and Prof Heusch[24] presents an outstanding comprehensive review of the mechanisms and signal transduction pathways in ischemic conditioning. The landmark CAESAR validation[23] is based on the principles of detailed conduct of experimental protocols, randomization, researcher blinding, a priori sample size calculation and exclusion criteria, appropriate statistical analyses, and assessment of reproducibility. For such proof of concept validation, authors decided to test ischemic (local) preconditioning as the intervention to reduce infarct size in 3 species

The opinions expressed in this article are not necessarily those of the editors or of the American Heart Association.

From the Centro Nacional de Investigaciones Cardiovasculares Carlos III (CNIC), Madrid, Spain (R.F.-J., B.I.); and Hospital Universitario Clínico San Carlos, Madrid, Spain (R.F.-J., B.I.).

Correspondence to Borja Ibanez, MD, PhD, Myocardial Pathophysiology Program, Centro Nacional de Investigaciones Cardiovasculares Carlos III (CNIC), Melchor Fernández Almagro, 3, 28029, Madrid, Spain. E-mail bibanez@cnic.es

(*Circ Res*. 2015;116:554-556.
DOI: 10.1161/CIRCRESAHA.115.305841.)

Circulation Research **is available at http://circres.ahajournals.org**
DOI: 10.1161/CIRCRESAHA.115.305841

(mouse, rabbit, and pig) at 3 different centers of the consortium (2 sites/species). Authors wisely chose ischemic preconditioning as a protective intervention because it is probably the most robust and reproducible cardioprotective intervention known to date. The mechanisms of protection during ischemic preconditioning are extensively presented in the review paper appearing in the same issue of the journal.[24]

The CAESAR authors and institutions involved in this work should be congratulated for their innovative and huge effort to achieve a rigorous experimental setting. Overall, this approach should result in a reduction of potential biases and consequently in an increase in the confidence of attributing the differences observed between groups of animals allocated to different interventions to the treatment under investigation rather than to confounding factors or to just random error. However, there are potential shortcomings in the implementation and universalization of the CAESAR methodology. Counterintuitively, the excessive protocol standardization to reduce data variance can come at a negative price in some cases. It has been postulated that highly environmental standardized conditions may reveal restricted conclusions to a concrete experimental setting with little external validity being a cause, rather than a cure, of poor study reproducibility[25] something that has been previously referred to as the standardization fallacy.[26] External validity of experimental studies can be also affected by inevitable species differences. Therefore, even with rigorous design and conduct of an experimental study, such as the one elegantly presented by CAESAR, the translation of animal results to the clinics may fail because of disparities between the model and the real-world patient. CAESAR tries to overcome this limitation by using >1 laboratory for each species, but in the end 2 laboratories closely associated and following the exact same methodology are virtually a single hyperspecialized unit. The adding of more laboratories, eventually using slight different approaches (eg, different strain of animals, different anesthetics, different methods for outcome assessment, etc.), can serve to further improve the salutary long-term benefits of CAESAR.

Even the best animal models are approximations to human physiology/pathophysiology, and it is fair to acknowledge that in most cases they are only partially resembling what is seen in a more complex human diseased system. As an example, aging and multiple comorbid conditions seen in patients included in regular clinical trials are barely present in the experimental setting. Obviously, the intrinsic limitations inherent to animal models do not invalidate the use of laboratory research. We are convinced that animal models are useful tools in biomedical research, but a call for rigor in experimental investigation as presented by CAESAR initiative is necessary to improve translation. In this regard, it is noteworthy that in the paper by Jones et al,[23] there seems to be a species-related effect size gradient: infarct size reduction by the applied preconditioning intervention was largest in mice, intermediate in rabbits, and smallest in pigs. This anecdotic findings highlight that the extrapolation of animal results into clinics highly depends on the species evaluated.

Another relevant aspect close to the topic here discussed is the positive results publication bias. The report of negative preclinical studies is an extremely hard endeavor, and many times animal studies yielding neutral results are never reported. CAESAR is certainly an endeavor of such relevance that a room for the report of negative preclinical studies should be identified. In this regard, it is noteworthy that Jones et al[23] acknowledge in their paper that 2 other agents have been tested by CAESAR, sodium nitrite and sildenafil citrate, and both failed to limit infarct size despite prior experimental studies reporting beneficial effects with these therapies. The best venue for reporting these negative findings in CAESAR is to be decided by the implicated institutions.

What is the ultimate translational relevance of the CAESAR initiative? This enterprise will certainly help in the better identification of therapies/interventions with chances to be tested in pilot clinical trials. Early identification of therapies with no (or limited) benefits will be of massive help for the scientific and pharmaceutical communities. The personal and economical costs associated with clinical trials is humongous and the proper early identification of potential failures is capital. There are some interventions that have already shown positive results in pilot clinical trials (for more details, we refer to the accompanying review paper by G. Heusch[24]). It is noteworthy that these positive experiences were always preceded by thorough preclinical studies.[9,11,27]

Emulating Julius Caesar and his legionaries, who built the first 2 bridges across the Rhine River to defeat Germanic tribes during the Gallic War in 53 BC, the CAESAR initiative[23] has built a new bridge that will help the translation expansion in the field of cardioprotection during STEMI.

Disclosures

None.

References

1. Task Force on the management of ST-segment elevation acute myocardial infarction of the European Society of Cardiology (ESC), Steg PG, James SK, Atar D, et al. ESC Guidelines for the management of acute myocardial infarction in patients presenting with ST-segment elevation. *Eur Heart J*. 2012;33:2569–2619.
2. American College of Emergency Physicians; Society for Cardiovascular Angiography and Interventions, O'Gara PT, Kushner FG, Ascheim DD, et al. 2013 ACCF/AHA guideline for the management of ST-elevation myocardial infarction: a report of the American College of Cardiology Foundation/American Heart Association Task Force on Practice Guidelines. *J Am Coll Cardiol*. 2013;61:e78–e140.
3. Maroko PR, Libby P, Ginks WR, Bloor CM, Shell WE, Sobel BE, Ross J Jr. Coronary artery reperfusion. I. Early effects on local myocardial function and the extent of myocardial necrosis. *J Clin Invest*. 1972;51:2710–2716. doi: 10.1172/JCI107090.
4. Ginks WR, Sybers HD, Maroko PR, Covell JW, Sobel BE, Ross J Jr. Coronary artery reperfusion. II. Reduction of myocardial infarct size at 1 week after the coronary occlusion. *J Clin Invest*. 1972;51:2717–2723. doi: 10.1172/JCI107091.
5. Ibanez B, Fuster V, Jiménez-Borreguero J, Badimon JJ. Lethal myocardial reperfusion injury: a necessary evil? *Int J Cardiol*. 2011;151:3–11. doi: 10.1016/j.ijcard.2010.10.056.
6. Larose E, Rodes-Cabau J, Pibarot P, et al. Predicting late myocardial recovery and outcomes in the early hours of ST-segment elevation myocardial infarction traditional measures compared with microvascular obstruction, salvaged myocardium, and necrosis characteristics by cardiovascular magnetic resonance. *J Am Coll Cardiol*. 2010;55:2459–2469.
7. Bøtker HE, Kharbanda R, Schmidt MR, et al. Remote ischaemic conditioning before hospital admission, as a complement to angioplasty, and effect on myocardial salvage in patients with acute myocardial infarction: a randomised trial. *Lancet*. 2010;375:727–734. doi: 10.1016/S0140-6736(09)62001-8.

8. Heusch G. Cardioprotection: chances and challenges of its translation to the clinic. *Lancet*. 2013;381:166–175. doi: 10.1016/S0140-6736(12)60916-7.
9. Ibanez B, Macaya C, Sanchez-Brunete V, et al. Effect of early metoprolol on infarct size in ST-segment-elevation myocardial infarction patients undergoing primary percutaneous coronary intervention: the Effect of Metoprolol in Cardioprotection During an Acute Myocardial Infarction (METOCARD-CNIC) trial. *Circulation*. 2013;128:1495–1503.
10. Piot C, Croisille P, Staat P, et al. Effect of cyclosporine on reperfusion injury in acute myocardial infarction. *N Engl J Med*. 2008;359:473–481.
11. Pizarro G, Fernandez-Friera L, Fuster V, et al. Long-term benefit of early pre-reperfusion metoprolol administration in patients with acute myocardial infarction: results from the METOCARD-CNIC trial (Effect of Metoprolol in Cardioprotection During an Acute Myocardial Infarction). *J Am Coll Cardiol*. 2014;63:2356–2362.
12. Vander Heide RS, Steenbergen C. Cardioprotection and myocardial reperfusion: pitfalls to clinical application. *Circ Res*. 2013;113:464–477. doi: 10.1161/CIRCRESAHA.113.300765.
13. Franco R, Cedazo-Minguez A. Successful therapies for Alzheimer's disease: why so many in animal models and none in humans? *Front Pharmacol*. 2014;5:146. doi: 10.3389/fphar.2014.00146.
14. Sena E, van der Worp HB, Howells D, Macleod M. How can we improve the pre-clinical development of drugs for stroke? *Trends Neurosci*. 2007;30:433–439. doi: 10.1016/j.tins.2007.06.009.
15. van der Worp HB, Howells DW, Sena ES, Porritt MJ, Rewell S, O'Collins V, Macleod MR. Can animal models of disease reliably inform human studies? *PLoS Med*. 2010;7:e1000245. doi: 10.1371/journal.pmed.1000245.
16. Bebarta V, Luyten D, Heard K. Emergency medicine animal research: does use of randomization and blinding affect the results? *Acad Emerg Med*. 2003;10:684–687.
17. Lecour S, Botker HE, Condorelli G, et al. ESC working group cellular biology of the heart: position paper: improving the preclinical assessment of novel cardioprotective therapies. *Cardiovasc Res*. 2014;104:399–411.
18. Fernandez-Jimenez R, Sanchez-Gonzalez J, Aguero J, et al. Myocardial edema after ischemia/reperfusion is not stable and follows a bimodal pattern: advanced imaging and histological tissue characterization. *J Am Coll Cardiol*. 2015; 65:315–323 doi: 10.1016/j.jacc.2014.11.004.
19. Bolli R, Becker L, Gross G, Mentzer R Jr, Balshaw D, Lathrop DA; NHLBI Working Group on the Translation of Therapies for Protecting the Heart from Ischemia. Myocardial protection at a crossroads: the need for translation into clinical therapy. *Circ Res*. 2004;95:125–134. doi: 10.1161/01.RES.0000137171.97172.d7.
20. Collins FS, Tabak LA. Policy: NIH plans to enhance reproducibility. *Nature*. 2014;505:612–613.
21. Hausenloy DJ, Baxter G, Bell R, et al. Translating novel strategies for cardioprotection: the Hatter Workshop Recommendations. *Basic Res Cardiol*. 2010;105:677–686. doi: 10.1007/s00395-010-0121-4.
22. Schwartz Longacre L, Kloner RA, Arai AE, et al; National Heart, Lung, and Blood Institute, National Institutes of Health. New horizons in cardioprotection: recommendations from the 2010 National Heart, Lung, and Blood Institute Workshop. *Circulation*. 2011;124:1172–1179.
23. Jones SP, Tang XL, Guo Y, et al. The NHLBI-Sponsored Consortium for preclinicAl assESsment of cARdioprotective Therapies (CAESAR): a new paradigm for rigorous, accurate, and reproducible evaluation of putative infarct-sparing interventions in mice, rabbits, and pigs. *Cir Res*. 2015;116:572–586. doi: 10.1161/CIRCRESAHA.116.305462.
24. Heusch G. The molecular basis of cardioprotection: signal 5 transduction in ischemic pre-, post- and remote conditioning. *Cir Res*. 2015;116:587–599.
25. Richter SH, Garner JP, Würbel H. Environmental standardization: cure or cause of poor reproducibility in animal experiments? *Nat Methods*. 2009;6:257–261. doi: 10.1038/nmeth.1312.
26. Würbel H. Behaviour and the standardization fallacy. *Nat Genet*. 2000;26:263. doi: 10.1038/81541.
27. Ibanez B, Prat-González S, Speidl WS, Vilahur G, Pinero A, Cimmino G, García MJ, Fuster V, Sanz J, Badimon JJ. Early metoprolol administration before coronary reperfusion results in increased myocardial salvage: analysis of ischemic myocardium at risk using cardiac magnetic resonance. *Circulation*. 2007;115:2909–2916. doi: 10.1161/CIRCULATIONAHA.106.679639.

KEY WORDS: Editorials ■ animal experimentation ■ infarction ■ ischemic preconditioning ■ random allocation ■ reperfusion ■ reproducibility of results

3.2 Chapter II. Translational implementation of cardiac magnetic resonance to the post-myocardial infarction heart

As a next step, the doctoral student was trained and capacitated by the host research group in the pig model of closed-chest MI and translational imaging methods to assess the post-MI heart. For such purpose, the doctoral student elaborated on a clinical observation done during his cardiology fellowship training: upon an acute MI, the systemic release of troponins seems to be disproportionately higher than that of total creatine kinase in patients with left ventricular hypertrophy. As a consequence, the prediction of infarct size based on the circulating levels of troponin might be confounded by the presence of left ventricular hypertrophy.[66] Although retrospective in nature, this was the first time that a different pattern of creatine kinase and troponin release was shown in MI patients with left ventricular hypertrophy.

This clinical observation was translated then to the preclinical laboratory at CNIC. A pig model of left ventricular hypertrophy secondary to pressure-overload by surgical banding of the ascending aorta was developed, and CMR used to assess left ventricular outcomes after MI. The hypothesis was then tested in the experimental setting, and translated again to the bedside by replicating the results in the METOCARD-CNIC trial; therefore completing a success translational journey. As a result, we have contributed to the literature with the following original research article for which I am the first author.

> Original research article #1. "*Impact of left ventricular hypertrophy on troponin release during acute myocardial infarction: new insights from a comprehensive translational study*".[67]

The lessons learned before about imaging of the post-MI heart were again applied in the clinical setting. Specifically, the association between the red blood cell content of marine omega-3 fatty acids and CMR measurements of MaR, infarct size, myocardial salvage and left ventricular ejection fraction was prospectively evaluated by using the METOCARD-CNIC data set. As a result, we have contributed to the literature with the following original research article for which I am the co-first author.

Original research article #2. "*Nutritional preconditioning by marine omega-3 fatty acids in patients with ST-segment elevation myocardial infarction: A METOCARD-CNIC trial substudy*".[68]

For the scientific documents published and contained in this chapter, I contributed as doctoral student in the following: design and plan the preclinical experiments, recruitment and follow-up of patients within the METOCARD-CNIC trial, perform the model of MI in the pig, collect and process blood and myocardial tissue samples for subsequent analysis, CMR imaging acquisition and analysis, statistical analysis, draft the manuscript, and elaborate and make critical input in the peer review process.

Original research article #1. "*Impact of left ventricular hypertrophy on troponin release during acute myocardial infarction: new insights from a comprehensive translational study*".[67]

ORIGINAL RESEARCH

Impact of Left Ventricular Hypertrophy on Troponin Release During Acute Myocardial Infarction: New Insights From a Comprehensive Translational Study

Rodrigo Fernández-Jiménez, MD; Jacobo Silva, MD, PhD; Sara Martínez-Martínez, PhD; Mª Dolores López-Maderuelo, PhD; Mario Nuno-Ayala, PhD; José Manuel García-Ruiz, MD; Ana García-Álvarez, MD, PhD; Leticia Fernández-Friera, MD, PhD; Tech Gonzalo Pizarro, MD; Jaime García-Prieto, BSc; David Sanz-Rosa, PhD; Gonzalo López-Martin; Antonio Fernández-Ortiz, MD, PhD; Carlos Macaya, MD, PhD; Valentin Fuster, MD, PhD; Juan Miguel Redondo, PhD; Borja Ibanez, MD, PhD

***Background*—**Biomarkers are frequently used to estimate infarct size (IS) as an endpoint in experimental and clinical studies. Here, we prospectively studied the impact of left ventricular (LV) hypertrophy (LVH) on biomarker release in clinical and experimental myocardial infarction (MI).

***Methods and Results*—**ST-segment elevation myocardial infarction (STEMI) patients (n=140) were monitored for total creatine kinase (CK) and cardiac troponin I (cTnI) over 72 hours postinfarction and were examined by cardiac magnetic resonance (CMR) at 1 week and 6 months postinfarction. MI was generated in pigs with induced LVH (n=10) and in sham-operated pigs (n=8), and serial total CK and cTnI measurements were performed and CMR scans conducted at 7 days postinfarction. Regression analysis was used to study the influence of LVH on total CK and cTnI release and IS estimated by CMR (gold standard). Receiver operating characteristic (ROC) curve analysis was performed to study the discriminatory capacity of the area under the curve (AUC) of cTnI and total CK in predicting LV dysfunction. Cardiomyocyte cTnI expression was quantified in myocardial sections from LVH and sham-operated pigs. In both the clinical and experimental studies, LVH was associated with significantly higher peak and AUC of cTnI, but not with differences in total CK. ROC curves showed that the discriminatory capacity of AUC of cTnI to predict LV dysfunction was significantly worse for patients with LVH. LVH did not affect the capacity of total CK to estimate IS or LV dysfunction. Immunofluorescence analysis revealed significantly higher cTnI content in hypertrophic cardiomyocytes.

***Conclusions*—**Peak and AUC of cTnI both significantly overestimate IS in the presence of LVH, owing to the higher troponin content per cardiomyocyte. In the setting of LVH, cTnI release during STEMI poorly predicts postinfarction LV dysfunction. LV mass should be taken into consideration when IS or LV function are estimated by troponin release. **(*J Am Heart Assoc*. 2015;4: e001218 doi: 10.1161/JAHA.114.001218)**

Key Words: creatine kinase • hypertrophy • magnetic resonance imaging • myocardial infarction • troponin

From the Centro Nacional de Investigaciones Cardiovasculares Carlos III (CNIC), Madrid, Spain (R.F.-J., S.M.-M., M.D.L.-M., M.N.-A., J.M.G.-R., A.G.-A., L.F.-F., G.P., J.G.-P., D.S.-R., G.L.-M., V.F., J.M.R., B.I.); Hospital Universitario Clínico San Carlos, Madrid, Spain (R.F.-J., J.S., A.F.-O., C.M., B.I.); Hospital Universitario Central de Asturias, Oviedo, Spain (J.M.G.-R.); Hospital Clinic, Barcelona, Spain (A.G.-A.); Hospital Universitario Montepríncipe, Madrid, Spain (L.F.-F.); Hospital Universitario Quirón Madrid UEM, Madrid, Spain (G.P.); The Zena and Michael A. Wiener CVI, Mount Sinai School of Medicine, New York, NY (V.F.).

Correspondence to: Borja Ibanez, MD, PhD, FESC, Atherothrombosis, Imaging and Epidemiology Department, Centro Nacional de Investigaciones Cardiovasculares Carlos III (CNIC), Melchor Fernández Almagro, 3, 28029 Madrid, Spain. E-mail: bibanez@cnic.es

Received June 21, 2014; accepted November 16, 2014.

Systemic release of cardiac biomarkers is commonly used to quantify the extent of cardiac damage after an acute myocardial infarction (AMI). Peak and area under the curve (AUC) of total creatine kinase (CK) and cardiac troponin (cTn) have been consistently shown to correlate with infarct size (IS) measured by reference standards: cardiac magnetic resonance (CMR),[1–3] single-photon emission computed tomography (SPECT),[4,5] and postmortem analysis.[6] Accurate quantification of IS is of value given that it correlates closely with long-term left ventricular (LV) performance and, more important, with clinical outcomes.[7] However, reference standard techniques for IS quantification (CMR or SPECT) are not widely available. Infarct size is therefore commonly estimated from the levels of cardiac biomarkers in peripheral blood, especially in clinical trials in which IS is used as an endpoint.[8,9]

We recently reported on a retrospective observational analysis showing that patients with LV hypertrophy (LVH) who suffer an ST-segment elevation myocardial infarction (STEMI) can have disproportional blood concentrations of cardiac troponin I (cTnI)/total CK, compared with STEMI patients with no LVH.[10] Given the high prevalence of LVH in the general population[11,12] and the importance of accurate IS quantification, unequivocal demonstration of the influence of LVH on biomarker release is of clinical and research value.

In the present study, we conducted a prospective analysis to determine whether LV mass influences cardiac biomarker release after STEMI. Biomarker estimates of IS were compared with state-of-the-art CMR, a gold standard for IS quantification, in STEMI patients from a prospective clinical trial, and a similar analysis was conducted in a controlled experimental pig STEMI model (with/without LVH) to gain insight into the underlying mechanisms. The main aims of the present study were to (1) analyze the influence of LVH on the cTnI/total CK release pattern after STEMI, (2) study the impact of LVH on IS quantification and LV ejection fraction (LVEF) prediction by these biomarkers, and (3) study the effect of LVH on cTnI expression in myocardial tissue samples from LVH and control pigs.

Methods

Clinical Study

Patients with first anterior STEMI presenting early (<6 hours) and undergoing primary angioplasty were recruited within the METOCARD-CNIC trial.[13,14] A prespecified analysis within this trial was the study of the association between cTnI/total CK and CMR-measured LVH, IS, and LVEF. Inclusion/exclusion criteria can be found elsewhere.[15] Serial cTnI and total CK measurements were taken in 140 patients, and data from these patients were used for the current analysis. All patients underwent CMR studies at 5 to 7 days (1 week)[13] and 6 months[14] after STEMI. This study was approved by the ethics committee, and patients signed informed consent.

CMR protocol

A detailed description of the CMR protocol and methods for imaging analysis has been reported elsewhere[15] and is detailed below. A comprehensive CMR study was performed with dedicated sequences to evaluate cardiac function and myocardial necrosis. Scans were performed with a 3.0-T magnet (Achieva Tx; Philips Medical Systems, Best, the Netherlands), with vectorcardiographic gating and a dedicated cardiac 32-channel phased-array surface coil. All sequences were acquired during expiration breath-hold mode. After standard localizer scan, contiguous short-axis slices were acquired to cover the whole LV. For functional cine imaging, we first ran a balanced turbo field echo steady-state free precession (SSFP) with a sensitivity encoding fast parallel imaging technique sequence. Typical parameters were voxel size 1.6×2 mm, slices 13, slice thickness 8 mm, gap 0 mm, cardiac phases 30, repetition time (TR) 3.5 ms, echo time (TE) 1.7 ms, flip angle (FA) 40°, sensitivity encoding 1.5, averages 1, and field of view (FOV) 360×360 mm. Delayed enhancement images to assess necrotic myocardium were acquired with a T1-weighted two-dimensional (2D) segmented inversion recovery turbo field echo (2D IR-TFE) sequence performed 10 to 15 minutes after intravenous administration of 0.20 mmol of gadopentate dimeglumine contrast agent (Magnevist; Schering AG, Berlin, Germany) per kg body weight.[16] The delayed enhancement images were thus acquired in short-axis slices that matched function imaging and had the following parameters: voxel size 1.5×1.5 mm; slices 13; slice thickness 8 mm; gap 0; TR 6.1; TE 3.0; inversion time 250 to 350 (optimized to null normal myocardium); FA 25°; TFE factor 20; averages 1; and FOV 360×360 mm.

CMR data analysis

Blinded analyses were undertaken by the core laboratory at the Centro Nacional de Investigaciones Cardiovasculares Carlos III (CNIC). Data were quantified with dedicated software (QMass MR 7.5; Medis, Leiden, the Netherlands). LV mass, LVEF, and extent of necrosis were determined. LV mass was normalized to body surface area according to Du Bois' formula.[17] Myocardial necrosis (IS), expressed as a percentage of LV mass (the gold standard for IS quantification), was defined according the extent of delayed gadolinium enhancement.[18]

Measurement of cTnI and total CK

Blood samples (3 mL) were taken from a peripheral vein into clot activator tubes for serum total CK analysis and into lithium-heparin tubes for analysis of plasma cTnI. Samples were prepared from blood by centrifugation following standard procedures. Total-CK was assessed with a standard enzymatic method on an Olympus AU2700 analyzer (Beckman Coulter Clinical Diagnostics, Nyon, Switzerland). cTnI was assessed by a chemoluminescence immunoassay on a Dimension Vista system (Siemens Healthcare Diagnostics, Deerfield, IL) or the AccuTnI paramagnetic chemoluminescence immunoassay on an Access-2 analyzer (Beckman Coulter Clinical Diagnostics) with reagents provided by the manufacturer. Blood samples for biomarkers were obtained on admission, every 4 hours during the first 12 hours post-STEMI, and then every 12 hours up to 72 hours post-STEMI.

Animal Study

Experimental procedures were performed in castrated male Large-White pigs. The study protocol was approved by the institutional animal research committee and conducted in accord with recommendations of the Guide for the Care and Use of Laboratory Animals.

Generation of pressure-overload LVH

Pressure-overload LVH was induced in 10 four-week-old Large-White pigs (10 to 14 kg) by surgical banding of the ascending aorta. Sedation was induced by intramuscular injection of ketamine (20 mg/kg), xylazine (2 mg/kg), and midazolam (0.5 mg/kg) and then maintained with sevoflurane. Continuous intravenous infusion of fentanyl served as an analgesic during surgery and a single dose of prophylactic antibiotic with cefuroxime was administered just before the procedure. Mechanical endotracheal ventilation was controlled by external respirator. A minimally invasive right lateral thoracotomy was performed in the fourth intercostal space. Through a small pericardiotomy, the ascending aorta was constricted ≈3 cm above the aortic valve with a rigid polyethylene band adjusted to 70% of the measured perimeter of the aorta. In all cases, the band was tied to fit snugly around the aorta, but did not create a palpable thrill. The small pericardiotomy was left open, the pneumothorax evacuated with a chest tube, and the chest wall and skin incisions were closed. After surgery and before the animals recovered from anesthesia, intramuscular (0.01 mg/kg) buprenorphine was administered as a postoperative analgesia. In 8 sham-operated animals, the same procedure was followed, but the band was not tightened. All animals were returned to the farm to grow for an average of 16 weeks before myocardial infarction (MI) procedure.

MI procedure

AMI was induced in all pigs 4 to 5 months after surgery when animals reached a weight of 60 to 70 kg. The protocol of AMI induction has been detailed elsewhere.[19,20] In summary, anesthesia was induced in all animals as described above and maintained by continuous intravenous infusion of ketamine (2 mg/kg/h), xylazine (0.2 mg/kg/h), and midazolam (0.2 mg/kg/h). All animals were intubated and mechanically ventilated with oxygen (fraction of inspired O_2: 28%). Central venous and arterial lines were placed and a single bolus of unfractioned heparin (300 mg/kg) was administered immediately before introduction of the catheter. A continuous infusion of amiodarone (300 mg/h) was maintained during the procedure in all pigs to prevent malignant ventricular arrhythmias. The left anterior descending coronary artery immediately distal to the origin of the first diagonal branch was occluded for 60 minutes with an angioplasty balloon introduced with a catheter inserted by the percutaneous femoral route. Balloon location and state of inflation were monitored angiographically. After balloon deflation, a coronary angiogram was recorded to confirm patency of the coronary artery. In cases of ventricular fibrillation, a biphasic defibrillator was used to deliver nonsynchronized shocks. During their recuperation, animals were cared for by dedicated veterinarians and technicians at the CNIC.

CMR protocol

A baseline CMR scan was performed in each pig immediately before AMI induction to assess baseline LV mass and LVEF. A second CMR study was performed 7 days after AMI in order to assess IS and LV performance. Pigs were anesthetized by intramuscular injection of ketamine, xylacine, and midazolam as described above, and anesthesia was maintained by continuous intravenous infusion of midazolam (0.2 mg/kg/h). All studies were performed using a Philips 3-Tesla Achieva Tx whole-body scanner (Philips Medical Systems) equipped with a 32-element cardiac phased-array surface coil. To evaluate global LV motion, segmented cine SSFP sequences were performed to acquire 13 to 15 contiguous short-axis slices covering the heart from the base to the apex (FOV of 280×280 mm; slice thickness of 8 mm without gap; TR 2.8 ms; TE 1.4 ms, FA 45°; cardiac phases 25; voxel size 1.8×1.8 mm; and 3 NEX [number of excitations]). Delayed enhancement imaging of infarct size was performed 10 to 15 minutes after intravenous administration of 0.20 mmol of gadopentate dimeglumine contrast agent per kg of body weight[16] using an inversion-recovery spoiled turbo field echo sequence (FOV of 280×280 mm; 13 to 15 short-axis slices with a thickness of 8 mm and no gap; TR 5.6 ms; TE 2.8 ms; voxel size 1.6×1.6 mm; time interval optimized to null normal myocardium; trigger delay longest; bandwidth, 304 Hz per pixel; and 2 NEX).

CMR data analysis

All CMR images were analyzed using dedicated software (QMass MR 7.5; Medis) by 2 observers experienced in CMR analysis and blinded to the LVH induction procedure. LV cardiac borders were traced in each cine image to obtain LV end-diastolic volume (LVEDV), end-systolic volume (LVESV), and LVEF. In the tracing convention used, the papillary muscles were included as part of the LV cavity volume. LVEDV and LVESV were determined using a summation of disks ("Simpson's rule") method. Ejection fraction (EF) was computed as EF=(LVEDV−LVESV)/LVEDV. LV epicardial borders were also traced on the end-diastolic images, with LV mass computed as the end-diastolic myocardial volume (ie, the difference between the epicardial and endocardial volumes)

multiplied by myocardial density (1.05 g/mL). Values of LV volume and LV mass normalized to body surface area were calculated with Brody's formula.[21] Myocardial necrosis (IS), expressed as a percentage of LV mass (the gold standard for IS quantification), was defined according the extent of delayed gadolinium enhancement.[18] Necrosis was identified as hyperintense regions, defined as >50% of maximum myocardial signal intensity (full width at half maximum), with manual adjustment when needed. If present, a central core of hypointense signal within the area of increased signal was included in the late gadolinium enhancement analysis.

Measurement of cTnI and total CK

Blood samples (3 mL) were taken from the femoral vein into clot activator tubes for serum total CK analysis and into lithium-heparin tubes for analysis of plasma cTnI. Samples were prepared from blood by centrifugation separation. Total CK was measured by an enzymatic method, according to the manufacturer's recommendations, and cardiac TnI was assayed using an automated colorimetric immunoassay with reagents provided by the manufacturer. Both biomarkers were determined on a Dimension RxL Max system (Siemens Healthcare Diagnostics). Blood samples for biomarker measurement were obtained from a femoral vein at baseline (before AMI procedure), minute 0 (just before coronary occlusion), minute 60 (immediately before reperfusion), and every hour over 6 hours following reperfusion.

Immunofluorescence Analysis of cTnI in Myocardial Tissue Samples

MI greatly influences myocardial protein tissue content,[22] prompting us to measure myocardial tissue content of cTnI in an additional set of 8 pigs (n=4 banded-LVH; n=4 sham-operated controls). When they reached the target weight (60 to 70 kg), these pigs underwent the baseline CMR scan and were sacrificed (they did not undergo AMI induction). Myocardial samples were collected within minutes of euthanasia from the anterior and posterolateral mid-ventricular wall, fixed in formalin, embedded in paraffin, and analyzed by immunofluorescence to measure expression of cTnI and cardiomyocyte perimeter. A detailed description is given below.

Heart samples from banded LVH (n=4) and normal pigs (n=4) were fixed in 10% formalin at 4°C for 24 hours and embedded in paraffin. For epitope unmasking, heart sections (5 μm) were treated with 10 mmol/L of trisodium citrate 0.05% Tween 20 (pH 6.0) for 3 minutes at 125°C. Sections were then permeabilized with 0.25% Triton X-100 in PBS for 10 minutes and blocked with 2% BSA in PBS (blocking buffer) for 1 hour at room temperature. Blocked sections were incubated with a mouse monoclonal anti-cardiac troponin I antibody (2 μg/mL, ab19615; Abcam, Cambridge, MA) or control mouse IgG (sc2025; Santa Cruz Biotechnology, Santa Cruz, CA) in blocking buffer for 2 hours at room temperature. After incubation with secondary anti-mouse Alexa-647 antibody (Invitrogen, Carlsbad, CA) for 45 minutes at room temperature, sections were stained with fluorescein isothiocyanate-conjugated lectin from wheat (FITC-WGA; 100 μg/mL in PBS, L-4895; Sigma-Aldrich, St. Louis, MO) overnight at 4°C to delineate the perimeter of cardiomyocytes. Finally, nuclei were stained by incubating slides with 4′,6-diamidino-2-phenylindole, and slides were mounted with Mowiol-Dabco mounting medium. Images were captured with a fluorescence confocal microscope (Leica SPE, DM 2500; Leica Microsystems, Buffalo Grove, IL) fitted with an ×40 objective. ImageJ software (National Institutes of Health, Bethesda, MD) was used to quantify mean fluorescence intensities corresponding to cTnI and cardiomyocyte cross-sectional area. The captured images of 20 random fields in a section from each pig (4 pigs per group) were quantified, and an average value was calculated for each pig.

Statistical Analysis

For quantitative variables, data are expressed as mean±SD and compared by parametric methods. Non-normal data are reported as medians and interquartile range (IQR) and were compared by nonparametric methods. Owing to the small sample size in the experimental study, all data were compared using nonparametric methods irrespective of the normality test. For categorical data, percentages were compared using exact methods.

Multiple linear regression analysis was used to study the influence of indexed LV mass on total CK and cTnI values, adjusted for infarct size measured by CMR. Variance of data on peak and AUC of total CK and cTnI release tends to be proportional to the mean; therefore, we used a square-root transformation for these variables when included in the regression analysis. Indexed LV mass was analyzed either as a continuous or as a categorical variable. For the experimental study, pigs were categorized according the presence or absence of LVH (yes/no) at baseline (before MI), which perfectly coincided with banding or sham operation, respectively. In the clinical study, patients were classified into 3 categories (LVH tertiles) according to indexed LV mass and sex.[23] Nonparametric ROC (receiver operating characteristic) curve analyses were performed in the clinical study to assess the discriminatory capacity of AUC of cTnI and total CK to predict LV dysfunction at 1 week and 6 months after STEMI. In addition, several predictive multiple regression models were estimated based on our human data to correct infarct sizing for troponin when LVH is present (upper tertile of indexed LV mass), being the final model selected according to

parsimonious criteria and predictive capacity. All statistical analyses were performed using commercially available software (Stata 12.0; StataCorp LP, College Station, TX).

Results

Clinical Study

Baseline characteristics and CMR data are presented in Table 1. Patients in the upper LVH tertile showed a ≈50% higher CMR-measured absolute and indexed LV mass, compared with those in the lower LVH tertile (Figure 1). Infarct size (% of LV mass) and LVEF on 1-week CMR did not differ between the lower and upper LVH tertiles (Figure 2).

Peak cTnI (median [IQR]) was 154.0 ng/mL (90.4 and 266.3 ng/mL) in the upper LVH tertile versus 98.1 ng/mL (36.2 and 191.3 ng/mL) in the lower LVH tertile (P=0.02; Figure 3A). AUC of cTnI (median [IQR]) was 3640 ng/mL (2335 and 5143 ng/mL) in the upper LVH tertile versus 2539 ng/mL (995 and 4616 ng/mL) in the lower LVH tertile (P=0.03; Figure 3B). In contrast, no significant differences were found in peak and AUC of total CK between the upper and lower LVH tertiles (Figure 4). Biomarker release data in the 3 population tertiles are summarized in Table 2.

In the regression analysis, higher LV mass was associated with significantly higher peak and AUC cTnI, after adjustment for IS evaluated by the gold standard (% of LV mass on 1-week CMR). This difference was observed both when indexed LV mass was categorized (upper versus lower LVH tertiles; P=0.009 and P=0.01 for peak and AUC cTnI, respectively; Figure 5A and 5B) and when it was evaluated as a continuous variable (P<0.001 and P=0.003 for peak and AUC cTnI, respectively; see Table 3). In contrast, indexed LV mass showed no significant association with peak or AUC of total CK, either when it was categorized or when it was evaluated as a continuous variable.

The discriminatory capacity of AUC of cTnI to predict post-STEMI LV dysfunction (LVEF ≤40%) on 1-week CMR was significantly worse for patients with LVH (upper LVH tertile, 0.71; 95% confidence interval [CI], 0.55 to 0.87; lower LVH tertile, 0.92; 95% CI, 0.84 to 0.99; P=0.02; Figure 6A). A sensitivity analysis using other clinically relevant LVEF cutoffs showed similar results (Figure 6B). AUC of cTnI was similarly poor at predicting long-term (6 months post-STEMI) severe

Table 1. Characteristics and Cardiac Magnetic Resonance Data in the Clinical Study

	Lower Tertile of Indexed LV Mass (n=47)	Middle Tertile of Indexed LV Mass (n=46)	Upper Tertile of Indexed LV Mass (n=47)	*P* Value*	*P* Value†
Age, y	58.7 (11.9)	59.7 (12.0)	56.7 (10.6)	0.45	0.23
Male, %	89.4	89.1	89.4	1.00	1.00
Hypertension, %	40.4	45.7	31.9	0.41	0.40
Dyslipidemia, %	53.2	44.4	36.2	0.26	0.15
Diabetes, %	12.8	30.4	14.9	0.08	1.00
Smoking (active), %	51.1	50.0	55.3	0.91	0.84
Body mass index, kg/m^2	27.9 (3.1)	28.3 (3.7)	28.0 (4.4)	0.86	0.94
Body surface area, m^2	1.93 (0.15)	1.90 (0.14)	1.89 (0.17)	0.40	0.20
Symptom-onset-to-balloon time, minute	190.8 (61.1)	186.0 (57.7)	212.7 (77.3)	0.12	0.13
TIMI grade 3 post-PTCA, %	68.1	69.6	76.6	0.67	0.49
Prereperfusion i.v. metoprolol, %	46.8	54.3	44.7	0.49	1.00
LV mass, g	93.1 (12.9)	110.1 (13.6)	136.6 (22.2)	<0.0001	<0.0001
Indexed LV mass, g/m^2	48.1 (5.1)	57.7 (4.5)	72.3 (10.9)	<0.0001	<0.0001
Infarct size (% of LV) at day 5 to 7	21.4 (12.6)	19.7 (11.1)	23.0 (10.7)	0.37	0.52
LVEF (%) at day 5 to 7	44.4 (9.7)	47.4 (9.4)	44.2 (7.3)	0.17	0.92
LVEF (%) at 6 months	47.18 (10.85)	50.8 (10.0)	46.48 (9.90)	0.11	0.75

Continuous variables are reported as means (SD) and compared by parametric methods (1-way ANOVA for comparison between all tertiles, and 2-tailed Student *t* test for comparison between upper and lower tertile of indexed LV mass). Categorical variables are reported as percentages and compared by Fisher's exact test. LV indicates left ventricle; LVEF, left ventricular ejection fraction; PTCA, percutaneous transluminal coronary angioplasty; TIMI, thrombolysis in myocardial infarction.

*P value for comparison between all tertiles.

†P value for comparison between upper and lower tertile of indexed LV mass.

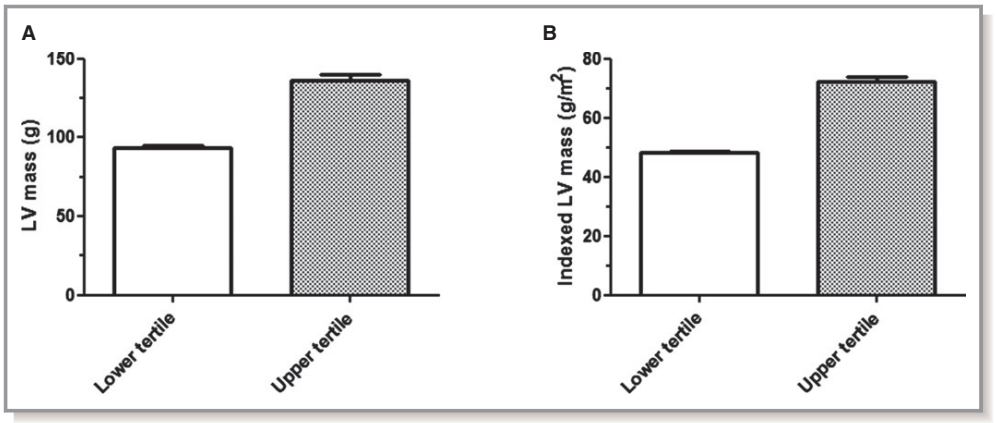

Figure 1. Left ventricular mass differences in patients presenting with STEMI. Patients in the upper tertile showed ≈50% higher absolute LV mass (A) and indexed LV mass (B): 136.6±22.2 g and 72.3±10.9 g/m^2 in the upper tertile versus 93.1±12.9 g and 48.1±5.1 g/m^2 in the lower tertile, respectively (P<0.0001 for both comparisons). Bars represent mean and SEM. LV indicates left ventricular; STEMI, ST-segment elevation myocardial infarction.

LVEF depression (≤35%) for patients with LVH (upper LVH tertile, 0.74; 95% CI, 0.59 to 0.90; lower LVH tertile, 0.92; 95% CI, 0.84 to 1.00; P=0.04). In contrast, the discriminatory capacity of AUC of total CK to predict LV dysfunction did not differ significantly between LVH tertiles at any cutoff or time point.

Animal Study

Six pigs (4 of 10 banded, and 2 of 8 sham-operated) died during AMI induction as a result of refractory ventricular fibrillation. The final population for analytical purposes was thus 12 pigs (6/group). Baseline characteristics and CMR data are presented in Table 4. Banded pigs had ≈30% higher absolute and indexed LV mass (Figure 7). Infarct size (% of LV mass) and LVEF on day 7 CMR did not differ between banded and sham-operated groups (Figure 8).

Peak cTnI (median [IQR]) was 183.4 ng/mL (171.4 and 194.3 ng/mL) in the banded group versus 153.1 ng/mL (132.6 and 169.7 ng/mL) in sham-operated controls (P=0.04; Figure 9A). AUC of cTnI (median [IQR]) was 55 230 ng/mL (52 537 and 57 598 ng/mL) in the banded group versus 45 817 ng/mL (41 998 and 50 365 ng/mL) in sham-operated controls (P=0.04; Figure 9B). In contrast, peak and

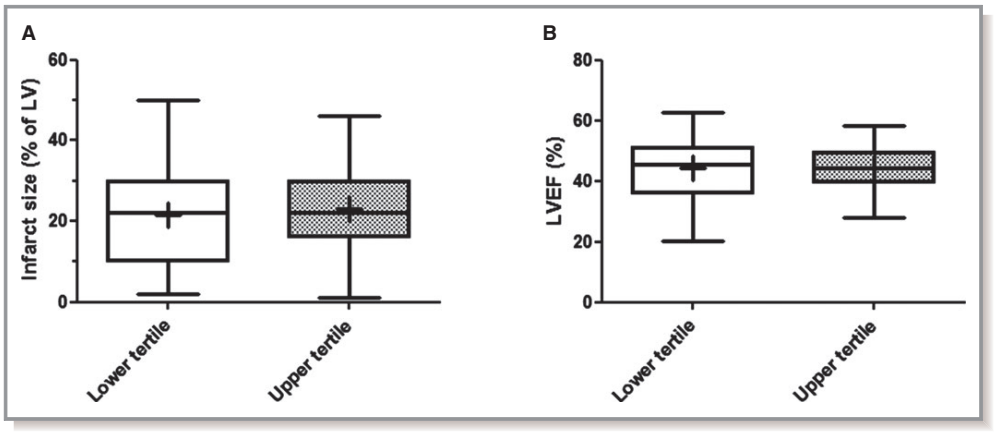

Figure 2. Distributional plots of infarct size (A) and left ventricular ejection fraction (B) measured by magnetic resonance in STEMI patients 1 week after infarction and classified in upper and lower tertiles of indexed LV mass. No between-tertile differences were detected: infarct size 23.0±1.6% in the upper LVH tertile versus 21.4±1.8% in the lower tertile; LVEF 44.2±1.1% in the upper tertile versus 44.4±1.4% in the lower tertile (P>0.50 for both comparisons). Box plots show median values and interquartile range (Tukey's method); crosses represent mean values. LV indicates left ventricular; LVEF, LV ejection fraction; LVH, LV hypertrophy; STEMI, ST-segment elevation myocardial infarction.

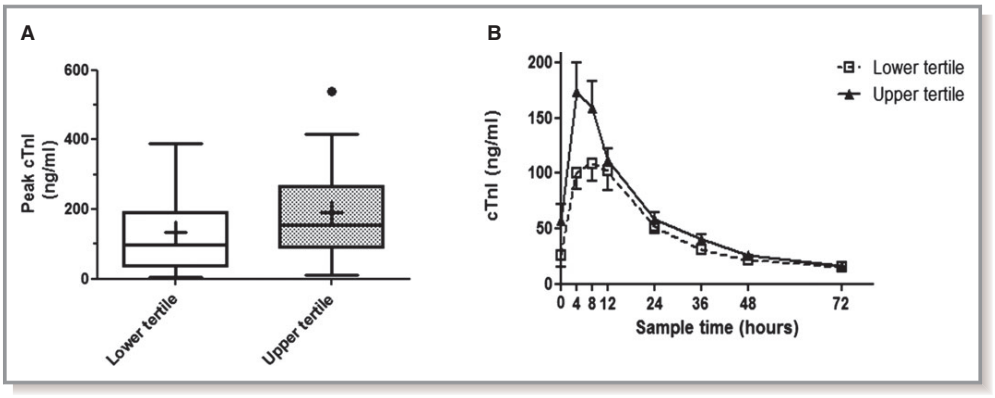

Figure 3. Differences in peripheral blood concentrations of cTnI between lower and upper tertiles of indexed LV mass in patients presenting with STEMI. A, Box plots of peak cTnI, showing median values and interquartile range (Tukey's method); crosses represent mean values. B, Time profile of cTnI readings after STEMI (mean±SEM). cTnI indicates cardiac troponin I; LV, left ventricular; STEMI, ST-segment elevation myocardial infarction.

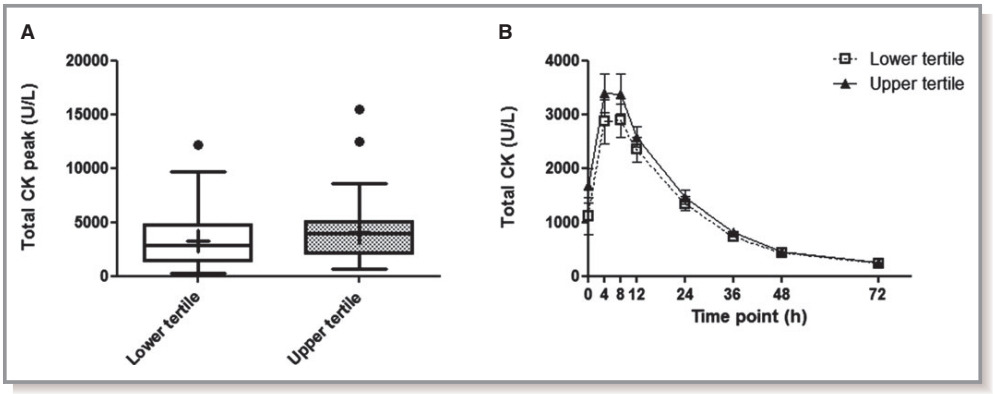

Figure 4. A, Peak total CK in STEMI patients in the lower and upper LVH tertiles in the clinical study. Box plots show median values and interquartile range (IQR; Tukey's method) of total CK; crosses represent mean values. The median (IQR) of the peak in the upper tertile was 4003 (2064 to 5065) versus 2829 UI/L (1348 to 4720) in the lower tertile (P>0.10). B, AUC of total CK in the lower and upper LVH tertiles. Data are presented as mean±SEM. The median (IQR) AUC of total CK in the upper tertile was 67 841 (40 759 to 99 692) versus 54 365 UI/L (28 573 to 83 894) in the lower tertile (P>0.10). AUC indicates area under the curve; CK, creatine kinase; LVH, left ventricular hypertrophy; STEMI, ST-segment elevation myocardial infarction.

AUC of total CK did not differ significantly between banded and sham-operated groups.

In the regression analysis, higher LV mass was associated with a significantly higher peak and AUC cTnI, after adjustment for IS evaluated by the gold standard (% of LV mass on day 7 CMR). This difference was observed both when indexed LV mass was categorized (yes/no; P<0.001 and P=0.001 for peak and AUC cTnI, respectively; Figure 10A

Table 2. Biomarker Release Data in the Clinical Study

	Lower Tertile of Indexed LV Mass (n=47)	Middle Tertile of Indexed LV Mass (n=46)	Upper Tertile of Indexed LV Mass (n=47)
Peak of cTnI, ng/mL	98.1 (36.2 to 191.3)	98.3 (29.4 to 200.3)	154.0 (90.4 to 266.3)
AUC of cTnI, ng/mL	2539 (995 to 4616)	2021 (741 to 4913)	3640 (2335 to 5143)
Peak of total CK, UI/L	2829 (1348 to 4720)	2176 (897 to 4471)	4003 (2064 to 5065)
AUC of total CK, UI/L	54 365 (28 573 to 83 894)	45 573 (21 230 to 74 260)	67 841 (40 759 to 99 692)

Data are presented as median (interquartile range). Data are not adjusted by actual infarct size as measured by cardiac magnetic resonance. AUC indicates area under the curve; CK, creatine kinase; cTnI, cardiac troponin I; LV, left ventricle.

A

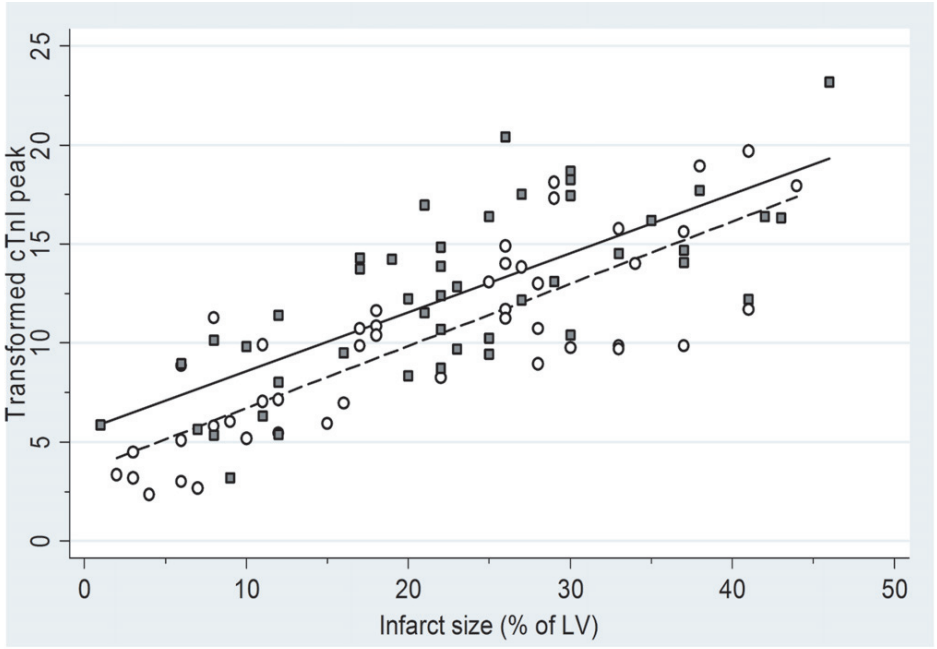

B

	Transformed mean		Adjusted difference (1)		
	Lower tertile(2)	Upper tertile (3)	Difference	95% CI	p-value
Peak of cTnI	10,46	12,87	1,87	0,47-3,27	0,009
AUC of cTnI	50,15	59,48	6,84	1,66-12,02	0,011

(1)Difference in transformed peak and AUC of cTnI between tertiles, adjusted for infarct size as assessed by the gold standard (% of LV mass on one-week CMR); (2) Lower tertile of indexed LV mass; (3) Upper tertile of indexed LV mass .

Figure 5. A, Scatter plots and fitted values of transformed (square-root) peak cTnI in STEMI patients versus infarct size evaluated by the gold standard (% of LV mass on 1-week CMR). Plots are shown for patients in the lower tertile of indexed LV mass (white circles and dash line) and in the upper tertile (gray squares and solid line). B, Differences in transformed peak and AUC of cTnI between the upper and lower indexed LV mass tertiles, adjusted for infarct size as assessed by the CMR gold standard. AUC indicates area under the curve; CI, confidence interval; CMR, cardiac magnetic resonance; cTnI, cardiac troponin I; LV, left ventricle; STEMI, ST-segment elevation myocardial infarction.

and 10B) and when it was evaluated as a continuous variable (*P*=0.023 and *P*=0.035 for peak and AUC cTnI, respectively; see Table 5). In contrast, indexed LV mass showed no significant association with peak or AUC of total CK, either when it was categorized or when it was evaluated as a continuous variable.

Table 3. Elevated LV Mass in STEMI Patients in the Clinical Study Is Significantly Associated With High Peak and AUC of cTnI, After Adjustment for Infarct Size

	Adjusted Difference	95% CI	*P* Value
Transformed peak of cTnI	0.87	0.41 to 1.33	<0.001
Transformed AUC of cTnI	2.59	0.87 to 4.30	0.003

The table shows adjusted differences in transformed peak and transformed AUC of cTnI for every 10-g/m^2 increase in indexed LV mass, adjusted for infarct size as assessed by the gold standard (% of LV mass on 1-week CMR). AUC indicates area under the curve; CI, confidence interval; CMR, cardiac magnetic resonance; cTnI, cardiac troponin I; LV, left ventricle; STEMI, ST-segment elevation myocardial infarction.

A

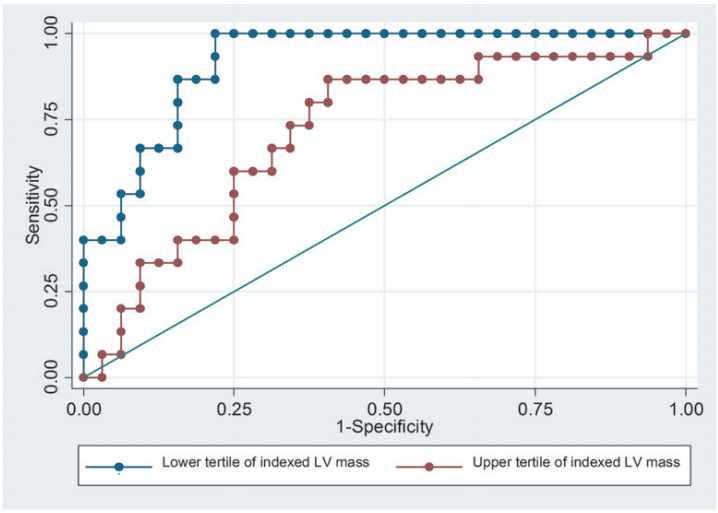

B

	Lower tertile of indexed LV mass		Upper tertile of indexed LV mass		
Cut-off point	ROC area	Asymptotic 95% CI	ROC area	Asymptotic 95% CI	P value
LVEF ≤ 35%	0.95	0.90-1.00	0.62	0.29-0.95	0.047
LVEF ≤ 40%	0.92	0.84-0.99	0.71	0.55-0.87	0.023
LVEF ≤ 50%	0.96	0.92-1.00	0.73	0.53-0.94	0.030

Figure 6. A, Discriminatory capacity of AUC of cTnI to predict LV dysfunction (LVEF ≤40%) on 1-week CMR in STEMI patients in the lower and upper indexed LV mass tertiles. B, Sensitivity analysis performed according to clinically relevant LVEF cut-offs. AUC indicates area under the curve; CI, confidence interval; CMR, cardiac magnetic resonance; cTnI, cardiac troponin I; LV, left ventricle; LVEF, LV ejection fraction; ROC, receiver operating characteristic; STEMI, ST-segment elevation myocardial infarction.

Histological evaluation showed that ventricular cardiomyocytes from banded pigs were significantly larger than those of sham-operated pigs (P=0.021; Figures 11 and 12A). Quantification of total cTnI per cardiomyocyte on immunostained sections revealed significantly higher cTnI content per cell in banded pigs (P=0.043; Figures 11 and 12B).

Discussion

The present study shows that, for a given infarct size determined by CMR, peak and AUC of cTnI are unusually high in patients with LVH and in pigs with induced LVH. In contrast, LVH had no effect on peak or AUC of total CK.

Table 4. Characteristics and Cardiac Magnetic Resonance Data of the Animal Study Population

	Sham-Operated Group (n=6)	Banded Group (n=6)	*P* Value
Weight, kg	63.8 (6.1)	66.9 (2.8)	0.23
Body surface area, m^2	1.12 (0.07)	1.16 (0.03)	0.23
LV mass, g	81.7 (8.3)	107.4 (16.7)	0.004
Indexed LV mass, g/m^2	72.9 (3.4)	92.8 (13.8)	0.004
Baseline LVEF, %	54.9 (5.2)	57.6 (3.9)	0.42
Infarct size (% of LV)	27.8 (5.0)	25.0 (3.3)	0.42
LVEF (%) at day 7	38.2 (8.0)	39.7 (6.3)	0.87

Continuous variables are reported as means (SD) and compared by a nonparametric test (Wilcoxon's rank-sum test). LV indicates left ventricle; LVEF, left ventricular ejection fraction.

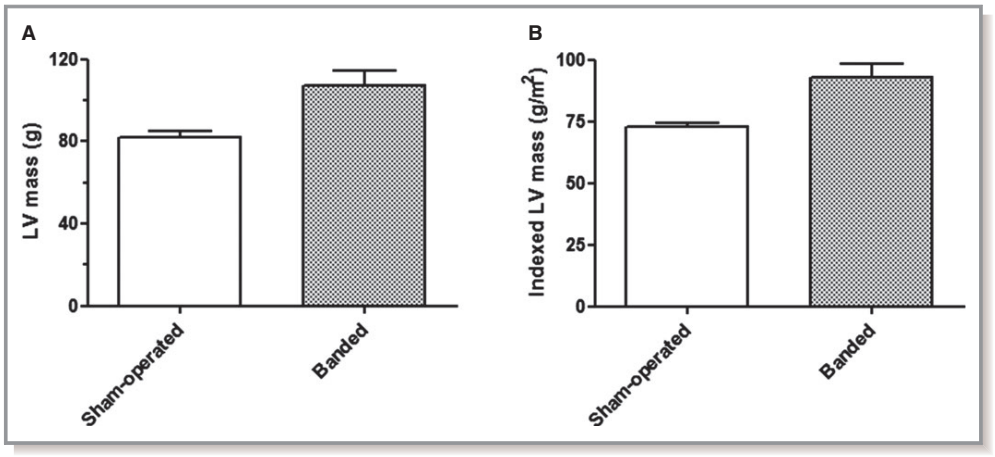

Figure 7. LV mass differences between sham-operated pigs and pigs with banding of the aorta to induce LVH. Absolute (A) and indexed (B) LV mass were ≈30% higher in the banded pigs: 107.4±16.7 g and 92.8±13.8 g/m^2 in the banded group versus 81.7±8.3 g and 72.9±3.4 g/m^2 in the sham-operated group (P<0.01 for both comparisons). Bars represent mean and SEM. LV indicates left ventricle; LVH, left ventricular hypertrophy.

ROC analysis shows that cTnI release during a STEMI is a less-accurate predictor of short- and long-term LV impairment in the presence of LVH. Moreover, cardiomyocytes from pigs with LVH have a higher cTnI content compared with cardiomyocytes from nonhypertrophied hearts. The same findings were consistently found in patients enrolled in a contemporary clinical trial and in a controlled large-animal study.

Quantification of the extent of myocardial necrosis after STEMI is of clinical and research interest. CMR has become the gold standard for accurate in vivo quantification of IS.[1] However, CMR is not widely available and is logistically challenging. Biomarkers of cardiac damage released to the systemic circulation after STEMI have, for many years, been used as surrogate markers of IS. For several decades, peak and AUC of total CK was the preferred biomarker. The more specific cardiac troponins were introduced later and are increasingly used. Peak and AUC of total CK and cTnI have been shown to correlate well with IS measured by gold-standard techniques. Owing to their cardiac specificity, troponins have become the reference biomarker for estimating IS and thus for predicting long-term clinical outcomes

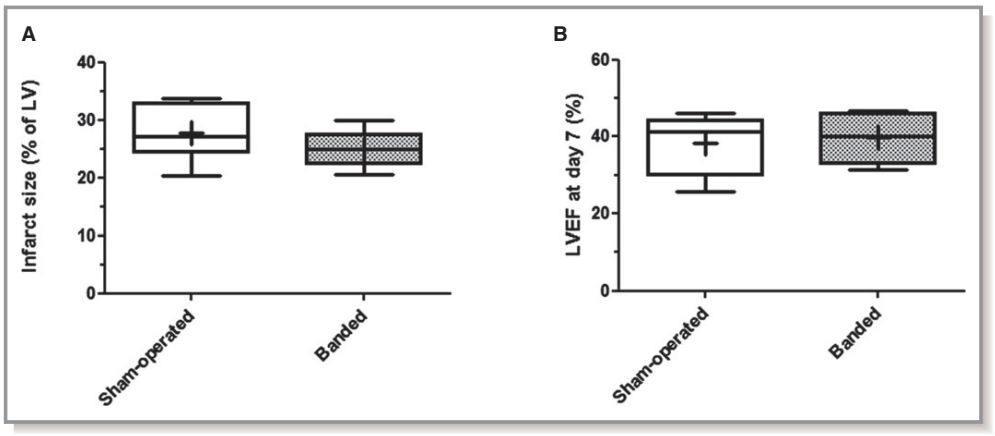

Figure 8. Distributional plots of infarct size (A) and LVEF (B) measured by magnetic resonance in sham-operated and banded pigs 1 week after infarction. No differences were detected between groups for either parameter: infarct size, 25.0±3.3% banded versus 27.8±5.0% sham-operated; LVEF, 39.7±6.3% banded versus 38.2±8.0% sham-operated (P>0.40 for both comparisons). Box plots show median values and interquartile range (Tukey's method); crosses represent mean values. LV indicates left ventricle; LVEF, LV ejection fraction.

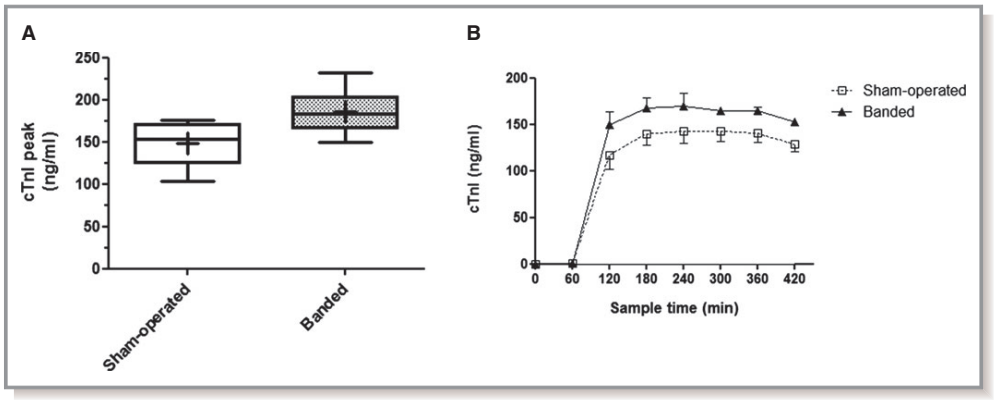

Figure 9. Postinfarction differences in peripheral blood concentrations of cTnI between sham-operated and pigs with banding of the aorta to induce LVH. A, Box plots of peak cTnI, showing median values and interquartile range (Tukey's method); crosses represent mean values. B, Time profile of cTnI readings after induced MI (mean±SEM). cTnI indicates cardiac-troponin I; LVH, left ventricular hypertrophy; MI, myocardial infarction.

after STEMI,[4,24] and, consequently, many experimental studies and clinical trials use cardiac troponins as the primary outcome measure.[8,25,26] It is therefore important to identify confounders that affect the release and quantification of cardiac troponins. Given the high prevalence of LVH in the general population (20% to 25%),[11,12] and especially in the MI population (50%),[27] it is of great importance to know whether LV mass affects the systemic release of biomarkers after an AMI. Notably, stratification according to hypertension—the most frequent cause of LVH—may be insufficient to control the effect of LV mass on biomarker release, given that approximately one third of patients with hypertension are unaware that they are hypertensive.[28]

Our analysis of total CK and cTnI showed that whereas hypertrophied hearts release more cTnI than control hearts upon AMI, hypertrophy does not affect total CK release. The CK system is important for intracellular energy production and utilization and is abundantly present in tissues with high metabolic demand. There are 4 electrophoretically distinct CK isoenzymes—BB, MB, MM, and the mitochondrial forms (mi-CK)—with CK-MB predominating in the adult heart.[29] Animal models of LVH consistently show that hypertrophic cardiomyocytes switch to a fetal CK isoenzyme pattern, increasing expression of CK-MB and CK-BB at the expense of reduced expression of CK-MM and mi-CK in order to increase energy yield; these changes balance out so that total CK levels in the hypertrophied myocardium are unaltered.[30–35] In contrast, it is intuitive to argue that cardiomyocyte content of troponin would increase with hypertrophy as part of the general increase in cardiomyocyte content of contractile units and associated contractile proteins. Thus, in the setting of LVH, the release of troponins will be disproportionally high after STEMI, whereas total CK release will not be affected. Regarding this specific issue, we estimated a final predictive model to correct infarct sizing for troponin when LVH is present. Thus, it was estimated that, in patients with LVH (upper tertile of indexed LV mass), peak of cTnI overestimates infarct size by 30%, as measured on CMR. Most research on the CK system took place in the 1980s and 1990s, when the troponins were still

Table 5. Experimentally Increased LV Mass in Pigs Is Significantly Associated With High Peak and AUC of cTnI, After Adjustment for Infarct Size

	Adjusted Difference	95% CI	*P* Value
Transformed peak of cTnI	0.67	0.12 to 1.22	0.023
Transformed AUC of cTnI	9.62	0.82 to 18.42	0.035
Transformed peak of total CK	2.72	−27.06 to 32.51	0.841
Transformed AUC of total CK	72.18	−446.31 to 590.68	0.760

On the other hand, increased LV mass in pigs is not associated with higher peak and AUC of total CK. The table shows adjusted differences in transformed peak and transformed AUC of cTnI and total CK for every 10-g/m^2 increase in indexed LV mass, adjusted for infarct size as assessed by the gold standard (% of LV mass on 1-week CMR). AUC indicates area under the curve; CK, creatine kinase; CMR, cardiac magnetic resonance; cTnI, cardiac troponin I; LV, left ventricle.

A

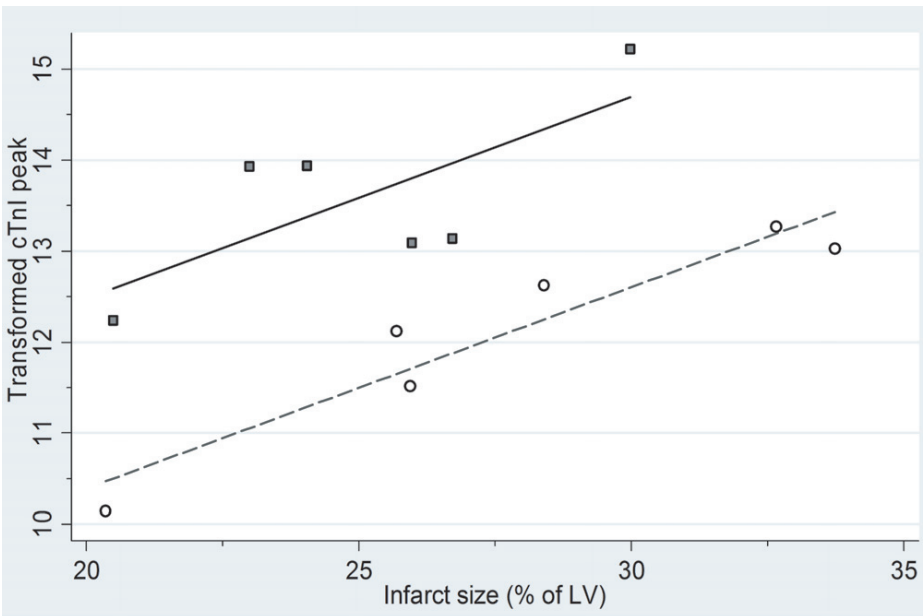

B

	Transformed mean		Adjusted difference (1)		
	Sham	Banded	Difference	95% CI	p-value
Peak of cTnI	12,12	13,59	2,09	1,26- 2,92	<0,001
AUC of TnI	211,01	231,51	30,60	16,32- 44,87	0,001

(1) Difference in transformed peak and AUC of cTnI between sham-operated and banded pigs, adjusted for infarct size as assessed by the gold standard (% of LV mass on one-week CMR).

Figure 10. A, Scatter plots and fitted values of transformed (square-root) peak postinfarction cTnI versus infarct size evaluated by the gold standard (% of LV mass on 1-week CMR). Plots are shown for sham-operated (white circles and dash line) and banded pigs (gray squares and solid line). B, Differences in transformed peak and AUC of cTnI between sham-operated and banded pigs, adjusted for infarct size as assessed by the CMR gold standard. AUC indicates area under the curve; CI, confidence interval; CMR, cardiac magnetic resonance; cTnI, cardiac-troponin I; LV, left ventricle.

unknown. The subsequent development of specific methods to accurately quantify troponins has established the use of this biomarker, and the high sensitivity and specificity of troponins for detecting even mild cardiac damage has represented a big step forward in the early triage of patients with chest pain. The influence of LVH on cTnI release after myocardial damage reported here does not invalidate the use of troponins as surrogate markers, but shows the need to take LV mass into account as an important potential confounding factor in clinical and research evaluations. These considerations could be especially important in determining the significance of small increases in circulating troponin in patients presenting to the emergency department, given that troponin readings in patients with LVH may give a false-positive diagnosis of MI.[36] In this regard, mild increases in troponin-I[37–40] or troponin-T[41] have been reported in patients with LVH in the absence of chest pain or any other acute condition. In addition, it has been recently reported that cardiac troponin concentrations correlate with LV mass index independent of coronary artery disease status in patients with aortic valve stenosis.[42,43] Presence of a dynamic pattern (rise and/or fall) in cardiac troponin values along with clinical evidence of ischemia can be of help to confirm the diagnosis of MI in these contexts. Although the aims of our study were beyond these important issues, our data support that, for a given small stress to the myocar-

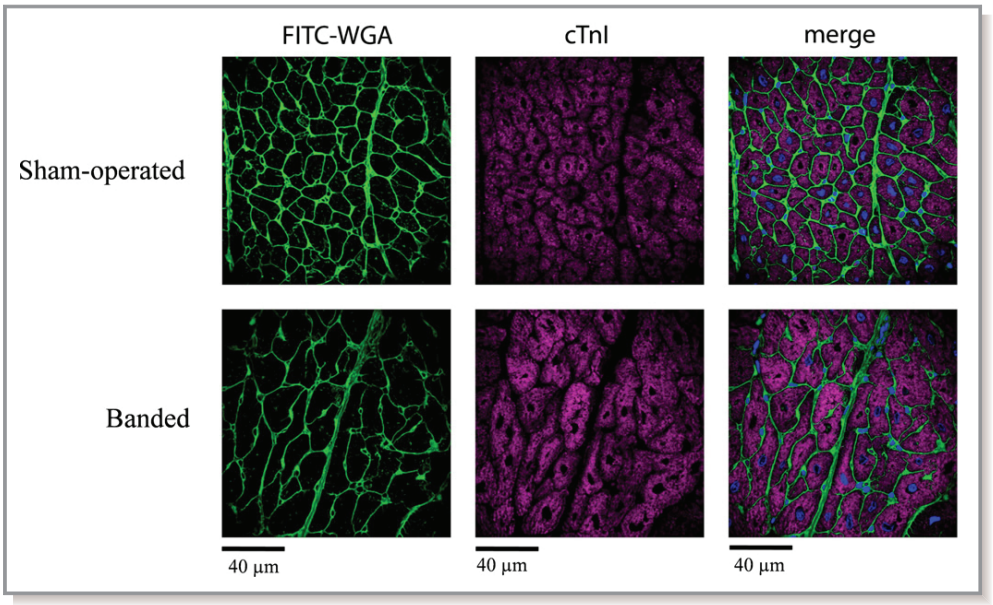

Figure 11. Representative immunofluorescence images of cTnI (pink, center) and cell membrane stained with FITC-WGA (green, left) in heart sections from sham-operated pigs (top) and hypertrophic (banded) pigs (bottom). Merged images are shown on the right. Nuclei are stained blue. cTnI indicates cardiac troponin I; FITC-WGA, fluorescein-isothiocyanate–conjugated lectin from wheat.

dium, troponin release in patients with LVH might be larger than in patients with normal LV mass.

In summary, our results show that LVH influences troponin release upon cardiac damage both in STEMI patients and in a controlled large-animal study, associated with higher expression of cTnI in cardiomyocytes from LVH hearts. These data have clinical implications given that many clinical trials use troponin release as a surrogate endpoint of the extent of cardiac damage and IS.

Limitations

Total CK circulating levels are potentially influenced by skeletal muscle trauma (including animal handling, intramus-

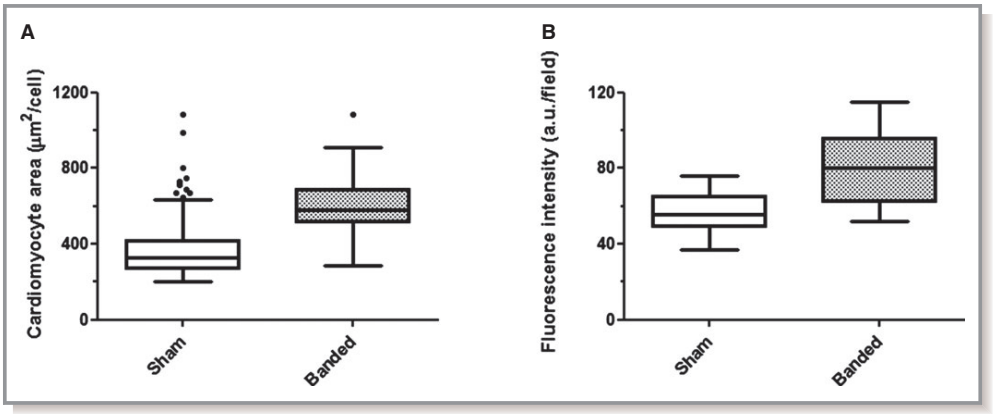

Figure 12. A, Cardiomyocyte area in banded and sham-operated pigs with no induced myocardial infarction. Box plots (Tukey's method) represent individual data (all random analyzed fields) from all pigs (4 pigs/group). Median (IQR) cardiomyocyte size was 579.3 μm^2 (516.9 to 685.7) in banded pigs and 326.2 μm^2 (271.0 to 420.0) in sham-operated pigs (P=0.021). B, Immunofluorescence of cardiac troponin I in banded and sham-operated pigs with no induced myocardial infarction. Box plots (Tukey's method) represent individual data (all random analyzed fields) from all pigs (4 pigs/group). Median (IQR) immunofluorescence intensity was 80 arbitrary units/field (62 to 96) in the banded pigs and 55.5 a.u./field (49.5 to 65) in sham-operated pigs (P=0.043). IQR indicates interquartile range.

cular injections, or surgical procedures).[44,45] Although we cannot completely exclude a significant influence of animal manipulation in total CK release, baseline total CK values were not different among groups. Of note, blood sample collections for biomarker measurement were performed 4 to 5 months after thoracotomy, thus unlikely to interfere in total CK release.

CK-MB was not systematically measured in the clinical study because it is no longer routinely evaluated in our environment. Similarly, CK-MB was not assessed in the animal study owing to lack of specificity of available antibodies and species differences in detected CK-MB activity.[46] In addition, activity of CK-MB has been shown to be very low in pigs,[47] thus being much less cardiac specific of myocardial damage than expected in humans owing to a very low CK-MB/total CK ratio in the cardiac muscle.[48] Of note, because of previously mentioned increase expression of CK-MB during ventricular hypertrophy,[30–35] we can speculate that CK-MB measurement overestimates actual infarct size similar to cTn. Although CK-MB has been used for years as the cardiac-specific biomarker of myocardial damage, cTn is currently the preferred biomarker because of its significantly higher cardiac tissue specificity.[9,49]

None of the cTnI assays used in this study are considered ultrasensitive. However, the conclusions from the present work are not likely to be affected by this fact given that high sensitivity is not needed to measure the levels observed both in pigs and humans in the context of STEMI.

The Siemens Dimension RxL assay was designed for detection of human cTnI. However, several findings anticipate its acceptable use in blood samples derived from pigs: (1) There is an almost perfect match between pigs and humans regarding amino acid sequences of the residues (epitopes) recognized by the antibodies of this kit (see www.ifcc.org/ifcc-scientific-division/documents-of-the-sd/troponinassay-analyticalcharacteristics2013/) when performing a Basic Local Alignment Search Tool (BLAST) test; (2) this assay has been shown to have good cTnI immunoreactivity in serum collected from rats and dogs,[50] which have identical amino acid sequence in these epitopes to pigs; and (3) blood and cardiac tissue collected from pigs has been shown to have good cross-reactivity to the antibodies used in a previous first-generation kit from the same manufacturer, which recognized the same epitopes with the same method.[51,52]

Conclusions

Peak and AUC of cTnI significantly overestimate infarct size in the presence of LVH, a phenomenon probably owing to the increased cTnI content in hypertrophied cardiomyocytes. Consistent with these findings, the discriminatory capacity of cTnI to predict LV dysfunction is significantly worse for patients with LVH. LV mass should therefore be considered when infarct size and LV function are estimated by troponin release.

Acknowledgments

The authors thank Angel Macias for high-quality CMR acquisition; Tamara Córdoba, Oscar Sanz, Eugenio Fernández, and the rest of teams at the CNIC animal facility and farm for outstanding animal care and support; Marta García for blood sample processing and biomarker measurements in the animal study; and Simon Bartlett (CNIC) for English editing.

Sources of Funding

This work was supported by an award from the Fondo de Investigación Sanitaria (FIS 10/02268) and by the competitive grant "CNIC translational 01/2009." Fernández-Jiménez is the recipient of a Rio Hortega fellowship. The "Red de Investigación Cardiovascular (RIC)" of the Spanish Ministry of Health supports Ibanez (RD 12/0042/0054) and Redondo (RD 12/0042/0022). The "Centro Nacional de Investigaciones Cardiovasculares Carlos III (CNIC)" is supported by the Spanish Ministry of Economy and Competitiveness and the Pro-CNIC Foundation.

Disclosures

None.

References

1. Choi KM, Kim RJ, Gubernikoff G, Vargas JD, Parker M, Judd RM. Transmural extent of acute myocardial infarction predicts long-term improvement in contractile function. *Circulation*. 2001;104:1101–1107.
2. Wu E, Judd RM, Vargas JD, Klocke FJ, Bonow RO, Kim RJ. Visualisation of presence, location, and transmural extent of healed Q-wave and non-Q-wave myocardial infarction. *Lancet*. 2001;357:21–28.
3. Younger JF, Plein S, Barth J, Ridgway JP, Ball SG, Greenwood JP. Troponin-I concentration 72 h after myocardial infarction correlates with infarct size and presence of microvascular obstruction. *Heart*. 2007;93:1547–1551.
4. Chia S, Senatore F, Raffel OC, Lee H, Wackers FJ, Jang IK. Utility of cardiac biomarkers in predicting infarct size, left ventricular function, and clinical outcome after primary percutaneous coronary intervention for ST-segment elevation myocardial infarction. *JACC Cardiovasc Interv*. 2008;1:415–423.
5. Licka M, Zimmermann R, Zehelein J, Dengler TJ, Katus HA, Kubler W. Troponin T concentrations 72 hours after myocardial infarction as a serological estimate of infarct size. *Heart*. 2002;87:520–524.
6. Hackel DB, Reimer KA, Ideker RE, Mikat EM, Hartwell TD, Parker CB, Braunwald EB, Buja M, Gold HK, Jaffe AS, Muller JE, Raabe DS, Rude RE, Sobel BE, Stone PH, Roberts R, and the MILIS Study Group. Comparison of enzymatic and anatomic estimates of myocardial infarct size in man. *Circulation*. 1984;70:824–835.
7. Kelle S, Roes SD, Klein C, Kokocinski T, de Roos A, Fleck E, Bax JJ, Nagel E. Prognostic value of myocardial infarct size and contractile reserve using magnetic resonance imaging. *J Am Coll Cardiol*. 2009;54:1770–1777.
8. Heusch G. Cardioprotection: chances and challenges of its translation to the clinic. *Lancet*. 2013;381:166–175.
9. Leonardi S, Armstrong PW, Schulte PJ, Ohman EM, Newby LK. Implementation of standardized assessment and reporting of myocardial infarction in

contemporary randomized controlled trials: a systematic review. *Eur Heart J*. 2013;34:894–902d.

10. Fernandez-Jimenez R, Lopez-Romero P, Suarez-Barrientos A, Garcia-Rubira JC, Fernandez-Ortiz A, Fuster V, Macaya C, Ibanez B. Troponin release overestimates infarct size in presence of left ventricular hypertrophy. *J Am Coll Cardiol*. 2012;60:640–641.
11. Drazner MH, Dries DL, Peshock RM, Cooper RS, Klassen C, Kazi F, Willett D, Victor RG. Left ventricular hypertrophy is more prevalent in blacks than whites in the general population: the Dallas Heart Study. *Hypertension*. 2005;46:124–129.
12. Ferrara AL, Vaccaro O, Cardoni O, Panarelli W, Laurenzi M, Zanchetti A. Is there a relationship between left ventricular mass and plasma glucose and lipids independent of body mass index? Results of the Gubbio Study. *Nutr Metab Cardiovasc Dis*. 2003;13:126–132.
13. Ibanez B, Macaya C, Sanchez-Brunete V, Pizarro G, Fernandez-Friera L, Mateos A, Fernandez-Ortiz A, Garcia-Ruiz JM, Garcia-Alvarez A, Iniguez A, Jimenez-Borreguero J, Lopez-Romero P, Fernandez-Jimenez R, Goicolea J, Ruiz-Mateos B, Bastante T, Arias M, Iglesias-Vazquez JA, Rodriguez MD, Escalera N, Acebal C, Cabrera JA, Valenciano J, Perez de Prado A, Fernandez-Campos MJ, Casado I, Garcia-Rubira JC, Garcia-Prieto J, Sanz-Rosa D, Cuellas C, Hernandez-Antolin R, Albarran A, Fernandez-Vazquez F, de la Torre-Hernandez JM, Pocock S, Sanz G, Fuster V. Effect of early metoprolol on infarct size in ST-segment-elevation myocardial infarction patients undergoing primary percutaneous coronary intervention: the effect of metoprolol in cardioprotection during an acute myocardial infarction (METOCARD-CNIC) trial. *Circulation*. 2013;128:1495–1503.
14. Pizarro G, Fernandez-Friera L, Fuster V, Fernandez-Jimenez R, Garcia-Ruiz JM, Garcia-Alvarez A, Mateos A, Barreiro MV, Escalera N, Rodriguez MD, de Miguel A, Garcia-Lunar I, Parra-Fuertes JJ, Sanchez-Gonzalez J, Pardillos L, Nieto B, Jimenez A, Abejon R, Bastante T, Martinez de Vega V, Cabrera JA, Lopez-Melgar B, Guzman G, Garcia-Prieto J, Mirelis JG, Zamorano JL, Albarran A, Goicolea J, Escaned J, Pocock S, Iniguez A, Fernandez-Ortiz A, Sanchez-Brunete V, Macaya C, Ibanez B. Long-term benefit of early pre-reperfusion metoprolol administration in patients with acute myocardial infarction: results from the METOCARD-CNIC trial (effect of metoprolol in cardioprotection during an acute myocardial infarction). *J Am Coll Cardiol*. 2014;63:2356–2362.
15. Ibanez B, Fuster V, Macaya C, Sanchez-Brunete V, Pizarro G, Lopez-Romero P, Mateos A, Jimenez-Borreguero J, Fernandez-Ortiz A, Sanz G, Fernandez-Friera L, Corral E, Barreiro MV, Ruiz-Mateos B, Goicolea J, Hernandez-Antolin R, Acebal C, Garcia-Rubira JC, Albarran A, Zamorano JL, Casado I, Valenciano J, Fernandez-Vazquez F, de la Torre JM, Perez de Prado A, Iglesias-Vazquez JA, Martinez-Tenorio P, Iniguez A. Study design for the "effect of metoprolol in cardioprotection during an acute myocardial infarction" (METOCARD-CNIC): a randomized, controlled parallel-group, observer-blinded clinical trial of early pre-reperfusion metoprolol administration in ST-segment elevation myocardial infarction. *Am Heart J*. 2012;164:473–480.e475.
16. Kim RJ, Albert TS, Wible JH, Elliott MD, Allen JC, Lee JC, Parker M, Napoli A, Judd RM. Performance of delayed-enhancement magnetic resonance imaging with gadoversetamide contrast for the detection and assessment of myocardial infarction: an international, multicenter, double-blinded, randomized trial. *Circulation*. 2008;117:629–637.
17. Du Bois D, Du Bois EF. Clinical calorimetry: tenth paper a formula to estimate the approximate surface area if height and weight be known. *Arch Intern Med*. 1916;XVII:863–871.
18. Thiele H, Kappl MJ, Conradi S, Niebauer J, Hambrecht R, Schuler G. Reproducibility of chronic and acute infarct size measurement by delayed enhancement-magnetic resonance imaging. *J Am Coll Cardiol*. 2006;47:1641–1645.
19. Ibanez B, Cimmino G, Prat-Gonzalez S, Vilahur G, Hutter R, Garcia MJ, Fuster V, Sanz J, Badimon L, Badimon JJ. The cardioprotection granted by metoprolol is restricted to its administration prior to coronary reperfusion. *Int J Cardiol*. 2011;147:428–432.
20. Ibanez B, Prat-Gonzalez S, Speidl WS, Vilahur G, Pinero A, Cimmino G, Garcia MJ, Fuster V, Sanz J, Badimon JJ. Early metoprolol administration before coronary reperfusion results in increased myocardial salvage: analysis of ischemic myocardium at risk using cardiac magnetic resonance. *Circulation*. 2007;115:2909–2916.
21. Brody S. A comparison of growth curves of man and other animals. *Science*. 1928;67:43–46.
22. Sharkey SW, Murakami MM, Smith SA, Apple FS. Canine myocardial creatine kinase isoenzymes after chronic coronary artery occlusion. *Circulation*. 1991;84:333–340.
23. Koerbin G, Abhayaratna WP, Potter JM, Apple FS, Jaffe AS, Ravalico TH, Hickman PE. Effect of population selection on 99th percentile values for a high sensitivity cardiac troponin I and T assays. *Clin Biochem*. 2013;46:1636–1643.
24. Boden H, Ahmed TA, Velders MA, van der Hoeven BL, Hoogslag GE, Bootsma M, le Cessie S, Cobbaert CM, Delgado V, van der Laarse A, Schalij MJ. Peak and fixed-time high-sensitive troponin for prediction of infarct size, impaired left ventricular function, and adverse outcomes in patients with first ST-segment elevation myocardial infarction receiving percutaneous coronary intervention. *Am J Cardiol*. 2013;111:1387–1393.
25. Hallen J. Troponin for the estimation of infarct size: what have we learned? *Cardiology*. 2012;121:204–212.
26. Tardif JC, Tanguay JF, Wright SS, Duchatelle V, Petroni T, Gregoire JC, Ibrahim R, Heinonen TM, Robb S, Bertrand OF, Cournoyer D, Johnson D, Mann J, Guertin MC, L'Allier PL. Effects of the P-selectin antagonist inclacumab on myocardial damage after percutaneous coronary intervention for non-ST-segment elevation myocardial infarction: results of the SELECT-ACS trial. *J Am Coll Cardiol*. 2013;61:2048–2055.
27. Carluccio E, Tommasi S, Bentivoglio M, Buccolieri M, Filippucci L, Prosciutti L, Corea L. Prognostic value of left ventricular hypertrophy and geometry in patients with a first, uncomplicated myocardial infarction. *Int J Cardiol*. 2000;74:177–183.
28. Hyman DJ, Pavlik VN. Characteristics of patients with uncontrolled hypertension in the United States. *N Engl J Med*. 2001;345:479–486.
29. Trask RV, Billadello JJ. Tissue-specific distribution and developmental regulation of M and B creatine kinase mRNAs. *Biochim Biophys Acta*. 1990;1049:182–188.
30. Ingwall JS, Kramer MF, Fifer MA, Lorell BH, Shemin R, Grossman W, Allen PD. The creatine kinase system in normal and diseased human myocardium. *N Engl J Med*. 1985;313:1050–1054.
31. Jameel MN, Zhang J. Myocardial energetics in left ventricular hypertrophy. *Curr Cardiol Rev*. 2009;5:243–250.
32. Nascimben L, Ingwall JS, Pauletto P, Friedrich J, Gwathmey JK, Saks V, Pessina AC, Allen PD. Creatine kinase system in failing and nonfailing human myocardium. *Circulation*. 1996;94:1894–1901.
33. Smith SH, Kramer MF, Reis I, Bishop SP, Ingwall JS. Regional changes in creatine kinase and myocyte size in hypertensive and nonhypertensive cardiac hypertrophy. *Circ Res*. 1990;67:1334–1344.
34. Vatner DE, Ingwall JS. Effects of moderate pressure overload cardiac hypertrophy on the distribution of creatine kinase isozymes. *Proc Soc Exp Biol Med*. 1984;175:5–9.
35. Ye Y, Wang C, Zhang J, Cho YK, Gong G, Murakami Y, Bache RJ. Myocardial creatine kinase kinetics and isoform expression in hearts with severe LV hypertrophy. *Am J Physiol Heart Circ Physiol*. 2001;281:H376–H386.
36. Sherwood MW, Kristin Newby L. High-sensitivity troponin assays: evidence, indications, and reasonable use. *J Am Heart Assoc*. 2014;3:e000403 doi: 10.1161/JAHA.113.000403.
37. Eggers KM, Lind L, Venge P, Lindahl B. Factors influencing the 99th percentile of cardiac troponin I evaluated in community-dwelling individuals at 70 and 75 years of age. *Clin Chem*. 2013;59:1068–1073.
38. Hamwi SM, Sharma AK, Weissman NJ, Goldstein SA, Apple S, Canos DA, Pinnow EE, Lindsay J. Troponin-I elevation in patients with increased left ventricular mass. *Am J Cardiol*. 2003;92:88–90.
39. McKie PM, Heublein DM, Scott CG, Gantzer ML, Mehta RA, Rodeheffer RJ, Redfield MM, Burnett JC Jr, Jaffe AS. Defining high-sensitivity cardiac troponin concentrations in the community. *Clin Chem*. 2013;59:1099–1107.
40. Xanthakis V, Larson MG, Wollert KC, Aragam J, Cheng S, Ho J, Coglianese E, Levy D, Colucci WS, Michael Felker G, Benjamin EJ, Januzzi JL, Wang TJ, Vasan RS. Association of novel biomarkers of cardiovascular stress with left ventricular hypertrophy and dysfunction: implications for screening. *J Am Heart Assoc*. 2013;2:e000399 doi: 10.1161/JAHA.113.000399.
41. de Lemos JA, Drazner MH, Omland T, Ayers CR, Khera A, Rohatgi A, Hashim I, Berry JD, Das SR, Morrow DA, McGuire DK. Association of troponin T detected with a highly sensitive assay and cardiac structure and mortality risk in the general population. *JAMA*. 2010;304:2503–2512.
42. Chin CWL, Shah ASV, McAllister DA, Joanna Cowell S, Alam S, Langrish JP, Strachan FE, Hunter AL, Maria Choy A, Lang CC, Walker S, Boon NA, Newby DE, Mills NL, Dweck MR. High-sensitivity troponin I concentrations are a marker of an advanced hypertrophic response and adverse outcomes in patients with aortic stenosis. *Eur Heart J*. 2014;35(34):2312–2321. doi: 10.1093/eurheartj/ehu189
43. Rosjo H, Andreassen J, Edvardsen T, Omland T. Prognostic usefulness of circulating high-sensitivity troponin T in aortic stenosis and relation to echocardiographic indexes of cardiac function and anatomy. *Am J Cardiol*. 2011;108:88–91.
44. Wolf RE, Graeber GM, Burge JR, DeShong JL, MacDonald JL, Zajtchuk R. Evaluation of serum creatine kinase and lactate dehydrogenase in experimental myocardial infarction, atriotomies, and thoracotomies. *Ann Thorac Surg*. 1986;41:378–386.

45. Bertinchant JP, Robert E, Polge A, Marty-Double C, Fabbro-Peray P, Poirey S, Aya G, Juan JM, Ledermann B, de la Coussaye JE, Dauzat M. Comparison of the diagnostic value of cardiac troponin I and T determinations for detecting early myocardial damage and the relationship with histological findings after isoprenaline-induced cardiac injury in rats. *Clin Chim Acta*. 2000;298:13–28.

46. Walker DB. Serum chemical biomarkers of cardiac injury for nonclinical safety testing. *Toxicol Pathol*. 2006;34:94–104.

47. Thoren-Tolling K, Jonsson L. Creatine kinase isoenzymes in serum of pigs having myocardial and skeletal muscle necrosis. *Can J Comp Med*. 1983;47:207–216.

48. Fredericks S, Merton GK, Lerena MJ, Heining P, Carter ND, Holt DW. Cardiac troponins and creatine kinase content of striated muscle in common laboratory animals. *Clin Chim Acta*. 2001;304:65–74.

49. Newby LK, Jesse RL, Babb JD, Christenson RH, De Fer TM, Diamond GA, Fesmire FM, Geraci SA, Gersh BJ, Larsen GC, Kaul S, McKay CR, Philippides GJ, Weintraub WS. ACCF 2012 expert consensus document on practical clinical considerations in the interpretation of troponin elevations: a report of the American College of Cardiology Foundation task force on clinical expert consensus documents. *J Am Coll Cardiol*. 2012;60:2427–2463.

50. Apple FS, Murakami MM, Ler R, Walker D, York M. Analytical characteristics of commercial cardiac troponin I and T immunoassays in serum from rats, dogs, and monkeys with induced acute myocardial injury. *Clin Chem*. 2008;54:1982–1989.

51. O'Brien PJ, Smith DE, Knechtel TJ, Marchak MA, Pruimboom-Brees I, Brees DJ, Spratt DP, Archer FJ, Butler P, Potter AN, Provost JP, Richard J, Snyder PA, Reagan WJ. Cardiac troponin I is a sensitive, specific biomarker of cardiac injury in laboratory animals. *Lab Anim*. 2006;40:153–171.

52. O'Brien PJ, Landt Y, Ladenson JH. Differential reactivity of cardiac and skeletal muscle from various species in a cardiac troponin I immunoassay. *Clin Chem*. 1997;43:2333–2338.

Original research article #2. "*Nutritional preconditioning by marine omega-3 fatty acids in patients with ST-segment elevation myocardial infarction: A METOCARD-CNIC trial substudy*".[68]

International Journal of Cardiology 228 (2017) 828–833

Contents lists available at ScienceDirect

International Journal of Cardiology

journal homepage: www.elsevier.com/locate/ijcard

Nutritional preconditioning by marine omega-3 fatty acids in patients with ST-segment elevation myocardial infarction: A METOCARD-CNIC trial substudy

Aleix Sala-Vila, DPharm PhD [a,b,1], Rodrigo Fernández-Jiménez, MD [c,d,1], Gonzalo Pizarro, MD [c,e], Carlos Calvo, BSc [a,b], Jose M García-Ruiz, MD [c], Leticia Fernández-Friera, MD PhD [c,f], Maite D Rodriguez, RN [c], Noemí Escalera, BPT [c], Jorge Palazuelos, MD PhD [i], Angel Macías, Tech [c], Braulio Pérez-Asenjo, BPT [c], Antonio Fernández-Ortiz, MD PhD [c,d], Emilio Ros, MD PhD [a,b], Valentín Fuster, MD PhD [c,g], Borja Ibáñez, MD PhD [c,h,*]

[a] Lipid Clinic, Endocrinology and Nutrition Service, Hospital Clínic, Institut d'Investigacions Biomèdiques August Pi i Sunyer (IDIBAPS), Barcelona, Spain
[b] CIBER Fisiopatología de la Obesidad y Nutrición (CIBEROBN), Instituto de Salud Carlos III (ISCIII), Spain
[c] Centro Nacional de Investigaciones Cardiovasculares Carlos III (CNIC), Madrid, Spain
[d] Cardiovascular Institute, Hospital Clínico San Carlos, Madrid, Spain
[e] Hospital Universitario Quirón, Universidad Europea de Madrid, Spain
[f] Hospital Universitario Montepríncipe, Madrid, Spain
[g] The Zena and Michael A. Wiener Cardiovascular Institute, Icahn School of Medicine at Mount Sinai, New York, NY, United States
[h] IIS, Fundación Jiménez Díaz, Madrid, Spain
[i] Hospital Universitario Central de la Defensa Gómez Ulla, Madrid, Spain

ARTICLE INFO

Article history:
Received 25 August 2016
Accepted 6 November 2016
Available online 9 November 2016

Keywords:
Fatty acids
Myocardial infarction
Nutrition

ABSTRACT

Background: Marine omega-3 eicosapentaenoic acid (EPA) is readily incorporated into cardiomyocyte membranes, partially displacing the omega-6 arachidonic acid (AA). Whereas AA is a substrate for pro-inflammatory eicosanoids, the release of EPA from cell membranes generates anti-inflammatory lipid mediators, contributing to the infarct-limiting effect observed experimental models. Clinical data are lacking.
Methods: In this observational study conducted in 100 patients with a reperfused anterior ST-elevation myocardial infarction (STEMI), at hospital admission we quantified by gas-chromatography the red blood cell proportions of AA, EPA, and the AA:EPA ratio, a valid surrogate for cardiomyocyte membrane content. Patients underwent cardiac magnetic resonance imaging in the acute phase (one week post-STEMI), and at long-term (6 months) follow-up. Infarct size (delayed gadolinium enhancement) and cardiac function (left ventricular ejection fraction [LVEF]) were correlated with exposures of interest by multivariate regression analysis.
Results: AA:EPA ratio directly related to acute infarct size (coefficient [95% CI]: 6.19 [1.68 to 10.69], $P = 0.008$) and inversely to long-term LVEF (coefficient [95% CI]: −4.02 [−7.15 to −0.89], $P = 0.012$). EPA inversely related to acute infarct size (coefficient [95% CI]: −6.58; [−11.46 to −1.70]; $P = 0.009$), while a direct association with LVEF at follow-up (coefficient [95% CI]: 3.67 [0.25 to 7.08]; $P = 0.036$) was observed.
Conclusions: A low AA:EPA ratio in red blood cells at the time of STEMI is associated with smaller acute infarct size and preserved long-term ventricular function. Our results are consistent with prior work in experimental models and add to the notion of omega-3 fatty acids as a healthy fat.
Trial registration: http://www.clinicaltrials.gov/NCT01311700

Abbreviations: AA, arachidonic acid (C20:4n-6); CMR, cardiac magnetic resonance; DHA, docosahexaenoic acid (C22:6n-3); EPA, eicosapentaenoic acid (C20:5n-3); IHD, ischemic heart disease; LCn3PUFA, long-chain n-3 (omega-3) polyunsaturated fatty acids; LVEF, left ventricular ejection fraction; RBC, red blood cell; STEMI, ST-segment elevation myocardial infarction.

* Corresponding author at: Translational Laboratory for Cardiovascular Imaging and Therapy, Centro Nacional de Investigaciones Cardiovasculares Carlos III (CNIC), Melchor Fernández Almagro, 3 & Department of Cardiology, Instituto de Investigación Sanitaria, Fundación Jiménez Díaz, Madrid, Spain.
E-mail address: bibanez@cnic.es (B. Ibáñez).
[1] These authors contributed equally to this study.

http://dx.doi.org/10.1016/j.ijcard.2016.11.214
0167-5273/

1. Introduction

Ischemic heart disease (IHD), the leading cause of death worldwide [1], can be prevented by a variety of dietary components [2]. Among them, intake of long-chain omega-3 polyunsaturated fatty acids (LCn3PUFA), mainly eicosapentaenoic acid (C20:5n-3, EPA) and docosahexaenoic acids (C22:6n-3, DHA), is associated with a lower risk of IHD, particularly sudden cardiac death, in individuals without prior cardiovascular disease [3]. The link is controversial for secondary prevention [4], which can be mostly explained by the universal statin treatment after myocardial infarction and by the fact that myocardial infarction survivors are no longer deficient in LCn3PUFA, as recently pointed out [5]. Based on large epidemiologic studies, the American Heart Association recommended consuming at least two servings per week of fish, preferably fatty fish [6].

Dietary LCn3PUFA readily displace the omega-6 arachidonic acid (C20:4n-6, AA) from membranes [7]. Such replacement modifies the production of eicosanoids and other lipid mediators by the cyclooxygenase, lipoxygenase, and cytochrome P450 pathways [8,9]. Myocardial ischemia triggers the release of free AA and the ensuing formation of pro-inflammatory eicosanoids, which are believed to amplify ischemic tissue damage in animal models and in patients with myocardial infarction [10,11]. In contrast, the release of EPA from cardiac membranes under ischemic conditions leads to the generation of anti-inflammatory eicosanoids [7–9].

Long-term diet-induced displacement of AA of cardiomyocyte membranes by EPA may thus have beneficial effects in the event of ST-segment elevation myocardial infarction (STEMI), protecting the myocardium during the ischemia/reperfusion process and improving post-infarction ventricular function and remodeling. This strategy would be of interest in public health, given that infarct size and chronic left ventricular ejection fraction (LVEF) are major determinants of post-STEMI mortality and morbidity [12,13]. Experimental models have consistently reported a nutritional preconditioning-like effect of diets supplemented with LCn3PUFA in the heart [14–19], but clinical data are confined to a recent study reporting that treatment with doses of 4 g/d of LCn3PUFA after myocardial infarction improves cardiac remodeling [20]. The issue of whether regular fish eaters who sustain a first STEMI may have less extensive cardiac damage than non-eaters remains to be explored. In observational studies, the optimal approach to address this issue is by using the fatty acid composition of body tissues, given the difficulties of accurately measuring fat intake from the diet records [21].

We therefore hypothesized that cardiomyocite membrane AA replacement by EPA supplied by the usual diet, in the absence of omega-3 supplementation, would relate to smaller myocardial injury and result in better chronic left ventricle contractile function at the time of a first STEMI. Given that routine myocardial biopsy is not safe in the acute phase of STEMI, we measured the AA:EPA ratio in red blood cells (RBC) – a well validated surrogate for cardiomyocyte membrane fatty acid content [22,23] unaffected in the subacute phase of a cardiac event [24] – at the time of STEMI and studied its association with acute infarct size and long-term cardiac function as assessed by state-of-the-art cardiac magnetic resonance (CMR) [25].

2. Material and methods

This observational study is a substudy of the METOCARD-CNIC clinical trial (http://www.clinicaltrials.gov. Unique identifier: NCT01311700. EUDRACT number: 2010-019939-35) [26–28].

2.1. Design and study participants

The METOCARD-CNIC trial showed that in patients suffering a first STEMI, early intravenous metoprolol administration prior to primary percutaneous coronary intervention reduces acute infarct size [27] and preserves long-term LVEF, thereby reducing the incidence of severe left ventricle systolic dysfunction and lowering heart failure admissions [28]. The study protocol has been described in detail elsewhere [26]. Participants were recruited between November 2010 and October 2012. Inclusion criteria were age 18 to 80 years, Killip class ≤ II anterior STEMI, and anticipated symptom onset-to-reperfusion time ≤ 6 h. Aside from allocation to pre-reperfusion intravenous metoprolol or control, all patients received state-of-the-art treatment according to clinical guidelines, including long-term oral treatment with β-blockers. The study, which complied with the Declaration of Helsinki, was approved by the institutional review boards of each participating center, and all eligible candidates provided written informed consent. Complete information was available in 100 STEMI patients ($n = 50$, treated with intravenous metoprolol administration prior to primary percutaneous coronary intervention; and $n = 50$ controls, no receiving metoprolol) who agreed to participate in this substudy (Supplementary Fig. 1).

2.2. RBC membrane fatty acid analysis

Overnight fasting period (>10 h) blood samples were drawn during hospital admission and were stored at −80 °C until fatty acid analysis. The RBC fatty acid profile was determined as described [29]. In brief, whole blood cells were hemolysed and the pellet (>99.5% RBC membranes) was obtained by centrifugation. After that, the cell membrane pellet was dissolved in 1 ml BF_3 methanol solution and transferred to a screw-cap test-tube, which was heated for 10 min at 100 °C to hydrolyze and methylate glycerophospholipid fatty acids. The extracts were cooled and fatty acid methyl esters were isolated by adding 300 μl of n-hexane. The tubes were centrifuged and an aliquot of the upper layer was transferred into an automatic injector vial equipped with a 300 μl volume adapter. Fatty acid methyl esters were separated by gas-chromatography using an Agilent HP 7890 Gas Chromatograph equipped with a 30 m × 0.25 μm × 0.25 mm SupraWAX-280 capillary column (Teknokroma, Barcelona, Spain), an autosampler, and a flame ionization detector. The amount of each fatty acid is expressed as a percentage of the total identified fatty acids in the sample.

2.3. Dietary assessment

To assess the consumption of foods rich in the fatty acids of interest (seafood) in the months prior to the STEMI, a random subsample ($n = 36$) underwent an adaptation of a validated semiquantitative food-frequency questionnaire [30] at baseline in a face-to-face interview. Information on seafood products was collected in eight items (uncanned fatty fish; lean fish; smoked/salted fish; molluscs; shrimp, prawn and crayfish; octopus, baby squid and squid; fatty fish canned in oil; fatty fish canned in salted water). EPA and DHA intake was estimated by multiplying the frequency of each item for the fatty acid composition of the servings consumed and averaging intake to daily amounts. Nutrient composition was estimated from Spanish food composition tables [31].

2.4. CMR procedure

A detailed description of the CMR protocol and analytical methods is reported elsewhere [26]. Analyses were undertaken by the core laboratory at the Centro Nacional de Investigaciones Cardiovasculares Carlos III (CNIC). Data were quantified with dedicated software (QMass MR 7.5; Medis, Leiden, the Netherlands). Main CMR outcomes included the extent of edema (myocardium at risk) defined by high signal intensity on T2-weighted imaging; the extent of necrosis (infarct size) defined by the degree of abnormal delayed gadolinium enhancement on T1 inversion-recovery sequences; and LVEF. Acute CMR was scheduled to be performed 5 to 7 days after infarction, and patients underwent follow-up CMR 6 months after the index event.

2.5. Statistical analysis

Normal distribution of each data subset was assessed using graphical methods and the Shapiro–Wilk test. Levene's test was performed to test the homogeneity of variances. For quantitative variables following a normal distribution, data are expressed as mean and standard deviation (SD), while non-normal data are reported as medians and interquartile range. For categorical variables, data are expressed as frequencies and percentages. Multiple linear regression analysis was used to study the association between RBC fatty acids (AA:EPA ratio, AA, and EPA) and CMR outcomes (infarct size at 5–7 days after infarction, and LVEF at 6 months after infarction). In addition to unadjusted models, we constructed models adjusted for area at risk, which is the main determinant of infarct size, and by early intravenous metoprolol administration (yes/no), given that it has been shown to reduce infarct size [27] and improve long-term LVEF [28]. Potential confounding factors (age, sex, body mass index, diabetes, dyslipidemia, and hypertension) were investigated, and the final model was selected according to parsimonious criteria and no relevant change in the precision of the estimation. Any explored fatty acid variable followed a normal distribution; therefore in the regression analysis these variables were processed by a logarithmic transformation (EPA and the AA:EPA ratio) or a square transformation (AA). Standard diagnostic checks on the residuals from the fitted models showed no evidence of any failure of the assumption of normality and homogeneity of the residual variance. Sperman's correlation coefficient was used to study the association between the calculated intake of EPA + DHA and the RBC proportions of EPA and AA:EPA ratio at the time of STEMI. Statistical significance was set at an alpha value of 0.05. All statistical analyses were performed using commercially available software (Stata 12.0).

3. Results

Baseline clinical characteristics and treatment regimens of the study population are shown in Table 1. Demographic, anthropometric, and clinical characteristics of patients included in this substudy were similar to those of the overall study cohort (data not shown). 15% of participants were treated with statins before STEMI, while the full cohort received statin treatment at 6 months. RBC membrane fatty acid composition at hospital admission is presented in Table 2. Acute and follow-up CMR data are summarized in Table 3.

In a randomly selected subset of subjects at baseline ($n = 36$), the mean (SD) of fatty fish, lean fish, and total fish was 38.3 g/d (22.1), 27.7 g/d (16.2) and 101.4 g/d (45.8), respectively. The calculated mean EPA + DHA intake was 1006 mg/d (502). Attesting to the validity of the questionnaire, the Spearman's correlation coefficient between calculated intake of EPA + DHA and AA:EPA ratio in RBC at the time of STEMI was −0.384 ($P = 0.021$), while the value for EPA in RBC was 0.392 ($P = 0.018$).

Univariate associations between CMR-assessed acute infarct size were −0.141 ($P = 0.161$); 0.112 ($P = 0.269$), and 0.173 ($P = 0.086$) for RBC EPA, AA, and AA:EPA ratio, respectively. The values for long-term LVEF were 0.130 ($P = 0.198$), −0.225 ($P = 0.024$), and −0.185 ($P = 0.065$), respectively. Multivariate associations are shown in Tables 4, 5, and eTable 1. The AA:EPA ratio showed a significant direct association with acute infarct size (coefficient: 6.19; 95% CI: 1.68 to 10.69; $P = 0.008$; Table 4) and a significant inverse association with LVEF at 6 months (coefficient: −4.02; 95% CI: −7.15 to −0.89; $P = 0.012$; Table 4). Significant associations were found for EPA (inverse with infarct size at baseline [coefficient: −6.58; 95% CI: −11.46 to −1.70; $P = 0.009$], and direct with LVEF at follow-up [coefficient: 3.67; 95% CI: 0.25 to 7.08; $P = 0.036$]) (Table 5). AA showed a significant inverse association with long-term LVEF (coefficient: −0.02; 95% CI: −0.03 to 0.00; $P = 0.022$) (eTable 1).

Table 1
Clinical characteristics and treatment regimens at baseline in 100 patients with anterior STEMI.

Variable	Mean (SD)	Range
Age, y	58.1 (11.5)	34.3 to 80.8
Male sex, n (%)	86 (86.0)	–
Body mass index, kg/m^2	27.4 (3.5)	21.1 to 40.4
Hypertension, n (%)	40 (40.0)	–
Smoking status, n (%)		–
Current	54 (54.0)	
Ex-smoker (0–10 y before)	7 (7.0)	
Dyslipidemia, n (%)	44 (44.0)	–
Treatment with statins, n (%)	15 (15.0)	–
Diabetes mellitus, n (%)	20 (20.0)	–
Ischemia duration, min[a]	190.6 (62.9)	60 to 345
Killip class I at admission, n (%)	94 (94.0)	–
Infarct artery lesion location, n (%)		–
Proximal LAD	21 (21.0)	
Mid LAD	67 (67.0)	
Distal LAD	7 (7.0)	
Diagonal	2 (2.0)	
Other	3 (3.0)	
TIMI grade 0–1 flow before PCI, n (%)	83 (83.0)	–
Successful PCI, n (%)[b]	98 (98.0)	–
Treatment at the time of PCI, n (%)		–
Heparin	95 (95.0)	
Aspirin	100 (100.0)	
Thienopyiridine	98 (98.0)	
Thrombus aspiration	89 (89.0)	
GP IIb/IIIa during PCI	66 (66.0)	

[a] Time from symptom onset to reperfusion.
[b] Defined as TIMI grade 2 to 3 flow after percutaneous coronary intervention.

Table 2
Red blood cell fatty acids at hospital admission.

Fatty acid (% of total fatty acids)	Median (interquartile range)
C14:0	1.86 (1.00 to 2.76)
C16:0	20.63 (19.93 to 21.48)
C18:0	10.51 (9.85 to 11.56)
C20:0	0.10 (0.08 to 0.12)
C22:0	0.14 (0.11 to 0.17)
C24:0	0.29 (0.22 to 0.35)
Sum of saturated fatty acids	33.79 (32.77 to 34.84)
C16:1n-7 *cis*	0.67 (0.54 to 0.88)
C18:1n-9 *cis*	14.78 (14.11 to 16.34)
C18:1n-9 *trans*	1.26 (1.15 to 1.34)
C20:1n-9	0.19 (0.16 to 0.23)
C24:1n-9	0.37 (0.27 to 0.45)
Sum of monounsaturated fatty acids	17.41 (16.50 to 18.97)
C18:2n-6	12.70 (11.56 to 14.07)
C18:3n-6	0.17 (0.12 to 0.22)
C20:2n-6	0.25 (0.22 to 0.30)
C20:3n-6	1.89 (1.64 to 2.20)
C20:4n-6 (AA, arachidonic acid)	20.13 (18.63 to 22.04)
C22:4n-6	2.44 (2.10 to 2.78)
C22:5n-6	0.46 (0.38 to 0.56)
Sum of n-6 polyunsaturated fatty acids	38.21 (36.60 to 41.18)
C18:3n-3	0.12 (0.10 to 0.16)
C20:5n-3 (EPA, eicosapentaenoic acid)	0.83 (0.62 to 1.13)
C22:5n-3	1.85 (1.67 to 2.04)
C22:6n-3 (DHA, docosahexaenoic acid)	6.67 (5.79 to 7.58)
Omega-3 index (C20:5n-3 + C22:6n-3)	7.70 (6.52 to 8.64)
AA:EPA ratio	24.97 (18.14 to 32.74)

4. Discussion

In this substudy of the METOCARD-CNIC trial, we found that reduced AA:EPA ratio in RBC membranes at the time of STEMI was associated with smaller infarctions and improved long-term LVEF. Despite its observational design, our study investigated the preconditioning-like properties of omega-3 fatty acids in humans, a notion only explored in animal models heretofore. We determined the LCn3PUFA profile in RBC, which is known to mirror dietary LCn3PUFA intake [21,29] and it is a validated surrogate for cardiac fatty acid status in humans, as previously demonstrated in studies undertaken in heart transplant recipients [23] and in patients undergoing cardiac bypass surgery [24]. Our unprecedented findings suggest that replacement of AA with EPA in the phospholipids of cell membranes (including cardiomyocytes), which can be achieved through the regular intake of fatty fish or fish oil, might contribute improving prognosis in the event of a STEMI.

Advances in reperfusion have reduced the acute mortality associated with STEMI, the leading cause of death worldwide, and attention has since turned to the improvement of survivors' quality of life and life expectancy [14]. In this regard, declining cardiac function emerged as an important and powerful predictor of clinical outcomes in post-infarction patients [13]. As a result, pharmacological and device-based therapies have been implemented to reduce long-term mortality

Table 3
Baseline and long-term magnetic resonance imaging data.

	Baseline (5 to 7 days after infarction)		Long-term (6 mo after infarction)	
Variable	Mean (SD)	Range	Mean (SD)	Range
LVEDV, mL	173.9 (36.7)	100.2 to 301.6	190.1 (43.1)	108.7 to 327.7
LVESV, mL	94.9 (32.1)	33.3 to 217.7	101.7 (41.0)	39.9 to 229.2
LV mass, g	110.8 (25.8)	57.7 to 186.1	85.8 (20.0)	40.5 to 139.4
Edema, g	35.4 (16.5)	0 to 75.7	–	–
Edema, % LV	28.2 (11.7)	0 to 52.0	–	–
Infarct size, g	24.7 (17.7)	0 to 79.8	14.8 (10.8)	0.0 to 42.4
LVEF, %	46.4 (9.7)	26.7 to 67.2	48.0 (10.8)	26.8 to 68.4

LVEDV, left ventricular end-diastolic volume; LVESV, left ventricular end-systolic volume; LV, left ventricle; LVEF, left ventricular ejection fraction.

Table 4
Independent determinants of acute infarct size (grams of LV tissue) and long-term left ventricular ejection fraction (%), including the ratio of C20:4n-6 to C20:5n-3 (AA:EPA ratio) in red blood cells at baseline.

Acute infarct size					
Variable	Coef. (95% CI)	*P*	F (3, 96)	Prob > F	Adj R-squared
Edema, % of LV	1.08 (0.88 to 1.29)	<0.001	42.58	<0.001	0.56
Metoprolol, yes	−5.12 (−9.79 to −0.44)	0.032			
AA:EPA ratio[a]	6.19 (1.68 to 10.69)	0.008			
Long-term left ventricular ejection fraction					
Variable	Coef. (95% CI)	*P*	F (3, 96)	Prob > F	Adj R-squared
Edema, % of LV	−0.58 (−0.72 to −0.44)	<0.001	25.97	<0.001	0.43
Metoprolol, yes	2.59 (−0.65 to 5.83)	0.116			
AA:EPA ratio[a]	−4.02 (−7.15 to −0.89)	0.012			

CI, confidence interval; LV, left ventricle.
[a] Logarithmic-transformed variable.

associated with low LVEF. The cost of these treatment strategies, however, precludes their universal implementation, particularly in developing countries [32]. By showing that long-term LVEF relates to the cell membrane fatty acid profile at the time of infarction, which is known to be modulated by dietary habits during the preceding weeks [21,33], we add on the notion of fish-derived LCn3PUFA as healthy fat for the heart.

The associations found for EPA and for the AA:EPA ratio, a surrogate of AA displacement by EPA, are mechanistically supported by the opposite effects on ischemia of recently discovered cytochrome P450-derived metabolites of AA and EPA [9,10]. Of note, an EPA-derived compound, resolvin E1, has been found to protect rat cardiomyocytes against ischemia-reperfusion injury and to limit infarct size when administered intravenously before reperfusion [34]. Our finding adds plausibility to the hypothesis linking cardiovascular risk to the relative proportions of precursors of harmful and protective lipid mediators (AA and EPA, respectively), which was raised by Dyerberg more than 30 years ago in an attempt to explain the low incidence of myocardial infarction among the Inuit of Greenland despite their high dietary intake of marine fat [35]. In line with our results, three studies from Japan, a country in which fish consumption is customarily high, reported that serum AA/EPA ratio directly related to hampered cardiac stability [36] and to an increased incidence of major adverse cardiac events after an ischemic insult [37,38]. However, the use of fatty acid composition of total serum, which does not reflect long-term intake as accurately as adipose tissue or RBC do [21], precludes the attribution of observed effects to membrane changes upon long-term EPA intake. In contrast, the turnover of RBC (120-day lifespan) makes RBC a suitable sample for objective assessment of LCn3PUFA status, with stability documented over a 6-week period [33] and importantly, in a subacute phase of a cardiac event [24]. This guarantees that the RBC fatty acid composition during hospital admission is representative of the fatty acid profile at the time of STEMI.

In line with the known notion that LCn3PUFA content in body tissues mirrors dietary intake of EPA and DHA, we inquired about fish and shellfish consumption in a subset (36%) of our population. To address this, we adapted a validated food-frequency questionnaire [30] previously used to relate dietary estimate EPA + DHA intake to RBC LCn3PUFA status in a Spanish population [29].Accordingly, we found a significant association between RBC AA:EPA ratio and estimated LCn3PUFA intake, with a Spearman's correlation coefficient concurring with previous literature [21]. The subset providing dietary data reported a mean EPA + DHA intake of 1006 mg/d, which largely exceeds the recommendation for the primary prevention of IHD [6]. This, in turn, is due to the high consumption of fatty fish (mean 38 g/d) within the months prior to STEMI in our study, a figure that concurs with reports from other Spanish populations [39].

Our study has limitations, such as the relatively small number of study subjects and the related low statistical power to detect clinical events during follow-up. The reason for a lack of a pre-specified sample size is that this is a study conducted in a subset of a clinical trial exploring changes in infarct size and LVEF after early intravenous metoprolol administration, and ours was an exploratory study with a sample large enough to detect a link between dietary determinants prior to admission and LVEF 6 months after infarction. A second limitation is that the food-frequency questionnaire was only administered to a subgroup of patients, and dietary intakes could not be adjusted for total energy intake because only seafood-derived items were investigated. Finally, a cause-effect relationship would only be established by a randomized clinical trial involving a nutritional intervention in a large population at high risk of STEMI followed for several years. The study also has strengths, such as the use of state-of-the-art CMR technology to evaluate heart anatomy and function, the use of an

Table 5
Independent determinants of acute infarct size (grams of LV tissue) and long-term left ventricular ejection fraction (%), including the proportion of EPA (C20:5n-3) in red blood cells at baseline.

Acute infarct size					
Variable	Coef. (95% CI)	*P*	F (3, 96)	Prob > F	Adj R-squared
Edema, % of LV	1.10 (0.90 to 1.30)	<0.001	42.40	<0.001	0.56
Metoprolol, yes	−4.92 (−9.60 to −0.24)	0.040			
EPA[a]	−6.58 (−11.46 to −1.70)	0.009			
Long-term left ventricular ejection fraction					
Variable	Coef. (95% CI)	*P*	F (3, 96)	Prob > F	Adj R-squared
Edema, % of LV	-0.59 (−0.73 to −0.45)	<0.001	24.85	<0.001	0.42
Metoprolol, yes	2.48 (−0.80 to 5.75)	0.136			
EPA[a]	3.67 (0.25 to 7.08)	0.036			

CI, confidence interval; LV, left ventricle.
[a] Logarithmic-transformed variable.

objective and stable biomarker of long-term fatty acid intake (reinforced by the association with calculated intake of EPA + DHA in a subset of our sample), and the adjustment for well-known confounders in multivariable analyses.

In conclusion, we report that a low AA:EPA ratio in RBC membranes at the time of STEMI is associated with presumed protection against myocardial injury, as reflected by reduced infarct size and improved long-term LVEF. Our results, which are consistent with the current model of the pathogenesis of myocardium damage upon ischemia/reperfusion, add plausibility to a hypothesis only tested in experimental models heretofore. The findings might contribute to explain also the primary prevention of fatal IHD, particularly sudden cardiac death, ascribed to the *anti*-arrhythmic properties of LCn3PUFA fatty acids. This overall supports the notion that consumption of seafood, fatty fish in particular, is a valid strategy for improving cardiovascular health, as recommended by several scientific society guidelines [6,40].

Supplementary data to this article can be found online at http://dx.doi.org/10.1016/j.ijcard.2016.11.214.

Author contributions

BI had full access to all the data in the study and takes responsibility for the integrity of the data and the accuracy of the data analysis. Study concept and design: AS-V and BIC. Acquisition of data: all authors. Analysis and interpretation of data: all authors. Drafting of the manuscript: AS-V, RF-J, GP, ER, and BI. Critical revision of the manuscript for important intellectual content: all authors. Statistical analysis: RF-J. Obtained funding: BI. Administrative, technical, or material support: NE. Supervision: BI.

Conflict of interest disclosures

ER has received research funding from the California Walnut Commission (including an unrestricted educational grant) and is a non-paid member of the Commission's scientific advisory committee. The other authors report no conflicts. None of the funding sources played a role in the design, collection, analysis, or interpretation of the data or in the decision to submit the manuscript for publication.

Funding sources

This work was supported by the Centro Nacional de Investigaciones Cardiovasculares Carlos III (CNIC), through CNIC Translational Grant 01-2009. Other sponsors were the Spanish Ministry of Health and Social Policy (EC10-042), the Mutua Madrileña Foundation (AP8695-2011), and a Master Research Agreement (MRA) between Philips Healthcare and the CNIC (CNIC translational 01-2009). AS-V holds a Miguel Servet I fellowship from the Ministry of Economy and Competitiveness through the Instituto de Salud Carlos III (CP12/03299). RF-J is a recipient of non-overlapping grants from the Ministry of Economy and Competitiveness through the Instituto de Salud Carlos III (Rio Hortega fellowship); and the Fundació Jesús Serra, the Fundación Interhospitalaria de Investigación Cardiovascular (FIC) and CNIC (FICNIC fellowship). BI is recipient of the ISCIII Fondo de Investigación Sanitaria grants and ERDF/FEDER funds (PI10/02268, PI13/01979 and RETIC# RD12/0042/0054) related to this topic. GP, LF-F, NE, and BI are members of the Spanish Red de Investigación Cardiovascular (RIC; Program 4: HISPANICVS). The CNIC is supported by the MINECO and the Pro CNIC Foundation, and is a Severo Ochoa Center of Excellence (MINECO award SEV-2015-0505). BI is Princess of Girona awardee in Science. CIBEROBN is an initiative of Instituto de Salud Carlos III, Spain.

Acknowledgements

We are indebted to the participants in the trial. Simon Bartlett (CNIC) provided English editing.

References

[1] M. Naghavi, GBD 2013 Mortality and Causes of Death Collaborators, Global, regional, and national age–sex specific all-cause and cause-specific mortality for 240 causes of death, 1990–2013: a systematic analysis for the Global Burden of Disease Study 2013, Lancet 385 (9963) (2015) 117–171.
[2] D. Mozaffarian, L.J. Appel, L. Van Horn, Components of a cardioprotective diet: new insights, Circulation 123 (24) (2011) 2870–2891.
[3] D. Mozaffarian, J.H. Wu, Omega-3 fatty acids and cardiovascular disease: effects on risk factors, molecular pathways, and clinical events, J. Am. Coll. Cardiol. 58 (20) (2011) 2047–2067.
[4] E.C. Rizos, E.E. Ntzani, E. Bika, M.S. Kostapanos, M.S. Elisaf, Association between omega-3 fatty acid supplementation and risk of major cardiovascular disease events: a systematic review and meta-analysis, JAMA 308 (10) (2012) 1024–1033.
[5] W.S. Harris, Are n-3 fatty acids still cardioprotective? Curr. Opin. Clin. Nutr. Metab. Care 16 (2) (2013) 141–149.
[6] P.M. Kris-Etherton, W.S. Harris, L.J. Appel, Omega-3 fatty acids and cardiovascular disease: new recommendations from the American Heart Association, Arterioscler. Thromb. Vasc. Biol. 23 (2) (2003) 151–152.
[7] P.L. McLennan, Cardiac physiology and clinical efficacy of dietary fish oil clarified through cellular mechanisms of omega-3 polyunsaturated fatty acids, Eur. J. Appl. Physiol. 114 (7) (2014) 1333–1356.
[8] M. Guichardant, C. Calzada, N. Bernoud-Hubac, M. Lagarde, E. Vericel, Omega-3 polyunsaturated fatty acids and oxygenated metabolism in atherothrombosis, Biochim. Biophys. Acta 1851 (4) (2015) 485–495.
[9] C. Westphal, A. Konkel, W.H. Schunck, CYP-eicosanoids — a new link between omega-3 fatty acids and cardiac disease? Prostaglandins Other Lipid Mediat. 96 (1–4) (2011) 99–108.
[10] C.M. Jenkins, A. Cedars, R.W. Gross, Eicosanoid signalling pathways in the heart, Cardiovasc. Res. 82 (2) (2009) 240–249.
[11] H. Qiu, J.Y. Liu, D. Wei, N. Li, E.N. Yamoah, B.D. Hammock, N. Chiamvimonvat, Cardiac-generated prostanoids mediate cardiac myocyte apoptosis after myocardial ischaemia, Cardiovasc. Res. 95 (3) (2012) 336–345.
[12] C.W. Yancy, M. Jessup, B. Bozkurt, et al., American College of Cardiology Foundation, American Heart Association Task Force on Practice Guidelines, American College of Cardiology Foundation/American Heart Association Task Force on Practice Guidelines, 2013 ACCF/AHA guideline for the management of heart failure: a report of the American College of Cardiology Foundation/American Heart Association task force on practice guidelines, J. Am. Coll. Cardiol. 62 (16) (2013) e147–e239.
[13] B. Ibáñez, G. Heusch, M. Ovize, F. Van de Werf, Evolving therapies for myocardial ischemia/reperfusion injury, J. Am. Coll. Cardiol. 65 (14) (2015) 1454–1471.
[14] S. al Makdessi, M. Brändle, M. Ehrt, H. Sweidan, R. Jacob, Myocardial protection by ischemic preconditioning: the influence of the composition of myocardial phospholipids, Mol. Cell. Biochem. 145 (1) (1995) 69–73.
[15] S. Pepe, P.L. McLennan, Cardiac membrane fatty acid composition modulates myocardial oxygen consumption and postischemic recovery of contractile function, Circulation 105 (19) (2002) 2303–2308.
[16] J. McGuinness, T.G. Neilan, A. Sharkasi, D. Bouchier-Hayes, J.M. Redmond, Myocardial protection using an omega-3 fatty acid infusion: quantification and mechanism of action, J. Thorac. Cardiovasc. Surg. 132 (1) (2006) 72–79.
[17] G.G. Abdukeyum, A.J. Owen, P.L. McLennan, Dietary (n-3) long-chain polyunsaturated fatty acids inhibit ischemia and reperfusion arrhythmias and infarction in rat heart not enhanced by ischemic preconditioning, J. Nutr. 138 (10) (2008) 1902–1909.
[18] S. Zeghichi-Hamri, M. de Lorgeril, P. Salen, M. Chibane, J. de Leiris, F. Boucher, F. Laporte, Protective effect of dietary n-3 polyunsaturated fatty acids on myocardial resistance to ischemia–reperfusion injury in rats, Nutr. Res. 30 (12) (2010) 849–857.
[19] I. Rondeau, S. Picard, T.M. Bah, L. Roy, R. Godbout, G. Rousseau, Effects of different dietary ω-6/3 polyunsaturated fatty acids ratios on infarct size and the limbic system after myocardial infarction, Can. J. Physiol. Pharmacol. 89 (3) (2011) 169–176.
[20] B. Heydari, S. Abdullah, J.V. Pottala, R. Shah, S. Abbasi, D. Mandry, S.A. Francis, H. Lumish, B.B. Ghoshhajra, U. Hoffmann, E. Appelbaum, J.H. Feng, R. Blankstein, M. Steigner, J.P. McConnell, W. Harris, E.M. Antman, M. Jerosch-Herold, R.Y. Kwong, Effect of omega-3 acid ethyl esters on left ventricular remodeling after acute myocardial infarction: the OMEGA-REMODEL randomized clinical trial, Circulation 134 (5) (2016) 378–391.
[21] L. Hodson, C.M. Skeaff, B.A. Fielding, Fatty acid composition of adipose tissue and blood in humans and its use as a biomarker of dietary intake, Prog. Lipid Res. 47 (5) (2008) 348–380.
[22] W.S. Harris, S.A. Sands, S.L. Windsor, H.A. Ali, T.L. Stevens, A. Magalski, C.B. Porter, A.M. Borkon, Omega-3 fatty acids in cardiac biopsies from heart transplantation patients: correlation with erythrocytes and response to supplementation, Circulation 110 (12) (2004) 1645–1649.
[23] R.G. Metcalf, L.G. Cleland, R.A. Gibson, K.C. Roberts-Thomson, J.R. Edwards, P. Sanders, R. Stuklis, M.J. James, G.D. Young, Relation between blood and atrial fatty acids in patients undergoing cardiac bypass surgery, Am. J. Clin. Nutr. 91 (3) (2010) 528–534.
[24] H. Aarsetoey, R. Aarsetoey, T. Lindner, H. Staines, W.S. Harris, D.W. Nilsen, Low levels of the omega-3 index are associated with sudden cardiac arrest and remain stable in survivors in the subacute phase, Lipids 46 (2) (2011) 151–161.
[25] C.M. Kramer, M.J. Budoff, Z.A. Fayad, et al., American College of Cardiology Foundation, American Heart Association, American College of Physicians Task Force on Clinical Competence and Training, ACCF/AHA 2007 clinical competence statement on vascular imaging with computed tomography and magnetic resonance: a report of the American College of Cardiology Foundation/American Heart Association/

American College of Physicians Task Force on Clinical Competence and Training: developed in collaboration with the Society of Atherosclerosis Imaging and Prevention, the Society for Cardiovascular Angiography and Interventions, the Society of Cardiovascular Computed Tomography, the Society for Cardiovascular Magnetic Resonance, and the Society for Vascular Medicine and Biology, Circulation 116 (11) (2007) 1318–1335.

[26] B. Ibanez, V. Fuster, C. Macaya, et al., Study design for the "effect of METOprolol in CARDioproteCtioN during an acute myocardial InfarCtion" (METOCARD-CNIC): a randomized, controlled parallel-group, observer-blinded clinical trial of early pre-reperfusion metoprolol administration in ST-segment elevation myocardial infarction, Am. Heart J. 164 (4) (2012) 473–480.

[27] B. Ibanez, C. Macaya, V. Sánchez-Brunete, et al., Effect of early metoprolol on infarct size in ST-segment-elevation myocardial infarction patients undergoing primary percutaneous coronary intervention: the effect of metoprolol in cardioprotection during an acute myocardial infarction (METOCARD-CNIC) trial, Circulation 128 (14) (2013) 1495–1503.

[28] G. Pizarro, L. Fernández-Friera, V. Fuster, et al., Long-term benefit of early pre-reperfusion metoprolol administration in patients with acute myocardial infarction: results from the METOCARD-CNIC trial (effect of metoprolol in Cardioprotection during an acute myocardial infarction), J. Am. Coll. Cardiol. 63 (22) (2014) 2356–2362.

[29] A. Sala-Vila, W.S. Harris, M. Cofán, A.M. Pérez-Heras, X. Pintó, R.M. Lamuela-Raventós, M.I. Covas, R. Estruch, E. Ros, Determinants of the omega-3 index in a Mediterranean population at increased risk for CHD, Br. J. Nutr. 106 (3) (2011) 425–431.

[30] J.D. Fernández-Ballart, J.L. Piñol, I. Zazpe, D. Corella, P. Carrasco, E. Toledo, M. Perez-Bauer, M.A. Martínez-González, J. Salas-Salvadó, J.M. Martín-Moreno, Relative validity of a semi-quantitative food-frequency questionnaire in an elderly Mediterranean population of Spain, Br. J. Nutr. 103 (12) (2010) 1808–1816.

[31] O. Moreiras, A. Carbajal, L. Cabrera, C. Cuadrado, Tablas de Composición de Alimentos (Food Composition Tables), Ediciones Pirámide, S.A, Madrid, 2005.

[32] E.F. Long, G.W. Swain, A.A. Mangi, Comparative survival and cost-effectiveness of advanced therapies for end-stage heart failure, Circ. Heart Fail. 7 (3) (2014) 470–478.

[33] W.S. Harris, R.M. Thomas, Biological variability of blood omega-3 biomarkers, Clin. Biochem. 43 (3) (2010) 338–340.

[34] K.T. Keyes, Y. Ye, Y. Lin, C. Zhang, J.R. Perez-Polo, P. Gjorstrup, Y. Birnbaum, Resolvin E1 protects the rat heart against reperfusion injury, Am. J. Physiol. Heart Circ. Physiol. 299 (1) (2010) H153–H164.

[35] J. Dyerberg, H.O. Bang, E. Stoffersen, S. Moncada, J.R. Vane, Eicosapentaenoic acid and prevention of thrombosis and atherosclerosis? Lancet 2 (8081) (1978) 117–119.

[36] M. Nodera, H. Suzuki, S. Yamada, M. Kamioka, T. Kaneshiro, Y. Kamiyama, Y. Takeishi, Association of serum n-3/n-6 polyunsaturated fatty acid ratio with T-wave alternans in patients with ischemic heart disease, Int. Heart J. 56 (6) (2015) 613–617.

[37] M. Ueeda, T. Doumei, Y. Takaya, N. Ohnishi, A. Takaishi, S. Hirohata, T. Miyoshi, R. Shinohata, S. Usui, S. Kusachi, Association of serum levels of arachidonic acid and eicosapentaenoic acid with prevalence of major adverse cardiac events after acute myocardial infarction, Heart Vessel. 26 (2) (2011) 145–152.

[38] T. Domei, H. Yokoi, S. Kuramitsu, et al., Ratio of serum n-3 to n-6 polyunsaturated fatty acids and the incidence of major adverse cardiac events in patients undergoing percutaneous coronary intervention, Circ. J. 76 (2) (2012) 423–429.

[39] A.A. Welch, E. Lund, P. Amiano, et al., Variability of fish consumption within the 10 European countries participating in the European Investigation into Cancer and Nutrition (EPIC) study, Public Health Nutr. 5 (6B) (2002) 1273–1285.

[40] J. Perk, G. De Backer, H. Gohlke, et al., European guidelines on cardiovascular disease prevention in clinical practice (version 2012). The Fifth Joint Task Force of the European Society of Cardiology and Other Societies on Cardiovascular Disease Prevention in Clinical Practice (constituted by representatives of nine societies and by invited experts). Developed with the special contribution of the European Association for Cardiovascular Prevention & Rehabilitation (EACPR), Eur. Heart J. 33 (13) (2012) 1635–1701;
Erratum inEur. Heart J. 33 (17) (2012) 2126.

3.3 Chapter III. Temporal dynamics and pathophysiology of the edematous response after myocardial infarction

A similar translational strategy as described before was followed for the research work performed to study the temporal dynamics and pathophysiology of the edematous response after MI. The overall research hypothesis emerged after the preliminary observation that the visualization of the post-MI edema qualitatively varied among individuals in the experimental setting.

In this process, we initially performed an in vivo validation of a CMR sequence for fast and accurate myocardial T2 mapping (T2 gradient-spin-echo [GraSE]) that could be easily integrated in routine protocols, and used in our subsequent experimental and clinical work for an accurate quantification and tracking of myocardial edema. This study represents the first validation of any parametric T2 sequence for myocardial water quantification against the gold standard. As a result, we have contributed to the literature with the following original research article for which I am the first author.

> Original research article #3. "*Fast T2 gradient-spin-echo (T2-GraSE) mapping for myocardial edema quantification: first in vivo validation in a porcine model of ischemia/reperfusion*".[69]

Then, we challenged the accepted view of the development of post-I/R myocardial edema in the preclinical setting. Through state-of-the-art CMR analysis and histological validation in a pig model of I/R, we showed for the first time that the edematous reaction during the first week after reperfusion is not stable, instead follows a bimodal pattern. As a result, we have contributed to the literature with the following original research article for which I am the first author.

> Original research article #4. "*Myocardial edema after ischemia/reperfusion is not stable and follows a bimodal pattern: imaging and histological tissue characterization*".[70]

Later, we studied the pathophysiology underlying the bimodal edematous reaction after MI in the preclinical setting. For such a purpose, a series of experiments were

designed including (1) a variety of strategies to modulate post-MI tissue composition (short-duration ischemia, permanent coronary occlusion, systemic administration of steroids, and coronary pre- and post-conditioning); (2) in-depth tissue characterization by CMR; (3) different time points for imaging and sample collection within the first week after MI; and (4) myocardial characterization at the cellular and molecular level by the use of histology, immunohistochemistry and proteomic tissue analysis. As a result, we have contributed to the literature with 3 original research articles for which I am first or co-first author. The work on proteomic myocardial tissue analysis after MI is only mentioned here and the manuscript is not included as part of this dissertation since the doctoral candidate is co-first author as second position in the manuscript.[71]

Original research article #5. "P*athophysiology underlying the bimodal edema phenomenon after myocardial ischemia/reperfusion*".[72]

Original research article #6. "*Effect of ischemia duration and protective interventions on the temporal dynamics of tissue composition after myocardial infarction*".[73]

Finally, we challenged the accepted view of the development of post-I/R myocardial edema in the clinical setting in a collaborative effort with researchers located at the *Hospital Universitario de Salamanca*. Thus, we were able to demonstrate for the first time that post-MI edema in patients follows a bimodal pattern that affects CMR estimates of MaR and salvage. Remarkably, CMR scans timing and sequences were designed as per protocol of our previous preclinical studies, becoming the first comprehensive evaluation of patients with ST-segment elevation MI by serial CMR to include the hyperacute postreperfusion period (i.e. the first 3 hours after primary PCI). During the analysis and writing phases of this work, the doctoral student performed a multidisciplinary training program that included the use and post-processing of cardiovascular imaging techniques at Mount Sinai Hospital (New York, United States of America) which complemented the skills and knowledge previously acquired. As a result, we have contributed to the literature with the following original research article for which I am the first author.

Original research article #7. "*Dynamic edematous response of the human heart to myocardial infarction: implications for assessing myocardial area at risk and salvage*".[74]

The results presented in this thesis work have received great attention. Thus, part of the work described here has been presented by the doctoral student in renowned international scientific congresses. Similarly, the demonstration of a bimodal edema phenomenon in the post-ischemic myocardium in pigs, and then in humans, has generated an ongoing intense controversy in the scientific community as it will be discussed later. As a result, we have contributed to the literature with 4 letters to the editor so far for which I am the first author.

Letter to the Editor #1. "*Reply: myocardial edema should be stratified according to the state of cardiomyocytes within the ischemic region*".[75]

Letter to the Editor #2. "*Reply: myocardial salvage, area at risk by T2W CMR: the resolution of the retrospective radio wave paradigm?*".[76]

Letter to the Editor #3. "*Reply: waves of edema seem implausible*".[77]

Letter to the Editor #4. "*Letter by Fernandez-Jimenez et al regarding article, Protective effects of ticagrelor on myocardial injury after infarction*".[78]

For the scientific documents published and contained in this chapter, I contributed as doctoral student in the following: design and plan the preclinical experiments and clinical study, develop and perform the different models of MI in the pig, collect and process myocardial tissue samples for subsequent analysis, CMR imaging acquisition and analysis, statistical analysis, draft the manuscript, and elaborate and make critical input in the peer review process.

Original research article #3. "*Fast T2 gradient-spin-echo (T2-GraSE) mapping for myocardial edema quantification: first in vivo validation in a porcine model of ischemia/reperfusion*".[69]

Part of this work was presented by the doctoral student at the 64th American College of Cardiology´s Annual Scientific Sessions, in San Diego (March 2015; California, USA). The communication received the *Best Abstract Award*: "the American College of Cardiology and the Spanish Society of Cardiology recognized Rodrigo Fernandez-Jimenez as first author of the highest ranking abstract submitted from Spain and accepted for presentation at the American College of Cardiology´s Annual Scientific Sessions in San Diego (March 2015; California, USA)".

Fernández-Jiménez et al. Journal of Cardiovascular Magnetic Resonance (2015) 17:92
DOI 10.1186/s12968-015-0199-9

Journal of Cardiovascular Magnetic Resonance

RESEARCH Open Access

Fast T2 gradient-spin-echo (T2-GraSE) mapping for myocardial edema quantification: first in vivo validation in a porcine model of ischemia/reperfusion

Rodrigo Fernández-Jiménez[1,2†], Javier Sánchez-González[1,3†], Jaume Aguero[1], María del Trigo[1], Carlos Galán-Arriola[1], Valentin Fuster[1,4] and Borja Ibáñez[1,5*]

Abstract

Background: Several T2-mapping sequences have been recently proposed to quantify myocardial edema by providing T2 relaxation time values. However, no T2-mapping sequence has ever been validated against actual myocardial water content for edema detection. In addition, these T2-mapping sequences are either time-consuming or require specialized software for data acquisition and/or post-processing, factors impeding their routine clinical use. Our objective was to obtain in vivo validation of a sequence for fast and accurate myocardial T2-mapping (T2 gradient-spin-echo [GraSE]) that can be easily integrated in routine protocols.

Methods: The study population comprised 25 pigs. Closed-chest 40 min ischemia/reperfusion was performed in 20 pigs. Pigs were sacrificed at 120 min ($n = 5$), 24 h ($n = 5$), 4 days ($n = 5$) and 7 days ($n = 5$) after reperfusion, and heart tissue extracted for quantification of myocardial water content. For the evaluation of T2 relaxation time, cardiovascular magnetic resonance (CMR) scans, including T2 turbo-spin-echo (T2-TSE, reference standard) mapping and T2-GraSE mapping, were performed at baseline and at every follow-up until sacrifice. Five additional pigs were sacrificed after baseline CMR study and served as controls.

Results: Acquisition of T2-GraSE mapping was significantly (3-fold) faster than conventional T2-TSE mapping. Myocardial T2 relaxation measurements performed by T2-TSE and T2-GraSE mapping demonstrated an almost perfect correlation ($R^2 = 0.99$) and agreement with no systematic error between techniques. The two T2-mapping sequences showed similarly good correlations with myocardial water content: $R^2 = 0.75$ and $R^2 = 0.73$ for T2-TSE and T2-GraSE mapping, respectively.

Conclusions: We present the first in vivo validation of T2-mapping to assess myocardial edema. Given its shorter acquisition time and no requirement for specific software for data acquisition or post-processing, fast T2-GraSE mapping of the myocardium offers an attractive alternative to current CMR sequences for T2 quantification.

Keywords: Cardiovascular magnetic resonance, T2-mapping, Imaging, Myocardial infarction, Edema, Water content

* Correspondence: bibanez@cnic.es
†Equal contributors
[1]Centro Nacional de Investigaciones Cardiovasculares Carlos III (CNIC), Madrid, Spain
[5]Department of Cardiology, Instituto de Investigación Sanitaria, Fundación Jiménez Díaz Hospital, Madrid, Spain
Full list of author information is available at the end of the article

Background

Cardiovascular magnetic resonance (CMR) has emerged as a popular and useful tool for noninvasive myocardial tissue characterization [1]. CMR provides valuable anatomical and functional information through high spatial resolution images and soft tissue contrast, without exposing patients to ionizing radiation. There is particular interest in using CMR to detect and track myocardial water content, because edema is a feature of many cardiovascular conditions [2–4]. T2-weighted (T2W) CMR sequences have been used for this task [5], but several problems inherent to these sequences have limited the widespread acceptance of this sequence to detect edema [6]. New T2-mapping sequences have recently been proposed to overcome some of these limitations [7–10] and provide absolute quantification of myocardial T2 relaxation times that can be compared among studies, the reference standard being T2 turbo-spin-echo (T2-TSE) [11, 12]. However, these methods are either time-consuming or require specialized software for data acquisition and/or post-processing, factors which limit their routine clinical use.

It is noteworthy that no T2-mapping sequence has ever been validated for quantification of myocardial water content against direct measurement by a gold standard technique. The validity of T2-mapping sequences for this task has been assumed based on their ability to retrospectively delineate the hypoperfused myocardial territory supplied by the occluded coronary artery (the area at risk). However, regional T2 relaxation time in the post-ischemia/reperfusion area is affected by tissue characteristics [13, 14], the application of cardioprotective therapies [15, 16], and the timing of image acquisition [17], and therefore the evidence supporting the validity of T2-mapping for myocardial edema quantification is weak.

In this study, we sought to provide in vivo validation of a sequence for fast and accurate T2-mapping of the myocardium using the gradient-spin-echo (GraSE) technique [18], which could be rapidly and easily integrated in daily protocols as it is commercially available from many vendors. To achieve this goal, we used a closed-chest pig model of ischemia/reperfusion in which animals were serially scanned and sacrificed at different time-points after reperfusion for direct quantification of myocardial water content.

Methods

General considerations and study design

Experimental procedures were performed in castrated male Large-White pigs weighing 30 to 40 kg. The study population comprised a total of 25 pigs. The experimental protocol was approved by the Institutional Animal Research Committee and conducted in accordance with recommendations of the Guide for the Care and Use of Laboratory Animals. The study design is summarized in Fig. 1. Briefly, reperfused acute myocardial infarction was induced in 20 pigs by closed-chest 40-min left anterior descending coronary artery occlusion followed by reperfusion. Pigs were sacrificed at 120 min ($n = 5$, Group 2), 24 h ($n = 5$, Group 3), 4 days ($n = 5$, Group 4) and 7 days ($n = 5$, Group 5) after reperfusion. CMR scans, including T2-TSE mapping (current standard) and T2-GraSE mapping sequences were performed at every follow-up until sacrifice (animals sacrificed at day 7 thus underwent baseline, 120 min, 24 h, day 4, and day 7 CMR). Five pigs (Group 1) were sacrificed with no other intervention than baseline CMR, and served as controls (healthy non-infarcted heart). Animals were sacrificed immediately after the last follow-up CMR, and myocardial tissue samples from ischemic and remote areas were rapidly collected for determination of water content.

Myocardial infarction procedure

The protocol of ischemia/reperfusion has been detailed elsewhere [17]. In summary, anesthesia was induced by intramuscular injection of ketamine (20 mg/kg), xylazine (2 mg/kg), and midazolam (0.5 mg/kg) and maintained by continuous intravenous infusion of ketamine (2 mg/kg/h), xylazine (0.2 mg/kg/h) and midazolam (0.2 mg/kg/h). All animals were intubated and mechanically ventilated with oxygen (inspired O_2 28 %). Central venous and arterial lines were placed and a single bolus of unfractioned heparin (300 mg/kg) was administered before any further procedure. The left anterior descending coronary artery immediately distal to the origin of the first diagonal branch was occluded for 40 min with an angioplasty balloon introduced thorough a catheter inserted via the percutaneous femoral route. Balloon location and state of inflation were monitored angiographically. After balloon deflation, a coronary angiogram was recorded to confirm patency of the coronary artery. A continuous infusion of amiodarone (300 mg/h) was maintained during the procedure in all pigs to prevent malignant ventricular arrhythmias. In cases of ventricular fibrillation, a biphasic defibrillator was used to deliver non-synchronized shocks. At intermediate follow-up time points, animals were recovered and cared for by a dedicated team of veterinarians and technicians.

CMR protocol

Baseline CMR was performed immediately before myocardial infarction and subsequently repeated at post-infarction follow-up time points until sacrifice. All scans were performed during free breathing in a Philips 3-T Achieva Tx whole body scanner (Philips Healthcare, Best, the Netherlands) equipped with a 32-element phased-array cardiac coil. The imaging protocol included a standard segmented cine steady-state free-precession

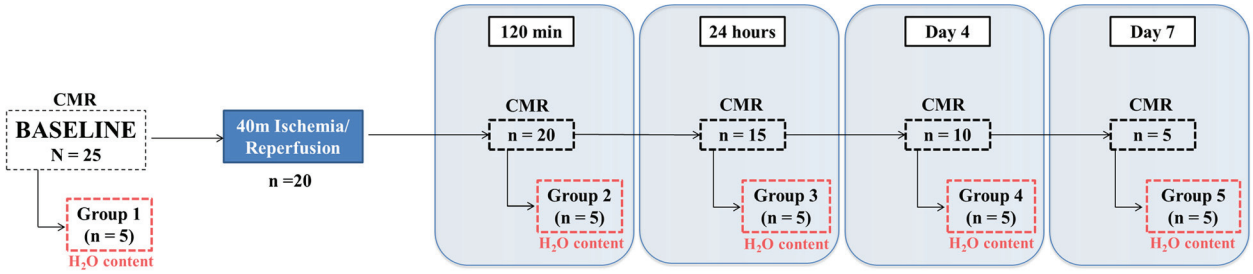

Fig. 1 Study design. The study population comprised 5 groups of pigs ($n = 5$/group). Groups 2 to 5 were subjected to 40 min ischemia/reperfusion (I/R) and were sacrificed at different time-points during the first week after reperfusion and heart tissue extracted for direct quantification of myocardial water content. Five pigs (Group 1) were sacrificed with no intervention other than baseline cardiovascular magnetic resonance (CMR), and served as controls. CMR scans including T2-TSE and T2-GraSE mapping sequences were performed at all follow-up stages until sacrifice, so that animals sacrificed at day 7 underwent baseline, 120 min, 24 h, day 4 and day 7 CMR

(SSFP) sequence to provide high quality anatomical references, a T2- turbo spin multi-echo mapping sequence (T2-TSE), and a T2- gradient spin echo mapping sequence (T2-GraSE). The imaging parameters for the SSFP sequence were FOV of 280x280, slice thickness of 6 mm with no gap, TR 2.8 ms, TE 1.4 ms, flip angle 45°, cardiac phases 30, voxel size 1.8×1.8 mm^2, and 3 NEX. The imaging parameters for the T2-TSE mapping were FOV 300×300 with and acquisition voxel size of 1.8×1.8 mm^2 and slice thickness 8 mm, TR 2 heartbeats, and ten echo times ranging from 4.9 to 49 ms. The imaging parameters for the T2-GraSE mapping were FOV 300×300 with an acquisition voxel size of 1.8×2.0 mm^2 and slice thickness 8 mm, TR 2 heartbeats, and eight echo times ranging from 6.7 to 53.6 ms, EPI factor 3. Both T2 mapping sequence where black blood triggered with a trigger delay placed at mid-diastole. Both T2-mapping sequences are schematized in Fig. 2. SSFP was performed to acquire 13–15 contiguous short axis slices covering the heart from the base to the apex, whereas T2-maps were acquired in a mid-apical ventricular short axis slice corresponding to the same anatomical level in all studies, in order to track T2 relaxation time changes across time.

CMR data analysis

CMR images were analyzed using dedicated software (MR Extended Work Space 2.6, Philips Healthcare, The Netherlands). T2-maps were automatically generated on the acquisition scanner by fitting the SI of all echo times to a monoexponential decay curve at each pixel with a maximum likelihood expectation maximization algorithm. T2 relaxation maps were quantitatively analyzed by placing a wide transmural region of interest (ROI) at the ischemic and remote areas of the corresponding slice in all studies. The masking was defined in the first echo image to improve the contrast between the cardiac muscle and the cavity. Higher T2 values in this interface can be found due to slow flow artifact; therefore, ROIs were carefully placed avoiding those areas from the analysis to minimize contamination on the reported T2 values. Hypointense areas suggestive of microvascular obstruction or hemorrhage were included in the ROI for T2 quantification purposes.

Quantification of myocardial water content

Paired myocardial samples were collected within the first 5 min of sacrifice from the infarcted and remote myocardium of all pigs. Tissue samples were immediately blotted to remove surface moisture and introduced into glass containers previously weighed on a high-precision scale. The containers were weighed before and after drying for 48 h at 100 °C in a desiccating oven. Tissue water content was calculated as follows: water content (%) = [(wet weight – dry weight)/wet weight] × 100. An empty container was weighed before and after desiccation as an additional calibration control.

Statistical analysis

Normal distribution was checked using graphical methods and a Shapiro-Wilk test. For quantitative variables showing a normal distribution, data are expressed as mean ± standard deviation. For quantitative variables showing a non-normal distribution, data are reported as medians with first and third quartiles. Agreement of T2 relaxation time measurements between T2-TSE and T2-GraSE mapping techniques was evaluated by the square of Pearson's correlation coefficient, the intraclass correlation coefficient for two-way random effect models, and Bland-Altman analysis [19]. Association between T2 relaxation time measurements performed by T2-TSE and T2-GraSE, and water content was evaluated by the square of Pearson's correlation coefficient. The significance of the difference between these correlation coefficients was performed using the Fisher r-to-z transformation and the *cortesti* user-written command for Stata. Statistical significance was set at a two-tailed probability

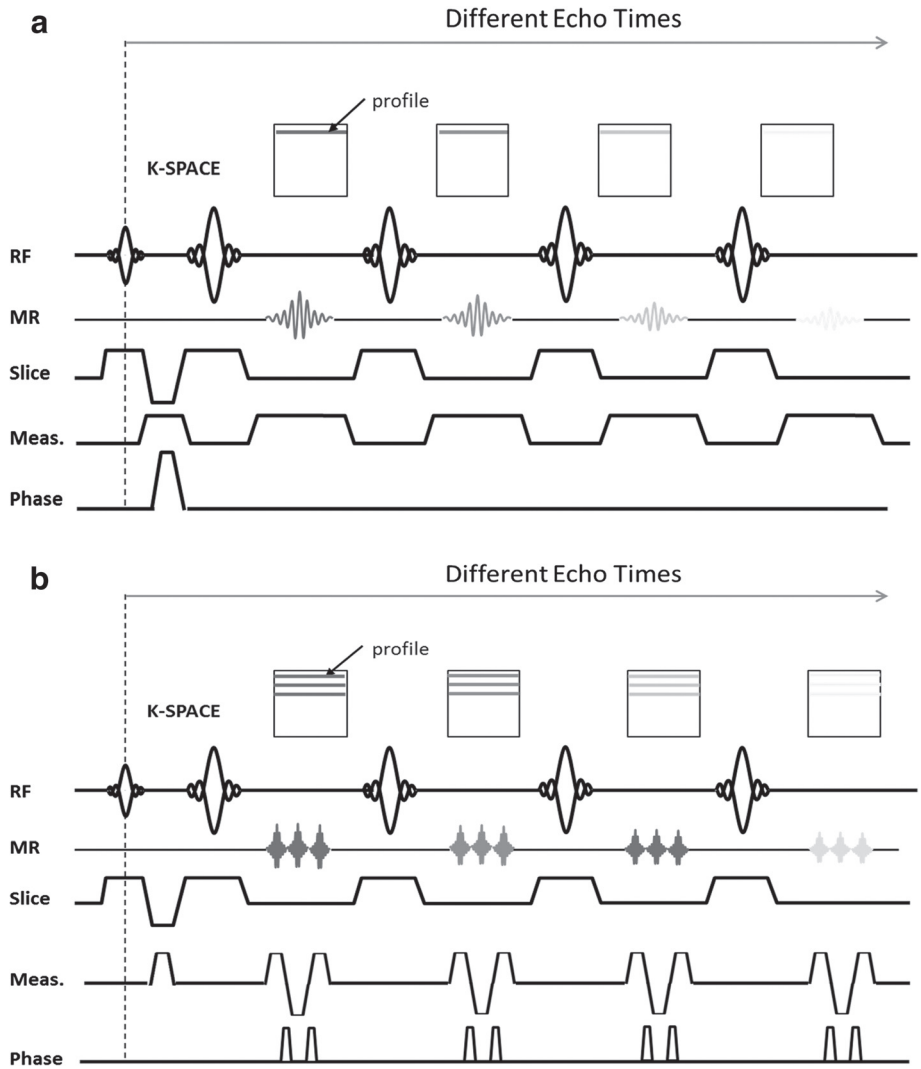

Fig. 2 Detail of T2-TSE and T2-GraSE mapping sequences. General scheme of Turbo Spin Echo (TSE) and Gradient Spin Echo (GraSE) mapping sequences. For the TSE a single k-space line is acquired for every excitation requiring as many excitations as k-space lines in the image (**a**). Conversely, for the GraSE sequence an echo planar imaging (EPI) readout is interleaved between each refocusing pulse, so that as many k-space lines are acquired as there are EPI factors, thus allowing shorter scan times (**b**). RF: radiofrequency pulse. MR: magnetic resonance signal. Meas.: measurement encoding

level of 0.05. All statistical analyses were performed using commercially available software (Stata 12.0). The authors had full access to the data and take responsibility for its integrity.

Results

Duration of sequence acquisition and T2 relaxation time measurements performed by T2-TSE and T2-GraSE mapping

Mean study acquisition length was 189 ± 19 s for T2-TSE mapping and 65 ± 8 s for T2-GraSE mapping ($p < 0.001$). T2 relaxation time measurements obtained by T2-TSE and T2-GraSE mapping at different follow-up points in the ischemic and remote myocardium are summarized in Table 1 and Table 2, respectively.

Agreement of T2 relaxation time measurements performed by T2-TSE and T2-GraSE mapping

T2 relaxation time measurements obtained by T2-TSE mapping and T2-GraSE mapping showed almost perfect correlation ($R^2 = 0.99$, Fig. 3a). Intraclass correlation coefficients (ICC) evaluating absolute agreement and consistency of agreement between both T2 mapping techniques showed an excellent concordance between sequences (ICC > 0.96 for all evaluations, Table 3). Bland-Altman analysis showed a good agreement between sequences (Fig. 3b). Representative T2-mapping images obtained by T2-TSE and T2-GraSE from the same pig subjected to 40 min of ischemia and 7 days of reperfusion are shown in Fig. 4.

Table 1 T2 relaxation time (ms) in the ischemic myocardium measured by T2-TSE and T2-GraSE mapping sequences at different time-points during the first week after ischemia/reperfusion

T2 relaxation time (ms)						
		Baseline	R-120 min	R-24 h	R-Day4	R-Day7
Group 1 (Control)	TSE	47.7 (4.0)				
	GraSE	48.0 (4.7)				
Group 2 (I/R-120 min)	TSE	48.7 (0.6)	73.3 (10.0)			
	GraSE	49.9 (2.5)	76.5 (7.8)			
Group 3 (I/R-24 h)	TSE	46.5 (1.9)	72.4 (12.3)	45.9 (5.3)		
	GraSE	48.3 (4.8)	73.9 (10.0)	42.9 (4.5)		
Group 4 (I/R-4 days)	TSE	45.9 (1.6)	73.5 (4.2)	42.7 (9.3)	55.1 (13.2)	
	GraSE	45.0 (3.7)	78.7 (10.8)	42.6 (8.5)	54.3 (14.1)	
Group 5 (I/R-7 days)	TSE	47.2 (3.5)	72.6 (14.2)	47.0 (2.9)	64.9 (7.9)	78.4 (10.6)
	GraSE	46.5 (3.0)	74.8 (14.4)	46.7 (4.9)	66.4 (8.3)	78.9 (11.7)
Pooled	TSE	47.2 (2.6)	72.9 (9.9)	45.2 (6.2)	60.0 (11.5)	78.4 (10.6)
	GraSE	47.6 (3.9)	76.0 (10.3)	44.1 (6.1)	60.4 (12.6)	78.9 (11.7)

Values are mean (standard deviation). I/R: ischemia/reperfusion. TSE: turbo spin echo. GraSE: gradient spin echo. CMR T2 relaxation times measured by T2-TSE mapping in the ischemic myocardium of these pigs have been reported [17]

Association between T2 relaxation time measurements and directly measured water content

Directly determined myocardial water content showed a good correlation with T2 relaxation time measurements performed by T2-TSE mapping ($R^2 = 0.75$, $p < 0.001$; Fig. 5a) and by T2-GraSE mapping ($R^2 = 0.73$, $p < 0.001$; Fig. 5b). No statistically significant differences between these correlations were observed.

Discussion

In this study we present an in vivo validation of a CMR sequence for fast and accurate T2-mapping of the heart using the gradient-spin-echo (GraSE) technique that can be easily integrated in routine protocols, overcoming some of the limitations of current CMR mapping sequences for myocardial T2 quantification. For this endeavor we developed a closed-chest large animal model of ischemia/reperfusion in which animals had serial CMR scans and were sacrificed at serial time-points after reperfusion for direct quantification of myocardial water content. Two mapping sequences were used to quantify myocardial T2 relaxation time: the well-established reference T2-TSE technique and the newer T2-GraSE technique, which further speeds up the TSE sequence [18].

Table 2 T2 relaxation time (ms) in the remote myocardium measured by T2-TSE and T2-GraSE mapping sequences at different time-points during the first week after ischemia/reperfusion

T2 relaxation time (ms)						
		Baseline	R-120 min	R-24 h	R-Day4	R-Day7
Group 1 (Control)	TSE	46.1 (1.5)				
	GraSE	45.7 (1.8)				
Group 2 (I/R-120 min)	TSE	46.8 (1.8)	47.0 (1.0)			
	GraSE	47.2 (1.6)	48.4 (2.0)			
Group 3 (I/R-24 h)	TSE	46.2 (2.6)	48.6 (3.0)	45.2 (0.6)		
	GraSE	46.8 (1.9)	47.2 (5.2)	44.8 (1.2)		
Group 4 (I/R-4 days)	TSE	45.5 (0.8)	48.3 (4.0)	47.5 (3.1)	48.2 (2.9)	
	GraSE	44.8 (1.1)	45.5 (4.6)	45.9 (3.9)	49.1 (1.4)	
Group 5 (I/R-7 days)	TSE	46.7 (1.5)	48.5 (3.7)	51.4 (5.0)	50.1 (1.8)	50.0 (3.3)
	GraSE	44.6 (2.3)	46.5 (2.9)	51.0 (3.5)	49.0 (1.5)	49.3 (5.0)
Pooled	TSE	46.3 (1.7)	48.1 (3.0)	48.0 (4.1)	49.1 (2.5)	50.0 (3.3)
	GraSE	45.8 (1.9)	47.0 (3.7)	47.2 (4.0)	49.0 (1.4)	49.3 (5.0)

Values are mean (standard deviation). I/R: ischemia/reperfusion. TSE: turbo spin echo. GraSE: gradient spin echo. CMR T2 relaxation times measured by T2-TSE mapping in the remote myocardium of these pigs have been reported [17]

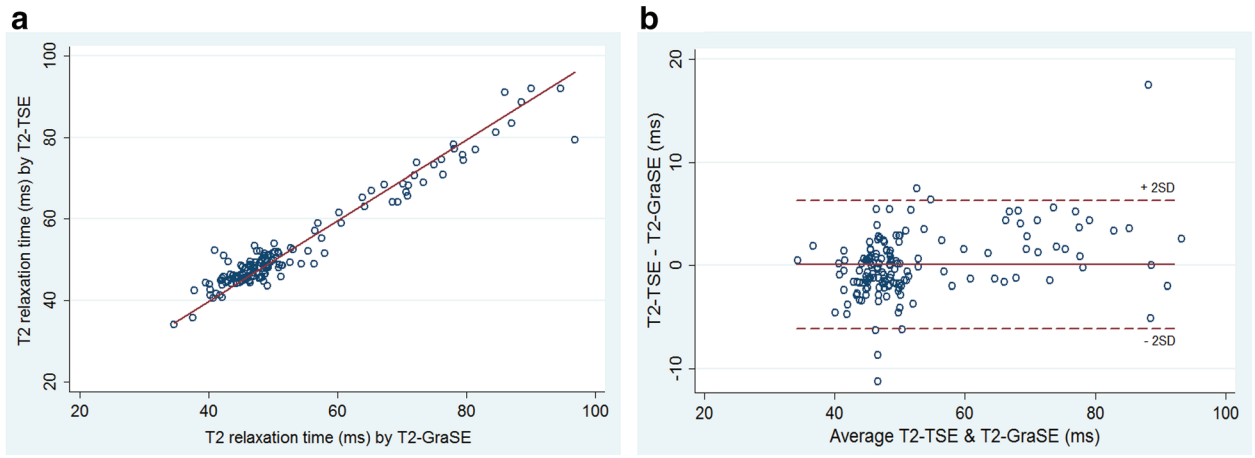

Fig. 3 Assessment of agreement between T2 relaxation times measured by T2-TSE and T2-GraSE mapping. (**a**) Scatter plot showing almost perfect linear correlation ($R^2 = 0.99$) of T2 relaxation times measured by T2-TSE and T2-GraSE mapping. (**b**) Bland-Altman analysis demonstrated excellent agreement between T2 relaxation readings from both T2-mapping sequences. The mean T2 relaxation time difference (T2-GraSE – T2-TSE) was 0.1 ms (agreement interval 95 %: −6.2 to 6.3 ms). The percentages of cases above and below the limits were 2.0 % and 2.7 %. The Spearman correlation coefficient between T2 relaxation time differences (T2-GraSE – T2-TSE) and mean T2 relaxation times (T2-GraSE & T2-TSE) was 0.33 ($p < 0.001$)

The translational pig model of myocardial infarction used in this study allows examination of a wide range of myocardial T2 relaxation times and myocardial water content [17], and produced values that closely mimic those clinically observed in several pathological conditions, strengthening the present validation.

Accurate noninvasive detection and quantification of myocardial edema is of great scientific and clinical interest given the occurrence of edema in several cardiovascular diseases and its usefulness for diagnosis and its correlation with ventricular remodeling and prognosis [20–22]. Many studies over the past decades have investigated the use of CMR with T2-weighted (T2W) sequences to monitor in the post-ischemic myocardium, since this approach is considered especially suited to the detection of high water content in this setting [23]. However, several problems inherent to T2W-CMR have limited the widespread uptake of this sequence for the detection of edema [6]. These problems include variations in surface coil sensitivity, motion artifacts, incomplete blood suppression, and the subjectivity of image interpretation [24].

Table 3 Absolute agreement and consistency of agreement between T2 relaxation times measured by T2-TSE and T2-GraSE mapping

		ICC	95 % CI
Absolute agreement	Individual	0.967	0.954–0.976
	Average	0.982	0.976–0.988
Consistency of agreement	Individual	0.966	0.954–0.976
	Average	0.983	0.977–0.988

ICC: intraclass correlation coefficient. CI: confidence interval. TSE: turbo spin echo. GraSE: gradient spin echo

A number of T2-mapping sequences have been recently proposed as a route to overcoming some of these limitations [7–9] and providing absolute quantification of regional T2 relaxation times that can be compared across studies. However, these methods are either time-consuming or require specialized software for data acquisition and/or post-processing, factors that impede their clinical routine use. Compared with these other approaches, T2-GraSE mapping has many advantages, including an acceptable acquisition time for integration into daily clinical CMR protocols, reduced energy requirements, and the use of standard post-processing methods. In this study, T2-GraSE mapping was 3-times faster than conventional reference standard T2-TSE mapping due to the interleaving of the EPI readout between two consecutive 180° pulses. The applicability of myocardial T2-mapping using the GraSE technique in humans has been reported recently [12, 25]; however, these studies mostly examined healthy hearts and therefore a narrow range of myocardial T2 relaxation times, and did not validate the sequence against directly determined tissue water content. Our study provides robust validation of T2-GraSE over a wide spectrum of myocardial T2 relaxation times and water contents that reflect a range of potential clinical scenarios.

Descriptions of previous T2-mapping sequences have relied on their ability to retrospectively identify the hypoperfused myocardial territory supplied by the occluded coronary artery—the area at risk—and there are no published data validating these techniques against true myocardial water content. Regional T2 relaxation time in the ischemic area can be altered depending on tissue characteristics [13, 14], the application of cardioprotective therapies

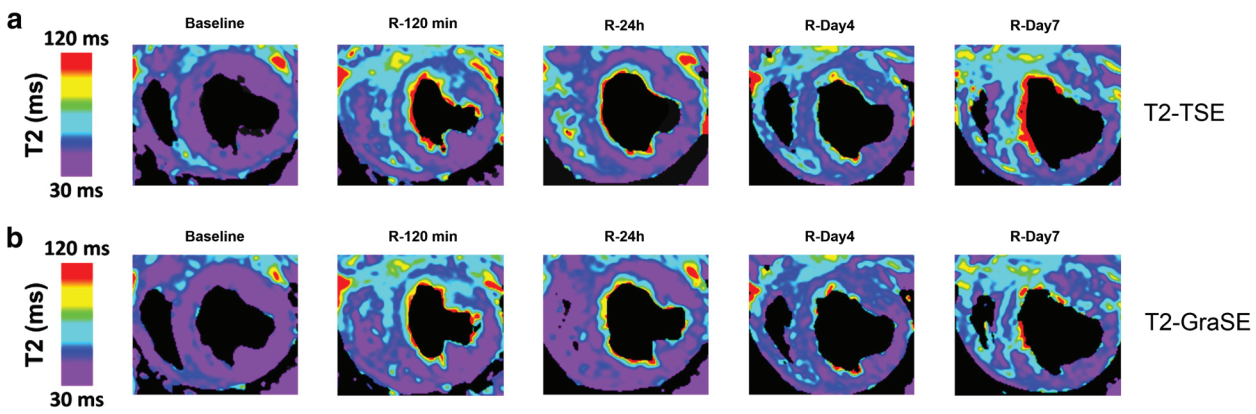

Fig. 4 Representative images of serial T2-TSE and T2-GraSE mapping. Representative T2-mapping images for all time-points from the same pig subjected to 40 min I/R and sacrificed at day 7 after reperfusion. **a** T2-TSE images. **b** T2-GraSE images. All T2 maps were scaled between 30 and 120 ms. All sequences were acquired with black-blood preparation prepulse. For better visualization, generated T2 maps were masked to remove background signal. The masking was defined in the first echo image to improve the contrast between the cardiac muscle and the cavity. R: Reperfusion

[15, 16] or the timing of imaging acquisition [17], highlighting the need of establishing the relationship between T2-mapping and true myocardial water content directly quantified in the tissue. This question has been explored in only a few studies conducted over 20 years ago [26–30], and these studies were performed in low magnetic fields or with excised hearts, factors well known to affect T2 relaxation time [31]. The present study is thus the first to provide in vivo validation of T2-mapping against actual tissue myocardial water content in magnetic fields used in current clinical practice. We believe it is important to assess the association between actual water content and T2 relaxation time at 3 Tesla since no clear relationship has been established between these parameters at different field strength. In this regard, in vitro analysis have demonstrated an increase on myocardial T2 at 3 Tesla systems compared to 1.5Tesla [32], while in-vivo studies suggest equivalent T2 values at 3-Tesla with those previously reported at 1.5 Tesla [33].

Our data demonstrate similarly good correlation between myocardial water content and both T2-mapping techniques examined. In our study ≈ 25-30 % of T2

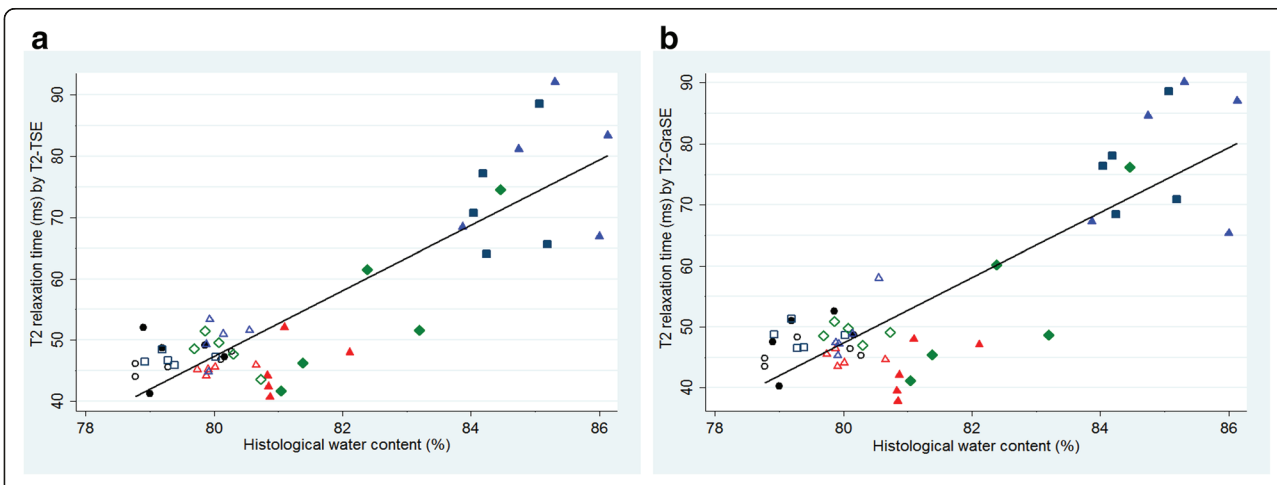

Fig. 5 Association between T2 relaxation time and directly measured water content. **a** Scatter plot demonstrating good correlation between T2 relaxation times measured by T2-TSE mapping and directly measured myocardial water content. **b** Scatter plot demonstrating similarly good correlation between T2 relaxation times measured by T2-GraSE mapping and directly measured myocardial water content. For each panel, individual data represent values from pigs sacrificed at baseline (black circles), 120 min (navy squares), 24 h (red triangles), 4 days (green diamonds) and 7 days (blue triangles) after reperfusion. Solid symbols represent data for ischemic myocardium and hollow symbols represent data for remote myocardium. Therefore, a total of 50 individual points for each correlation are shown which corresponds to two samples per pig (ischemic and remote myocardium) from 5 groups of 5 pigs each sacrificed at the different time-points

relaxation time variance was not completely explained by water content changes, highlighting the influence on T2 values of other tissue characteristics and components [6, 17] including the proportion of free/bound water as well as its location (intracellular/extracellular) in the tissue [34]. These data should be taken into account when interpreting clinical studies using these sequences.

In summary, we provide in vivo validation of a CMR sequence for fast and accurate T2-mapping of the heart using the gradient-spin-echo (GraSE) technique. This approach can be easily integrated in routine protocols since it is available for all equipment, and overcomes some of the limitations of current CMR mapping sequences for T2 quantification.

Limitations

Although tissue changes in the post-I/R myocardium in pigs are similar to those in humans, we cannot rule out the existence of subtle histological differences between human and pig after infarction. As a consequence, the ≈ 30 % of T2 relaxation time variance that was not completely explained by water content changes in the present study might differ slightly from the value in humans. However, experimental studies allow validation, as shown here with the direct quantification of myocardial water content.

The pig is one of the most clinically translatable large animal models for the study of myocardial infarction and related issues due to its anatomical and functional similarities to humans [35], and also shows similar T2 values in the ischemic and remote myocardium to those seen in humans [8, 12].

In this study the ROIs for T2 relaxation time quantification covered the entire wall thickness and were individually adjusted by hand to carefully avoid the right and left ventricular cavities. The ROIs therefore might include different myocardial states (e.g., hemorrhage, microvascular obstruction, collagen) given that reperfused myocardium is a very heterogeneous condition [36]. However, we adopted this approach to match the analysis of water content, which was evaluated in the entire wall thickness. Both T2 mapping sequences did not apply any correction for respiratory motion. However, all scans were performed during free breathing; therefore animals had an abdominal breathing pattern with minimal chest movement in antero-posterior direction minimizing the ghosting artefacts in short axis view. Three-dimensional (3D) T2-mapping sequences have been very recently described and might benefit from higher spatial resolution, therefore reducing partial-volume averaging effects and misregistration between images [37, 38]. However, the proposed implementation of the T2-GraSE mapping can be performed in many modern scanners in a reasonable acquisition time, while 3D T2-mapping normally take longer acquisition times.

Conclusions

We provide the first in vivo validation of T2-mapping for the assessment of myocardial edema. Given its shorter acquisition time, high accuracy in quantifying T2 relaxation time and no requirement for specific software for data acquisition or post-processing, fast T2-GraSE mapping of the heart is an attractive alternative to current CMR sequences for T2 quantification.

Abbreviations

CMR: cardiovascular magnetic resonance; EPI: echo planar imaging; FOV: field of view; GraSE: gradient spin echo; I/R: ischemia/reperfusion; NEX: number of excitations; ROI: region of interest; T2W: T2 weighted; TE: echo time; TR: repetition time; TSE: turbo spin echo.

Competing interests

The authors declare that they have no competing interests.

Authors' contributions

RFJ carried out the experimental procedures, participated in the data analysis and design of the study, performed the statistical analysis and drafted the manuscript. JSG conceived and carried out the application of the sequence, participated in images acquisition and design of the study, and helped to draft the manuscript. JA helped to perform experimental procedures and to draft the manuscript. MT carried out the data analysis, and helped to perform experimental procedures and to draft the manuscript. CGA helped to perform experimental procedures and to draft the manuscript. BI participated in the design of the study. BI and VF coordinated and helped to draft the manuscript. All authors read and approved the final manuscript; and agree to be accountable for all aspects of the work in ensuring that questions related to the accuracy or integrity of any part of the work are appropriately investigated and resolved.

Acknowledgements

We are greatly indebted to Gonzalo J Lopez-Martin who carried out images acquisition. We thank Tamara Córdoba, Oscar Sanz, Eugenio Fernández and other members of the CNIC animal facility and farm for outstanding animal care and support. Simon Bartlett (CNIC) provided English editing.

Funding sources

This work was supported by a competitive grant from the Ministry of Economy and Competitiveness (MINECO) through the Carlos III Institute of Health -Fondo de Investigación Sanitaria (PI13/01979)-, the Fondo Europeo de Desarrollo Regional (FEDER, RD: SAF2013-49663-EXP), and in part by the FP7-PEOPLE-2013-ITN *Next generation training in cardiovascular research and innovation-Cardionext*. Rodrigo Fernández-Jiménez is recipient of a *Rio Hortega* fellowship from the Ministry of Economy and Competitiveness through the *Instituto de Salud Carlos III*, and a FICNIC fellowship from the *Fundació Jesús Serra*, the *Fundación Interhospitalaria de Investigación Cardiovascular* (FIC) and the *Centro Nacional de Investigaciones Cardiovasculares Carlos III* (CNIC). Javier Sánchez-González is an employee of Philips Healthcare. Jaume Aguero is a FP7-PEOPLE-2013-ITN-Cardionext fellow. Carlos Galán-Arriola is recipient of a "Contrato Predoctoral de Formación en *Investigación* en Salud (PFIS), FI14/00356". This study forms part of a Master Research Agreement (MRA) between CNIC and Philips Healthcare. Borja Ibanez is supported by the *Red de Investigación Cardiovascular* (RIC) of the Spanish Ministry of Health (RD 12/0042/0054). The CNIC is supported by the Spanish Ministry of Economy and Competitiveness and the Pro-CNIC Foundation.

Author details

[1]Centro Nacional de Investigaciones Cardiovasculares Carlos III (CNIC), Madrid, Spain. [2]Hospital Universitario Clínico San Carlos, Madrid, Spain. [3]Philips Healthcare, Madrid, Spain. [4]The Zena and Michael A. Wiener CVI, Mount Sinai School of Medicine, New York, NY, USA. [5]Department of Cardiology, Instituto de Investigación Sanitaria, Fundación Jiménez Díaz Hospital, Madrid, Spain.

Received: 18 June 2015 Accepted: 28 October 2015
Published online: 04 November 2015

References

1. Friedrich MG. Tissue characterization of acute myocardial infarction and myocarditis by cardiac magnetic resonance. JACC Cardiovasc Imaging. 2008;1(5):652–62. doi:10.1016/j.jcmg.2008.07.011.
2. Thavendiranathan P, Walls M, Giri S, Verhaert D, Rajagopalan S, Moore S, et al. Improved detection of myocardial involvement in acute inflammatory cardiomyopathies using T2 mapping. Circ Cardiovasc Imaging. 2012;5(1):102–10. doi:10.1161/CIRCIMAGING.111.967836.
3. Usman AA, Taimen K, Wasielewski M, McDonald J, Shah S, Giri S, et al. Cardiac magnetic resonance T2 mapping in the monitoring and follow-up of acute cardiac transplant rejection: a pilot study. Circ Cardiovasc Imaging. 2012;5(6):782–90. doi:10.1161/CIRCIMAGING.111.971101.
4. Zia MI, Ghugre NR, Connelly KA, Strauss BH, Sparkes JD, Dick AJ, et al. Characterizing myocardial edema and hemorrhage using quantitative T2 and T2* mapping at multiple time intervals post ST-segment elevation myocardial infarction. Circ Cardiovasc Imaging. 2012;5(5):566–72. doi:10.1161/CIRCIMAGING.112.973222.
5. Wright J, Adriaenssens T, Dymarkowski S, Desmet W, Bogaert J. Quantification of myocardial area at risk with T2-weighted CMR: comparison with contrast-enhanced CMR and coronary angiography. JACC Cardiovasc Imaging. 2009;2(7):825–31. doi:10.1016/j.jcmg.2009.02.011.
6. Croisille P, Kim HW, Kim RJ. Controversies in cardiovascular MR imaging: T2-weighted imaging should not be used to delineate the area at risk in ischemic myocardial injury. Radiology. 2012;265(1):12–22. doi:10.1148/radiol.12111769.
7. Ugander M, Bagi PS, Oki AJ, Chen B, Hsu LY, Aletras AH, et al. Myocardial edema as detected by pre-contrast T1 and T2 CMR delineates area at risk associated with acute myocardial infarction. JACC Cardiovasc Imaging. 2012;5(6):596–603. doi:10.1016/j.jcmg.2012.01.016.
8. Verhaert D, Thavendiranathan P, Giri S, Mihai G, Rajagopalan S, Simonetti OP, et al. Direct T2 quantification of myocardial edema in acute ischemic injury. JACC Cardiovasc Imaging. 2011;4(3):269–78. doi:10.1016/j.jcmg.2010.09.023.
9. van Heeswijk RB, Feliciano H, Bongard C, Bonanno G, Coppo S, Lauriers N, et al. Free-breathing 3 T magnetic resonance T2-mapping of the heart. JACC Cardiovasc Imaging. 2012;5(12):1231–9. doi:10.1016/j.jcmg.2012.06.010.
10. Salerno M, Kramer CM. Advances in parametric mapping with CMR imaging. JACC Cardiovasc Imaging. 2013;6(7):806–22. doi:10.1016/j.jcmg.2013.05.005.
11. Maudsley AA. Modified Carr-Purcell-Meiboom-Gill sequence for NMR fourier imaging applications. J Magn Reson (1969). 1986;69(3):488–91. http://dx.doi.org/10.1016/0022-2364(86)90160-5.
12. Sprinkart A, Luetkens J, Traber F, Doerner J, Gieseke J, Schnackenburg B, et al. Gradient Spin Echo (GraSE) imaging for fast myocardial T2 mapping. J Cardiovasc Magn Reson. 2015;17(1):12.
13. Mikami Y, Sakuma H, Nagata M, Ishida M, Kurita T, Komuro I, et al. Relation between signal intensity on T2-weighted MR images and presence of microvascular obstruction in patients with acute myocardial infarction. AJR Am J Roentgenol. 2009;193(4):W321–6. doi:10.2214/AJR.09.2335.
14. Lotan CS, Bouchard A, Cranney GB, Bishop SP, Pohost GM. Assessment of postreperfusion myocardial hemorrhage using proton NMR imaging at 1.5 T. Circulation. 1992;86(3):1018–25.
15. Thuny F, Lairez O, Roubille F, Mewton N, Rioufol G, Sportouch C, et al. Post-conditioning reduces infarct size and edema in patients with ST-segment elevation myocardial infarction. J Am Coll Cardiol. 2012;59(24):2175–81. doi:10.1016/j.jacc.2012.03.026.
16. White SK, Frohlich GM, Sado DM, Maestrini V, Fontana M, Treibel TA, et al. Remote Ischemic Conditioning Reduces Myocardial Infarct Size and Edema in Patients With ST-Segment Elevation Myocardial Infarction. JACC Cardiovasc Interv. 2015;8(1):178–88. doi:10.1016/j.jcin.2014.05.015.
17. Fernandez-Jimenez R, Sanchez-Gonzalez J, Aguero J, Garcia-Prieto J, Lopez-Martin GJ, Garcia-Ruiz JM, et al. Myocardial edema after ischemia/reperfusion is not stable and follows a bimodal pattern: imaging and histological tissue characterization. J Am Coll Cardiol. 2015;65(4):315–23. doi:10.1016/j.jacc.2014.11.004.
18. Oshio K, Feinberg DA. GRASE (Gradient- and spin-echo) imaging: a novel fast MRI technique. Magn Reson Med. 1991;20(2):344–9.
19. Bland JM, Altman DG. Statistical methods for assessing agreement between two methods of clinical measurement. Lancet. 1986;1(8476):307–10.
20. Friedrich MG, Kim HW, Kim RJ. T2-weighted imaging to assess post-infarct myocardium at risk. JACC Cardiovasc Imaging. 2011;4(9):1014–21. doi:10.1016/j.jcmg.2011.07.005.
21. Kubanek M, Sramko M, Maluskova J, Kautznerova D, Weichet J, Lupinek P, et al. Novel predictors of left ventricular reverse remodeling in individuals with recent-onset dilated cardiomyopathy. J Am Coll Cardiol. 2013;61(1):54–63. doi:10.1016/j.jacc.2012.07.072.
22. Zagrosek A, Abdel-Aty H, Boye P, Wassmuth R, Messroghli D, Utz W, et al. Cardiac magnetic resonance monitors reversible and irreversible myocardial injury in myocarditis. JACC Cardiovasc Imaging. 2009;2(2):131–8. doi:10.1016/j.jcmg.2008.09.014.
23. Arai AE, Leung S, Kellman P. Controversies in cardiovascular MR imaging: reasons why imaging myocardial T2 has clinical and pathophysiologic value in acute myocardial infarction. Radiology. 2012;265(1):23–32. doi:10.1148/radiol.12112491.
24. Pennell D. Myocardial salvage: retrospection, resolution, and radio waves. Circulation. 2006;113(15):1821–3. doi:10.1161/CIRCULATIONAHA.105.618942.
25. Bonner F, Janzarik N, Jacoby C, Spieker M, Schnackenburg B, Range F, et al. Myocardial T2 mapping reveals age- and sex-related differences in volunteers. J Cardiovasc Magn Reson. 2015;17(1):9. doi:10.1186/s12968-015-0118-0.
26. Boxt LM, Hsu D, Katz J, Detweiler P, McLaughlin S, Kolb TJ, et al. Estimation of myocardial water content using transverse relaxation time from dual spin-echo magnetic resonance imaging. Magn Reson imaging. 1993;11(3):375–83.
27. Scholz TD, Martins JB, Skorton DJ. NMR relaxation times in acute myocardial infarction: relative influence of changes in tissue water and fat content. Magn Reson Med. 1992;23(1):89–95.
28. Wisenberg G, Prato FS, Carroll SE, Turner KL, Marshall T. Serial nuclear magnetic resonance imaging of acute myocardial infarction with and without reperfusion. Am Heart J. 1988;115(3):510–8.
29. Garcia-Dorado D, Oliveras J, Gili J, Sanz E, Perez-Villa F, Barrabes J, et al. Analysis of myocardial oedema by magnetic resonance imaging early after coronary artery occlusion with or without reperfusion. Cardiovasc Res. 1993;27(8):1462–9.
30. Higgins CB, Herfkens R, Lipton MJ, Sievers R, Sheldon P, Kaufman L, et al. Nuclear magnetic resonance imaging of acute myocardial infarction in dogs: alterations in magnetic relaxation times. Am J Cardiol. 1983;52(1):184–8.
31. Liu P, Johnston DL, Brady TJ, Lutrario DM, Okada RD. The alterations of magnetic resonance relaxation parameters in excised myocardial tissue during NMR spectroscopy: the effects of time, environmental exposure and TTC staining. Magn Reson Imaging. 1989;7(1):109–13.
32. Stanisz GJ, Odrobina EE, Pun J, Escaravage M, Graham SJ, Bronskill MJ, et al. T1, T2 relaxation and magnetization transfer in tissue at 3T. Magn Reson Med. 2005;54(3):507–12. doi:10.1002/mrm.20605.
33. von Knobelsdorff-Brenkenhoff F, Prothmann M, Dieringer MA, Wassmuth R, Greiser A, Schwenke C, et al. Myocardial T1 and T2 mapping at 3 T: reference values, influencing factors and implications. J Cardiovasc Magn Reson. 2013;15:53. doi:10.1186/1532-429X-15-53.
34. Eitel I, Friedrich MG. T2-weighted cardiovascular magnetic resonance in acute cardiac disease. J Cardiovasc Magn Reson. 2011;13:13. doi:10.1186/1532-429X-13-13.
35. Fernández-Jiménez R, Fernández-Friera L, Sánchez-González J, Ibáñez B. Animal Models of Tissue Characterization of Area at Risk, Edema and Fibrosis. Curr Cardiovasc Imaging Rep. 2014;7(4):1–10. doi:10.1007/s12410-014-9259-z.
36. Fernandez-Jimenez R, Garcia-Prieto J, Sanchez-Gonzalez J, Aguero J, Lopez-Martin GJ, Galan-Arriola C, et al. Pathophysiology Underlying the Bimodal Edema Phenomenon After Myocardial Ischemia/Reperfusion. J Am Coll Cardiol. 2015;66(7):816–28. doi:10.1016/j.jacc.2015.06.023.
37. Ding H, Fernandez-de-Manuel L, Schar M, Schuleri KH, Halperin H, He L, et al. Three-dimensional whole-heart T2 mapping at 3T. Magn Reson Med. 2015;74(3):803–16. doi:10.1002/mrm.25458.
38. van Heeswijk RB, Piccini D, Feliciano H, Hullin R, Schwitter J, Stuber M. Self-navigated isotropic three-dimensional cardiac T2 mapping. Magn Reson Med. 2015;73(4):1549–54. doi:10.1002/mrm.25258.

Original research article #4. “*Myocardial edema after ischemia/reperfusion is not stable and follows a bimodal pattern: imaging and histological tissue characterization*”.[70]

Part of this work was presented by the doctoral student as Late Breaking Basic Science oral communication at the American Heart Association Scientific Sessions 2014, in Chicago (November 2014; Illinois, USA).

JOURNAL OF THE AMERICAN COLLEGE OF CARDIOLOGY
VOL. 65, NO. 4, 2015

ISSN 0735-1097/$36.00
PUBLISHED BY ELSEVIER INC.
http://dx.doi.org/10.1016/j.jacc.2014.11.004

ORIGINAL INVESTIGATIONS

Myocardial Edema After Ischemia/Reperfusion Is Not Stable and Follows a Bimodal Pattern

Imaging and Histological Tissue Characterization

Rodrigo Fernández-Jiménez, MD,*† Javier Sánchez-González, PhD,*‡ Jaume Agüero, MD,* Jaime García-Prieto, BSc,* Gonzalo J. López-Martín, Tech,* José M. García-Ruiz, MD,* Antonio Molina-Iracheta, DVM,* Xavier Rosselló, MD,* Leticia Fernández-Friera, MD, PhD,*§ Gonzalo Pizarro, MD,*‖ Ana García-Álvarez, MD, PhD,* Erica Dall'Armellina, MD, DPhil,¶ Carlos Macaya, MD, PhD,† Robin P. Choudhury, DM,¶ Valentin Fuster, MD, PhD,*# Borja Ibáñez, MD, PhD*†

ABSTRACT

BACKGROUND It is widely accepted that edema occurs early in the ischemic zone and persists in stable form for at least 1 week after myocardial ischemia/reperfusion. However, there are no longitudinal studies covering from very early (minutes) to late (1 week) reperfusion stages confirming this phenomenon.

OBJECTIVES This study sought to perform a comprehensive longitudinal imaging and histological characterization of the edematous reaction after experimental myocardial ischemia/reperfusion.

METHODS The study population consisted of 25 instrumented Large-White pigs (30 kg to 40 kg). Closed-chest 40-min ischemia/reperfusion was performed in 20 pigs, which were sacrificed at 120 min (n = 5), 24 h (n = 5), 4 days (n = 5), and 7 days (n = 5) after reperfusion and processed for histological quantification of myocardial water content. Cardiac magnetic resonance (CMR) scans with T2-weighted short-tau inversion recovery and T2-mapping sequences were performed at every follow-up stage until sacrifice. Five additional pigs sacrificed after baseline CMR served as controls.

RESULTS In all pigs, reperfusion was associated with a significant increase in T2 relaxation times in the ischemic region. On 24-h CMR, ischemic myocardium T2 times returned to normal values (similar to those seen pre-infarction). Thereafter, ischemic myocardium-T2 times in CMR performed on days 4 and 7 after reperfusion progressively and systematically increased. On day 7 CMR, T2 relaxation times were as high as those observed at reperfusion. Myocardial water content analysis in the ischemic region showed a parallel bimodal pattern: 2 high water content peaks at reperfusion and at day 7, and a significant decrease at 24 h.

CONCLUSIONS Contrary to the accepted view, myocardial edema during the first week after ischemia/reperfusion follows a bimodal pattern. The initial wave appears abruptly upon reperfusion and dissipates at 24 h. Conversely, the deferred wave of edema appears progressively days after ischemia/reperfusion and is maximal around day 7 after reperfusion. (J Am Coll Cardiol 2015;65:315–23) © 2015 by the American College of Cardiology Foundation.

From the *Centro Nacional de Investigaciones Cardiovasculares Carlos III (CNIC), Madrid, Spain; †Hospital Universitario Clínico San Carlos, Madrid, Spain; ‡Philips Healthcare, Madrid, Spain; §Hospital Universitario Montepríncipe, Madrid, Spain; ‖Hospital Universitario Quirón Universidad Europea de Madrid, Madrid, Spain; ¶Oxford Acute Vascular Imaging Centre, Division of Cardiovascular Medicine, Radcliffe Department of Medicine, University of Oxford, Oxford, United Kingdom; and #The Zena and Michael A. Wiener Cardiovascular Institute, Icahn School of Medicine at Mount Sinai, New York, New York. This work was supported by a competitive grant from the Ministry of Economy and Competitiveness (MINECO), Fondo Europeo de Desarrollo Regional (FEDER) Carlos III Institute of Health-Fondo de Investigación Sanitaria (PI13/01979), and in part by FP7-PEOPLE-2013-ITN

JACC VOL. 65, NO. 4, 2015
FEBRUARY 3, 2015:315–23

ABBREVIATIONS AND ACRONYMS

CMR = cardiac magnetic resonance

FOV = field of view

I/R = ischemia/reperfusion

NEX = number of excitations

ROI = region of interest

STIR = short-tau inversion recovery

TE = echo time

TR = repetition time

T2W = T2 weighted

Tissue characterization after myocardial ischemia/reperfusion (I/R) is of great scientific and clinical value. After myocardial I/R, there is an intense edematous reaction (due to abnormal fluid accumulation in the interstitial and/or cardiomyocyte compartments) in the post-ischemic myocardium (1–5). Cardiac magnetic resonance (CMR) is a noninvasive technique that allows accurate tissue characterization of the myocardium (6). In particular, T2-weighted (T2W) and T2-mapping CMR sequences have the potential to identify tissues with high water content (7). Few experimental studies have correlated post-I/R T2-CMR data with myocardial water content (2,8), and these validations were undertaken at different times after reperfusion. Many recent experimental and clinical studies have used these CMR sequences to retrospectively evaluate post-myocardial infarction edema on the basis of the assumptions that myocardial edema appears early after I/R, persists in a stable form for at least 1 week (9,10), and is accurately visualized by CMR.

SEE PAGE 324

However, the time chosen for the CMR examination varies significantly among studies, from 1 day (9,10) up to several weeks (9–16) after reperfusion. In addition, post-I/R T2W signal intensity and T2 relaxation time are affected by other factors besides water content: T2-CMR results can be modulated independently by hemorrhage (17,18), microvascular obstruction (19), and even cardioprotective therapies (20–22). There is, therefore, intense debate about the accuracy of CMR-based methods for detecting, quantifying, and tracking the post-infarction edematous reaction (7,23). Given the growing use of CMR technology to quantify post-I/R edema in clinical trials (24,25), a comprehensive characterization of the time course of post-I/R myocardial edema, including evaluation of both CMR and histological reference standards, is needed (22–24,26–28).

The present study aimed to comprehensively characterize myocardial edema and reperfusion-related tissue changes after I/R, covering from early to late reperfusion stages. For this, we performed a full CMR and histopathological study in a large animal (pig) model of I/R.

METHODS

STUDY DESIGN. Experiments were performed in castrated male Large-White pigs weighing 30 kg to 40 kg. A total of 25 pigs completed the full protocol and comprised the study population. The study was approved by the Institutional Animal Research Committee and conducted in accordance with the recommendations of the Guide for the Care and Use of Laboratory Animals. The study design is summarized in **Figure 1**. Five pigs (Group 1) served as controls and were sacrificed with no intervention other than baseline CMR. In 20 pigs, reperfused acute myocardial infarction (I/R) was induced experimentally by closed-chest 40-min left anterior descending coronary artery occlusion. These pigs were sacrificed at 120 min (n = 5, Group 2), 24 h (n = 5, Group 3), 4 days (n = 5, Group 4), and 7 days (n = 5, Group 5) after reperfusion. CMR scans, including T2W short-tau inversion recovery (STIR), T2-mapping, and delayed enhancement sequences, were performed at every follow-up stage until sacrifice (i.e., animals sacrificed on day 7 underwent CMR examinations at baseline, 120 min, 24 h, day 4, and day 7). After the last follow-up CMR scan, animals were immediately euthanized, and myocardial tissue samples from ischemic and remote areas were rapidly collected for evaluation of water content by histology.

MYOCARDIAL INFARCTION PROCEDURE. The I/R protocol has been detailed elsewhere (29). Anesthesia was induced by intramuscular injection of ketamine (20 mg/kg), xylazine (2 mg/kg), and midazolam (0.5 mg/kg), and maintained by continuous intravenous infusion of ketamine (2 mg/kg/h), xylazine (0.2 mg/kg/h), and midazolam (0.2 mg/kg/h). Animals

Next Generation Training in Cardiovascular Research and Innovation-Cardionext. This study forms part of a Master Research Agreement between CNIC and Philips Healthcare. QMass software use was partially supported by a scientific collaboration with Medis Medical Imaging Systems BV. The Spanish Ministry of Economy and Competitiveness and the Pro-CNIC Foundation support the CNIC. Dr. Fernández-Jiménez is a recipient of a Rio Hortega fellowship from the Ministry of Economy and Competitiveness through the Instituto de Salud Carlos III; and has received an FICNIC fellowship from the Fundació Jesús Serra, the Fundación Interhospitalaria de Investigación Cardiovascular, and the CNIC. Dr. Sánchez-González is an employee of Philips Healthcare. Dr. Aguero is an FP7-PEOPLE-2013-ITN-Cardionext fellow. All other authors have reported that they have no relationships relevant to the contents of this paper to disclose. Derek Yellon, PhD, DSc, served as Guest Editor for this paper.
Listen to this manuscript's audio summary by *JACC* Editor-in-Chief Dr. Valentin Fuster.
You can also listen to this issue's audio summary by *JACC* Editor-in-Chief Dr. Valentin Fuster.

Manuscript received October 19, 2014; revised manuscript received November 5, 2014, accepted November 6, 2014.

FIGURE 1 Study Design

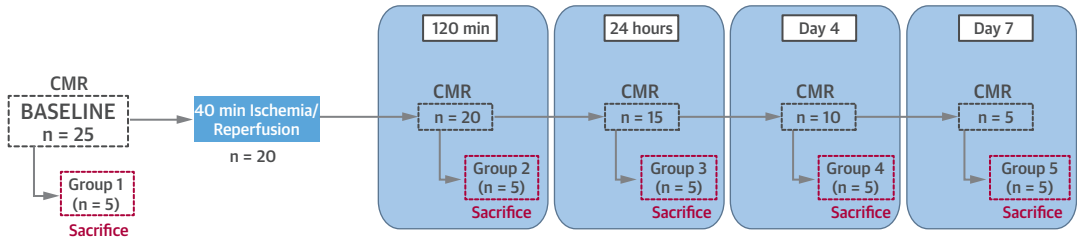

The study population comprised 5 groups of pigs (n = 5/group) used to characterize myocardial edema during the first week after ischemia/reperfusion. Cardiac magnetic resonance (CMR) scans, including T2-weighted short-tau inversion recovery and T2-mapping sequences, were performed at every follow-up until sacrifice (i.e., animals sacrificed on day 7 underwent baseline, 120-min, 24-h, day 4, and day 7 CMR).

were intubated and mechanically ventilated with oxygen (fraction of inspired O_2: 28%). Central venous and arterial lines were inserted, and a single bolus of unfractionated heparin (300 mg/kg) was administered at the onset of instrumentation. The left anterior descending coronary artery, immediately distal to the origin of the first diagonal branch, was occluded for 40 min with an angioplasty balloon introduced via the percutaneous femoral route using the Seldinger technique. Balloon location and maintenance of inflation were monitored angiographically. After balloon deflation, a coronary angiogram was recorded to confirm patency of the coronary artery. A continuous infusion of amiodarone (300 mg/h) was maintained during the procedure in all pigs to prevent malignant ventricular arrhythmias. In cases of ventricular fibrillation, a biphasic defibrillator was used to deliver nonsynchronized shocks.

CMR PROTOCOL. A baseline CMR scan was performed immediately before myocardial infarction and subsequent CMR scans were performed at post-infarction follow-up time points until sacrifice. All studies were performed in a Philips 3-T Achieva Tx whole-body scanner (Philips Healthcare, Best, the Netherlands) equipped with a 32-element phased-array cardiac coil. The imaging protocol included a standard segmented cine steady-state free-precession (SSFP) sequence to provide high-quality anatomical references, a T2-weighted triple inversion-recovery (T2W-STIR) sequence, a T2-turbo spin echo (TSE) mapping sequence, and a late gadolinium enhancement sequence. The imaging parameters for the SSFP sequence were field of view (FOV) of 280 × 280 mm, slice thickness 6 mm with no gaps, repetition time (TR) 2.8 ms, echo time (TE) 1.4 ms, flip angle 45°, cardiac phases 30, voxel size 1.8 × 1.8 mm, and 3 number of excitations (NEX). Imaging parameters for the T2W-STIR sequence were FOV 280 × 280 mm, slice thickness 6 mm, TR 2 heartbeats, TE 80 ms, voxel size 1.4 × 1.95 mm, delay 210 ms, end-diastolic acquisition, echo-train length 16, and 2 NEX. The imaging parameters for the T2-TSE mapping were FOV 300 × 300 mm, slice thickness 8 mm, TR 2 heartbeats, and 10 echo times ranging from 4.9 to 49.0 ms. Delayed enhancement imaging was performed 10 to 15 min after intravenous administration of 0.20 mmol of gadopentetate dimeglumine contrast agent per kg of body weight (30) using an inversion-recovery spoiled turbo field echo (IR-T1TFE) sequence with the following parameters: FOV of 280 × 280 mm, voxel size 1.6 × 1.6 mm, end-diastolic acquisition, thickness 6 mm with no gap, TR 5.6 ms, TE 2.8 ms, inversion delay time optimized to null normal myocardium, and 2 NEX. SSFP, T2W-STIR, and IR-T1TFE sequences were performed to acquire 13 to 15 contiguous short-axis slices covering the heart from the base to the apex. To track T2 relaxation time changes across time, T2 maps in all studies were acquired in midapical ventricular short-axis slices corresponding to the same anatomical level.

CMR DATA ANALYSIS. CMR images were analyzed using dedicated software (MR Extended Work Space 2.6, Philips Healthcare, and QMass MR 7.5, Medis, Leiden, the Netherlands) by 2 observers experienced in CMR analysis. T2 maps were automatically generated on the acquisition scanner by fitting the signal intensity of all echo times to a monoexponential decay curve at each pixel with a maximum likelihood expectation maximization algorithm. T2 relaxation maps were quantitatively analyzed by placing a wide transmural region of interest (ROI) at the ischemic and remote areas of the corresponding slice in all studies. Hypointense areas suggestive of microvascular obstruction or hemorrhage were included in the ROI for T2 quantification purposes. Delayed gadolinium-enhanced regions were defined as >50% of maximum myocardial signal intensity (full width at

FIGURE 2 Time Course of CMR T2 Relaxation Time and Corresponding Myocardial Water Content During the First Week After I/R

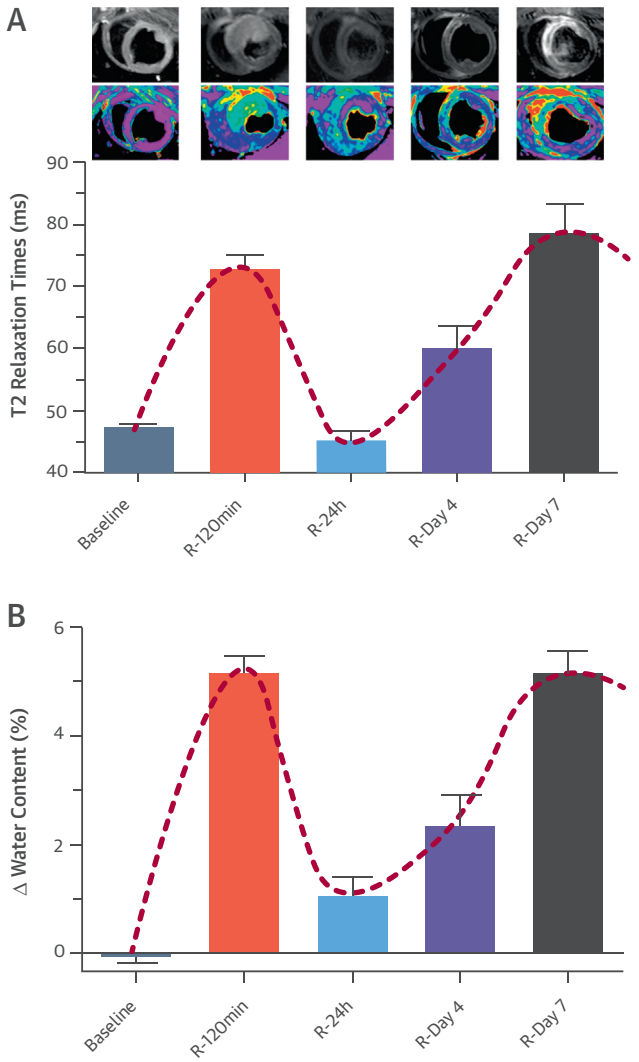

Note the parallel courses of cardiac magnetic resonance (CMR) fluctuations and histologically determined edema **(dashed red lines). (A)** Time course of absolute T2 relaxation time values (ms) in the ischemic myocardium during the first week after ischemia/reperfusion (I/R). **Bars** represent means and standard errors of the means. The **top of the panel** shows representative images from 1 animal that underwent 40-min/7-day I/R and CMR T2-weighted short-tau inversion recovery and T2-mapping examinations at all time points. All T2 maps were scaled between 30 and 120 ms. **(B)** Time course of absolute differences (%) in water content between ischemic (midapical anteroseptal left ventricular wall) and remote (posterolateral left ventricular wall) zones during the first week after I/R. **Bars** represent means and standard errors of the means. Absolute differences were 0.0 ± 0.2% for group 1 (sacrificed at baseline with no other intervention than CMR), 5.2 ± 0.6% for group 2 (I/R 120 min), 1.1 ± 0.7% for group 3 (I/R 24 h), 2.4 ± 1.3% for Group 4 (I/R 4 days), and 5.1 ± 1.0% for group 5 (I/R 7 days). All pairwise comparisons for the absolute differences in myocardial water content were explored, adjusting the p values for multiple comparisons using the Holm-Bonferroni correction. Comparisons between different groups remained statistically significant with the exception of the following: group 1 (control) vs. group 3 (I/R 24 h), group 3 (I/R 24 h) vs. group 4 (I/R 4 days), and group 2 (I/R 120 min) vs. group 5 (I/R 7 days).

half maximum) with manual adjustment when needed. If present, a central core of hypointense signal within the area of increased signal was included as late gadolinium-enhanced myocardium. Regional transmurality of contrast enhancement was evaluated in the same segments where ROIs for T2 quantification were placed with a scheme on the basis of the spatial extent of delayed enhancement tissue within each segment (31). Segments with more than 75% hyperenhancement were considered segments with transmural enhancement.

QUANTIFICATION OF MYOCARDIAL WATER CONTENT BY HISTOLOGY. Paired myocardial samples were collected within minutes of euthanasia from the infarcted and remote myocardia of all pigs. Tissue samples were immediately blotted to remove surface moisture and introduced into laboratory crystal containers previously weighed on a high-precision scale. The containers were weighed before and after drying for 48 h at 100°C in a desiccating oven. Tissue water content was calculated as follows: water content (%) = ([wet weight − dry weight]/wet weight) ×100. An empty container was weighed before and after desiccation as an additional calibration control.

STATISTICAL ANALYSIS. Normal distribution of each data subset was checked using graphical methods and a Shapiro-Wilk test. For quantitative variables showing a normal distribution, data are expressed as mean ± SD. Leven's test was performed to check the homogeneity of variances. A 1-way analysis of variance was conducted for comparison of myocardial water content among groups (from animals sacrificed at different time points). To take repeated measures into account, a generalized mixed model was conducted for comparison of T2 relaxation times among different time points. As this study was exploratory, all pairwise comparisons were explored, adjusting p values for multiple comparisons using the Holm-Bonferroni method. In all cases, data from the ischemic and remote myocardium (i.e., myocardial water content and T2 relaxation time values) were separately analyzed. All statistical analyses were performed using commercially available software (Stata version 12.0, StataCorp, College Station, Texas).

RESULTS

NATURAL EVOLUTION OF MYOCARDIAL EDEMA DURING THE FIRST WEEK AFTER I/R. CMR imaging. Baseline (i.e., before ischemia) mean T2 relaxation times were 47.2 ± 2.6 ms and 46.3 ± 1.7 ms for the midapical anteroseptal and posterolateral left ventricular walls, respectively. In all pigs, early

reperfusion (120-min CMR) was associated with a sharp and significant increase in T2 relaxation time above baseline, in the former ischemic area (mid-apical anteroseptal ventricular wall). T2 relaxation times returned to baseline values at 24 h post-I/R in all animals, but subsequently increased progressively, reaching post-I/R values on day 7 similar to those observed during early reperfusion. Albeit slight, a linear trend for a progressive increase in T2 relaxation times across different time points was observed in the remote myocardium. Figure 2A shows mean changes in T2 relaxation time in the ischemic myocardium as well as a representative example of 1 animal serially scanned at all time points. Measurements of T2 relaxation time in the ischemic and remote myocardium at different time points after I/R are summarized in Table 1. Changes observed in T2W-STIR and T2-TSE mapping were consistent in all animals, as seen in Figure 3, which shows images from 8 pigs scanned at the different time points. The transmural extent of infarction was >80% in all evaluated segments containing the ROIs for T2 relaxation time quantification.

Myocardial water content. Myocardial water content in noninfarcted myocardium (from animals in group 1) was 79.4 ± 0.6% and 79.4 ± 0.7% for the midapical anteroseptal and posterolateral left ventricular walls, respectively. In the ischemic myocardium, an abrupt increase in water content was detected at early reperfusion. Consistent with the CMR data, there was a systematic and significant decrease in tissue water content in the formerly ischemic region at 24 h, followed by a subsequent increase over the following days to reach values on day 7 similar to those observed at early reperfusion. A linear trend for a slight, but progressive increase in water content across different time points was observed in the remote myocardium. Time courses for absolute differences in water content between ischemic and remote myocardium are shown in Figure 2B. Table 2 summarizes measurements of water content in the ischemic and remote myocardium at different time points after I/R.

TABLE 1 Measurements of T2 Relaxation Time in the Ischemic and Remote Myocardium at Different Time Points During the First Week After Ischemia/Reperfusion

		T2 Relaxation Times (ms)				
		Baseline	R-120 min	R-24 h	R-Day 4	R-Day 7
Group 1 (Control)	IM	47.7 ± 4.0				
	Rem	46.1 ± 1.5				
Group 2 (I/R-120 min)	IM	48.7 ± 0.6	73.3 ± 10.0			
	Rem	46.8 ± 1.8	47.0 ± 1.0			
Group 3 (I/R-24 h)	IM	46.5 ± 1.9	72.4 ± 12.3	45.9 ± 5.3		
	Rem	46.2 ± 2.6	48.6 ± 3.0	45.2 ± 0.6		
Group 4 (I/R-4 days)	IM	45.9 ± 1.6	73.5 ± 4.2	42.7 ± 9.3	55.1 ± 13.2	
	Rem	45.5 ± 0.8	48.3 ± 4.0	47.5 ± 3.1	48.2 ± 2.9	
Group 5 (I/R-7 days)	IM	47.2 ± 3.5	72.6 ± 14.2	47.0 ± 2.9	64.9 ± 7.9	78.4 ± 10.6
	Rem	46.7 ± 1.5	48.5 ± 3.7	51.4 ± 5.0	50.1 ± 1.8	50.0 ± 3.3
Pooled	IM	**47.2 ± 2.6**	**72.9 ± 9.9**	**45.2 ± 6.2**	**60.0 ± 11.5**	**78.4 ± 10.6**
	Rem	**46.3 ± 1.7**	**48.1 ± 3.0**	**48.0 ± 4.1**	**49.1 ± 2.5**	**50.0 ± 3.3**

Values are mean ± SD. All pairwise comparisons for pooled serial T2 relaxation times were explored, adjusting p values for multiple comparisons using the Holm-Bonferroni correction. Comparisons between different time points in the ischemic myocardium remained statistically significant with the exception of the following: baseline vs. R-24 h, and R-120 min vs. R-day 7. **Bold** values are those that were compared and are also represented in Figure 2A.

IM = ischemic myocardium; Rem = remote myocardium.

DISCUSSION

The present experimental study challenges the accepted view of the development of post-ischemia/reperfusion myocardial edema. Through state-of-the-art CMR analysis and histological validation in a pig model of I/R, we show that the edematous reaction during the first week after reperfusion is not stable, instead following a bimodal pattern (Central Illustration). The first wave appears abruptly upon reperfusion and dissipates at 24 h. Conversely, the second wave of edema appears progressively days after I/R and increases to a maximum on post-reperfusion day 7. To the best of our knowledge, this is the first study to comprehensively characterize the time course of myocardial edema during the first week after I/R, covering from very early to late reperfusion stages. Because edema has been perceived as both stable and persistent during at least 1 week after myocardial I/R, it has been used increasingly both clinically and in the setting of clinical trials as a marker of "ischemic memory." Therefore, our findings that neither of these assumptions is accurate will have important translational implications.

As with most organs, water is a major component of healthy cardiac tissue. In steady-state conditions, myocardial water content is stable and mostly intracellular, with only a very small interstitial component contained within the extracellular matrix. Cardiac

TABLE 2 Measurements of Myocardial Water Content in the Ischemic and Remote Myocardium at Different Time Points During the First Week After I/R

	Water Content (%)				
	Group 1 (Control)	Group 2 (I/R-120 min)	Group 3 (I/R-24 h)	Group 4 (I/R-4 days)	Group 5 (I/R-7 days)
IM	79.4 ± 0.6	84.5 ± 0.5	81.2 ± 0.5	82.5 ± 1.4	85.2 ± 0.9
Rem	79.4 ± 0.7	79.4 ± 0.4	80.0 ± 0.4	80.1 ± 0.4	80.1 ± 0.3

Values are mean ± SD. All pairwise comparisons for myocardial water content were explored, adjusting p values for multiple comparisons using the Holm-Bonferroni correction. Comparisons between different groups in the ischemic myocardium remained statistically significant with the exception of the following: group 2 (I/R-120 min) vs. group 5 (I/R-7 days).

Abbreviations as in Table 1.

FIGURE 3 CMR T2W-STIR and T2 Mapping Images From Different Animals During the 1-Week Time Course After I/R

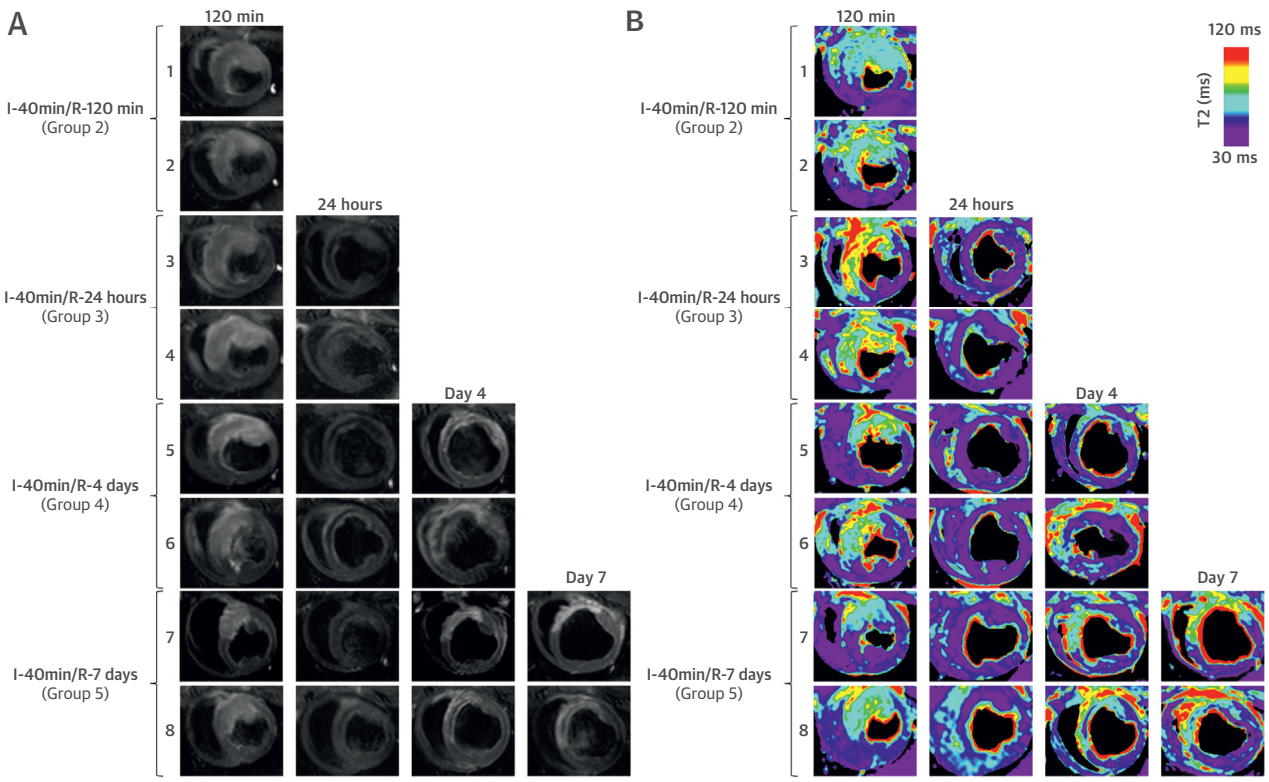

Serial CMR scans reveal highly consistent bimodal changes in image-determined myocardial edema during the first week after I/R, both in T2-weighted short-tau inversion recovery (T2W-STIR) imaging **(A)** and T2 mapping **(B)**. Images from 8 pigs at different time points are shown. All T2 maps were scaled between 30 and 120 ms. Abbreviations as in Figure 2.

edema occurs in numerous pathological conditions in which this homeostasis is disrupted, and affects both fluid accumulation outside cells (interstitial edema) and within cardiomyocytes (cellular edema). In the context of myocardial infarction, edema appears initially in the form of cardiomyocyte swelling during the early stages of ischemia (5). Myocardial edema is then significantly exacerbated upon restoration of blood flow to the ischemic region. This increase is due to increased cell swelling (3) and, more importantly, to interstitial edema secondary to reactive hyperemia and leakage from damaged capillaries when the hydrostatic pressure is restored upon reperfusion (1,4).

CMR has emerged as a noninvasive technology that allows characterization of cardiac tissue after I/R (6), with T2-weighted (T2W) CMR sequences especially suited to detecting high water content in post-ischemic edematous cardiac muscle (7). Under the accepted dogma that myocardial edema appears early after I/R and is present for at least 1 week (9,10,24), numerous experimental and clinical studies have used T2W-CMR to retrospectively evaluate the edematous reaction associated with myocardial infarction. Although visually attractive, T2W imaging is subject to several technical limitations and does not offer quantitative T2 measurements that would allow for comparisons between different studies (32,33). Recently developed quantitative T2 relaxation maps (T2 mapping) have been proposed to overcome at least some of the limitations for the detection and quantification of myocardial edema (34,35). However, T2-mapping sequences have inherent limitations, are time-consuming, and are thus mostly used as a research tool and require further validation. Large animal models of I/R offer an ideal platform for such a validation (36), and, due to its anatomical and physiological similarities to the human heart, the pig is one of the most reliable models for studying I/R-related processes.

The disparate time points examined in different experimental and clinical studies are an important source of confusion in CMR evaluation of post-I/R

edema. As demonstrated in the present study, because T2 values in the ischemic myocardium fluctuate significantly during the first week after reperfusion, the timing of post-infarction imaging is critically important for noninvasive assessment of myocardial edema. In a previous study, Foltz et al. (37,38) suggested a similar myocardial T2 relaxation time course in a pig model of I/R, with CMR scans at days 0, 2, and 7 after reperfusion. However, this study lacked histological validation of myocardial water content, and the observed T2 value fluctuations were interpreted as reflecting the oxidative denaturation of hemoglobin to methemoglobin (17,39) rather than fluctuations in myocardial water content. The histological validation in the present study demonstrates the consistent appearance of 2 consecutive waves of edema during the first week after I/R, a groundbreaking concept in the field.

The first wave of edema appears soon after reperfusion and dissipates at 24 h. Interestingly, water content within the ischemic myocardium did not return to normal values, whereas T2 relaxation time in the ischemic ventricular wall dropped to baseline values. It is plausible that the decrease in T2 relaxation time observed at 24 h is due to at least 2 components: the classically described paramagnetic effect of hemoglobin denaturation products and the sharp decrease in myocardial water content at 24 h post-reperfusion reported here.

The second wave of edema appeared progressively in the days after I/R and was maximal at day 7. Interestingly, T2 abnormalities and increased water content in the ischemic region were ultimately as impressive as those observed at early reperfusion. Further studies are needed to elucidate the physiopathology underlying this bimodal edematous reaction after I/R. It is intuitive to argue that the first and second waves of post-I/R edema are related to different pathological phenomena, although this has not been demonstrated in the present work. Whereas the first wave seems to be directly related to reperfusion, the pathophysiology underlying the second wave is more challenging to decipher. We speculate that tissue changes during the first week of infarction (removal of cardiomyocyte debris from the extracellular compartment and its replacement by water, collagen homeostasis, and healing of tissue/inflammation, among others) could play a role in this second edematous reaction.

The data presented here might have implications for understanding the role of CMR in retrospective quantification of the post-infarction area at risk. Given that this study was not designed to correlate the actual anatomical area at risk (perfusion defect during ischemia) with the extension of CMR-visualized edema, any conclusions in this regard are speculative and distract from this study's main objective. Future studies should specifically evaluate the impact of the dual edema phenomenon on the role of CMR to accurately quantify area at risk.

The identification of the time course of post-I/R myocardial edema has important biological, diagnostic, prognostic, and therapeutic implications, and opens a route to further exploration of factors influencing this phenomenon.

STUDY LIMITATIONS. Extrapolation of the results of this experimental study to the clinic should be done with caution. The intensity and time course of bimodal post-I/R edema may be modified by several factors, such as the duration of ischemia, preexistence of collateral flow, and even the application of peri-reperfusion therapies to attenuate I/R damage. Nonetheless, the use of a large animal model is of

CENTRAL ILLUSTRATION Edematous Reaction After Ischemia/Reperfusion Follows a Bimodal Pattern: The Bimodal Edema Phenomenon

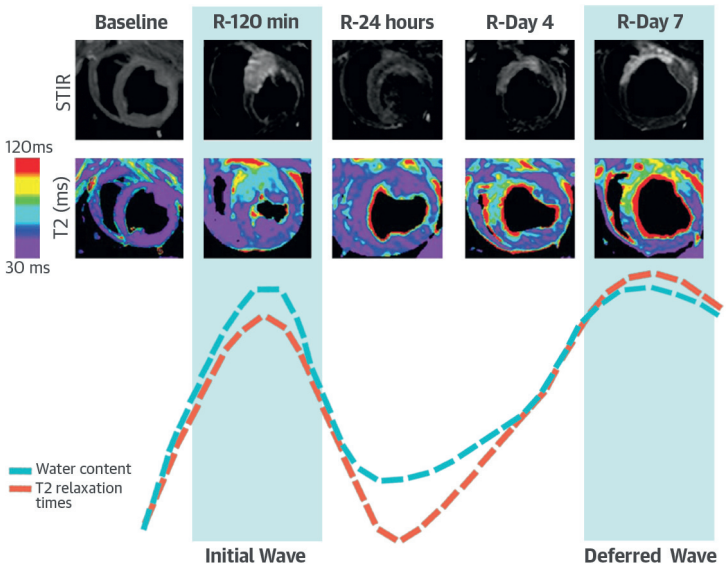

Fernández-Jiménez, R. et al. J Am Coll Cardiol. 2015; 65(4):315–23.

The development of myocardial edema is a well known phenomenon occurring after ischemia/reperfusion (myocardial infarction). This edematous reaction was long assumed to be stable for at least 1 week, but the post-ischemia/reperfusion phase was not previously tracked in a comprehensive serial study. In the present study, analysis of advanced cardiac magnetic resonance and histopathology showed that post-ischemia/reperfusion edema is bimodal. An initial wave of edema abruptly appears upon reperfusion and almost completely disappears at 24 h. A deferred wave appears later and increases progressively until day 7. STIR = short-tau inversion recovery.

great translational value, especially considering the difficulty of performing such a comprehensive serial CMR study (including 1 examination immediately upon reperfusion) in patients. The data presented in this study are robust and consistent, and the pig is one of the most clinically translatable large animal models for the study of I/R issues, because (unlike other mammals) its coronary artery anatomy and distribution are similar to those of humans (40) and it has minimal pre-existing coronary collateral flow (41). In addition, as shown here with the direct quantification of myocardial water content, experimental studies offer the possibility of histological validation.

In this study, the ROIs for quantification of T2 relaxation time were placed in the entire wall thickness, then were carefully and individually adjusted by hand to avoid the right and left ventricular cavities. Therefore, ROIs might include different myocardial states (i.e., hemorrhage, microvascular obstruction). We took this approach to mimic the histological water content evaluation, which was performed in the entire wall thickness. Given the parallel courses of T2 relaxation times and water content, we believe that the possible inclusion of different myocardial states had little effect on the results, although it might have had some influence on the differences in absolute T2 relaxation times between our study and others that used a different methodological approach to select ROIs.

CONCLUSIONS

Contrary to the accepted view, the present work consistently shows that edematous reaction during the first week after ischemia/reperfusion is not stable, but follows a bimodal pattern. The first wave of edema appears abruptly upon reperfusion and dissipates at 24 h. Conversely, the second wave appears progressively days after ischemia/reperfusion and is maximal around day 7 after reperfusion.

ACKNOWLEDGMENTS The authors are indebted to the contributions of Maria Del Trigo, Carlos Galán-Arriola, and David Sanz-Rosa. The authors also thank Tamara Córdoba, Oscar Sanz, Eugenio Fernández, and other members of the CNIC animal facility and farm for outstanding animal care and support, and Simon Bartlett (from the CNIC) for providing English editing.

REPRINT REQUESTS AND CORRESPONDENCE: Dr. Borja Ibáñez, Centro Nacional de Investigaciones Cardiovasculares Carlos III (CNIC), Melchor Fernández Almagro 3, 28029 Madrid, Spain. E-mail: bibanez@cnic.es.

PERSPECTIVES

COMPETENCY IN MEDICAL KNOWLEDGE: Myocardial edema that develops after acute infarction is a bimodal phenomenon with diagnostic, prognostic, and therapeutic implications.

TRANSLATIONAL OUTLOOK: Temporal variation in post-ischemic reperfusion edema should be considered in studies of cardiac magnetic resonance imaging for quantification of jeopardized myocardium.

REFERENCES

1. Bragadeesh T, Jayaweera AR, Pascotto M, et al. Post-ischaemic myocardial dysfunction (stunning) results from myofibrillar oedema. Heart 2008;94:166–71.

2. Garcia-Dorado D, Oliveras J, Gili J, et al. Analysis of myocardial oedema by magnetic resonance imaging early after coronary artery occlusion with or without reperfusion. Cardiovasc Res 1993;27:1462–9.

3. Kloner RA, Ganote CE, Whalen DA Jr., Jennings RB. Effect of a transient period of ischemia on myocardial cells. II. Fine structure during the first few minutes of reflow. Am J Pathol 1974;74:399–422.

4. Turschner O, D'Hooge J, Dommke C, et al. The sequential changes in myocardial thickness and thickening which occur during acute transmural infarction, infarct reperfusion and the resultant expression of reperfusion injury. Eur Heart J 2004;25:794–803.

5. Whalen DA Jr., Hamilton DG, Ganote CE, Jennings RB. Effect of a transient period of ischemia on myocardial cells. I. Effects on cell volume regulation. Am J Pathol 1974;74:381–97.

6. Friedrich MG. Tissue characterization of acute myocardial infarction and myocarditis by cardiac magnetic resonance. J Am Coll Cardiol Img 2008;1:652–62.

7. Arai AE, Leung S, Kellman P. Controversies in cardiovascular MR imaging: reasons why imaging myocardial T2 has clinical and pathophysiologic value in acute myocardial infarction. Radiology 2012;265:23–32.

8. Wisenberg G, Prato FS, Carroll SE, Turner KL, Marshall T. Serial nuclear magnetic resonance imaging of acute myocardial infarction with and without reperfusion. Am Heart J 1988;115:510–8.

9. Carlsson M, Ubachs JF, Hedstrom E, et al. Myocardium at risk after acute infarction in humans on cardiac magnetic resonance: quantitative assessment during follow-up and validation with single-photon emission computed tomography. J Am Coll Cardiol Img 2009;2:569–76.

10. Dall'Armellina E, Karia N, Lindsay AC, et al. Dynamic changes of edema and late gadolinium enhancement after acute myocardial infarction and their relationship to functional recovery and salvage index. Circ Cardiovasc Imaging 2011;4:228–36.

11. Aletras AH, Tilak GS, Natanzon A, et al. Retrospective determination of the area at risk for reperfused acute myocardial infarction with T2-weighted cardiac magnetic resonance imaging: Histopathological and displacement encoding with stimulated echoes (dense) functional validations. Circulation 2006;113:1865–70.

12. Berry C, Kellman P, Mancini C, et al. Magnetic resonance imaging delineates the ischemic area at risk and myocardial salvage in patients with acute

myocardial infarction. Circ Cardiovasc Imaging 2010;3:527–35.

13. Friedrich MG, Abdel-Aty H, Taylor A, et al. The salvaged area at risk in reperfused acute myocardial infarction as visualized by cardiovascular magnetic resonance. J Am Coll Cardiol 2008;51:1581–7.

14. Ibanez B, Macaya C, Sanchez-Brunete V, et al. Effect of early metoprolol on infarct size in ST-segment-elevation myocardial infarction patients undergoing primary percutaneous coronary intervention: the effect of metoprolol in cardioprotection during an acute myocardial infarction (METOCARD-CNIC) trial. Circulation 2013;128:1495–503.

15. Thiele H, Hildebrand L, Schirdewahn C, et al. Impact of high-dose N-acetylcysteine versus placebo on contrast-induced nephropathy and myocardial reperfusion injury in unselected patients with ST-segment elevation myocardial infarction undergoing primary percutaneous coronary intervention: the LIPSIA-N-ACC (Prospective, Single-Blind, Placebo-Controlled, Randomized Leipzig Immediate Percutaneous Coronary Intervention Acute Myocardial Infarction N-ACC) trial. J Am Coll Cardiol 2010;55:2201–9.

16. Wright J, Adriaenssens T, Dymarkowski S, Desmet W, Bogaert J. Quantification of myocardial area at risk with T2-weighted CMR: comparison with contrast-enhanced CMR and coronary angiography. J Am Coll Cardiol Img 2009;2:825–31.

17. Lotan CS, Miller SK, Cranney GB, Pohost GM, Elgavish GA. The effect of postinfarction intramyocardial hemorrhage on transverse relaxation time. Magn Reson Med 1992;23:346–55.

18. O'Regan DP, Ahmed R, Karunanithy N, et al. Reperfusion hemorrhage following acute myocardial infarction: assessment with T2* mapping and effect on measuring the area at risk. Radiology 2009;250:916–22.

19. Mikami Y, Sakuma H, Nagata M, et al. Relation between signal intensity on t2-weighted MR images and presence of microvascular obstruction in patients with acute myocardial infarction. AJR Am J Roentgenol 2009;193:W321–6.

20. Hausenloy DJ, Baxter G, Bell R, et al. Translating novel strategies for cardioprotection: the hatter workshop recommendations. Basic Res Cardiol 2010;105:677–86.

21. Thuny F, Lairez O, Roubille F, et al. Post-conditioning reduces infarct size and edema in patients with ST-segment elevation myocardial infarction. J Am Coll Cardiol 2012;59:2175–81.

22. White SK, Frohlich GM, Sado DM, et al. Remote ischemic conditioning reduces myocardial infarct size and edema in patients with ST-segment elevation myocardial infarction. J Am Coll Cardiol Intv 2015;8:177–87.

23. Croisille P, Kim HW, Kim RJ. Controversies in cardiovascular MR imaging: T2-weighted imaging should not be used to delineate the area at risk in ischemic myocardial injury. Radiology 2012;265:12–22.

24. Eitel I, Friedrich MG. T2-weighted cardiovascular magnetic resonance in acute cardiac disease. J Cardiovasc Magn Reson 2011;13:13.

25. Schwitter J, Arai AE. Assessment of cardiac ischaemia and viability: role of cardiovascular magnetic resonance. Eur Heart J 2011;32:799–809.

26. Garcia-Dorado D, Andres-Villarreal M, Ruiz-Meana M, Inserte J, Barba I. Myocardial edema: a translational view. J Mol Cell Cardiol 2012;52:931–9.

27. Ghugre NR, Pop M, Barry J, Connelly KA, Wright GA. Quantitative magnetic resonance imaging can distinguish remodeling mechanisms after acute myocardial infarction based on the severity of ischemic insult. Magn Reson Med 2013;70:1095–105.

28. Klocke FJ. Cardiac magnetic resonance measurements of area at risk and infarct size in ischemic syndromes. J Am Coll Cardiol 2010;55:2489–90.

29. Garcia-Prieto J, Garcia-Ruiz JM, Sanz-Rosa D, et al. Beta3 adrenergic receptor selective stimulation during ischemia/reperfusion improves cardiac function in translational models through inhibition of MPTP opening in cardiomyocytes. Basic Res Cardiol 2014;109:422.

30. Kim RJ, Albert TS, Wible JH, et al. Performance of delayed-enhancement magnetic resonance imaging with gadoversetamide contrast for the detection and assessment of myocardial infarction: An international, multicenter, double-blinded, randomized trial. Circulation 2008;117:629–37.

31. Wu E, Judd RM, Vargas JD, et al. Visualisation of presence, location, and transmural extent of healed Q-wave and non-Q-wave myocardial infarction. Lancet 2001;357:21–8.

32. Pennell D. Myocardial salvage: retrospection, resolution, and radio waves. Circulation 2006;113:1821–3.

33. Arai AE. Using magnetic resonance imaging to characterize recent myocardial injury: utility in acute coronary syndrome and other clinical scenarios. Circulation 2008;118:795–6.

34. Ugander M, Bagi PS, Oki AJ, et al. Myocardial edema as detected by pre-contrast T1 and T2 CMR delineates area at risk associated with acute myocardial infarction. J Am Coll Cardiol Img 2012;5:596–603.

35. Verhaert D, Thavendiranathan P, Giri S, et al. Direct T2 quantification of myocardial edema in acute ischemic injury. J Am Coll Cardiol Img 2011;4:269–78.

36. Fernandez-Jimenez R, Fernández-Friera L, Sanchez-Gonzalez J, Ibanez B. Animal models of tissue characterization of area at risk, edema and fibrosis. Curr Cardiovasc Imaging Rep 2014;7:1–10.

37. Foltz WD, Yang Y, Graham JJ, et al. MRI relaxation fluctuations in acute reperfused hemorrhagic infarction. Magn Reson Med 2006;56:1311–9.

38. Foltz WD, Yang Y, Graham JJ, et al. T2 fluctuations in ischemic and post-ischemic viable porcine myocardium in vivo. J Cardiovasc Magn Reson 2006;8:469–74.

39. Lotan CS, Bouchard A, Cranney GB, Bishop SP, Pohost GM. Assessment of postreperfusion myocardial hemorrhage using proton NMR imaging at 1.5 T. Circulation 1992;86:1018–25.

40. Weaver ME, Pantely GA, Bristow JD, Ladley HD. A quantitative study of the anatomy and distribution of coronary arteries in swine in comparison with other animals and man. Cardiovasc Res 1986;20:907–17.

41. Maxwell MP, Hearse DJ, Yellon DM. Species variation in the coronary collateral circulation during regional myocardial ischaemia: a critical determinant of the rate of evolution and extent of myocardial infarction. Cardiovasc Res 1987;21:737–46.

KEY WORDS CMR, MRI, myocardial infarction, pig, T2, water content

Original research article #5. “P*athophysiology underlying the bimodal edema phenomenon after myocardial ischemia/reperfusion*”.[72]

JOURNAL OF THE AMERICAN COLLEGE OF CARDIOLOGY
© 2015 BY THE AMERICAN COLLEGE OF CARDIOLOGY FOUNDATION
PUBLISHED BY ELSEVIER INC.

VOL. 66, NO. 7, 2015
ISSN 0735-1097/$36.00
http://dx.doi.org/10.1016/j.jacc.2015.06.023

Pathophysiology Underlying the Bimodal Edema Phenomenon After Myocardial Ischemia/Reperfusion

Rodrigo Fernández-Jiménez, MD,*† Jaime García-Prieto, BSc,* Javier Sánchez-González, PhD,*‡ Jaume Agüero, MD,* Gonzalo J. López-Martín, RT,* Carlos Galán-Arriola, DVM,* Antonio Molina-Iracheta, DVM,* Roisin Doohan, BSc,* Valentin Fuster, MD, PhD,*§ Borja Ibáñez, MD, PhD*†

ABSTRACT

BACKGROUND Post-ischemia/reperfusion (I/R) myocardial edema was recently shown to follow a consistent bimodal pattern: an initial wave of edema appears on reperfusion and dissipates at 24 h, followed by a deferred wave that initiates days after infarction, peaking at 1 week.

OBJECTIVES This study examined the pathophysiology underlying this post-I/R bimodal edematous reaction.

METHODS Forty instrumented pigs were assigned to different myocardial infarction protocols. Edematous reaction was evaluated by water content quantification, serial cardiac magnetic resonance T2-mapping, and histology/immunohistochemistry. The association of reperfusion with the initial wave of edema was evaluated in pigs undergoing 40-min/80-min I/R and compared with pigs undergoing 120-min ischemia with no reperfusion. The role of tissue healing in the deferred wave of edema was evaluated by comparing pigs undergoing standard 40-min/7-day I/R with animals subjected to infarction without reperfusion (chronic 7-day coronary occlusion) or receiving post-I/R high-dose steroid therapy.

RESULTS Characterization of post-I/R tissue changes revealed maximal interstitial edema early on reperfusion in the ischemic myocardium, with maximal content of neutrophils, macrophages, and collagen at 24 h, day 4, and day 7 post-I/R, respectively. Reperfused pigs had significantly higher myocardial water content at 120 min and T2 relaxation times on 120 min cardiac magnetic resonance than nonreperfused animals. Permanent coronary occlusion or high-dose steroid therapy significantly reduced myocardial water content on day 7 post-infarction. The dynamics of T2 relaxation times during the first post-infarction week were altered significantly in nonreperfused pigs compared with pigs undergoing regular I/R.

CONCLUSIONS The 2 waves of the post-I/R edematous reaction are related to different pathophysiological phenomena. Although the first wave is secondary to reperfusion, the second wave occurs mainly because of tissue healing processes. (J Am Coll Cardiol 2015;66:816–28) © 2015 by the American College of Cardiology Foundation.

From the *Centro Nacional de Investigaciones Cardiovasculares Carlos III, Madrid, Spain; †Hospital Universitario Clínico San Carlos, Madrid, Spain; ‡Philips Healthcare, Madrid, Spain; and §The Zena and Michael A. Wiener Cardiovascular Institute, Mount Sinai School of Medicine, New York, New York. This work was supported by a competitive grant from the Spanish Ministry of Economy and Competitiveness through the Carlos III Institute of Health-Fondo de Investigación Sanitaria (PI13/01979), the Fondo Europeo de Desarrolo Regional (FEDER, RD: SAF2013-49663-EXP), and in part by the FP7-PEOPLE-2013-ITN Next generation training in cardiovascular research and innovation-Cardionext. This study forms part of a Master Research Agreement between the Centro Nacional de Investigaciones Cardiovasculares Carlos III (CNIC) and Philips Healthcare. The CNIC is supported by the Ministry of Economy and Competitiveness and the Pro-CNIC Foundation. Dr. Fernández-Jiménez holds a Rio Hortega fellowship from the Ministry of Economy and Competitiveness through the Instituto de Salud Carlos III; and a FICNIC fellowship from the Fundació Jesús Serra, the Fundación Interhospitalaria de Investigación Cardiovascular, and the Centro Nacional de Investigaciones Cardiovasculares Carlos III (CNIC). Dr. Sánchez-González is employed by Philips. Dr. Agüero is an FP7-PEOPLE-2013-ITN-Cardionext fellow. Dr. Ibáñez is supported by the Red de Investigación Cardiovascular of the Spanish Ministry of Health (RD 12/0042/0054). All other authors have reported that they have no relationships relevant to the contents of this paper to disclose. João A.C. Lima, MD, served as Guest Editor for this paper.
Listen to this manuscript's audio summary by *JACC* Editor-in-Chief Dr. Valentin Fuster.

Manuscript received May 19, 2015; accepted June 9, 2015.

Post-myocardial infarction (MI) tissue characterization offers the possibility of predicting long-term remodeling and evaluating the impact of interventions aimed at preserving cardiac function. Reperfusion, the basis of myocardial protection during infarction, alters post-MI tissue composition compared with the nonreperfused setting (1,2). Nonetheless, most current knowledge of tissue modifications in the post-infarcted myocardium is based on observations in nonreperfused hearts. There is therefore a need for comprehensive tissue characterization in the context of ischemia/reperfusion (I/R).

SEE PAGE 829

The post-I/R myocardium is characterized by an intense edematous reaction confined to the post-ischemic region (3–7) assumed to appear early after I/R and persist in stable form for at least 1 week (8,9). It has been used both experimentally and clinically as a marker of ischemic "memory." Noninvasive evaluation of this post-I/R edematous reaction has become possible with the development of T2-weighted and T2-mapping cardiac magnetic resonance (CMR) sequences able to accurately detect increases in water content (10–12). Innumerable clinical and experimental reports have been based on the unimodal hypothesis of a persistent edematous reaction during the first week after I/R. However, we recently showed that the post I/R edematous reaction is not constant, but rather follows a bimodal pattern, with an initial wave of edema appearing abruptly on reperfusion and dissipating at 24 h, followed by a deferred wave of edema appearing several days after I/R, increasing to a maximum on post-reperfusion day 7 (13). These experimental observations challenge the accepted view (14) and call for a mechanistic study to unravel the pathophysiological mechanisms underlying this newly recognized phenomenon.

In the present study, we used a large animal model (pig) of MI to characterize the tissue changes taking place in the post I/R myocardium by histological and CMR methods. Under the hypothesis that the initial wave of edema is a direct consequence of reperfusion while the deferred wave is caused by healing processes, we manipulated each wave independently through the use of reperfused and nonreperfused MI models, and exposure to high-dose steroid therapy, interventions that are known to alter healing processes.

METHODS

STUDY DESIGN, PROTOCOLS, AND IMAGING ANALYSIS. The study population was 40 castrated male Large-White pigs. The study (Figure 1) was approved by the Institutional Animal Research Committee and conducted in accordance with recommendations of the Guide for the Care and Use of Laboratory Animals. MI was generated by 40-min angioplasty-balloon occlusion of the mid-left anterior descending (LAD) coronary artery followed by balloon deflation and re-establishment of blood flow (15). Short follow-up (120 min) nonreperfused MI was achieved by maintaining balloon inflation until sacrifice and heart excision. Long follow-up (7 days) nonreperfused MI was achieved by implanting an intravascular CMR-compatible coil in the mid-LAD to generate permanent coronary occlusion. Full methods can be found in the Online Appendix.

ABBREVIATIONS AND ACRONYMS

CMR = cardiac magnetic resonance
I/R = ischemia/reperfusion
LAD = left anterior descending
MI = myocardial infarction

Myocardial water content was quantified in samples from the infarcted and remote myocardium of all pigs by using the desiccating technique as the reference standard: water content (%) = [(wet weight − dry weight)/wet weight] ×100. Samples of ischemic myocardium were analyzed by histology and immunohistochemistry. Histological sections were stained with hematoxylin and eosin and Masson trichrome, and with antibodies against F4/80 (macrophages) and PM1 (neutrophils).

CMR examinations were performed immediately before MI and at subsequent post-MI follow-up time points until sacrifice. Examinations were conducted with a Philips 3-Tesla Achieva Tx whole body scanner (Philips Healthcare, Best, the Netherlands) equipped with a 32-element phased-array cardiac coil. The imaging protocol included a standard segmented cine steady-state free-precession sequence to provide high-quality anatomic references, a T2-weighted triple short-tau inversion recovery sequence, and T2 turbo spin multiecho mapping. The imaging parameters are detailed in the Online Appendix.

CMR images were analyzed using dedicated software (MR Extended Work Space 2.6, Philips Healthcare) by 2 experienced observers blinded to group allocation.

STATISTICAL ANALYSIS. Normal distribution of each data subset was checked using graphical methods and a Shapiro-Wilk test. For quantitative variables showing a normal distribution, data are expressed as mean ± SD. For quantitative variables showing a non-normal distribution, data are expressed as median and interquartile range. A Kruskal-Wallis test was conducted for comparison of hemorrhage, number of inflammatory cells, and collagen content among groups over the histopathological time course. Given the hypothesis-driven nature of the study, comparisons between groups of pigs sacrificed at

FIGURE 1 Study Design

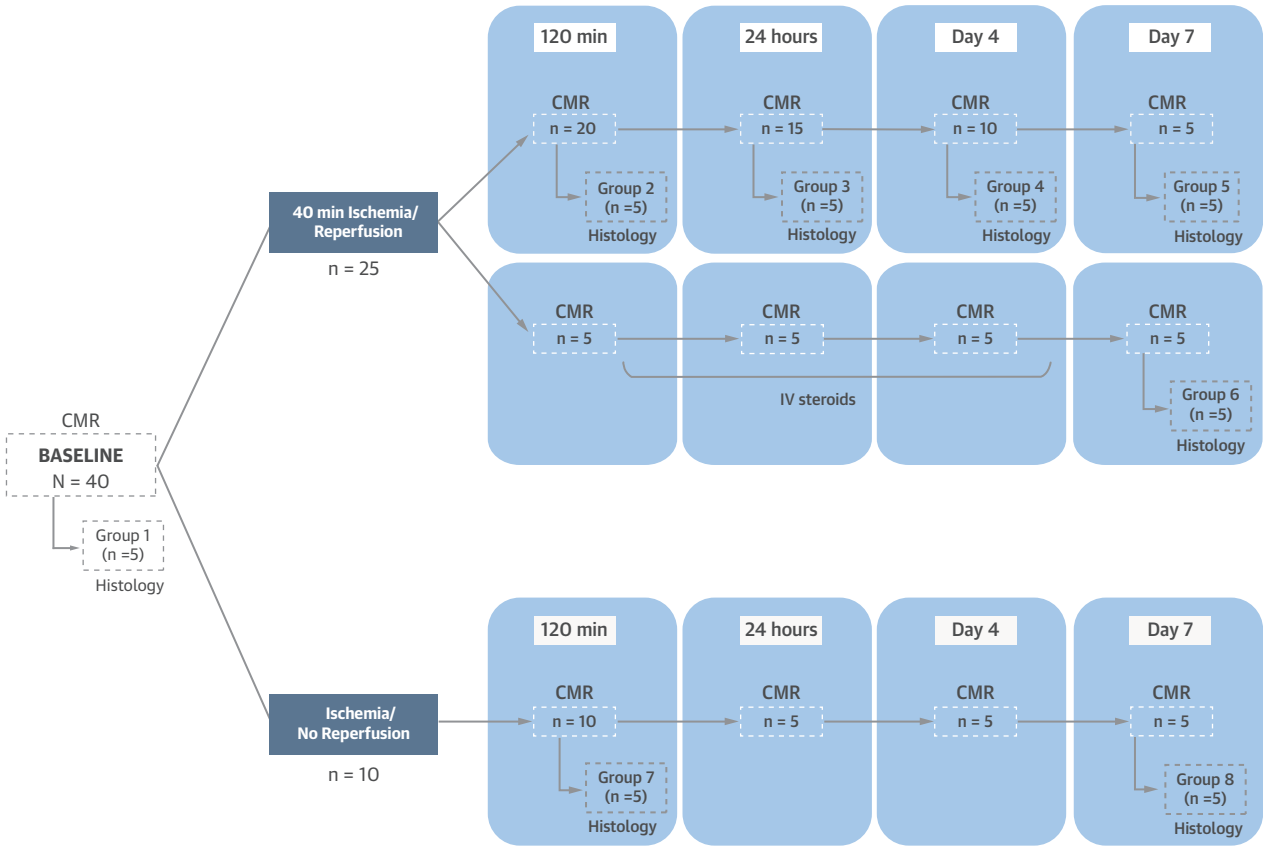

The study population comprised 8 groups of pigs (n = 5 per group). Groups 1 to 5 were used for the histopathological characterization of myocardial tissue changes during the first week post-ischemia/reperfusion. Groups 6 to 8 were used to decipher the mechanisms underlying the bimodal edematous reaction in the first week after ischemia/reperfusion. Cardiac magnetic resonance (CMR) scans were performed at all follow-up stages until sacrifice, so that animals sacrificed at day 7 underwent baseline, 120 min, 24 h, day 4, and day 7 CMR. CMR data and myocardial water content from animals in groups 1 to 5 have been reported previously (13).
IV = intravenous.

post-infarction day 7 were planned in advance. Quantitative variables showing a normal distribution were therefore compared using a two-tailed Student *t* test, whereas quantitative variables showing a non-normal distribution were compared using a Wilcoxon rank sum test. All statistical analyses were performed with Stata 12.0 (StataCorp, College Station, Texas).

TABLE 1 Tissue Changes in the Ischemic Myocardium During Week 1 Post-I/R

	R-120 Min	R-24 H	R-Day 4	R-Day 7	p Value
Hemorrhage, score 0–5	0 (0–1)	2 (2–3)	4 (3–5)	1 (0–2)	0.02
Neutrophils,* n/mm^2	69.0 ± 94.7	677.6 ± 318.3	454.5 ± 312.5	94.9 ± 86.8	<0.01
Macrophages,* n/mm^2	5.5 ± 11.0	20.6 ± 30.1	154.4 ± 295.8	12.6 ± 20.5	<0.01
Collagen,† %	0 ± 0	0 ± 0	4.5 ± 1.1	13.3 ± 3.2	<0.01

Values are median (interquartile range) or mean ± SD. Interstitial hemorrhage is graded from 0 (absence) to 5 (very severe). p value for among-group comparison. *In the lesion area. †In the granulation tissue area.
I = ischemia; R = reperfusion.

RESULTS

DYNAMICS OF TISSUE CHANGES DURING THE FIRST WEEK AFTER REPERFUSED MI. To characterize changes associated with the 2 waves of edema, we first studied histological changes during the first week after standard I/R. Samples for this analysis came from a group of animals whose bimodal CMR and water content results were previously reported (13). The time course of tissue changes in the post-I/R myocardium is summarized in Table 1 and illustrated in Figure 2A with representative staining images in Figure 2B. The density of infiltrating neutrophils was maximal at 24 h post-I/R and remained high at day 4

before dropping significantly by day 7 post-I/R. The density of infiltrating macrophages also increased significantly from day 1 to a peak on day 4 before dropping significantly at day 7. Interstitial hemorrhage was apparent at 24 h, peaking on day 4 post-I/R. There was no evidence of increased collagen deposition until day 4, with a further increase in content observed at post-I/R day 7.

INITIAL WAVE OF EDEMA AND REPERFUSION. To study the potential association between the initial wave of edema and reperfusion, a new group of 5 pigs (Group 7 in Figure 1) underwent ischemia (angioplasty-balloon mid-LAD coronary occlusion) and were sacrificed after 120-min CMR without being reperfused. When compared with animals undergoing 40-min coronary occlusion followed by 80-min reperfusion (Group 2 in Figure 1), myocardial water content in the ischemic region of the nonreperfused pigs was significantly lower than in reperfused animals sacrificed at the same time (80.8 ± 0.4% vs. 84.5 ± 0.5%; $p < 0.0001$) (Figure 3A).

CMR results agreed with histological water content data: although baseline (pre-ischemia) T2 relaxation times in nonreperfused and reperfused pigs were similar (45.3 ± 1.4 ms vs. 48.7 ± 0.6 ms), the 120-min CMR T2 relaxation times in the ischemic region of nonreperfused pigs were significantly lower than those of reperfused pigs (57.0 ± 3.0 ms vs. 73.3 ± 10.0 ms;

FIGURE 2 Histopathological Changes in the Ischemic Myocardium During the First Week After Ischemia/Reperfusion

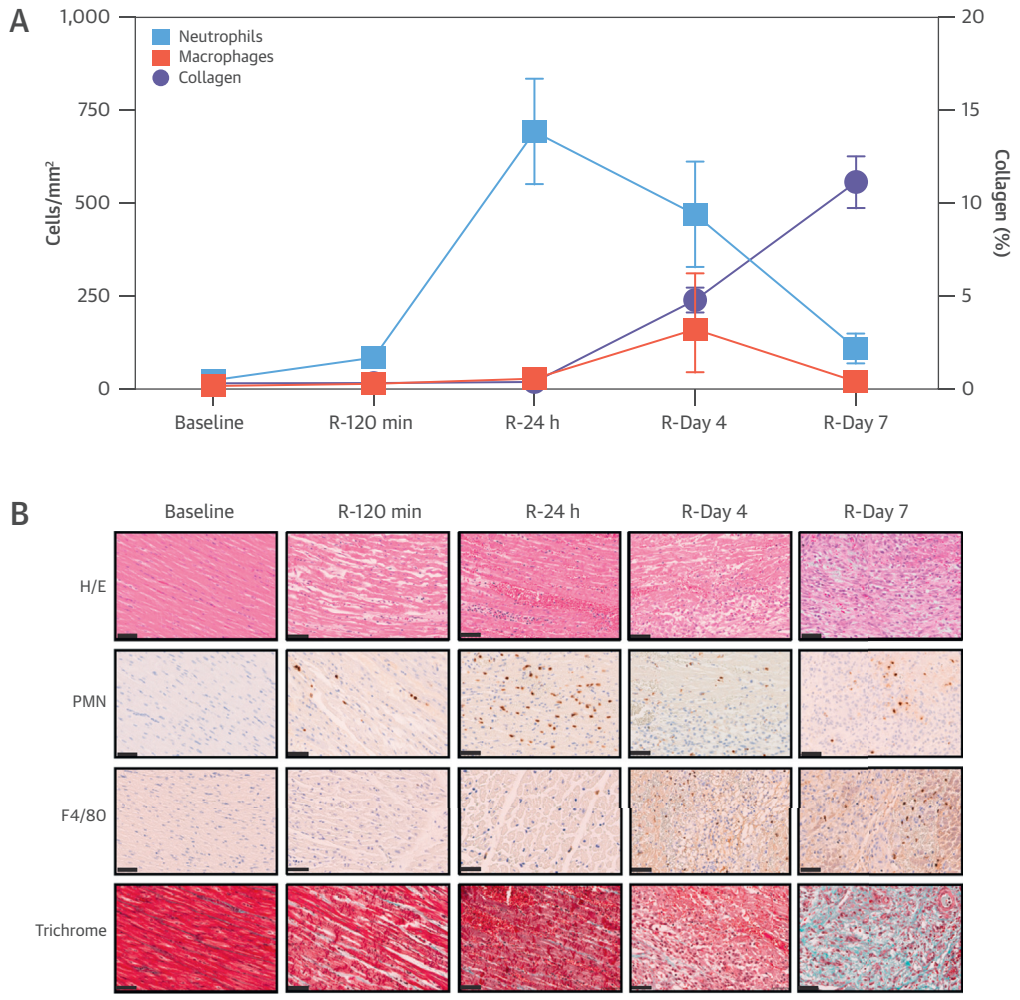

Neutrophil and macrophage density in the lesion area and collagen content in the granulation tissue **(A)** and representative images of histological changes in the ischemic myocardium **(B)** during the first week post-ischemia/reperfusion. For each time point, images are shown of staining with hematoxylin and eosin (H/E), anti-PM1, anti-F4/80, and Masson trichrome. Data are mean ± SEM. PMN = polymorphonuclear leukocytes; R = reperfusion.

FIGURE 3 Effect of Preventing Reperfusion on the Initial Wave of Post-Myocardial Infarction Edema

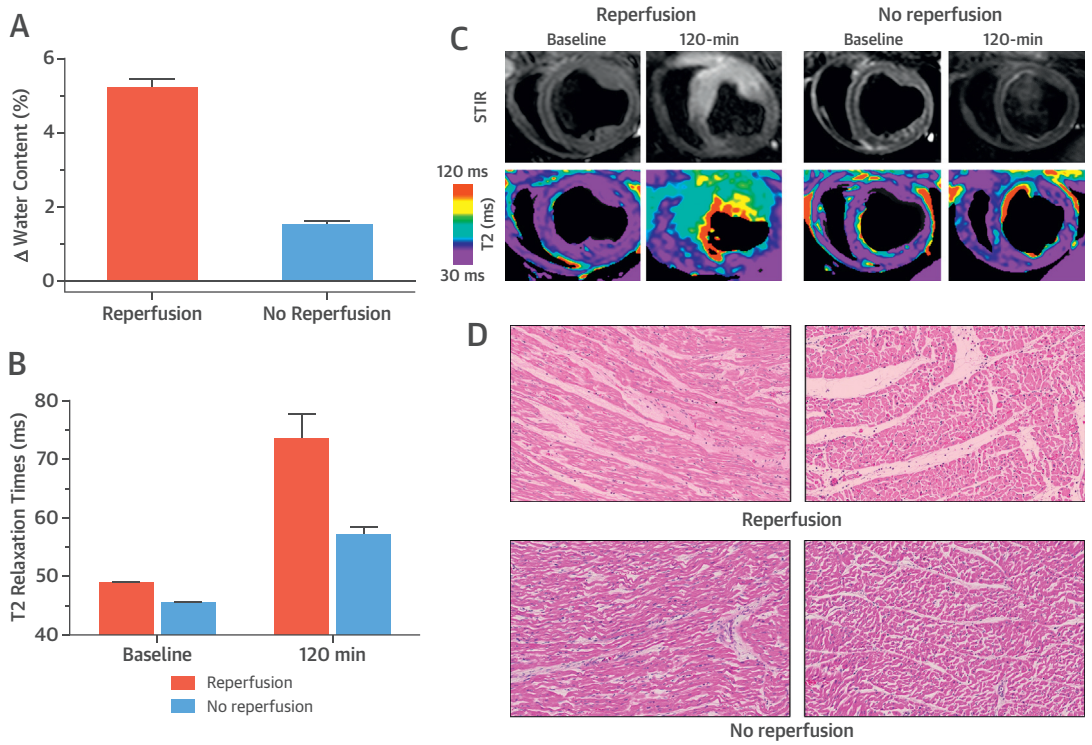

Mean differences in absolute water content at 120 min from ischemia onset between the ischemic and remote myocardial regions were 5.2% for reperfused pigs and 1.5% for nonreperfused pigs **(A)**; the latter showed an ≈70% lower relative increase in myocardial water content in the ischemic area. The nonreperfused pigs also demonstrated significantly lower 120-min cardiac magnetic resonance T2 relaxation times in the ischemic region **(B)**. Representative T2-weighted triple short-tau inversion recovery (STIR) and T2-mapping images **(C)** from representative pigs subjected to ischemia with reperfusion (40-min ischemia plus 80-min reperfusion) and with no reperfusion (120-min ischemia). Data are mean ± SEM; all T2 maps were scaled between 30 and 120 ms. Representative images of ischemic myocardial tissue stained with hematoxylin and eosin from 2 reperfused **(D, top)** and 2 nonreperfused **(D, bottom)** pigs sacrificed at 120 min after ischemia onset. Note the evident increase in extracellular space, most probably caused by extracellular edema, in reperfused pigs compared with nonreperfused animals.

$p < 0.01$) (Figure 3B). In agreement with quantitative T2 maps, qualitative T2-weighted signal intensity in nonreperfused pigs was significantly lower than that in reperfused pigs, with the intensity at 120-min CMR in the former similar to that observed pre-ischemia (baseline) (Figure 3C). Histological analysis revealed significantly less interstitial edema in the ischemic area of nonreperfused pig hearts (Figure 3D).

DEFERRED WAVE OF EDEMA AND MI HEALING. To study the potential association between the deferred wave of edema and MI healing, we modified tissue healing in the post-infarcted myocardium with 2 independent strategies: permanent coronary occlusion and high-dose steroid therapy.

Five pigs were subjected to chronic occlusion without reperfusion by delivery of a CMR-compatible coil to the mid-LAD (Group 8 in Figure 1). All animals underwent serial CMR examinations (baseline, 120 min, days 1, 4, and 7) and were sacrificed after day 7 CMR. Permanent occlusion of the coronary artery significantly attenuated the deferred wave of edema, with myocardial water content in the ischemic region at day 7 significantly lower in the nonreperfused pigs than in reperfused pigs—Group 5 (82.5 ± 1.0% vs. 85.2 ± 0.9%; $p < 0.01$) (Figure 4A).

Permanent coronary occlusion altered the dynamics of serial CMR T2 relaxation times (Figures 4B and 5). In agreement with the outcome of acute occlusion experiments, T2 relaxation times in the ischemic region on 120-min CMR were significantly lower in nonreperfused pigs, whereas T2 relaxation times at 24-h CMR did not differ between nonreperfused and reperfused pigs. Thereafter, T2 relaxation times diverged; at day 4, a trend toward lower T2 relaxation

FIGURE 4 Effect of Preventing Reperfusion on the Deferred Wave of Post-Myocardial Infarction Edema

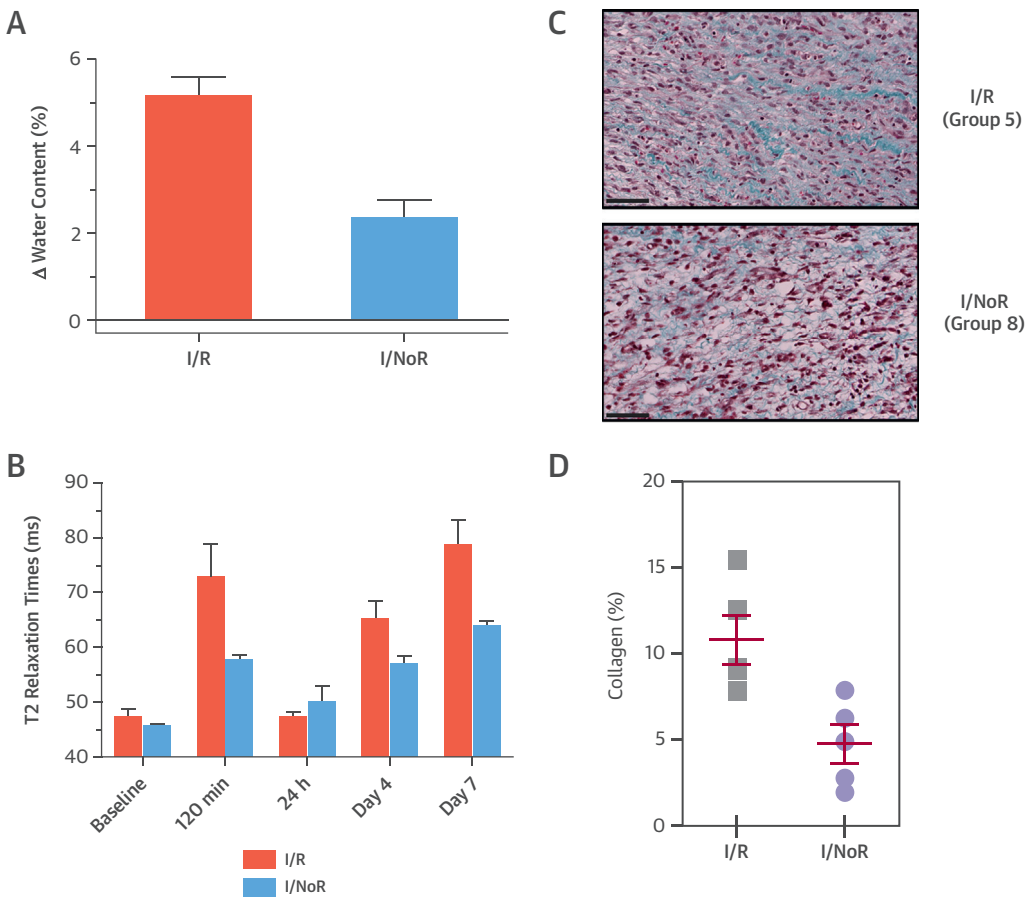

Mean differences in absolute myocardial water content on day 7 between the ischemic and remote regions were 5.1% in reperfused and 2.3% in nonreperfused pigs **(A)**; the latter showed an ≈55% lower relative increase in myocardial water content in the ischemic area. Absolute T2 relaxation times in the ischemic myocardium during the first week after ischemia/reperfusion (I/R) in reperfused and nonreperfused pigs show divergence over time **(B)**. Data are mean ± SEM. Representative Masson trichrome staining of ischemic myocardium sections taken from reperfused **(top)** and nonreperfused **(bottom)** pigs at day 7 after ischemia onset **(C)**. Collagen is stained **light blue**. Lack of reperfusion produced a lower collagen density in the lesion area **(D)**. The chart shows data from individual animals together with mean ± SEM. NoR = no reperfusion.

times was detected in the ischemic myocardium of chronically nonreperfused pigs. Consistent with the water content analysis, at day 7 this difference was statistically significant (63.8 ± 2.5 ms in nonreperfused pigs vs. 78.4 ± 10.6 ms in reperfused pigs; $p = 0.02$) (Figures 4B and 5).

Histological analysis at day 7 post-infarction revealed different healing patterns per reperfusion status. Permanent occlusion resulted in lower collagen density in the lesion area (4.7 ± 2.4% vs. 10.8 ± 3.1%; $p = 0.01$) (Figures 4C and 4D). The extent of necrosis within the lesion area was significantly higher in the nonreperfused pigs (68.9 ± 21.7% vs. 8.9 ± 12.7%; $p < 0.001$) (Figure 6), and the proportion of granulation tissue was correspondingly lower (31.1 ± 21.7% vs. 91.1 ± 12.7%; $p < 0.001$) (Figure 6).

Five pigs underwent 40-min/7-day I/R and received high intravenous doses of steroids, commencing after the 120-min CMR (Group 6 in Figure 1). All animals underwent serial CMR examinations (baseline, 120 min, days 1, 4, and 7) and were sacrificed after day 7 CMR. The pigs received 3 doses of intravenous methylprednisolone (30 mg/kg/dose) within the first 24 h post-I/R, followed by 1 daily dose of intravenous methylprednisolone (30 mg/kg) on the following 3 days.

Administration of steroids significantly altered the deferred wave of edema, with myocardial water

FIGURE 5 Effect of Preventing Reperfusion on Myocardial T2 Relaxation Time

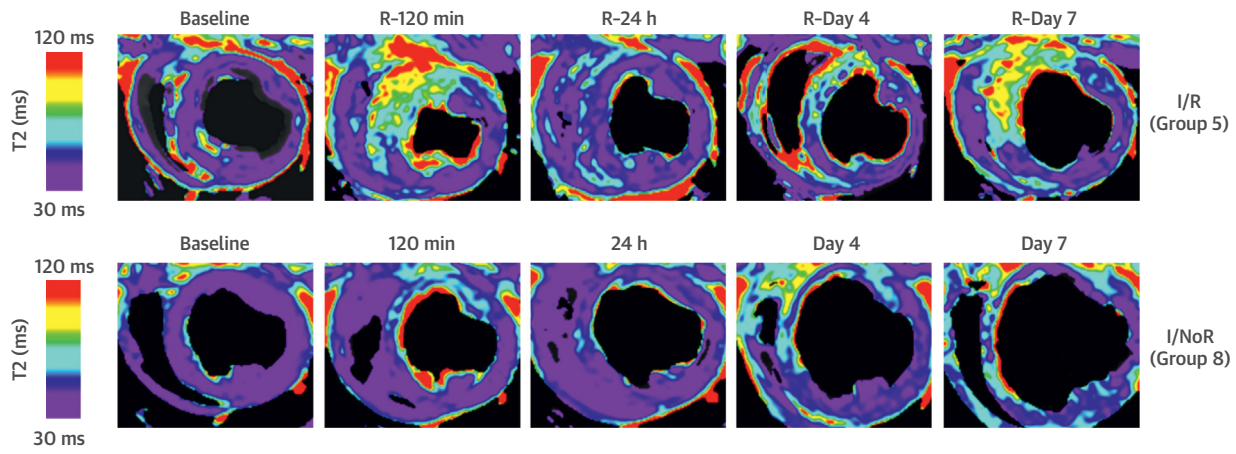

Permanent coronary occlusion altered the dynamics of serial cardiac magnetic resonance T2 relaxation times in the ischemic region as it is shown by these representative T2-mapping images from reperfused and nonreperfused pigs for all time points. All T2 maps were scaled between 30 and 120 ms. Abbreviations as in Figures 2 and 4.

content significantly lower in the ischemic region at day 7 than in the untreated pigs in Group 5 (83.3 ± 0.8% vs. 85.2 ± 0.4% for steroid-treated and untreated pigs, respectively; $p = 0.01$) (Figure 7A). This effect was not accompanied by significant differences in T2 relaxation times on day 7 CMR (77.3 ± 13.0 ms steroid-treated vs. 78.4 ± 10.6 ms untreated; $p > 0.10$) or at any of the earlier time points evaluated (Figures 7B and 8).

According to the histological analysis, high-dose steroid therapy resulted in lower collagen density in the lesion area (6.1 ± 3.4% vs. 10.8 ± 3.1%; $p = 0.05$) (Figures 7C and 7D). The proportions of necrosis and granulation tissue within the lesion area were similar in the 2 groups: 17.3 ± 18.7% and 82.7 ± 18.7%, respectively, in steroid-treated pigs vs. 8.9 ± 12.7% and 91.1 ± 12.7% in nontreated pigs ($p > 0.10$) (Figure 6). Water content and hemorrhage scores in the myocardium of pigs sacrificed on day 7 after ischemia onset is summarized in Table 2.

DISCUSSION

Recent work has shown that the edematous reaction in the reperfused post-infarcted myocardium is not stable, but follows a bimodal pattern. An initial wave of edema appears on reperfusion, abating almost completely by 24 h, followed by a deferred wave that initiates days after I/R and peaks around 1 week after infarction (13). In the present study, we explored the possible mechanisms underlying these 2 waves of post-I/R edema through a comprehensive histopathological analysis and state-of-the-art CMR serial evaluations in the pig model. Our results show that the 2 waves of post-I/R edema are produced by different processes that can be independently modulated (Central Illustration). The absence of reperfusion almost completely abolishes the initial wave, indicating that it is a direct consequence of the reperfusion process. The deferred wave is substantially altered by interventions that impair healing in the post-infarcted myocardium (absence of reperfusion and high-dose steroid therapy), thus implicating tissue healing processes in this second phase of edema. Elucidation of the pathophysiology underlying bimodal post-I/R edema has potential translational implications in diagnosis, prognosis, and therapy. Pharmacological or other interventions targeting the pathways implicated in the initial or deferred waves of post-I/R edema could contribute to better cardiac recovery and remodeling, and thus improve prognosis in patients experiencing an acute MI. Additionally, this study provides a comprehensive histological characterization of the dynamic changes occurring in a large animal model of reperfused MI.

Water is the major component of healthy cardiac tissue. In steady-state conditions, myocardial water content is stable and mostly intracellular, with only a very small interstitial component in the extracellular matrix. During MI, edema occurs initially as cardiomyocyte swelling during the early stages of

FIGURE 6 Effect of Nonreperfusion and High-Dose Steroid Therapy on the Proportion of Necrosis/Granulation Tissue Within the Healing Myocardium

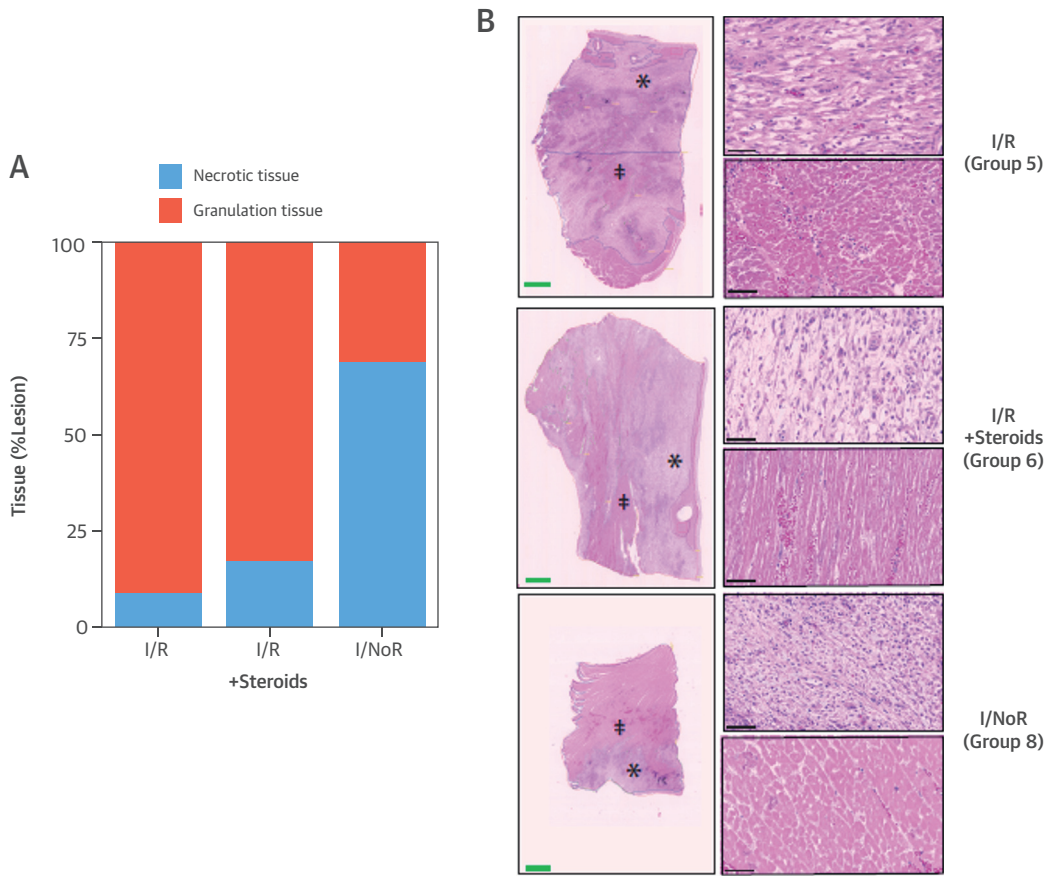

(A) Proportion of necrosis and granulation tissue within the lesion area of pigs sacrificed on day 7 after ischemia onset. **(B)** Histological sections stained with hematoxylin and eosin show features of myocardial infarction repair in pigs sacrificed on day 7 after ischemia onset: full transverse sections of infarcted myocardium (**left**; ×1 magnification) and granulation tissue **(upper subpanel)** and necrotic tissue **(lower subpanel)** (**right**; ×40) from 1 representative pig per group.*Granulation tissue. ‡Necrotic tissue. Abbreviations as in Figure 4.

ischemia (7). Myocardial edema is then exacerbated significantly on restoration of blood flow to the ischemic region. This reperfusion-associated increase seems to be caused by increased cell swelling (5) and, more importantly, by interstitial edema secondary to reactive hyperemia and leakage from capillaries damaged when hydrostatic pressure is restored on reperfusion (3,6). For many years, this myocardial edema was believed to remain stable for at least 1 week (8–10); this view led many experimental studies and clinical trials to rely on the ability of CMR and other imaging tools to retrospectively evaluate post-MI edema (10–12). The concept of stable post-I/R edema was recently challenged in an experimental analysis by our group in a pig model of I/R, revealing the bimodal pattern of the edematous response (13). The present study confirms our original description of a bimodal response and provides insight into the underlying pathophysiological mechanisms.

The association between the initial, hyperacute edematous response and the reperfusion process has been reported previously (2,16). In agreement with those studies, here we show that the absence of reperfusion almost completely abolishes the early increase in water content and the CMR-measured regional T2 relaxation times in the ischemic myocardium. Indirect histological detection of interstitial edema (increased extracellular volume) was consistent with the water content and CMR data. Our study demonstrates that the reperfusion-driven hyperacute edematous reaction (4) is exhausted after 24 h; moreover, these processes can be visualized and

FIGURE 7 Effect of High-Dose Steroid Therapy on the Deferred Wave of Post-Myocardial Infarction Edema

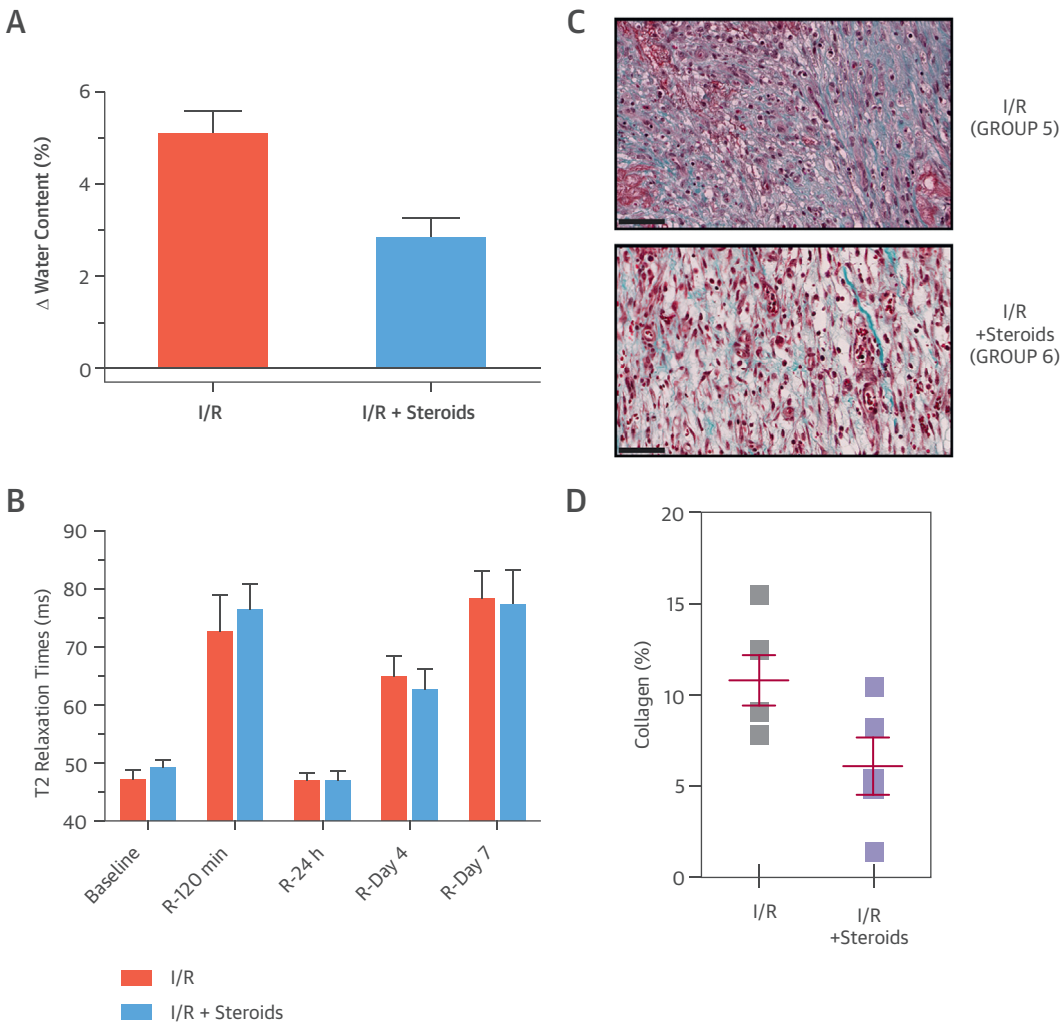

Mean differences in absolute water content between the ischemic and remote myocardial regions were 5.1% in reperfused nontreated pigs and 2.8% in reperfused steroid-treated pigs **(A)**; the latter showed an ≈45% lower relative increase in myocardial water content in the ischemic area. Absolute T2 relaxation times in the ischemic myocardium during the first week post-I/R were similar in nontreated and steroid-treated pigs **(B)**. Data are mean ± SEM. Masson trichrome staining of ischemic myocardium sections taken from nontreated **(top)** and steroid-treated **(bottom)** pigs on day 7 post-I/R **(C)**. Steroid treatment showed a lower collagen density in the lesion area **(D)**. The chart shows data from individual animals together with mean ± SEM. Abbreviations as in Figure 4.

quantified by state-of-the-art contemporaneous T2 CMR sequences, a finding of special translational relevance. Although water content in the ischemic myocardium decreases significantly during the first 24 h post-reperfusion, it does not return to normal values, whereas T2 relaxation time does decrease to values seen in the pre-ischemia baseline scan (13). These data indicate that myocardial water content may not be the only factor influencing post-infarction T2 relaxation time. The fact that the interstitial hemorrhage was more pronounced at 24 h than early after reperfusion (Table 2) suggests a possible contribution from the well-described paramagnetic effect of hemoglobin denaturation products (17).

We hypothesized that the deferred wave of edema might be related to early healing, a process coinciding with the deferred edema wave. To test this hypothesis, we used 2 independent strategies to manipulate this biological phenomenon: high-dose steroid therapy and absence of reperfusion. Steroids are well known to interfere with collagen deposition in healing infarcts (18,19) and absence of reperfusion is

FIGURE 8 Effect of High-Dose Steroid Therapy on Myocardial T2 Relaxation Time

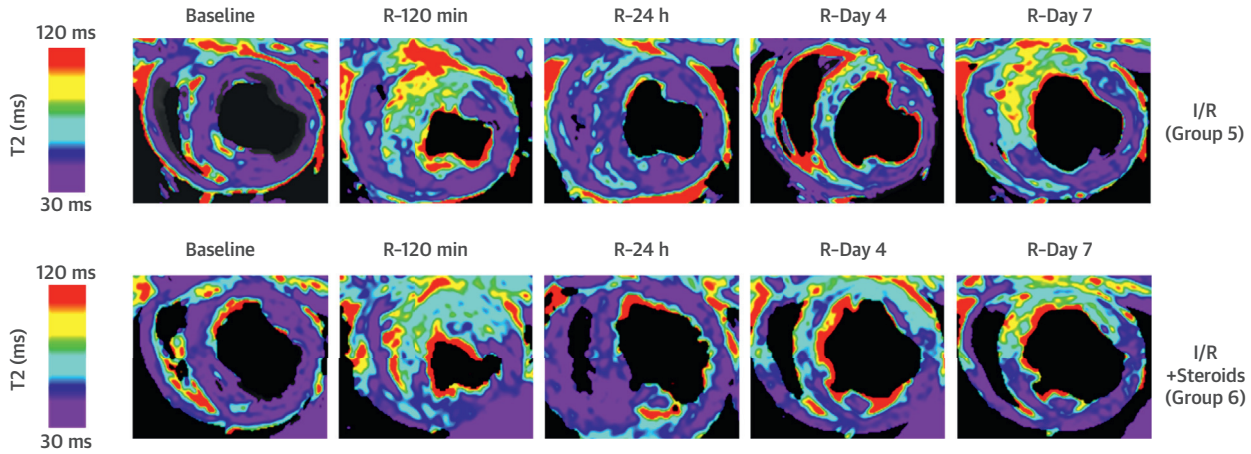

Treatment with high-dose steroid therapy did not alter the dynamics of serial cardiac magnetic resonance T2 relaxation times in the ischemic region as it is shown by these representative T2-mapping images from reperfused nontreated and treated pigs for all time points. All T2 maps were scaled between 30 and 120 ms. Abbreviations as in Figures 2 and 4.

associated with significant delay to healing (1,2,20), in contrast with reperfusion, which accelerates this process. Both interventions altered the deferred wave of edema, as demonstrated by the significant reductions in water content in the ischemic myocardium of steroid-treated and nonreperfused animals compared with reperfused animals not receiving steroids. CMR data in nonreperfused pigs paralleled the water content measures, with T2 relaxation times at day 7 significantly lower than in reperfused pigs.

However, T2 relaxation times in steroid-treated pigs did not differ from values in untreated pigs. This apparent discrepancy might be explained by the effect of steroid therapy on collagen content: myocardial tissue from steroid-treated pigs showed a significant reduction in collagen content compared with untreated pigs, in agreement with previous reports (18). Collagen deposition correlates inversely with CMR T2 relaxation times (21–23); this effect may thus have compensated for the reduced water content, resulting in no net alteration in CMR T2 relaxation time in untreated pigs. The counterbalancing effects of water and collagen content highlight the likelihood that CMR T2 relaxation time is a composite measure of several phenomena occurring in the post-I/R myocardium. Collagen deposition was also reduced by permanent occlusion, where CMR T2 relaxation times and water content were consistent with each other. Notably, the infarct composition was different in steroid-treated and nonreperfused hearts at day 7. The proportions of necrosis and granulation tissue within the myocardial lesion were similar in steroid-treated and standard reperfused pigs, whereas lesions in the nonreperfused pigs had a much higher proportion of necrotic tissue, indicating a delay to healing. Several factors might contribute to the discrepancies in water content and T2 relaxation time observed between nonreperfused pigs and steroid-treated reperfused pigs: distinct healing characteristics; different myocardial perfusion status related to circulation-induced increases in T2 relaxation time (24); and indirect influences, such as inflammation (25,26) and angiogenesis (27).

The results of the present study show that the 2 waves of post-I/R edema are caused by different phenomena that can be independently modulated.

TABLE 2 Myocardial Water Content and Hemorrhage Score in Pigs*

	40 Min/7 Days I/R (Group 5)	40 Min/7 Days I/R + 7-Day Coronary Steroid Therapy (Group 6)	40 Min/7 Days I/R + 7-Day Coronary Occlusion (Group 8)	p Value†	p Value‡
Water content, ischemic, %	85.2 ± 0.9	83.3 ± 0.8	82.5 ± 1.0	0.01	<0.01
Water content, remote, %	80.1 ± 0.3	80.4 ± 0.3	80.2 ± 0.4	NS	NS
Hemorrhage, score 0–5	1 (0–2)	0 (0–3)	1 (1–2)	NS	NS

Values are mean ± SD or median (interquartile range). Interstitial hemorrhage is graded from 0 (absence) to 5 (very severe). *Sacrificed on day 7 after ischemia onset. †Comparison between Group 5 (I/R with no other intervention) and Group 6 (I/R plus steroid therapy). ‡Comparison between Group 5 (I/R with no other intervention) and Group 8 (I/No R).

NS = not significant; other abbreviations as in Table 1.

CENTRAL ILLUSTRATION **Mechanisms Underlying the Bimodal Edema Phenomenon After Myocardial Ischemia/Reperfusion**

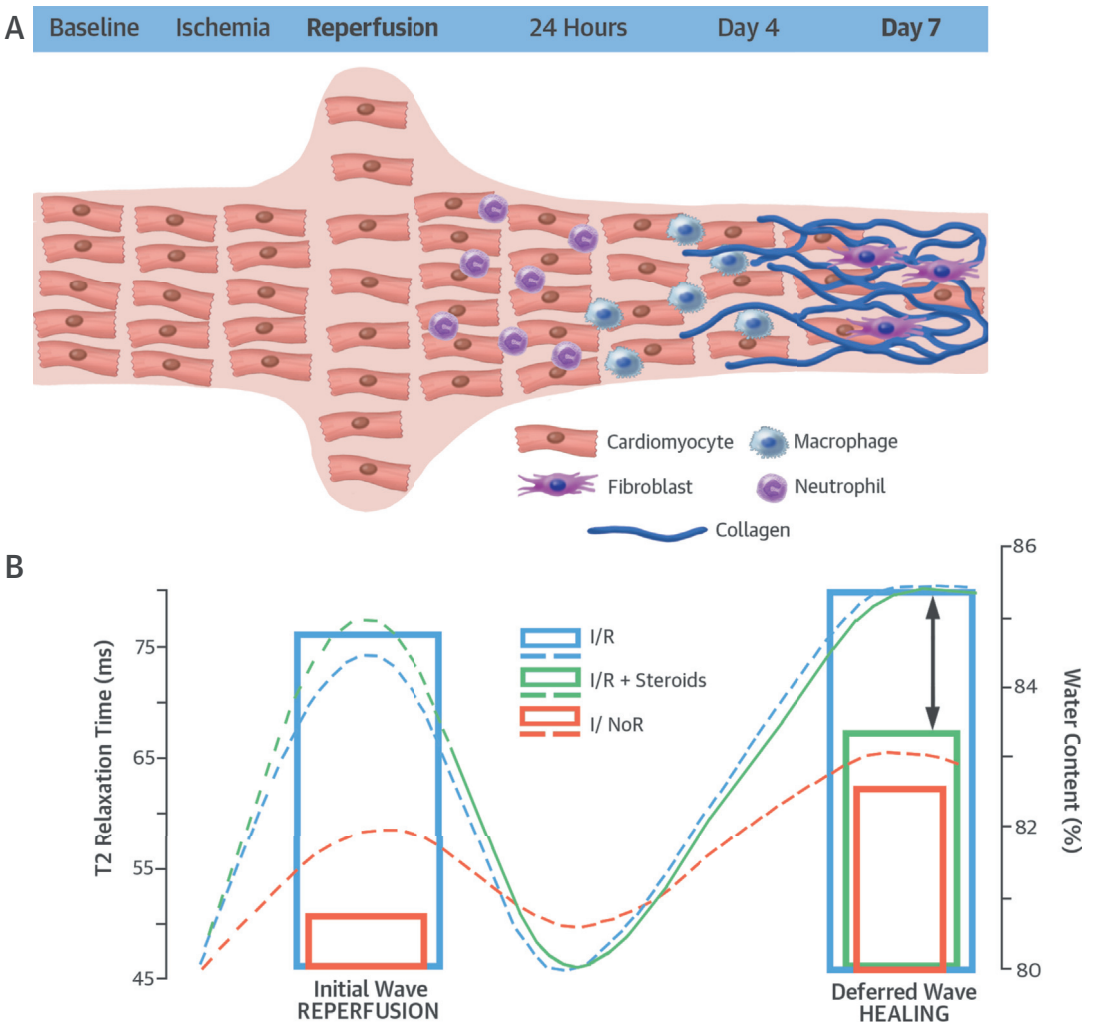

Fernández-Jiménez, R. et al. J Am Coll Cardiol. 2015; 66(7):816–28.

Two distinct waves of edema emerge within the first week after ischemia/reperfusion (I/R) because of different pathophysiological processes. The initial wave, appearing abruptly on reperfusion, is a direct consequence of the reperfusion process itself, whereas the deferred wave, appearing progressively days after I/R, is mainly caused by tissue healing processes. **(A)** Reperfusion is associated with a very abrupt edematous reaction that separates myocardial fibers from each other, resolving by day 1. Post-infarction, an initial neutrophil infiltration (peaking by day 1) is followed by macrophage infiltration (peaking by day 4). From day 4 on, necrotic cardiomyocytes are progressively replaced by granulation tissue and collagen. **(B)** Myocardial water content was evaluated by histology. **Boxes** represent water content measurements in pigs; **blue** = regular I/R protocol; **salmon** = permanent coronary occlusion (nonreperfused myocardial infarction; initial edema wave abrogated, deferred wave significantly attenuated); **green** = I/R plus steroid therapy (deferred wave significantly attenuated). The **lines** show cardiac magnetic resonance T2 relaxation time course in the ischemic myocardium; **blue** = first week after infarction (2 peaks closely track the water content changes); **salmon** = nonreperfused myocardial infarction (both waves of cardiac magnetic resonance-evaluated edema significantly attenuated); and **green** = I/R plus steroid therapy (**continuous line** after initiation of therapy). In this last case, T2 relaxation time does not track attenuation of the deferred wave as evaluated by the histological reference standard, highlighting the need for caution in interpreting cardiac magnetic resonance analysis of the post-myocardial infarction heart. **Double arrowed line** = discrepancy between water content and T2 relaxation time at day 7 in steroid group. NoR = no reperfusion.

Although the initial wave is mainly caused by the reperfusion itself, the deferred wave of edema is mainly caused by healing processes. Additionally, the present study shows that myocardial T2 relaxation time seems to be affected by dynamic factors occurring during the repair of the infarcted tissue, highlighting the need for caution in interpreting CMR analysis of the post-MI heart.

STUDY LIMITATIONS. Extrapolation of the results of this experimental study to the clinic should be done cautiously. Nonetheless, the pig is one of the most clinically translatable large animal models for the study of I/R issues given its similar coronary artery anatomy and distribution to humans and minimal pre-existing coronary collateral flow. The use of a large animal model is of great translational value (28), especially considering the difficulty of performing such a comprehensive serial CMR study (including 1 examination immediately on reperfusion) and histological validation in patients. The time course of tissue changes in the post-I/R myocardium in pigs, albeit slightly shorter, is similar to that in humans (21). Moreover, the process of infarct healing is qualitatively similar in both species, in that infarct healing involves a sequential infiltration of neutrophils and macrophages, removal of necrotic myocytes, formation of granulation tissue, and collagen deposition. The present study does not provide information on the localization of the elevated water content within the myocardial tissue; indeed, there are no reliable methods to distinguish between intracellular and interstitial increases in myocardial water content (25).

In this study, the regions of interest for T2 relaxation time quantification included the entire wall thickness and were individually adjusted by hand to carefully avoid the right and left ventricular cavities. Regions of interest might therefore include different myocardial states (e.g., hemorrhage or microvascular obstruction). We took this approach to mimic the histological evaluation of water content, which assesses the entire wall thickness. We believe that the possible inclusion of different myocardial states had little effect on the results relating to the pathophysiology of bimodal edema given that this biological process has also been measured by histological means in the present study. However, it might have had some influence on the differences in absolute T2 relaxation times between our study and others taking a different approach to region of interest selection.

CONCLUSIONS

The present study elucidates the pathophysiology underlying the bimodal edematous reaction after I/R. The initial wave of edema, appearing abruptly on reperfusion and dissipating at 24 h, is directly secondary to the reperfusion process itself. The deferred wave of edema, appearing progressively days after I/R and peaking around day 7, is mainly caused by tissue healing processes.

ACKNOWLEDGMENTS The authors thank Tamara Córdoba, Oscar Sanz, Eugenio Fernández, and other members of the Centro Nacional de Investigaciones Cardiovasculares Carlos III animal facility and farm for outstanding animal care and support, and Brenda Guijarro for assistance with histological sample processing. Simon Bartlett (Centro Nacional de Investigaciones Cardiovasculares Carlos III) provided English editing.

REPRINT REQUESTS AND CORRESPONDENCE: Dr. Borja Ibáñez, Translational Laboratory for Cardiovascular Imaging and Therapy, Centro Nacional de Investigaciones Cardiovasculares Carlos III, Melchor Fernández Almagro 3, 28029 Madrid, Spain. E-mail: bibanez@cnic.es.

PERSPECTIVES

COMPETENCY IN MEDICAL KNOWLEDGE: After ischemic injury, the course of myocardial edema is bimodal. Acute reperfusion is responsible for the initial acute edematous reaction, whereas healing is implicated in the later wave of edema.

TRANSLATIONAL OUTLOOK: Additional research is needed to develop pharmacological or other interventions that target pathways implicated in the initial or deferred waves of edema after post-ischemic reperfusion, and evaluate the efficacy of these strategies to accelerate cardiac recovery and improve clinical outcomes of patients with acute myocardial infarction.

REFERENCES

1. Vandervelde S, van Amerongen MJ, Tio RA, et al. Increased inflammatory response and neovascularization in reperfused vs. non-reperfused murine myocardial infarction. Cardiovasc Pathol 2006;15:83–90.

2. Reimer KA, Vander Heide RS, Richard VJ. Reperfusion in acute myocardial infarction: effect of timing and modulating factors in experimental models. Am J Cardiol 1993;72:13–21G.

3. Bragadeesh T, Jayaweera AR, Pascotto M, et al. Post-ischaemic myocardial dysfunction (stunning) results from myofibrillar oedema. Heart 2008;94:166–71.

4. Garcia-Dorado D, Oliveras J, Gili J, et al. Analysis of myocardial oedema by magnetic resonance imaging early after coronary artery occlusion with or without reperfusion. Cardiovasc Res 1993;27:1462–9.

5. Kloner RA, Ganote CE, Whalen DA Jr., Jennings RB. Effect of a transient period of ischemia on myocardial cells. II. Fine structure during the first few minutes of reflow. Am J Pathol 1974;74:399–422.

6. Turschner O, D'Hooge J, Dommke C, et al. The sequential changes in myocardial thickness and thickening which occur during acute transmural infarction, infarct reperfusion and the resultant expression of reperfusion injury. Eur Heart J 2004;25:794–803.

7. Whalen DA Jr., Hamilton DG, Ganote CE, Jennings RB. Effect of a transient period of ischemia on myocardial cells. I. Effects on cell volume regulation. Am J Pathol 1974;74:381–97.

8. Carlsson M, Ubachs JF, Hedstrom E, et al. Myocardium at risk after acute infarction in humans on cardiac magnetic resonance: quantitative assessment during follow-up and validation with single-photon emission computed tomography. J Am Coll Cardiol Img 2009;2:569–76.

9. Dall'Armellina E, Karia N, Lindsay AC, et al. Dynamic changes of edema and late gadolinium enhancement after acute myocardial infarction and their relationship to functional recovery and salvage index. Circ Cardiovasc Imaging 2011;4:228–36.

10. Arai AE, Leung S, Kellman P. Controversies in cardiovascular MR imaging: reasons why imaging myocardial T2 has clinical and pathophysiologic value in acute myocardial infarction. Radiology 2012;265:23–32.

11. Friedrich MG. Tissue characterization of acute myocardial infarction and myocarditis by cardiac magnetic resonance. J Am Coll Cardiol Img 2008;1:652–62.

12. Friedrich MG, Abdel-Aty H, Taylor A, et al. The salvaged area at risk in reperfused acute myocardial infarction as visualized by cardiovascular magnetic resonance. J Am Coll Cardiol 2008;51:1581–7.

13. Fernandez-Jimenez R, Sanchez-Gonzalez J, Aguero J, et al. Myocardial edema after ischemia/reperfusion is not stable and follows a bimodal pattern: imaging and histological tissue characterization. J Am Coll Cardiol 2015;65:315–23.

14. Kloner RA. New observations regarding post-ischemia/reperfusion myocardial swelling. J Am Coll Cardiol 2015;65:324–6.

15. Garcia-Prieto J, Garcia-Ruiz JM, Sanz-Rosa D, et al. β3 adrenergic receptor selective stimulation during ischemia/reperfusion improves cardiac function in translational models through inhibition of mPTP opening in cardiomyocytes. Basic Res Cardiol 2014;109:422.

16. Wisenberg G, Prato FS, Carroll SE, et al. Serial nuclear magnetic resonance imaging of acute myocardial infarction with and without reperfusion. Am Heart J 1988;115:510–8.

17. Lotan CS, Bouchard A, Cranney GB, et al. Assessment of postreperfusion myocardial hemorrhage using proton NMR imaging at 1.5 T. Circulation 1992;86:1018–25.

18. Kloner RA, Fishbein MC, Lew H, et al. Mummification of the infarcted myocardium by high dose corticosteroids. Circulation 1978;57:56–63.

19. Cutroneo KR, Rokowski R, Counts DF. Glucocorticoids and collagen synthesis: comparison of in vivo and cell culture studies. Coll Relat Res 1981;1:557–68.

20. Connelly CM, Ngoy S, Schoen FJ, Apstein CS. Biomechanical properties of reperfused transmural myocardial infarcts in rabbits during the first week after infarction: implications for left ventricular rupture. Circ Res 1992;71:401–13.

21. Jackowski C, Christe A, Sonnenschein M, et al. Postmortem unenhanced magnetic resonance imaging of myocardial infarction in correlation to histological infarction age characterization. Eur Heart J 2006;27:2459–67.

22. Koenig SH. Classes of hydration sites at protein-water interfaces: the source of contrast in magnetic resonance imaging. Biophys J 1995;69:593–603.

23. Reiter DA, Lin PC, Fishbein KW, et al. Multicomponent T2 relaxation analysis in cartilage. Magn Reson Med 2009;61:803–9.

24. Barth M, Moser E. Proton NMR relaxation times of human blood samples at 1.5 T and implications for functional MRI. Cell Mol Biol (Noisy-le-grand) 1997;43:783–91.

25. Garcia-Dorado D, Andres-Villarreal M, Ruiz-Meana M, et al. Myocardial edema: a translational view. J Mol Cell Cardiol 2012;52:931–9.

26. Bonner F, Borg N, Jacoby C, et al. Ecto-5'-nucleotidase on immune cells protects from adverse cardiac remodeling. Circ Res 2013;113:301–12.

27. Lambert JM, Lopez EF, Lindsey ML. Macrophage roles following myocardial infarction. Int J Cardiol 2008;130:147–58.

28. Fernández-Jiménez R, Fernández-Friera L, Sánchez-González J, Ibáñez B. Animal models of tissue characterization of area at risk, edema and fibrosis. Curr Cardiovasc Imaging Rep 2014;7:1–10.

KEY WORDS collagen, edema, healing, magnetic resonance, myocardial infarction, T2, tissue

APPENDIX For a supplemental Methods section, please see the online version of this article.

Original research article #6. "*Effect of ischemia duration and protective interventions on the temporal dynamics of tissue composition after myocardial infarction*".[73]

Part of this work was presented by the doctoral student at the 65th American College of Cardiology´s Annual Scientific Sessions, in Chicago (April 2016; Illinois, USA). The communication received a *Best Abstract Award*: "the American College of Cardiology and the Spanish Society of Cardiology recognized Rodrigo Fernandez-Jimenez as first author of the highest ranking abstract submitted from Spain and accepted for presentation at the American College of Cardiology´s Annual Scientific Sessions in Chicago (April 2016; Illinois, USA)".

Part of this work was presented by the doctoral student as Late Breaking Basic Science communication at the American Heart Association Scientific Sessions 2016, in New Orleans (November 2016; Louisiana, USA).

OPEN

Effect of Ischemia Duration and Protective Interventions on the Temporal Dynamics of Tissue Composition After Myocardial Infarction

Rodrigo Fernández-Jiménez, Carlos Galán-Arriola, Javier Sánchez-González, Jaume Agüero, Gonzalo J. López-Martín, Sandra Gomez-Talavera, Jaime Garcia-Prieto, Austin Benn, Antonio Molina-Iracheta, Manuel Barreiro-Pérez, Ana Martin-García, Inés García-Lunar, Gonzalo Pizarro, Javier Sanz, Pedro L. Sánchez, Valentin Fuster, Borja Ibanez

Rationale: **The impact of cardioprotective strategies and ischemia duration on postischemia/reperfusion (I/R) myocardial tissue composition (edema, myocardium at risk, infarct size, salvage, intramyocardial hemorrhage, and microvascular obstruction) is not well understood.**

Objective: **To study the effect of ischemia duration and protective interventions on the temporal dynamics of myocardial tissue composition in a translational animal model of I/R by the use of state-of-the-art imaging technology.**

Methods and Results: **Four 5-pig groups underwent different I/R protocols: 40-minute I/R (prolonged ischemia, controls), 20-minute I/R (short-duration ischemia), prolonged ischemia preceded by preconditioning, or prolonged ischemia followed by postconditioning. Serial cardiac magnetic resonance (CMR)-based tissue characterization was done in all pigs at baseline and at 120 minutes, day 1, day 4, and day 7 after I/R. Reference myocardium at risk was assessed by multidetector computed tomography during the index coronary occlusion. After the final CMR, hearts were excised and processed for water content quantification and histology. Five additional healthy pigs were euthanized after baseline CMR as reference. Edema formation followed a bimodal pattern in all 40-minute I/R pigs, regardless of cardioprotective strategy and the degree of intramyocardial hemorrhage or microvascular obstruction. The hyperacute edematous wave was ameliorated only in pigs showing cardioprotection (ie, those undergoing short-duration ischemia or preconditioning). In all groups, CMR-measured edema was barely detectable at 24 hours postreperfusion. The deferred healing-related edematous wave was blunted or absent in pigs undergoing preconditioning or short-duration ischemia, respectively. CMR-measured infarct size declined progressively after reperfusion in all groups. CMR-measured myocardial salvage, and the extent of intramyocardial hemorrhage and microvascular obstruction varied dramatically according to CMR timing, ischemia duration, and cardioprotective strategy.**

Conclusions: **Cardioprotective therapies, duration of index ischemia, and the interplay between these greatly influence temporal dynamics and extent of tissue composition changes after I/R. Consequently, imaging techniques and protocols for assessing edema, myocardium at risk, infarct size, salvage, intramyocardial hemorrhage, and microvascular obstruction should be standardized accordingly. (*Circ Res*. 2017;121:439-450. DOI: 10.1161/CIRCRESAHA.117.310901.)**

Key Words: edema ■ ischemic preconditioning ■ ischemic postconditioning ■ magnetic resonance imaging ■ reperfusion injury ■ translational medical research

Original received February 28, 2017; revision received June 2, 2017; accepted June 8, 2017. In May 2017, the average time from submission to first decision for all original research papers submitted to *Circulation Research* was 12.28 days.

From the Department of Clinical Research, Centro Nacional de Investigaciones Cardiovasculares Carlos III (CNIC), Madrid, Spain (R.F.-J., C.G.-A., J.A., G.J.L.-M., S.G.-T., J.G.-P., A.B., A.M.-I., I.G.-L., G.P., J.S., V.L., B.I.); Centro de Investigación Biomédica en Red de enfermedades CardioVasculares (CIBERCV) (R.F.-J., C.G.-A., J.A., S.G.-T., J.G.-P., M.B.-P., A.M.-G., I.G.-L., G.P., P.L.S., B.I.); Department of Cardiology, The Zena and Michael A. Wiener Cardiovascular Institute, Icahn School of Medicine at Mount Sinai, New York (R.F.-J., J.S., V.L.); Department of Clinical Research, Philips Healthcare, Madrid, Spain (J.S.-G.); Department of Cardiology, Hospital Universitario de Salamanca, Instituto de Investigación Biomédica de Salamanca, Spain (M.B.-P., A.M.-G., P.L.S.); Department of Cardiology, Hospital Universitario Quiron (I.G.-L.) and Complejo Hospitalario Ruber Juan Bravo (G.P.), European University of Madrid, Spain; and Department of Cardiology, IIS-Fundación Jiménez Díaz Hospital, Madrid, Spain (S.G.-T., B.I.).

The online-only Data Supplement is available with this article at http://circres.ahajournals.org/lookup/suppl/doi:10.1161/CIRCRESAHA.117.310901/-/DC1.

Correspondence to Borja Ibanez, MD, PhD, Translational Laboratory for Cardiovascular Imaging and Therapy, Centro Nacional de Investigaciones Cardiovasculares Carlos III, Melchor Fernández Almagro, 3, 28029 Madrid, Spain. E-mail bibanez@cnic.es

Novelty and Significance

What Is Known?

- Edema formation, inflammation, and microvascular injury contribute to irreversible loss of cardiac myocytes after myocardial I/R.
- The presence and extent of these processes and tissue healing are associated with outcome after MI.
- Evaluation of myocardial tissue composition changes by CMR imaging (ie, tissue characterization) serves as surrogate end points in experimental and clinical studies and clinical trials.

What New Information Does This Article Contribute?

- By using serial CMR exams in a translational large animal model of I/R, this study shows that the temporal dynamics and extent of post-MI tissue composition changes are greatly influenced by the application of cardioprotective interventions, the duration of the index ischemia, and the interplay between them.
- Rather than estimates of the ischemic area alone, the degree and spatial extent of myocardial edema seems to be a surrogate marker of ischemic insult severity.
- These findings highlight the need for protocol standardization when using post-MI imaging techniques to measure relevant end points in experimental and clinical studies.

Post-MI tissue composition is highly dynamic and could be characterized by CMR, which has been used to assess surrogate outcomes and efficacy end points in many experimental and clinical studies. However, there is paucity of studies tracking the temporal dynamics of these processes in a comprehensive manner. Our current work shows that the degree and extent of post-MI tissue composition changes (edema, necrosis, hemorrhage, and MVO) as assessed by CMR are greatly influenced by the time of image acquisition, duration of ischemia, cardioprotective strategies, and the interplay between them. Therefore, clinical and experimental imaging protocols for post-MI tissue characterization aiming at quantifying edema, myocardial area at risk, IS, myocardial salvage, IMH, and MVO should take into consideration these dynamics and be as standardized as possible.

Nonstandard Abbreviations and Acronyms

CMR	cardiac magnetic resonance
IMH	intramyocardial hemorrhage
I/R	ischemia/reperfusion
IR-TFE	inversion recovery turbo field echo
IS	infarct size
LAD	left anterior descending
LGE	late gadolinium enhancement
LV	left ventricle
LVEF	left ventricular ejection fraction
MaR	myocardium at risk
MDCT	multidetector computed tomography
MI	myocardial infarction
MVO	microvascular obstruction
ROI	region of interest
STIR	short-tau triple inversion-recovery
T2W	T2-weighted

Ischemia/reperfusion (I/R) results in a dramatic change of myocardial tissue composition, mainly in the first days after myocardial infarction (MI).[1,2] Edema formation, inflammation, microvascular injury, and ultimately healing, among other phenomena, accompany irreversible loss of cardiac myocytes after MI. Cardiac magnetic resonance (CMR) can noninvasively identify most of these phenomena; however, accounting for the temporal dynamics and factors affecting post-MI tissue composition might be crucial for a precise assessment of related imaging end points. To date, this has not been studied in a comprehensive manner.

Editorial, see p 326
Meet the First Author, see p 312

For years, the intense edematous reaction appearing in the postischemic region early after MI was thought to persist in stable form for at least 1 week.[3,4] On this basis, delineating the extent of post-MI edema by CMR rapidly became established as a measure of the original occluded coronary artery perfusion territory (myocardium at risk [MaR]).[5,6] Thus, the amount of salvaged myocardium[7]—a theoretically better surrogate of the effect of cardioprotective therapies[8]—has been estimated from quantifications of the extent of delayed gadolinium enhanced myocardium (infarct size [IS]) and the extent of myocardial edema (assumed to delineate the MaR) in the same imaging session. Consequently, multiple clinical and experimental studies have used CMR-measured edema and IS as end points, within a single imaging session performed at a variety of post-MI time points.[9] Recent evidence has challenged the view of a stable post-MI edema reaction, demonstrating dynamic changes in edema in a pig model of MI.[10,11] In this model, an initial hyperacute edema reaction on reperfusion resolves within 24 hours and is followed by a deferred healing-related edema wave occurring a few days after reperfusion. Notably, intramyocardial hemorrhage (IMH) and microvascular obstruction (MVO) can counteract the high-intensity edema signal on T2 sequences by reducing tissue T2 relaxation time. The impact of IMH and MVO on the bimodal edematous reaction is, thus, a matter of intense debate.[12–15] Moreover, the extent/degree of edema might be lower in patients undergoing infarct-limiting cardioprotective interventions.[16,17] Another variable that might differently affect post-MI tissue composition is ischemia duration.[18] However, CMR exams were performed at different time points in these studies, precluding a definitive interpretation.

In summary, temporal dynamics and extent of post-I/R key phenomena (edema, necrosis, MVO, and IMH) might be affected by duration of the index ischemic event, by the application of cardioprotective interventions and the interplay between them, but to date, this has not been studied in a comprehensive manner. To elucidate these, we designed an experimental study in which pigs underwent different myocardial I/R protocols. CMR was performed at baseline and at 120 minutes, 24 hours, 4 days, and 7 days after I/R for the serial noninvasive assessment of myocardial edema, extent of IMH and MVO, IS, and myocardial salvage. Histology and quantification of

myocardial water content by reference standard were performed at sacrifice immediately after the final CMR scan.

Methods

Study Design and MI Procedure

The study population comprised 25 Large White male pigs weighing 30 to 40 kg. The study was approved by the Institutional and Regional Animal Research Committees, and the study design is summarized in Online Figure I. Five pigs were euthanized with no intervention other than baseline CMR and served as reference healthy subjects. A group of 5 pigs underwent reperfused transmural acute MI by closed-chest I/R, consisting of 40-minute left anterior descending coronary artery occlusion followed by balloon deflation and reestablishment of blood flow,[10] and were euthanized at 7 days after I/R serving as controls. Three additional groups of 5 animals each underwent modified I/R protocols incorporating different protective strategies followed by sacrifice on day 7: preconditioning, 40-minute I/R preceded by three 5-minute cycles of balloon inflation/deflation in the left anterior descending; postconditioning, 40-minute I/R followed by four 1-minute cycles of balloon inflation/deflation in the left anterior descending; and short-duration ischemia, 20-minute I/R.

Arterial enhanced multidetector computed tomography (MDCT) was performed during the index coronary occlusion, between minute 10 and minute 20 of ischemia, to delineate the reference MaR (MDCT-MaR, hypoperfused region during coronary occlusion).[19] Comprehensive CMR exams were performed at baseline and at 120 minutes, 24 hours, day 4, and day 7 after I/R. Animals were immediately euthanized after the final follow-up CMR scan, and myocardial tissue samples from ischemic areas were rapidly collected for histology and evaluation of water content.

Full methods are provided in the Online Data Supplement.

Arterial Enhanced MDCT Protocol and Analysis

Arterial phase MDCT studies were performed on a 64-slice computed tomographic-scanner (Brilliance CT 64; Philips Healthcare, Cleveland, OH) after intravenous administration of iodinated contrast media.[19] MDCT images were analyzed using dedicated software (MR Extended Work Space 2.6; Philips Healthcare, Best, The Netherlands) by 2 observers blinded to group allocation. Short axes orientation were obtained from volumetric computed tomographic images by multiplanar reconstruction using equivalent anatomic coordinates used for T2-weighted short-tau triple inversion-recovery (T2W-STIR) planning acquisition. MaR and remote areas were visually identified based on contrast enhancement differences, manually delineated, and expressed as a percentage of left ventricle (LV) area.

Detailed information about imaging MDCT protocol and analysis is shown in the Online Data Supplement.

CMR Protocol and Analysis

Baseline CMR scans were performed immediately before MI, and scans were subsequently repeated at all postinfarction follow-up times until sacrifice. CMR examinations were conducted with a Philips 3-Tesla Achieva Tx whole body scanner (Philips Healthcare, Best, The Netherlands) equipped with a 32-element phased-array cardiac coil. The imaging protocol included a standard segmented cine steady-state free-precession sequence to provide high quality anatomic references and assessment of LV mass, wall thickness, and LV ejection fraction (LVEF); a T2W-STIR sequence to assess the extent of edema and IMH; a T2-gradient-spin-echo mapping sequence to provide precise myocardial T2 relaxation time properties;[20] and a T1-weighted inversion recovery turbo field echo sequence acquired 10 to 15 minutes after the administration of gadolinium contrast (late gadolinium enhancement [LGE]) to assess IS and MVO. To avoid any interference with T2 measures at immediate reperfusion, gadolinium contrast was not administered at baseline CMR scans. CMR images were analyzed using dedicated software (MR Extended Work Space 2.6; QMassMR 7.6; Medis, Leiden, The Netherlands) by 2 observers experienced in CMR analysis and blinded to group allocation. Detailed information about imaging protocol and parameters and CMR analysis can be found in the Online Data Supplement.

Myocardial Water Quantification and Histological Analysis

Paired myocardial samples were collected within minutes of sacrifice from the ischemic myocardium of all pigs. Myocardial water content was quantified by the desiccation technique and expressed as a percentage of wet weight.[10,11] Histological sections of the at-risk myocardium were stained with hematoxylin and eosin, Masson trichrome, and antineutrophil antibody.[11] Full methods are presented in the Online Data Supplement.

Statistical Analysis

Normal distribution of each data subset was checked using graphical methods and a Shapiro–Wilk test. Leven test was performed to check homogeneity of variances. For quantitative variables, data are expressed as mean±SD. A 1-way ANOVA was conducted for among-group comparison of myocardial water content and MDCT-MaR. To take account of repeated measures, generalized mixed models were applied for the study and comparison of the temporal evolution of T2, CMR-MaR, IS, IMH, MVO, and salvage myocardium within and between groups. Pairwise comparisons among groups and time points were performed and *P* value adjusted for multiple comparisons using the Hochberg method. Post hoc test of trends over time for imaging parameters by group was performed by using coefficients of orthogonal polynomials. A Kruskal–Wallis test was conducted to compare the number of inflammatory cells and collagen content among groups euthanized at day 7. Associations between measured T2 relaxation time and IMH, MVO, IS, and LVEF were evaluated by Pearson correlation coefficient. All statistical analyses were performed with Stata v12.0 (StataCorp, College Station, TX). Graphs were generated with Stata 12.0 or GraphPad-Prism v6.0 (GraphPad Software, Inc, La Jolla, CA).

Results

Impact of Cardioprotective Strategies and Ischemia Duration on T2 and Myocardial Water Content

T2 relaxation time determined at time points ≤7 days post-reperfusion are summarized in Table 1. As already reported, after 40-minute I/R, T2 relaxation times were significantly prolonged at reperfusion, almost completely normalized at

Table 1. Time Profile of Myocardial T2 Relaxation in the Ischemic Porcine Myocardium During the First Week After Different I/R Protocols and Cardioprotective Strategies

	T2 Relaxation Time, ms				
	Baseline	R-120 min	R-24 h	R-Day 4	R-Day 7
40-min I/R (controls)	46.5 (3.0)	74.8 (14.4)	46.7 (4.9)	66.4 (8.3)	78.9 (11.7)
40-min I/R+PostC	43.1 (4.1)	73.4 (8.8)	46.1 (2.5)	72.5 (17.0)	76.7 (16.8)
PreC+40-min I/R	43.1 (1.0)	62.5 (2.8)*	49.1 (1.2)	59.2 (10.8)*	57.6 (10.3)*
20-min I/R	46.6 (2.0)	58.3 (1.5)*	49.9 (1.9)	50.1 (3.1)*	48.7 (1.5)*

Values are mean (SD). No significant differences were found between groups at baseline. A bimodal T2 time course was observed for all 40-min I/R pigs, with no significant differences detected between 40-min I/R and 40-min I/R+PostC. In contrast, PreC blunted both T2 peaks, whereas after 20-min I/R, the first peak was blunted and the second, absent. I/R indicates ischemia/reperfusion; PostC, postconditioning; and PreC, preconditioning.

*Statistically significant differences ($P<0.05$) compared with the same time point in the 40-min I/R (control) group. *P* value is adjusted for multiple comparisons among groups for each time point.

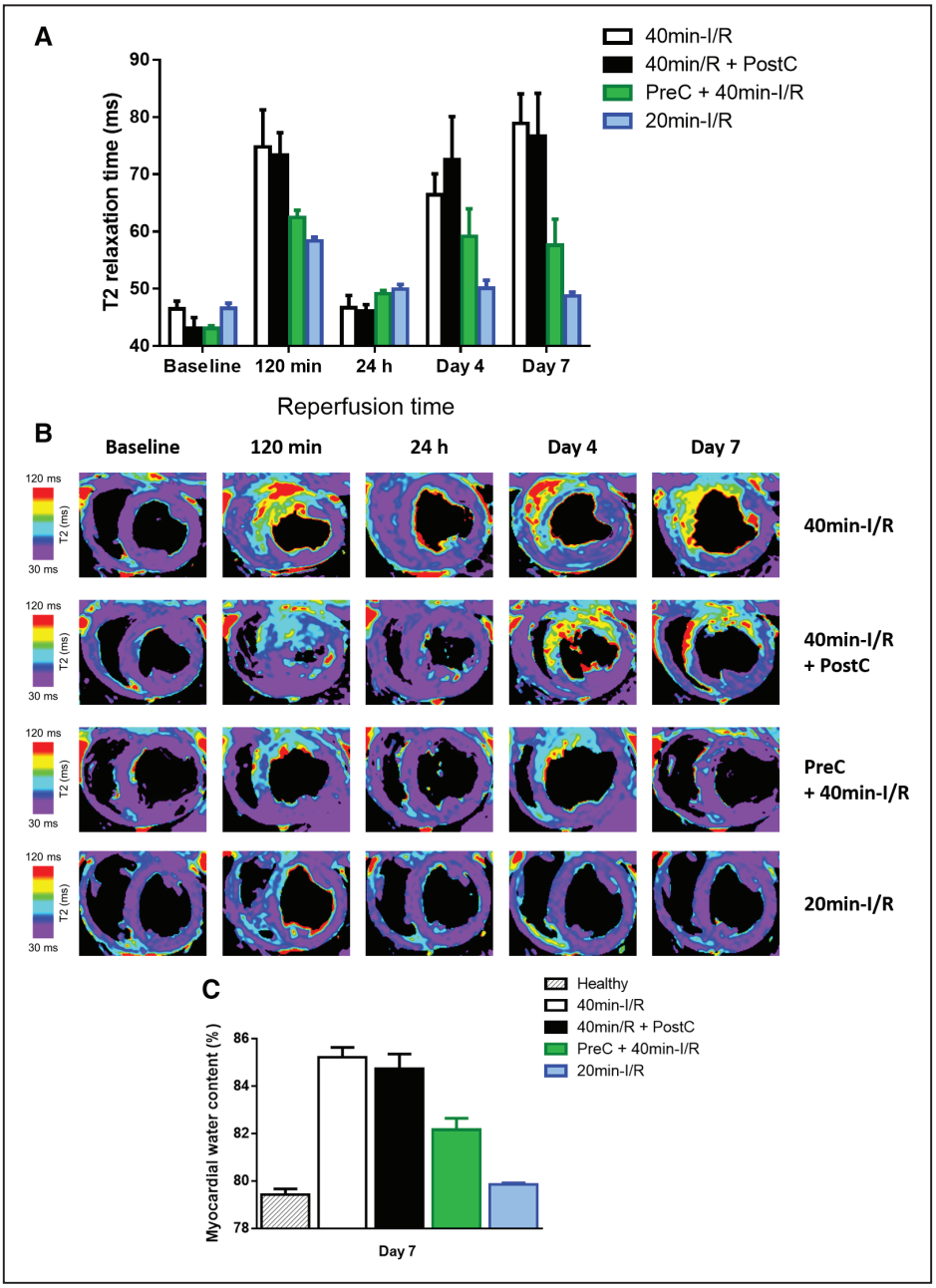

Figure 1. Time profile of T2 relaxation time and measurements of myocardial water content in the ischemic myocardium after different ischemia/reperfusion (I/R) protocols. **A**, Time profile of absolute T2 relaxation time (ms) in the ischemic myocardium of pigs undergoing different I/R protocols. Data are shown as mean±standard error of the mean. **B**, Representative serial cardiac magnetic resonance T2-mapping images from pigs that underwent 40-min I/R (control), 40-min I/R followed by postconditioning (PostC), 40-min I/R preceeded by preconditioning (PreC), or 20-min I/R; examinations were made at baseline, 120 min, 24 h, 4 d, and 7 d after reperfusion. All T2 maps were scaled between 30 and 120 ms. **C**, Measurements of myocardial water content (%) in healthy pigs and in the ischemic myocardium of pigs subjected to different I/R protocols and euthanized at day 7 after I/R. Myocardial water content (mean±SD, %) in the healthy pig myocardium was 79.4±0.6%. Myocardial water content (mean±SD, %) in the ischemic myocardium of pigs undergoing 40-min I/R (controls), 40-min I/R+PostC, 40-min I/R preceded by PreC, and 20-min I/R (short-duration ischemia) at day 7 after I/R was 85.2±0.9%, 84.7±1.4%, 82.2±1.1%, and 79.8±0.2%, respectively. Between-group differences of water content in the ischemic myocardium remained statistically significant with the exception of 40-min I/R+PostC vs 40-min I/R and 20-min I/R vs healthy. Data represented are means±standard error of the mean.

24 hours, then increasing again to reach a peak on day 7.[10] Preconditioning before 40-minute I/R resulted in a significantly shorter T2 relaxation time at reperfusion and an earlier and shorter deferred peak, occurring on day 4 rather than day 7. Conversely, postconditioning had no effect on edema dynamics, with animals showing the standard bimodal pattern with an initial peak at reperfusion and a deferred T2 prolongation peaking on day 7 (Figure 1A and 1B). Pigs subjected to short-duration ischemia (20-minute I/R) showed a unimodal pattern of edema, with T2 prolongation at reperfusion, albeit blunted compared with 40-minute I/R, and no deferred peak. True myocardial water content values in the

ischemic myocardium were comparable with those estimated from T2 relaxation times on day 7 CMR (Figure 1C).

Impact of Cardioprotective Strategies and Ischemia Duration on CMR-Measured MaR

Mean MaR measured by MDCT in the different groups was as follows (% of LV): 40-minute I/R (controls), 28.3±4.3%; preconditioning plus 40-minute I/R, 31.7±6.9%; 40-minute I/R plus postconditioning, 31.3±4.0%; and short-duration ischemia (20-minute I/R), 24.6±6.7% (statistically nonsignificant differences as compared with controls). Measurements of MaR determined by T2W-CMR in these groups at different times after reperfusion are summarized in Table 2.

CMR-measured MaR and T2 relaxation time showed similar time course patterns. Pigs subjected to 40-minute I/R with or without postconditioning had significant swelling of the formerly ischemic myocardium at reperfusion (Online Table I; Online Movies I through IV). Consequently, at early reperfusion, CMR-measured MaR as delineated by T2W-STIR was significantly higher than MaR measured by the reference standard MDCT in these pigs (Figure 2A and 2B). Conversely, preconditioned and 20-minute I/R pigs developed edema at reperfusion but without myocardial swelling (Online Table I; Online Movies V through VIII), and, therefore, MaR measured by CMR was similar to the value recorded by MDCT at this time point in these groups. In all study groups, the initial edema wave dissipated by 24 hours postreperfusion, and CMR measurements systematically underestimated MaR at this time point. On days 4 and 7 postreperfusion, CMR-measured MaR in control and postconditioned pigs was similar to MaR measured by MDCT. Conversely, in preconditioned pigs, CMR- and MDCT-measured MaR values were similar on day 4, but on day 7, CMR underestimated MaR because of partial resolution of the deferred edema wave, which appeared earlier, peaking on day 4. In pigs undergoing short-duration ischemia (20-minute I/R), CMR underestimated MaR at all time points after the first reperfusion scan because of the absence of the deferred edema wave.

Impact of Cardioprotective Strategies and Ischemia Duration on IS, Myocardial Salvage, IMH, and MVO

CMR measurements of IS and myocardial salvage after reperfusion are summarized in Table 2. IS was maximal at reperfusion and progressively shrank during the first week after MI in all groups. Whereas postconditioning had no effect on IS, preconditioning significantly reduced IS at all time points (Figure 3A and 3B). In pigs undergoing short-duration ischemia, IS was negligible at all time points. In parallel with the temporal variations in CMR-measured MaR, myocardial salvage estimated by CMR dynamically changed over time and according to the I/R protocol applied (Table 2). The time profile of myocardium salvage as assessed by reference MDCT-measured MaR and CMR IS is presented in Online Table II.

CMR measurements of IMH and MVO after reperfusion are summarized in Online Table III. IMH was apparent at 24 hours, peaking on day 4 post-I/R (Figure 2C), whereas MVO was apparent early after reperfusion, peaking on day 1 post-I/R and progressively decreasing thereafter (Figure 3C). Presence and extent of IMH and MVO were unaffected by postconditioning, significantly reduced by preconditioning, and negligible after short-duration ischemia.

Table 2. Time Profile of MaR, IS and Myocardial Salvage as Assessed by CMR During the First Week After Reperfused Myocardial Infarction in Pigs Subjected to Different I/R Protocols and Cardioprotective Strategies

Group	CMR Measure	Follow-Up			
		R-120 min	R-24 h	R-Day 4	R-Day 7
40-min I/R (controls)	MaR, % of LV	42.9 (5.7)	2.2 (1.7)	27.1 (3.4)	30.1 (2.3)
	IS, % of LV	39.2 (3.8)	30.2 (3.1)	28.2 (4.6)	25.4 (4.0)
	Myocardial salvage, %	8.3 (6.4)	–1310 (996)	–4.4 (14.2)	15.7 (13.3)
40-min I/R+PostC	MaR, % of LV	48.8 (6.2)*	1.9 (2.0)	33.9 (4.9)*	32.5 (3.2)
	IS, % of LV	46.2 (5.6)*	33.1 (3.4)	32.8 (4.5)*	30.4 (3.6)*
	Myocardial salvage, %	5.2 (4.8)	–1060 (513)	3.3 (3.9)	6.6 (3.0)
PreC+40-min I/R	MaR, % of LV	29.1 (1.4)*	4.2 (1.4)	24.6 (7.5)	17.2 (5.7)*
	IS, % of LV	21.0 (7.2)*	18.5 (10.2)*	7.5 (3.7)*	6.1 (4.7)*
	Myocardial salvage, %	28.2 (22.6)*	–389 (361)*	68.0 (13.6)*	64.0 (23.9)*
20-min I/R	MaR, % of LV	27.7 (3.3)*	3.6 (1.1)	4.2 (2.2)*	2.2 (1.9)*
	IS, % of LV	6.1 (4.5)*	3.0 (1.0)*	2.2 (0.8)*	1.5 (0.8)*
	Myocardial salvage, %	78.8 (13.7)*	17.3 (18.7)*	25.2 (75.5)	3.4 (79.0)

Values are mean (SD). A bimodal trend over time after reperfusion was observed for CMR-MaR and CMR-salvage ([CMR MaR–CMR IS]/CMR MaR, %) in all groups of pigs with the exception of the 20-min I/R group in which a negative linear trend or no clear trend was shown for CMR-MaR and salvage, respectively. In contrast, a strong negative linear trend over time was shown for IS in all groups. *P* values for significant trends were all <0.01. CMR indicates cardiac magnetic resonance; I/R, ischemia/reperfusion; IS, infarct size; LV, left ventricle; MaR, myocardium at risk; PostC, postconditioning; PreC, preconditioning; and R, reperfusion.

*Statistically significant differences ($P<0.05$) as compared with the same time point in the 40- min I/R (control) group. *P* value is adjusted for multiple comparisons among groups for each time point and imaging parameter.

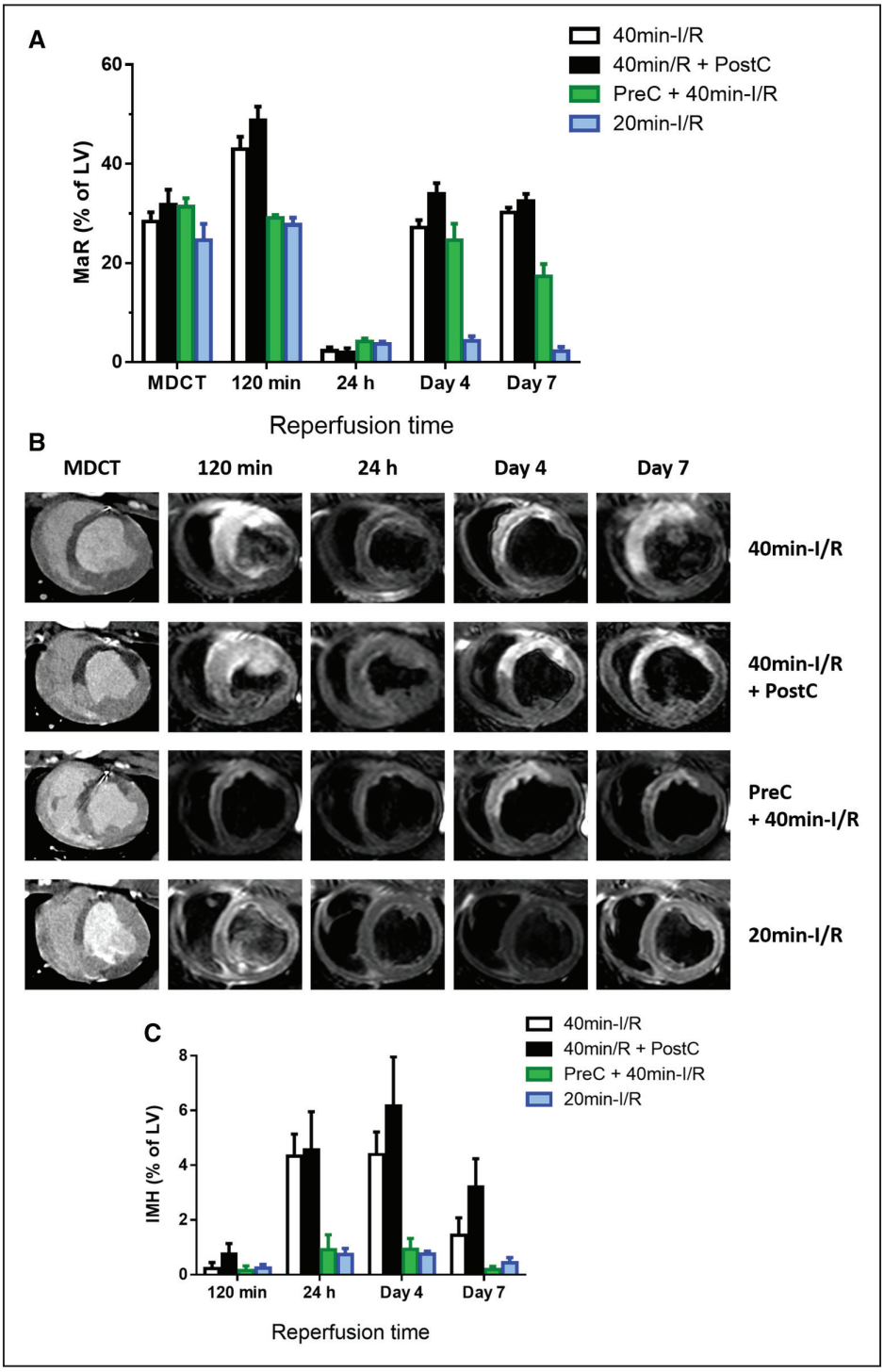

Figure 2. Time profile of cardiac magnetic resonance (CMR)-myocardium at risk (MaR) and intramyocardial hemorrhage (IMH) after different ischemia/reperfusion (I/R) protocols. **A**, Time profile of CMR-MaR measured by T2-weighted short-tau triple inversion-recovery (T2W-STIR) in pigs undergoing different I/R protocols. Arterial enhanced multidetector computed tomography (MDCT) was performed during coronary occlusion in all pigs as a reference measure of MaR. Data are shown as mean±standard error of the mean. **B**, Representative images from pigs that underwent 40-min I/R (control), 40-min I/R followed by postconditioning (PostC), 40-min I/R preceeded by preconditioning (PreC), or 20-min I/R; serial CMR T2W-STIR examinations were made at 120 min, 24 h, 4 d, and 7 d after reperfusion. Images are from the same pigs as those shown in the Figure. **C**, Temporal evolution of IMH in pigs subjected to different I/R protocols and followed ≤7 d after reperfusion. Data are means±standard error of the mean. LV indicates left ventricle.

Impact of Cardioprotective Strategies and Ischemia Duration on Histological Features of MI

The histological analysis of pigs euthanized at day 7 postreperfusion are summarized in Online Table IV. Postconditioning had no discernable effect on lesion size, granulation tissue content, neutrophil infiltration, or collagen content (Figure 4). Preconditioning resulted in smaller lesion areas, a higher proportion of granulation tissue, and lower neutrophil infiltration

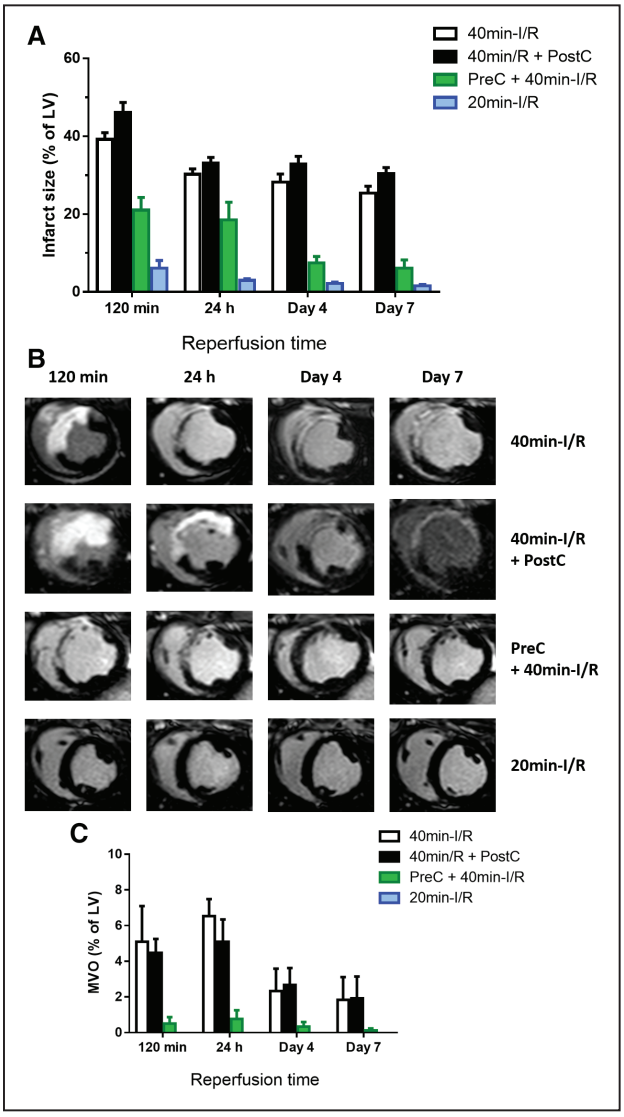

Figure 3. Time profile of cardiac magnetic resonance (CMR)-measured infarct size and microvascular obstruction (MVO) after different ischemia/reperfusion (I/R) protocols. A, Time profile of infarct size measured by T1-weighted inversion recovery turbo field echo (T1-IR-TFE) after administration of gadolinium to pigs undergoing different I/R protocols. Data are shown as mean±standard error of the mean. **B**, Representative images from pigs that underwent 40-min I/R (control), 40-min I/R followed by postconditioning (PostC), 40-min I/R preceded by preconditioning (PreC), or 20-min I/R; serial CMR T1-IR-TFE examinations were made at 120 min, 24 h, 4 d, and 7 d after reperfusion. Images are from same pigs as those shown in Figures 2 and 3. **C**, Temporal evolution of MVO in pigs subjected to different I/R protocols and followed ≤7 d after reperfusion. Data are means±standard error of the mean. Note that pigs subjected to 20-min I/R did not show MVO at any evaluated time point. LV indicates left ventricle.

and collagen content. Pigs undergoing short-duration ischemia showed no signs of tissue lesion and a low degree of neutrophil infiltration.

Association Between T2 and IMH, MVO, IS, and LVEF

Overall, T2 relaxation time in the ischemic region at 120 minutes post-I/R correlated positively with the degree of IMH and MVO: the longer the T2 at early reperfusion, the larger the extent of IMH and MVO. Conversely, the deferred T2 peak (highest value between day 4 and day 7) correlated positively with IS and inversely with LVEF: the greater the deferred T2 peak, the larger the infarct and the lower the LVEF on day 7 (Figure 5).

Discussion

In this study, we have comprehensively characterized the impact of cardioprotective strategies (preconditioning and postconditioning) and ischemia duration on the temporal evolution and extent of myocardial tissue composition changes (edema, necrosis, IMH, and MVO) by CMR. In all instances of necrosis (positive LGE at day 7), a bimodal edematous response is seen, regardless of the presence and degree of IMH or MVO; however, when necrosis is absent (in animals undergoing short-duration ischemia with no day-7 LGE), the edematous reaction is unimodal, with a blunted reperfusion-related edema wave and no healing-related deferred wave. Preconditioning, which significantly reduces IS, modulates the intensity of both the initial and deferred edema waves. The deferred wave also peaks earlier in preconditioned than in nonpreconditioned infarctions. CMR-measured IS declined progressively after reperfusion in all groups, whereas the extent of IMH and MVO varied according to CMR timing and protocol applied. T2 relaxation time in the ischemic area early after reperfusion is correlated with the severity of IMH and MVO, whereas the deferred peak of T2 relaxation time is strongly associated with IS and LVEF.

Consequently, imaging protocols for post-MI tissue characterization aiming at quantifying edema, MaR, IS, myocardial salvage, IMH, and MVO should account for these dynamics and be as standardized as possible (Figure 6).

Modulation of the Post-I/R Edema by Cardioprotecitve Strategies and Ischemia Duration

The possibility of protecting the myocardium during an acute MI (cardioprotection) has interested the scientific community for several decades.[2,21] Many studies use IS normalized to MaR as an acute end point, on the assumption that post-I/R edema is steady. However, recent studies suggest that the extent of edema might be influenced by cardioprotective conditioning interventions.[16,17] However, these previous clinical studies were not designed to address the effect of conditioning interventions on edema formation, and subjects underwent a single CMR examination that was not at the same time point for all individuals.[16,17]

Our results show that preconditioning (a potent cardioprotective strategy) and short ischemia duration have a major impact on the intensity and dynamics of post-MI edema (Figure 1). Preconditioning reduced the initial edema wave and also the deferred wave, which peaked early, on day 4, contrasting with the peak on day 7 in control animals. Shortening the duration of coronary occlusion to 20 minutes (20-minute I/R) also blunted initial edema wave, and in this case, the second edema wave was absent. These CMR results are consistent with histologically determined water content at day 7 after MI, which was reduced in pigs undergoing preconditioning and within the normal range in pigs undergoing short-duration ischemia (Figure 1C).

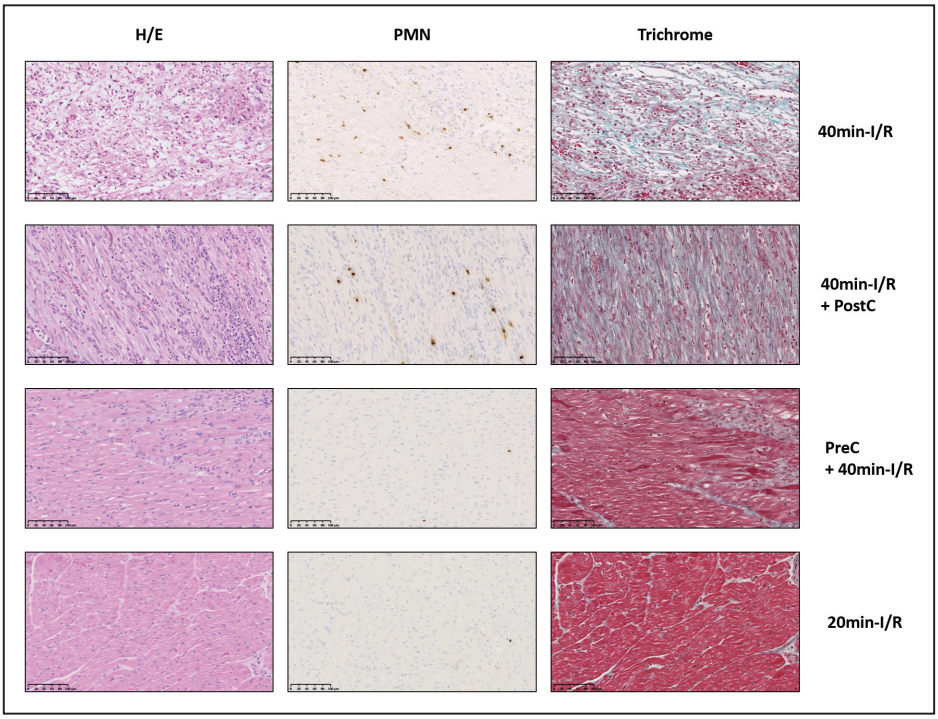

Figure 4. Impact of cardioprotection and ischemia duration on histological features of myocardial infarction. Representative histological images of porcine ischemic myocardium 7 d after 40-min ischemia/reperfusion (I/R; control), 40-min I/R followed by postconditioning (PostC), 40-min I/R preceded by preconditioning (PreC), and 20-min I/R. Images show staining with hematoxylin and eosin (H/E), antiPM1 antibody (PMN), and Masson trichrome. Stained sections were used to quantify lesion extent, proportion of necrosis and granulation tissue, neutrophil density, and percentage of collagen within granulation tissue. Note the scarce neutrophil infiltration in porcine myocardium subjected to PreC or 20-min I/R, accompanied by small patchy areas of granulation tissue (PreC) or its absence (20-min I/R). Scale bars, 100μM.

Impact of IMH and MVO on the Occurrence of the Bimodal Edematous Reaction

The extent of IMH and MVO varies as a function of time from the acute ischemic event.[11,12] IMH is moreover closely associated with the development of MVO, conferring a worse prognosis when present.[12] More importantly, in the present study, edema followed a bimodal T2 pattern in all pigs undergoing 40-minute I/R (with or without preconditioning or postconditioning) regardless of the degree of IMH or MVO (Figure 1), which was almost absent in preconditioned pigs (Figures 2C and 3C). Notably, all pigs, including those undergoing short-duration ischemia, showed a significant drop in T2 from the hyperacute phase to 24 hours postreperfusion (Figure 1). These findings suggest that the main driver of the drop in T2 is rapid resorption of the initial reperfusion-related edema, regardless of the degree of IMH and MVO, and reinforce the reality of bimodal post-MI edema. Nevertheless, IMH exerts some influence on T2 relaxation time, as we previously conceded,[10,11,14,20] and might explain the slightly less noticeable drop in T2 at 24 hours in pigs with almost no IMH or MVO (pigs given preconditioning or short-duration ischemia; Figure 1).

Impact of Cardioprotective Strategies and Ischemia Duration on CMR-Measured Myocardial Area at Risk and Salvage

Parametric T2 mapping improves the detection and quantification of myocardial edema;[20] however, this methodology is not universally available, contrasting with T2W-STIR, which is available from all major vendors. In this regard, CMR-measured MaR as delineated by the extent of edema on T2W-STIR imaging paralleled T2 relaxation time profile. The present study shows that the edema-sensitive T2W-STIR CMR sequence overestimates MaR (as compared with the reference standard, MDCT in this study) at early time points (120 minutes) after reperfusion in pigs subjected to 40-minute I/R with no protective strategies or undergoing postconditioning (which did not protect in this study). This overestimation is mainly driven by the massive swelling of the reperfused myocardium (Online Movies I through IV). By 24 hours, there is a systematic underestimation of MaR by CMR in all cases, mainly driven by the substantial resorption of edema and normalization of T2 relaxation time.[10] This underestimation resulted in biologically implausible negative myocardial salvage data at 24 hours in most pigs (Table 2). This finding reinforces the idea that MaR (and consequently salvaged myocardium) may not reliably be quantified by CMR around this time point. Conversely, on days 4 and 7, CMR-measured MaR was similar to MaR measured by MDCT (Figure 2A). However, the dynamics of postischemia edema are altered by cardioprotective strategies and ischemia duration, with further implications for CMR-measured MaR and salvage.

Thus, the smaller extent of edema at reperfusion in pigs that underwent preconditioning or short-duration ischemia (Figure 2) was associated with less prolonged T2 relaxation times (Figure 1) and lower degree of myocardial swelling. Interestingly, these 2 groups of cardioprotected animals had

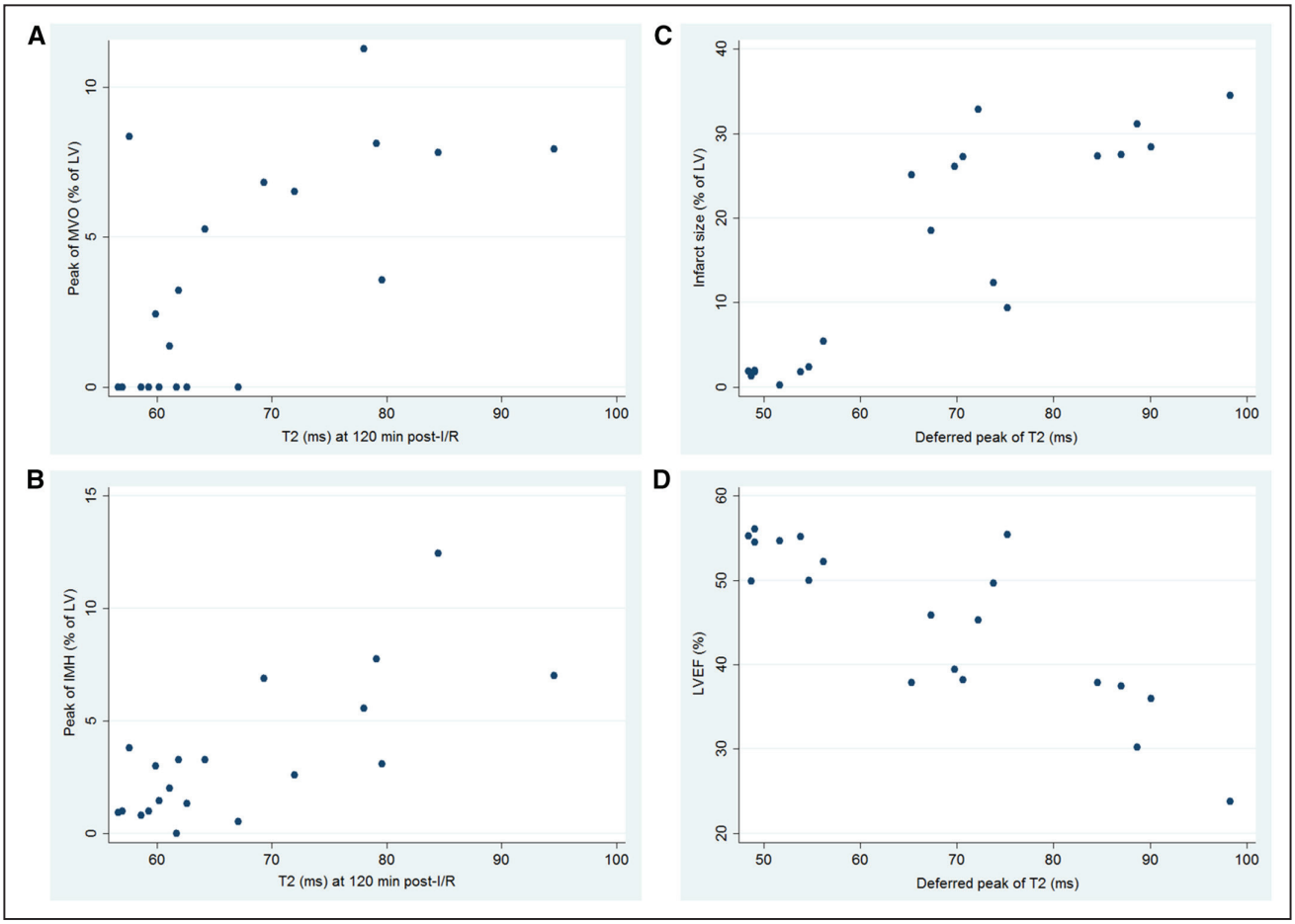

Figure 5. Association between T2, intramyocardial hemorrhage (IMH), microvascular obstruction (MVO), infarct size, and left ventricular ejection fraction (LVEF). Scatter plots showing positive association of T2 relaxation time in the ischemic myocardium during the hyperacute postreperfusion period (120 min) with (**A**) peak MVO (Pearson *r*=0.68) and (**B**) peak intramyocardial hemorrhage (Pearson *r*=0.75). **C** and **D**, The deferred T2 peak in the ischemic myocardium shows a strong positive association with day-7 infarct size (Pearson *r*=0.87) and a negative association with day-7 LVEF (Pearson *r*=−0.85). After adjustment for multiple testing, all *P* values for the correlations shown remained significant (*P*<0.05). Graphs include 4 groups of 5 pigs each undergoing 40-min ischemia/reperfusion (I/R; controls), 40-min I/R followed by postconditioning, 40-min I/R preceded by preconditioning, or 20-min I/R. LV indicates left ventricle.

significantly smaller infarcts on day 7 (Figure 3). The cardioprotection (reduced IS) afforded by preconditioning or short-duration ischemia was demonstrated by CMR (LGE; Figure 3) and histology (Figure 4). In pigs undergoing short-duration ischemia, necrosis was barely detectable, and so was edema and CMR-measured MaR from day 1 on, supporting the notion that the deferred edema wave is related to post-MI healing.[11] This would imply that interventions that protect the myocardium could affect edema dynamics, therefore, having an impact on CMR estimations of MaR and salvage, as suggested by indirect clinical evidence before.[16,17] However, whether any intervention that reduces IS diminishes myocardial edema remains to be demonstrated. A paradigmatic example of such interplay may be seen in the group subjected to short duration of ischemia (Table 2). In this group, IS is small and stable on day 1 (3.0% of LV), day 4 (2.2% of LV), and day 7 (1.5% of LV); however, a dramatic change is seen in CMR-measured salvage index (17.3%, 25.2%, and 3.4% of MaR on days 1, 4, and 7, respectively). Of note, when using the MaR standard reference MDCT value to calculate salvage, salvage index remains stable (87.4%, 90.0%, and 94.4% of MaR on days 1, 4, and 7, respectively; Online Table II). The latter measurements (based on MDCT-MaR) are consistent with the significant cardioprotective effect seen by early reperfusion (ie, short ischemia duration).

Decrease of CMR-Based IS During the First Week After MI

Previous studies show rapid resorption of LGE myocardium (a surrogate of IS) between ≈day 1 and day 7 after MI.[4,22] Consistent with these observations, our data show a progressive decrease of CMR-based IS in all study groups (Figure 3). The massive swelling of the early postreperfused myocardium might explain the large IS detected in our study 120 minutes after reperfusion. Interestingly, animals that underwent preconditioning showed LGE-positive myocardial regions early after reperfusion that became LGE negative by day 4 or day 7 CMR (Figure 3). This phenomenon might indicate early and transient expansion of extracellular volume without irreversible myocardial injury.[22] These data highlight the importance of performing CMR infarct imaging within a consistently defined and narrow time frame, preferably at the end of the first week, when using IS as an end point in clinical trials during

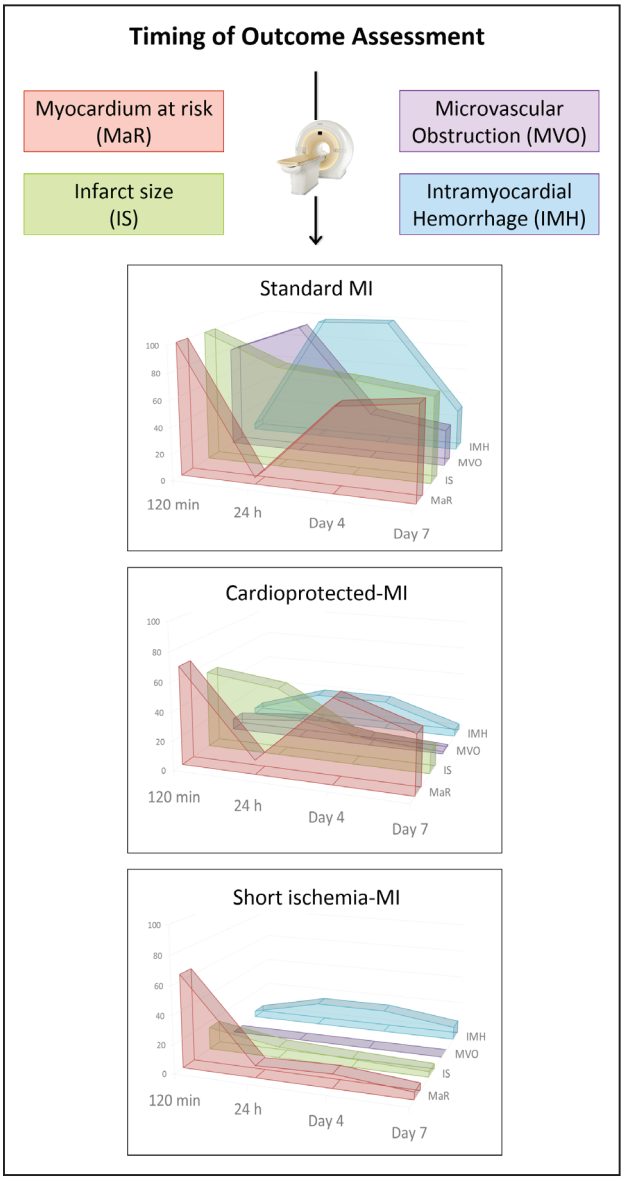

Figure 6. Effect of timing of evaluation, ischemia duration, and protective interventions on cardiac magnetic resonance (CMR)-measured individual outcomes after myocardial infarction (MI). By using state-of-the-art CMR imaging, we have demonstrated that the temporal dynamics and extent of post-MI tissue composition changes are greatly influenced by the timing of imaging acquisition, application of cardioprotective interventions, and the duration of the index ischemia. These findings highlight the need for protocol standardization when using post-MI imaging techniques to measure edema, myocardial area at risk, infarct size (IS), myocardial salvage, intramyocardial hemorrhage (IMH), and microvascular obstruction (MVO) in experimental and clinical studies. According to the data presented, establishing the appropriate timing to measure IMH and MVO could occur somewhere around the first 24 to 48 h post-MI; whereas the optimal timing to measure edema, myocardium at risk (MaR), IS, and salvage could occur somewhere between day 4 and day 7 after MI. Nevertheless, caution should be exercised when addressing post-MI tissue characterization by any means given that several components and factors might additionally impact the dynamics and complex changes which undergo the heart after MI. *y* axis numbers and graphs represent real data relative to the highest point on the chart for the given imaging outcome (MaR, IS, MVO, and IMH). A value of 100 is the highest value for the (*Continued*)

the acute post-MI period. Nevertheless, the fact that myocardial edema and LGE follow a disparate dynamic pattern after ischemia/reperfusion highlights the complexity of measuring myocardial salvage in real practice.

T2 as a Maker of Post-I/R Myocardial Injury

The ability to predict the fate of the myocardium early after MI would be of great clinical value. Myocardial edema contributes to impaired post-MI microvascular perfusion by increasing extravascular compression and might contribute to altered coronary physiology indices.[1,2] In this study, we show that T2 relaxation time in ischemic myocardium in the hyperacute CMR examination (after 2 hours of reperfusion) correlates with IMH and MVO—events that develop days after MI (Figure 5A and 5B). Conversely, the deferred T2 peak correlated directly with IS and inversely with LVEF—parameters associated with post-MI healing (Figure 5C and 5D). Therefore, myocardial T2 relaxation time might be a quantitative surrogate of the ischemic insult or therapeutic effect, rather than a surrogate of MaR.

However, these findings might apply only to the reperfused MI because the bimodal edema response is less pronounced in nonreperfused MI.[11] These findings warrant further experimental and clinical studies specifically addressing the prognostic significance of T2 at different time points and the perfusion status of the myocardium.

Limitations

Caution is needed when extrapolating experimental results to the clinic. However, the pig is one of the most clinically translatable large animal models for the study of reperfused MI.[23,24] The nature of our experimental study, that is, longitudinal follow-up, precluded individual histological gold standard measurements of area at risk (ie, Evans Blue by coronary reocclusion), IS (ie, triphenyl tetrazolium chloride), or MVO (thioflavin-S) at each time point. In addition, the heart was harvested at sacrifice to perform reference standard myocardial water content measurements and histological quantification of different tissue components, which otherwise might be altered by such procedures. It is fair to acknowledge that although previous studies have used histological standards to validate the use of CMR to measure IS and MVO[22,25] and MDCT to measure MaR,[19,26] there is probably no perfect noninvasive method for such purposes. In this regard, acutely detected LGE does not necessarily equate to irreversible injury and may contribute to severely distort estimates of salvaged myocardium when comparing against a prereperfusion reference standard to assess MaR.[22] Other reasons that might contribute to inaccurate estimations include damage extent beyond the boundaries of the actual MaR (defined as the hypoperfused region during coronary occlusion);[19] slightly shrinking of MaR in MDCT performed during coronary occlusion because of lack of perfusion in animal models with poor collateral circulation; and the presence of residual edema in salvaged

Figure 6 Continued. corresponding measure in controls (ie, pigs subjected to 40-min I/R) among all time points evaluated (120 min, day 1, day 4, and day 7 after reperfusion). A value of 50 means that the extent of the corresponding measure is half as the former highest value.

myocardium which might contribute to overestimate of IS early after reperfusion.[22] Hybrid imaging techniques have been proposed to overcome some of these issues;[27] however, further validation is needed.

Our study examined only anterior MI. The reasons for this choice include the avoidance of possible magnetic-field nonhomogeneity related to the inferolateral wall[6,28] and adherence to recommendations for patient selection in clinical trials of cardioprotective interventions.[21] The observed changes in tissue composition are likely to occur regardless of MI location; however, caution should be exercised when extrapolating other results, especially those regarding the association of T2 with ventricular outcome.

Our results do not necessarily invalidate the reported protective effects of the majority of preclinical postconditioning studies published.[29] However, our findings are in line with some recent experimental and clinical data.[29,30] In this regard, ischemic postconditioning did not reduce the incidence of clinical events in ST-segment–elevation MI (STEMI) patients in the DANAMI-3-iPOST trial (The Third Danish Study of Optimal Acute Treatment of Patients With ST Elevation Myocardial Infarction–Ischemic Postconditioning).[31] Moreover, this intervention did not reduce IS, myocardial salvage index, extent of MVO, or improve LVEF in the subset of patients who underwent CMR.[31] Interspecies differences, small sample size, the lack of comorbidities and comedications in animal experiments, and the diversity of postconditioning protocols applied might explain the ambivalent preclinical and clinical data.[29] Nevertheless, our goal was not to test the cardioprotective effect of postconditioning, but rather to use different protective strategies to characterize post-MI tissue over a range of injury severities. Indeed, the use of strategies that did not achieve cardioprotection reinforced our earlier results obtained by the standard I/R procedure.[10,11]

The regions of interest used to quantify T2 relaxation time in this study included the full wall thickness. The regions of interest might, therefore, include different myocardial states (such as hemorrhage or MVO). We took this approach to match our previous experimental work and because the differentiation of such small areas might be challenging. This might have contributed to the differences in absolute T2 relaxation time between our study and others taking a different approach to region of interest selection.

Conclusions

In a translational large animal model of myocardial I/R and by using CMR, we have shown that the temporal dynamics and extent of post-MI tissue composition changes are greatly influenced by application of cardioprotective interventions and the duration of the index ischemia. Post-MI LGE areas do not necessarily equate to necrotic myocardium because the extent of hyperenhanced ischemic tissue evolves rapidly during the first week after reperfusion. The magnitude of IMH and MVO varies according to ischemia duration and cardioprotection. The greatest divergences are seen in the degree and spatial extent of myocardial edema during the first week after MI, which seem to be a quantitative surrogate marker of ischemic damage or therapeutic effect.

These data highlight the need for protocol standardization when using post-MI imaging techniques to measure edema, MaR, IS, myocardial salvage, IMH, and MVO in experimental and clinical studies.

Acknowledgments

We thank Tamara Córdoba, Oscar Sanz, Eugenio Fernández, and other members of the Centro Nacional de Investigaciones Cardiovasculares Carlos III (CNIC) animal facility and farm for outstanding animal care and support and Roisin Doohan and Brenda Guijarro for assistance with histological sample processing. Simon Bartlett (CNIC) provided English editing. Pictures from multidetector computed tomography and cardiac magnetic resonance equipment (Online Figure I; Figure 6) are reproduced with the permission of Philips Healthcare.

Sources of Funding

This study was supported by a competitive grant from the Carlos III Institute of Health-Fondo de Investigacion Sanitaria and the European Regional Development Fund (ERDF/FEDER; PI10/02268 and PI13/01979), the Spanish Ministry of Economy, Industry, and Competitiveness (MEIC) and ERDF/FEDER (SAF2013-49663-EXP), and, in part, by the FP7-PEOPLE-2013-ITN Next generation training in cardiovascular research and innovation-Cardionext. R. Fernández-Jiménez holds a FICNIC fellowship from the Fundació Jesús Serra, the Fundación Interhospitalaria de Investigación Cardiovascular, and the Centro Nacional de Investigaciones Cardiovasculares Carlos III (CNIC). J. Agüero is a FP7-PEOPLE-2013-ITN-Cardionext fellow. This research program is part of an institutional agreement between FIIIS-Fundación Jiménez Díaz and CNIC. This study forms part of a Master Research Agreement between the CNIC and Philips Healthcare. This study is part of a bilateral research program between Hospital de Salamanca Cardiology Department and the CNIC. The CNIC is supported by the MEIC and the Pro CNIC Foundation and is a Severo Ochoa Center of Excellence (MEIC award SEV-2015-0505).

Disclosures

J. Sánchez-González is a Philips Healthcare employee. The other authors report no conflicts.

References

1. Heusch G. The coronary circulation as a target of cardioprotection. *Circ Res*. 2016;118:1643–1658. doi: 10.1161/CIRCRESAHA.116.308640.
2. Ibanez B, Heusch G, Ovize M, Van de Werf F. Evolving therapies for myocardial ischemia/reperfusion injury. *J Am Coll Cardiol*. 2015;65:1454–1471. doi: 10.1016/j.jacc.2015.02.032.
3. Carlsson M, Ubachs JF, Hedstrom E, Heiberg E, Jovinge S, Arheden H. Myocardium at risk after acute infarction in humans on cardiac magnetic resonance: quantitative assessment during follow-up and validation with single-photon emission computed tomography. *JACC Cardiovasc Imaging*. 2009;2:569–576. doi: 10.1016/j.jcmg.2008.11.018.
4. Dall'Armellina E, Karia N, Lindsay AC, Karamitsos TD, Ferreira V, Robson MD, Kellman P, Francis JM, Forfar C, Prendergast BD, Banning AP, Channon KM, Kharbanda RK, Neubauer S, Choudhury RP. Dynamic changes of edema and late gadolinium enhancement after acute myocardial infarction and their relationship to functional recovery and salvage index. *Circ Cardiovasc Imaging*. 2011;4:228–236. doi: 10.1161/CIRCIMAGING.111.963421.
5. Aletras AH, Tilak GS, Natanzon A, Hsu LY, Gonzalez FM, Hoyt RF Jr, Arai AE. Retrospective determination of the area at risk for reperfused acute myocardial infarction with T2-weighted cardiac magnetic resonance imaging: histopathological and displacement encoding with stimulated echoes (DENSE) functional validations. *Circulation*. 2006;113:1865–1870. doi: 10.1161/CIRCULATIONAHA.105.576025.
6. Friedrich MG, Kim HW, Kim RJ. T2-weighted imaging to assess post-infarct myocardium at risk. *JACC Cardiovasc Imaging*. 2011;4:1014–1021. doi: 10.1016/j.jcmg.2011.07.005.
7. Friedrich MG, Abdel-Aty H, Taylor A, Schulz-Menger J, Messroghli D, Dietz R. The salvaged area at risk in reperfused acute myocardial infarction as visualized by cardiovascular magnetic resonance. *J Am Coll Cardiol*. 2008;51:1581–1587. doi: 10.1016/j.jacc.2008.01.019.
8. Engblom H, Heiberg E, Erlinge D, Jensen SE, Nordrehaug JE, Dubois-Rande JL, Halvorsen S, Hoffmann P, Koul S, Carlsson M, Atar D, Arheden H. Sample size in clinical cardioprotection trials using myocardial salvage

index, infarct size, or biochemical markers as endpoint. *J Am Heart Assoc*. 2016;5:e002708. doi: 10.1161/JAHA.115.002708.
9. Kim HW, Van Assche L, Jennings RB, et al. Relationship of T2-weighted MRI myocardial hyperintensity and the ischemic area-at-risk. *Circ Res*. 2015;117:254–265. doi: 10.1161/CIRCRESAHA.117.305771.
10. Fernández-Jiménez R, Sánchez-González J, Agüero J, et al. Myocardial edema after ischemia/reperfusion is not stable and follows a bimodal pattern: imaging and histological tissue characterization. *J Am Coll Cardiol*. 2015;65:315–323. doi: 10.1016/j.jacc.2014.11.004.
11. Fernández-Jiménez R, García-Prieto J, Sánchez-González J, Agüero J, López-Martín GJ, Galán-Arriola C, Molina-Iracheta A, Doohan R, Fuster V, Ibáñez B. Pathophysiology underlying the bimodal edema phenomenon after myocardial ischemia/reperfusion. *J Am Coll Cardiol*. 2015;66:816–828. doi: 10.1016/j.jacc.2015.06.023.
12. Carrick D, Haig C, Ahmed N, Rauhalammi S, Clerfond G, Carberry J, Mordi I, McEntegart M, Petrie MC, Eteiba H, Hood S, Watkins S, Lindsay MM, Mahrous A, Welsh P, Sattar N, Ford I, Oldroyd KG, Radjenovic A, Berry C. Temporal evolution of myocardial hemorrhage and edema in patients after acute ST-segment elevation myocardial infarction: pathophysiological insights and clinical implications. *J Am Heart Assoc*. 2016;5:e002834.
13. Dharmakumar R. Building a unified mechanistic insight into the bimodal pattern of edema in reperfused acute myocardial infarctions: observations, interpretations, and outlook. *J Am Coll Cardiol*. 2015;66:829–831. doi: 10.1016/j.jacc.2015.05.074.
14. Fernández-Jiménez R, Fuster V, Ibanez B. Reply: "waves of edema" seem implausible. *J Am Coll Cardiol*. 2016;67:1869–1870. doi: 10.1016/j.jacc.2016.01.052.
15. Heusch P, Nensa F, Heusch G. Is MRI really the gold standard for the quantification of salvage from myocardial infarction? *Circ Res*. 2015;117:222–224. doi: 10.1161/CIRCRESAHA.117.306929.
16. Thuny F, Lairez O, Roubille F, et al. Post-conditioning reduces infarct size and edema in patients with ST-segment elevation myocardial infarction. *J Am Coll Cardiol*. 2012;59:2175–2181. doi: 10.1016/j.jacc.2012.03.026.
17. White SK, Frohlich GM, Sado DM, Maestrini V, Fontana M, Treibel TA, Tehrani S, Flett AS, Meier P, Ariti C, Davies JR, Moon JC, Yellon DM, Hausenloy DJ. Remote ischemic conditioning reduces myocardial infarct size and edema in patients with ST-segment elevation myocardial infarction. *JACC Cardiovasc Interv*. 2015;8:178–188. doi: 10.1016/j.jcin.2014.05.015.
18. Ghugre NR, Pop M, Barry J, Connelly KA, Wright GA. Quantitative magnetic resonance imaging can distinguish remodeling mechanisms after acute myocardial infarction based on the severity of ischemic insult. *Magn Reson Med*. 2013;70:1095–105. doi: 10.1002/mrm.24531.
19. Mewton N, Rapacchi S, Augeul L, Ferrera R, Loufouat J, Boussel L, Micolich A, Rioufol G, Revel D, Ovize M, Croisille P. Determination of the myocardial area at risk with pre- versus post-reperfusion imaging techniques in the pig model. *Basic Res Cardiol*. 2011;106:1247–1257. doi: 10.1007/s00395-011-0214-8.
20. Fernandez-Jimenez R, Sanchez-Gonzalez J, Aguero J, Del Trigo M, Galan-Arriola C, Fuster V, Ibanez B. Fast T2 gradient-spin-echo (T2-GraSE) mapping for myocardial edema quantification: first in vivo validation in a porcine model of ischemia/reperfusion. *J Cardiovasc Magn Reson*. 2015;17:92. doi: 10.1186/s12968-015-0199-9.
21. Hausenloy DJ, Botker HE, Engstrom T, Erlinge D, Heusch G, Ibanez B, Kloner RA, Ovize M, Yellon DM, Garcia-Dorado D. Targeting reperfusion injury in patients with ST-segment elevation myocardial infarction: trials and tribulations. *Eur Heart J*. 2017;38:935–941. doi: 10.1093/eurheartj/ehw145.
22. Jablonowski R, Engblom H, Kanski M, Nordlund D, Koul S, van der Pals J, Englund E, Heiberg E, Erlinge D, Carlsson M, Arheden H. Contrast-enhanced CMR overestimates early myocardial infarct size: mechanistic insights using ECV measurements on day 1 and day 7. *JACC Cardiovasc Imaging*. 2015;8:1379–1389. doi: 10.1016/j.jcmg.2015.08.015.
23. Fernández-Jiménez R, Fernández-Friera L, Sánchez-González J, Ibáñez B. Animal models of tissue characterization of area at risk, edema and fibrosis. *Curr Cardiovasc Imaging Rep*. 2014;7:1–10.
24. Heusch G, Skyschally A, Schulz R. The in-situ pig heart with regional ischemia/reperfusion - ready for translation. *J Mol Cell Cardiol*. 2011;50:951–963. doi: 10.1016/j.yjmcc.2011.02.016.
25. Wu KC. CMR of microvascular obstruction and hemorrhage in myocardial infarction. *J Cardiovasc Magn Reson*. 2012;14:68. doi: 10.1186/1532-429X-14-68.
26. van der Pals J, Hammer-Hansen S, Nielles-Vallespin S, Kellman P, Taylor J, Kozlov S, Hsu LY, Chen MY, Arai AE. Temporal and spatial characteristics of the area at risk investigated using computed tomography and T1-weighted magnetic resonance imaging. *Eur Heart J Cardiovasc Imaging*. 2015;16:1232–1240. doi: 10.1093/ehjci/jev072.
27. Nensa F, Poeppel T, Tezgah E, Heusch P, Nassenstein K, Mahabadi AA, Forsting M, Bockisch A, Erbel R, Heusch G, Schlosser T. Integrated FDG PET/MR imaging for the assessment of myocardial salvage in reperfused acute myocardial infarction. *Radiology*. 2015;276:400–407. doi: 10.1148/radiol.2015140564.
28. Fernández-Friera L, García-Ruiz JM, García-Álvarez A, Fernández-Jiménez R, Sánchez-González J, Rossello X, Gómez-Talavera S, López-Martín GJ, Pizarro G, Fuster V, Ibáñez B. Accuracy of area at risk quantification by cardiac magnetic resonance according to the myocardial infarction territory. *Rev Esp Cardiol (Engl Ed)*. 2017;70:323–330. doi: 10.1016/j.rec.2016.07.004.
29. Heusch G, Rassaf T. Time to give up on cardioprotection? a critical appraisal of clinical studies on ischemic pre-, post-, and remote conditioning. *Circ Res*. 2016;119:676–695. doi: 10.1161/CIRCRESAHA.116.308736.
30. Bodi V, Ruiz-Nodar JM, Feliu E, et al. Effect of ischemic postconditioning on microvascular obstruction in reperfused myocardial infarction. Results of a randomized study in patients and of an experimental model in swine. *Int J Cardiol*. 2014;175:138–146. doi: 10.1016/j.ijcard.2014.05.003.
31. Engstrøm T, Kelbæk H, Helqvist S, et al; Third Danish Study of Optimal Acute Treatment of Patients With ST Elevation Myocardial Infarction–Ischemic Postconditioning (DANAMI-3–iPOST) Investigators. Effect of ischemic postconditioning during primary percutaneous coronary intervention for patients with ST-segment elevation myocardial infarction: a randomized clinical trial. *JAMA Cardiol*. 2017;2:490–497. doi: 10.1001/jamacardio.2017.0022.

SUPPLEMENTAL MATERIAL

DETAILED METHODS

Study design

Experiments were performed on castrated male Large-White pigs weighing 30 to 40 kg. A total of 25 pigs completed the full protocol and comprised the study population. The study was approved by the Institutional and Regional Animal Research Committee. The study design is summarized in **Online Figure I**. Five pigs were sacrificed with no intervention other than baseline CMR, and served as reference healthy subjects. A group of 5 pigs underwent reperfused transmural acute myocardial infarction by closed-chest I/R, consisting of 40-minute left anterior descending (LAD) coronary artery occlusion followed by balloon deflation and reestablishment of blood flow,[1] and were sacrificed at 7 days after I/R serving as controls. Three additional groups of 5 animals each underwent modified I/R protocols incorporating different protective strategies followed by sacrifice on day 7: preconditioning, 40min-I/R preceded by three 5-minute cycles of balloon inflation/deflation in the LAD; postconditioning, 40min-I/R followed by four 1-minute cycles of balloon inflation/deflation in the LAD; and short-duration ischemia, 20min-I/R.

In all pigs, arterial enhanced multidetector computed tomography (MDCT) was performed during the index coronary occlusion, between minute 10 and minute 20 of ischemia, to delineate the reference MaR (hypoperfused region during coronary occlusion).[2] Comprehensive CMR exams were performed at baseline, and at 120min, 24h, day4, and day7 after I/R. Animals were immediately sacrificed after the final follow-up CMR scan, and myocardial tissue samples from ischemic areas were rapidly collected for histology and evaluation of water content.

Myocardial infarction procedure

The MI protocol is detailed elsewhere.[1, 3] Anesthesia was induced by intramuscular injection of ketamine (20 mg/kg), xylazine (2 mg/kg), and midazolam (0.5 mg/kg), and maintained by continuous intravenous infusion of ketamine (2 mg/kg/h), xylazine (0.2 mg/kg/h), and midazolam (0.2 mg/kg/h). Animals were intubated and mechanically ventilated with oxygen (fraction of inspired O_2: 28%). Central venous and arterial lines were inserted and a single bolus of unfractioned heparin (300 IU/kg) was administered at the onset of instrumentation. The left anterior descending coronary artery, immediately distal to the origin of the first diagonal branch, was occluded for 40 or 20 minutes with an angioplasty balloon introduced via the percutaneous femoral route using the Seldinger technique. Balloon location and maintenance of inflation were monitored angiographically. After balloon deflation, a coronary angiogram was recorded to confirm patency of the coronary artery. A continuous infusion of amiodarone (300 mg/h) was maintained during the procedure in all pigs to prevent malignant ventricular arrhythmias. In cases of ventricular fibrillation, a biphasic defibrillator was used to deliver non-synchronized shocks.

Conditioning strategies

In the postconditioned group, at the end of the 40 minutes coronary occlusion, coronary flow was reestablished for 1 min by deflating the angioplasty balloon. After 1 min of reflow, the balloon was re-inflated to occlude the coronary artery (low pressure, 4-6 atmospheres) at the same level for 1 minute. This procedure was repeated four times and then chronic coronary reperfusion was allowed.[4] In the pre-conditioning group, the angioplasty balloon was placed immediately distal to the first diagonal branch, and inflated 3 times for 5 min with low pressure (4 to 6 atmospheres) inflations, each separated by 5 min of reflow. At the end of the pre-conditioning protocol, the balloon was inflated for 40 minutes and then deflated to allow chronic reperfusion. Balloon location and maintenance of inflation were monitored angiographically in all cases for both procedures.

Arterial enhanced MDCT protocol

Arterial enhanced multidetector computed tomography (MDCT) was performed during the index coronary occlusion in all pigs, between minute 10 and minute 20 of ischemia, to delineate the reference MaR (hypoperfused region during coronary occlusion).[2] All MDCT studies were performed

on a 64-slice CT-scanner (Brilliance CT 64, Philips Healthcare, Cleveland, Ohio). The pigs were positioned supine, and all scans were performed in the cranio-caudal direction during free-breathing. Arterial phase MDCT was performed after intravenous administration of 60 ml iomeprol 400 mgI/ml (Iomeron 400, Bracco Imaging, Milano, Italy) at a flow rate of 3 ml/s followed by a 20-ml saline chaser bolus at the same flow rate. The scan delay was determined using a bolus tracking technique. Data acquisition started 15 seconds after a threshold of 180 Hounsfield Units was reached in a region of interest placed in the descending aorta.[2]
MDCT examinations were acquired using retrospective cardiac triggered at the 75% of the cardiac cycle with 64 x 0.625 mm collimation and a pitch of 0.2, 120 kV tube voltage, 800 mA tube current and tube rotation time of 400 ms. Image reconstruction was performed with a 512x512 matrix size over a 273x273mm^2 FOV and 0.45mm slice thickness by using high resolution filter (Xres Sharp).

Arterial enhanced MDCT analysis
MDCT images were analyzed using dedicated software (MR Extended Work Space 2.6, Philips Healthcare, Best, The Netherlands). Short axes orientation were obtained from volumetric CT images by multi-planar reconstruction using equivalent anatomical coordinates used for T2W-STIR planning acquisition. In order to have equivalent LV sections, MDCT studies had to be reconstructed in slices equivalent in thickness and level to the CMR ones. Thus, T2W-STIR and multi-planar reconstructed (MPR) short axis CT images were co-registered in 13 to 15 short-axis LV slices by one observer. To ensure CT as independent reference for MaR, endocardial and epicardial borders from MPR CT short-axis images were manually traced by a different observer blinded to the co-registration information; and MaR and remote areas were visually identified based on contrast enhancement differences, manually delineated, and expressed as a percentage of LV area.

CMR protocol
Baseline CMR scans were performed immediately before myocardial infarction and scans were subsequently repeated at all post-infarction follow-up times until sacrifice. CMR examinations were conducted with a Philips 3-Tesla Achieva Tx whole body scanner (Philips Healthcare, Best, the Netherlands) equipped with a 32-element phased-array cardiac coil. The imaging protocol included a standard segmented cine steady-state free-precession (SSFP) sequence to provide high quality anatomical references, and assessment of LV mass, wall thickness and left ventricular ejection fraction (LVEF); a T2-weighted short-tau triple inversion-recovery (T2W-STIR) sequence to assess the extent of edema and intramyocardial hemorrhage; a T2-gradient-spin-echo mapping (T2-GraSE map) sequence to provide precise myocardial T2 relaxation time properties;[5] and a T1-weighted inversion recovery turbo field echo (T1-IR-TFE) sequence acquired 10 to 15 minutes after the administration of gadolinium contrast to assess infarct size and microvascular obstruction. To avoid interference with T2 measures at immediate reperfusion, gadolinium contrast was not administered at baseline CMR scans. All sequences were acquired in free-breathing mode.
The imaging parameters for the SSFP sequence were FOV 280 x 280 mm, slice thickness 6 mm with no gap, TR 2.8 ms, TE 1.4 ms, flip angle 45°, cardiac phases 30, voxel size 1.8 x 1.8 mm, and 3 NEX. The imaging parameters for the T2W-STIR sequence were FOV 280 x 280, slice thickness 6 mm, TR 2 heartbeats, TE 80 ms, voxel size 1.4 x 1.9 mm, delay 210 ms, end-diastolic acquisition, echo-train length 16, and 2 NEX. The imaging parameters for the T2-GraSE mapping were FOV 300x300 with an acquisition voxel size of 1.8x2.0 mm^2 and slice thickness 8 mm, TR 2 heartbeats, eight echo times ranging from 6.7 to 53.6ms, and EPI factor 3. Late gadolinium enhancement imaging was performed 10 to 15 min after intravenous administration of 0.20 mmol of gadopentetate dimeglumine contrast agent per kg of body weight using a T1 inversion-recovery spoiled turbo field echo (T1-IR-TFE) sequence with the following parameters: FOV 280 × 280 mm, voxel size 1.6 × 1.6 mm, end-diastolic acquisition, thickness 6 mm with no gap, TR 5.6 ms, TE 2.8 ms, inversion delay time optimized to null normal myocardium, and 2 NEX.
SSFP, T2W-STIR, and T1-IR-TFE sequences were performed to acquire 13 to 15 contiguous short-axis slices covering the heart from the base to the apex, whereas T2-maps were acquired in a mid-apical ventricular short axis slice corresponding to the same anatomical level in all acquisitions in order to track T2 relaxation time changes over time.

CMR analysis

CMR images were analyzed using dedicated software (MR Extended Work Space 2.6, Philips Healthcare, The Netherlands; and QMassMR 7.6, Medis, Leiden, The Netherlands) by two observers experienced in CMR analysis and blinded to protocol allocation. Left ventricular (LV) mass, myocardial T2 relaxation time, and extent of edema, necrosis, intramyocardial hemorrhage (IMH) and microvascular obstruction (MVO) were determined.

LV cardiac borders were automatically traced with manual adjustment in each cine image to obtain LV end-diastolic volume (LVEDV), end-systolic volume (LVESV), and LVEF. In the tracing convention used, the papillary muscles were included as part of the LV cavity volume. LVEF was computed as LVEF (%) = (LVEDV-LVESV)/LVEDV. LV epicardial borders were also traced on the end-diastolic images to measure end-diastolic wall thickness at the myocardium at risk and remote areas, with LV mass computed as the end-diastolic myocardial volume (ie, the difference between the epicardial and endocardial volumes) multiplied by myocardial density (1.05 g/mL). Values of LV mass normalized to body surface area were calculated with the modified Brody's formula.[6]

T2-maps were automatically generated on the acquisition scanner by fitting the signal intensity of all echo times to a monoexponential decay curve at each pixel with a maximum likelihood expectation maximization algorithm. T2 relaxation maps were quantitatively analyzed by placing a wide transmural region of interest (ROI) at the ischemic area of the corresponding slice in all studies. Hypointense areas suggestive of microvascular obstruction or hemorrhage were included in the ROI for T2 quantification purposes.[1, 3, 5]

The extent of edema, expressed as a percentage of LV mass, was defined after manually tracing the endocardial and epicardial contours of T2W-STIR short-axis images. Abnormal areas were initially identified using the full-width at half-maximum (FWHM) method.[7, 8] Given that the solely use of FWHM may be prompt to inaccurate patchy estimations,[9, 10] extensive manual correction and visual border delineation were performed. Areas corresponding to slow-flow artifacts were carefully excluded from edematous area. Hypointense areas within the edematous zone, corresponding to intramyocardial hemorrhage (IMH), were included within the edematous region.[11, 12] Additionally, the size of the area of IMH was calculated by manual delineation of the hypointense areas on T2W-images,[11] and expressed as a percentage of LV mass. Manual delineation of clear hypointense areas was permitted in the absence of discernible hyperintense myocardium.

Myocardial necrosis (infarct size, IS), expressed as a percentage of LV mass, was defined according the extent of late gadolinium enhancement (LGE) after manually tracing the endocardial and epicardial contours on T1-IR-TFE short axis images. Abnormal areas were defined using the FWHM, with manual correction if needed. Hypointense black areas within the necrotic zone, corresponding to microvascular obstruction (MVO), were included within the necrotic area.[11, 12] Additionally, the size of the area MVO was calculated by manual delineation of the hypointense areas on LGE images,[11] and expressed as a percentage of LV mass.

Quantification of myocardial water content

Paired myocardial samples were collected within minutes of euthanasia from the ischemic myocardium of all pigs. Tissue samples were immediately blotted to remove surface moisture and introduced into laboratory crystal containers previously weighed on a high-precision scale. The containers were weighed before and after drying for 48 hours at 100°C in a desiccating oven. Tissue water content was calculated as follows: water content (%) = [(wet weight−dry weight)/wet weight] ×100. An empty container was weighed before and after desiccation as an additional calibration control.

Histological and immunnohistochemical analysis

Myocardial samples were collected within minutes of euthanasia from the ischemic (anteroseptal) mid-apical ventricular wall and processed as previously described.[3] Briefly, tissue samples were fixed in 10% neutral buffered formalin for 48 hours and processed by dehydrating the tissue in increasing concentrations of ethanol. Samples were then cleared in xylene, embedded in paraffin wax and cut into 4 micron sections.

For histopathological analysis sections were stained with Hematoxylin and Eosin (H&E) and Masson's Trichrome. Necrotic tissue was defined by the presence of typical signs of coagulative necrosis including marginal contraction bands, fading and eventually loss of nuclei and striation in cardiomyocytes. Granulation tissue was defined by the presence of loose collagen and abundant capillaries with a nearly complete removal of necrotic myocytes by infiltrated macrophages. Lesion area was defined as the sum of necrotic and granulation areas.
For immunohistochemical analysis sections were deparaffinized and antigen unmasking was performed using heat induced epitope retrieval with citrate buffer at pH6. Before incubation with primary antibodies, endogenous peroxidase was blocked by incubation with H_2O_2 for 5 minutes and endogenous antigens were blocked with fetal bovine serum for 20 minutes. Primary antibody used was mouse monoclonal anti-PM1 (BMA biomedicals; T-3503) to detect neutrophils. As secondary antibodies we used a HRP-conjugated goat anti-mouse (Dako; P0447) for PM1. Bound antibody was revealed by staining with diaminobenzidine and nuclei were counterstained with hematoxylin. All immunohistochemical procedures were performed using an automated autostainer (Autostainer Plus®, Dako).
For analysis, the images were digitalized with a scanner (Nanozoomer-RS C110730®, Hamamatsu) and examined with image analysis software (Tissuemorph®, Visiopharm) by an experienced veterinary pathologist blinded to experimental procedure performed. For the Trichrome staining analysis, we used the AEC-DAB 35% protocol instead of the H&E 12% protocol used before,[3] to increase sensitivity to changes in collagen content.

SUPPLEMENTAL FIGURES AND FIGURE LEGENDS

Online Figure I. Study design.
The study population comprised 25 pigs weighing 30-40 kg. Five pigs were sacrificed with no intervention other than baseline cardiac magnetic resonance (CMR), and served as healthy reference subjects. Four 5-pig groups underwent different closed-chest I/R protocols: 40-min-I/R (prolonged ischemia, controls), prolonged ischemia followed by postconditioning, prolonged ischemia preceded by preconditioning, or 20-min-I/R (short-duration ischemia). Arterial enhanced multidetector computed tomography was performed during coronary occlusion in all pigs as a reference standard for measuring the myocardial area at risk. Serial CMR-based tissue characterization was done in all pigs at baseline, and at 120-min, day1, day4, and day7 after I/R. Animals were sacrificed immediately after the final follow-up CMR scan, and myocardial tissue samples from ischemic areas were rapidly collected for histology and determination of water content.
CMR: cardiac magnetic resonance; I/R: ischemia/reperfusion; MDCT: multidetector computed tomography; PostC: postconditioning; PreC: preconditioning.

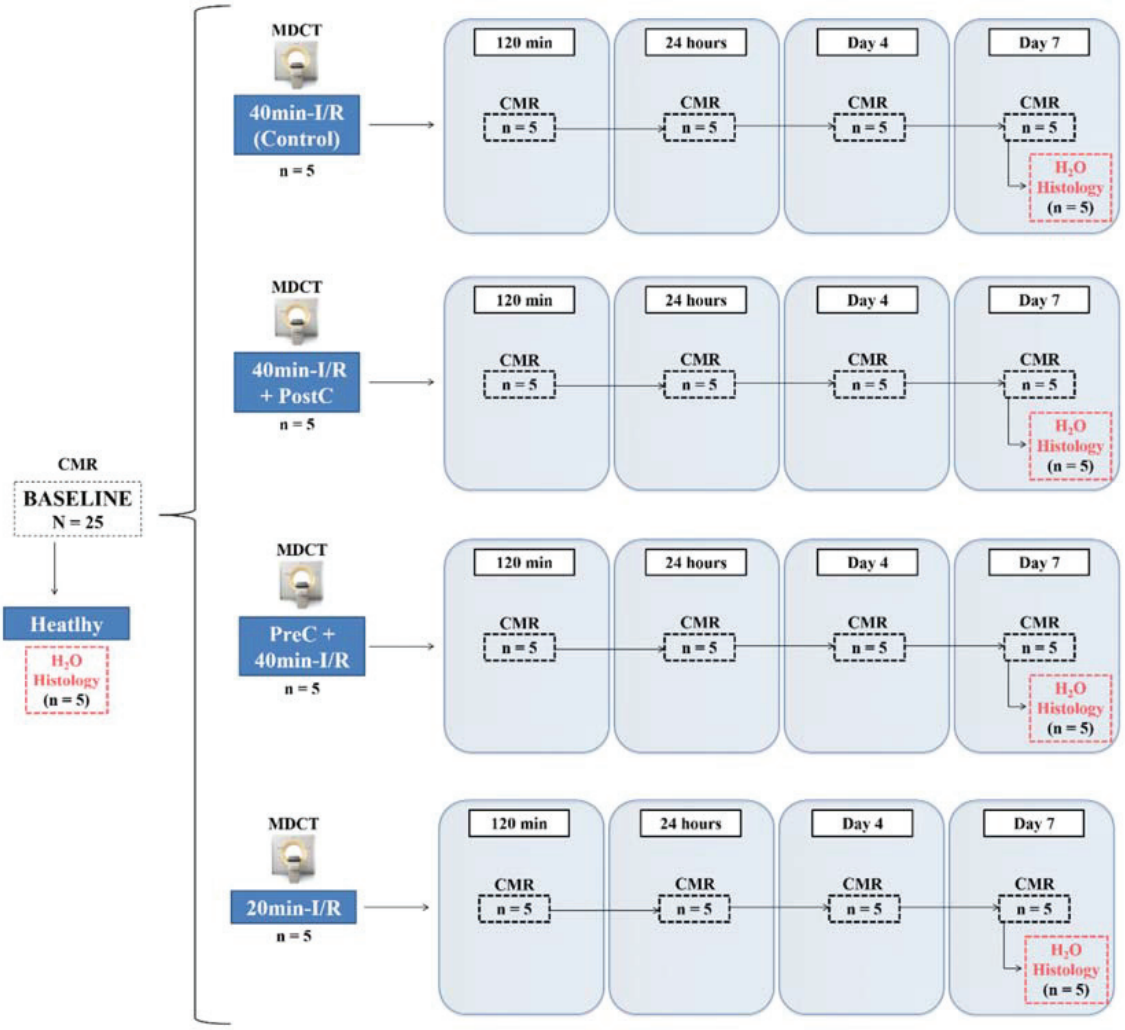

SUPPLEMENTAL TABLES

Online Table I. Temporal evolution of left ventricular mass, thickness, and positive- and negative-late gadolinium enhanced mass as assessed by cardiac magnetic resonance in pigs subjected to different I/R protocols and followed up to day 7 after I/R.

Group	CMR measure	Follow up				
		Baseline	**R-120min**	**R-24hours**	**R-Day4**	**R-Day7**
40min-I/R (Control)	LV mass, g/m^2	64.0 (7.4)	92.6 (6.0)	71.1 (4.7)	73.6 (5.2)	74.3 (4.7)
	Thickness ratio	1.06 (0.18)	2.08 (0.36)	1.23 (0.13)	1.17 (0.15)	1.08 (0.06)
	LGE (+) mass, g	-	25.9 (4.7)	17.2 (2.9)	16.8 (2.4)	14.6 (2.3)
	LGE (-) mass, g	-	39.9 (3.4)	39.6 (5.1)	43.0 (4.5)	43.5 (6.1)
40min-I/R + PostC	LV mass, g/m^2	53.3 (4.4)	77.7 (11.7)	54.1 (4.7)	59.7 (4.8)	60.5 (6.1)
	Thickness ratio	0.97 (0.20)	2.62 (0.62)	1.31 (0.13)	1.23 (0.13)	1.10 (0.23)
	LGE (+) mass, g	-	24.1 (6.6)	13.3 (1.7)*	16.1 (2.3)	14.8 (1.7)
	LGE (-) mass, g	-	27.5 (2.5)	27.1 (2.7)	33.1 (3.8)	34.0 (2.1)
PreC + 40min-I/R	LV mass, g/m^2	54.0 (9.5)	58.5 (8.6)	56.7 (6.2)	66.1 (9.9)	60.2 (6.2)
	Thickness ratio	1.13 (0.15)	1.34 (0.34)	1.22 (0.20)	1.21 (0.07)	1.24 (0.18)
	LGE (+) mass, g	-	8.8 (2.1)*	7.2 (3.6)*	3.1 (1.3)*	2.5 (1.8)*
	LGE (-) mass, g	-	34.8 (9.0)	34.0 (8.7)	39.9 (7.0)	41.0 (9.0)
20min-I/R	LV mass, g/m^2	56.30 (1.5)	57.60 (3.2)	57.10 (0.5)	59.60 (2.5)	60.80 (1.9)
	Thickness ratio	1.05 (0.10)	1.04 (0.14)	1.06 (0.08)	1.11 (0.04)	1.03 (0.12)
	LGE (+) mass, g	-	2.4 (1.8)*	1.2 (0.5)*	0.9 (0.3)*	0.6 (0.3)*
	LGE (-) mass, g	-	36.6 (2.6)	39.9 (2.4)	39.4 (3.9)	40.5 (4.1)

Values are mean (standard deviation). Table includes data from 4 groups of 5 pigs each undergoing 40min-I/R (controls), 40min-I/R plus postconditioning, 40min-I/R preceded by preconditioning, or 20min-I/R (short-duration ischemia). Total LV mass (g/m^2) and end-diastolic wall thickness ratio (MaR/remote) was assessed in standard segmented cine SSFP sequence; while LV mass showing positive or negative late gadolinium enhanced was assessed in T1-IR-TFE sequence.

No significant differences were found between time-points within same group in regards to total LV mass or wall thickness ratio, except for the R-120 min CMR in 40min-I/R and 40min-I/R plus post-conditioning, in which LV mass and thickness ratio was significantly higher than at the other time-points and groups due to the intense swelling of the ischemic myocardium at early reperfusion ($p<0.05$). Note that pigs subjected to 20min-I/R or preconditioning plus 40min-I/R did not show a significant increase of LV mass or thickness ratio at early reperfusion. P-value is adjusted for multiple comparisons.

Assessment of absolute LGE positive mass confirmed a cardioprotective effect in preconditioning and short-duration ischemia groups as compared to controls. A strong negative linear trend over time was shown for absolute LGE positive mass in all groups ($p<0.01$). *statistically significant differences ($p<0.05$) in regards to LGE positive areas as compared with the same time point in the 40min-I/R (control) group.

CMR: cardiac magnetic resonance; I/R: ischemia/reperfusion; PostC: post-conditioning; PreC: pre-conditioning; LV: left ventricle; g: grams; g/m^2: grams normalized for body surface area; LGE (+): late gadolinium enhanced positive; LGE (-): late gadolinium enhanced negative.

Online Table II. Time profile of myocardium salvage as assessed by multidetector computed tomography and cardiac magnetic resonance during the first week after reperfused myocardial infarction in pigs subjected to different I/R protocols and cardioprotective strategies.

Group	Follow up			
	R-120min	**R-24hours**	**R-Day4**	**R-Day7**
40min-I/R (Controls)	-40.0 (21.2)	-7.8 (14.2)	-0.9 (20.8)	9.1 (19.9)
40min-I/R + PostC	-50.7 (36.0)	-6.6 (13.7)	-5.1 (9.8)	2.3 (11.8)
PreC + 40min-I/R	34.1 (18.3)*	43.1 (28.6)*	76.3 (10.5)*	80.8 (14.2)*
20min-I/R	77.0 (12.4)*	87.4 (2.6)*	90.0 (4.3)*	94.4 (3.2)*

Values are mean (standard deviation).
The extent of myocardium at risk as assessed by MDCT reference standard during the index coronary occlusion (MDCT-MaR) was 28.3±4.3%, 31.3±4.0%, 31.7±6.9%, and 24.6±6.7% of LV; for pigs subjected to 40min-I/R (controls), 40min-I/R plus postcontitioning, preconditioning plus 40min-I/R, and 20min-I/R, respectively (statistically non-significant differences as compared to controls).
Myocardial salvage as assessed by MDCT/CMR [(MDCT MaR – CMR infarct size) / MDCT MaR, %] is presented in the table. Note that MDCT was performed only once (during the index ischemic event), while CMR was performed at all follow-up time-points.
A strong negative linear trend over time was shown for myocardial salvage as assessed with MDCT as reference standard for MaR in all groups ($p<0.01$).
*statistically significant differences ($p<0.05$) as compared with the same time point in the 40min-I/R (control) group. P-value is adjusted for multiple comparisons among groups for each time-point and imaging parameter.
CMR: cardiac magnetic resonance; MaR: myocardium at risk; I/R: ischemia/reperfusion; R: reperfusion; PostC: postconditioning; PreC: preconditioning.

Online Table III. Time course of intramyocardial hemorrhage and microvascular obstruction assessed by cardiac magnetic resonance up to day 7 after I/R in pigs subjected to different I/R protocols.

Group	CMR measure	Follow up			
		R-120min	**R-24hours**	**R-Day4**	**R-Day7**
40min-I/R (Control)	IMH, % of LV	0.2 (0.5)	4.3 (1.8)	4.4 (1.9)	1.4 (1.4)
	MVO, % of LV	5.1 (4.5)	6.5 (2.1)	2.3 (2.8)	1.8 (2.9)
40min-I/R + PostC	IMH, % of LV	0.7 (0.9)	4.6 (3.1)	6.2 (4.0)	3.2 (2.3)
	MVO, % of LV	4.5 (1.7)	5.1 (2.8)	2.7 (2.1)	1.9 (2.8)
PreC + 40min-I/R	IMH, % of LV	0.2 (0.4)	0.9 (1.2)*	0.9 (0.9)*	0.2 (0.3)
	MVO, % of LV	0.5 (0.8)*	0.8 (1.1)*	0.3 (0.6)	0.1 (0.2)
20min-I/R	IMH, % of LV	0.2 (0.3)	0.7 (0.5)*	0.7 (0.2)*	0.4 (0.4)
	MVO, % of LV	0*	0*	0	0

Values are mean (standard deviation). Table includes data from 4 groups of 5 pigs each undergoing 40min-I/R (controls), 40min-I/R plus postconditioning, 40min-I/R preceded by preconditioning, or 20min-I/R (short-duration ischemia). Note that the degree of intramyocardial hemorrhage and MVO was significantly lower at crucial time-points evaluated in pigs subjected to 20min-I/R or pre-conditioning plus 40min-I/R than in pigs subjected to 40min-I/R or 40min-I/R plus post-conditioning. *statistically significant differences ($p<0.05$) as compared with the same time point in the 40min-I/R (control) group. P-value is adjusted for multiple comparisons among groups for each time-point and imaging parameter.
CMR: cardiac magnetic resonance; I/R: ischemia/reperfusion; PostC: post-conditioning; PreC: pre-conditioning; IMH: intramyocardial hemorrhage; MVO: microvascular obstruction; LV: left ventricle.

Online Table IV. Histological features in the ischemic myocardium of pigs sacrificed at day 7 after I/R.

	Healthy	40min-I/R (Control)	40min-I/R + PostC	PreC + 40min-I/R	20min-I/R
Lesion, %	0.0 (0.0)	45.0 (39.7)	69.3 (25.7)	10.1 (8.0)*	0.0 (0.0)*
Necrosis†, %	0.0 (0.0)	8.9 (12.7)	9.0 (10.8)	0.3 (0.6)	0.0 (0.0)
Granulation tissue†, %	0.0 (0.0)	91.1 (12.7)	91.0 (10.8)	99.7 (0.6)	0.0 (0.0)*
Neutrophils, number/mm²	6.3 (1.5)	39.4 (43.4)	63.2 (45.5)	5.5 (3.3)	11.2 (2.3)
Collagen, %	0.0 (0.0)	30.4 (6.1)	31.2 (13.1)	18.8 (8.0)*	0.0 (0.0)*

Neutrophils are reported as the mean (standard deviation) number of cells per square millimeter in the histological section. Collagen content is reported as the mean (standard deviation) percentage within the granulation tissue area. Given that a more sensitive protocol was used to quantify collagen content, the value obtained for pigs subjected to 40min-I/R (control) differs from that previously published for the same group of pigs.[3]

*statistically significant differences ($p<0.05$) as compared to the 40min-I/R (control) group. Healthy animals were excluded from comparisons. P-value is adjusted for multiple comparisons among groups for each one of the histological features.

†Necrosis and granulation tissue as defined within the lesion area (see detailed methods).

I/R: ischemia/reperfusion; PostC: post-conditioning; PreC: pre-conditioning.

SUPPLEMENTAL REFERENCES

1. Fernandez-Jimenez R, Sanchez-Gonzalez J, Aguero J, Garcia-Prieto J, Lopez-Martin GJ, Garcia-Ruiz JM, Molina-Iracheta A, Rossello X, Fernandez-Friera L, Pizarro G, Garcia-Alvarez A, Dall'Armellina E, Macaya C, Choudhury RP, Fuster V and Ibanez B. Myocardial edema after ischemia/reperfusion is not stable and follows a bimodal pattern: imaging and histological tissue characterization. *J Am Coll Cardiol*. 2015;65:315-23.
2. Mewton N, Rapacchi S, Augeul L, Ferrera R, Loufouat J, Boussel L, Micolich A, Rioufol G, Revel D, Ovize M and Croisille P. Determination of the myocardial area at risk with pre- versus post-reperfusion imaging techniques in the pig model. *Basic Res Cardiol*. 2011;106:1247-57.
3. Fernandez-Jimenez R, Garcia-Prieto J, Sanchez-Gonzalez J, Aguero J, Lopez-Martin GJ, Galan-Arriola C, Molina-Iracheta A, Doohan R, Fuster V and Ibanez B. Pathophysiology Underlying the Bimodal Edema Phenomenon After Myocardial Ischemia/Reperfusion. *J Am Coll Cardiol*. 2015;66:816-28.
4. Bodi V, Ruiz-Nodar JM, Feliu E, Minana G, Nunez J, Husser O, Martinez-Elvira J, Ruiz A, Bonanad C, Monmeneu JV, Lopez-Lereu MP, Forteza MJ, de Dios E, Hervas A, Moratal D, Gomez C, Mainar L, Sanchis J, Mainar V, Valencia J, Diaz A, Noguera I, Chaustre F and Chorro FJ. Effect of ischemic postconditioning on microvascular obstruction in reperfused myocardial infarction. Results of a randomized study in patients and of an experimental model in swine. *Int J Cardiol*. 2014;175:138-46.
5. Fernandez-Jimenez R, Sanchez-Gonzalez J, Aguero J, Del Trigo M, Galan-Arriola C, Fuster V and Ibanez B. Fast T2 gradient-spin-echo (T2-GraSE) mapping for myocardial edema quantification: first in vivo validation in a porcine model of ischemia/reperfusion. *J Cardiovasc Magn Reson*. 2015;17:92.
6. Kelley KW, Curtis SE, Marzan GT, Karara HM and Anderson CR. Body surface area of female swine. *Journal of animal science*. 1973;36:927-30.
7. Aletras AH, Tilak GS, Natanzon A, Hsu LY, Gonzalez FM, Hoyt RF, Jr. and Arai AE. Retrospective determination of the area at risk for reperfused acute myocardial infarction with T2-weighted cardiac magnetic resonance imaging: histopathological and displacement encoding with stimulated echoes (DENSE) functional validations. *Circulation*. 2006;113:1865-70.
8. Fernandez-Friera L, Garcia-Ruiz JM, Garcia-Alvarez A, Fernandez-Jimenez R, Sanchez-Gonzalez J, Rossello X, Gomez-Talavera S, Lopez-Martin GJ, Pizarro G, Fuster V and Ibanez B. Accuracy of Area at Risk Quantification by Cardiac Magnetic Resonance According to the Myocardial Infarction Territory. *Revista espanola de cardiologia*. 2017;70:323-330.
9. McAlindon E, Pufulete M, Lawton C, Angelini GD and Bucciarelli-Ducci C. Quantification of infarct size and myocardium at risk: evaluation of different techniques and its implications. *European heart journal cardiovascular Imaging*. 2015;16:738-46.
10. Sjogren J, Ubachs JF, Engblom H, Carlsson M, Arheden H and Heiberg E. Semi-automatic segmentation of myocardium at risk in T2-weighted cardiovascular magnetic resonance. *J Cardiovasc Magn Reson*. 2012;14:10.
11. Robbers LF, Eerenberg ES, Teunissen PF, Jansen MF, Hollander MR, Horrevoets AJ, Knaapen P, Nijveldt R, Heymans MW, Levi MM, van Rossum AC, Niessen HW, Marcu CB, Beek AM and van Royen N. Magnetic resonance imaging-defined areas of microvascular obstruction after acute myocardial infarction represent microvascular destruction and haemorrhage. *Eur Heart J*. 2013;34:2346-53.
12. Valle-Caballero MJ, Fernandez-Jimenez R, Diaz-Munoz R, Mateos A, Rodriguez-Alvarez M, Iglesias-Vazquez JA, Saborido C, Navarro C, Dominguez ML, Gorjon L, Fontoira JC, Fuster V, Garcia-Rubira JC and Ibanez B. QRS distortion in pre-reperfusion electrocardiogram is a bedside predictor of large myocardium at risk and infarct size (a METOCARD-CNIC trial substudy). *Int J Cardiol*. 2016;202:666-73.

LEGENDS FOR VIDEO FILES

Online Videos I and II. Short-axis view of a standard segmented cine steady-state free-precession (SSFP) from a pig subjected to 40min-I/R (control) at baseline (Video I) and within the first two hours after reperfusion (Video II).

Online Videos III and IV. Short-axis view of a standard segmented cine steady-state free-precession (SSFP) from a pig subjected to 40min-I/R plus post-conditioning at baseline (Video III) and within the first two hours after reperfusion (Video IV).

Online Videos V and VI. Short-axis view of a standard segmented cine steady-state free-precession (SSFP) from a pig subjected to preconditioning plus 40min-I/R at baseline (Video V) and within the first two hours after reperfusion (Video VI).

Online Videos VII and VIII. Short-axis view of a standard segmented cine steady-state free-precession (SSFP) from a pig subjected to 20min-I/R at baseline (Video VII) and within the first two hours after reperfusion (Video VIII).

Original research article #7. "*Dynamic edematous response of the human heart to myocardial infarction: implications for assessing myocardial area at risk and salvage*".[74]

Part of this work was presented by the doctoral student at the American Heart Association Scientific Sessions 2015, in Orlando (November 2015; Florida, USA).

ORIGINAL RESEARCH ARTICLE

Dynamic Edematous Response of the Human Heart to Myocardial Infarction

Implications for Assessing Myocardial Area at Risk and Salvage

Editorial, see p 1301

BACKGROUND: Clinical protocols aimed to characterize the post–myocardial infarction (MI) heart by cardiac magnetic resonance (CMR) need to be standardized to take account of dynamic biological phenomena evolving early after the index ischemic event. Here, we evaluated the time course of edema reaction in patients with ST-segment–elevation MI by CMR and assessed its implications for myocardium-at-risk (MaR) quantification both in patients and in a large-animal model.

METHODS: A total of 16 patients with anterior ST-segment–elevation MI successfully treated by primary angioplasty and 16 matched controls were prospectively recruited. In total, 94 clinical CMR examinations were performed: patients with ST-segment–elevation MI were serially scanned (within the first 3 hours after reperfusion and at 1, 4, 7, and 40 days), and controls were scanned only once. T2 relaxation time in the myocardium (T2 mapping) and the extent of edema on T2-weighted short-tau triple inversion-recovery (ie, CMR-MaR) were evaluated at all time points. In the experimental study, 20 pigs underwent 40-minute ischemia/reperfusion followed by serial CMR examinations at 120 minutes and 1, 4, and 7 days after reperfusion. Reference MaR was assessed by contrast-multidetector computed tomography during the index coronary occlusion. Generalized linear mixed models were used to take account of repeated measurements.

RESULTS: In humans, T2 relaxation time in the ischemic myocardium declines significantly from early after reperfusion to 24 hours, and then increases up to day 4, reaching a plateau from which it decreases from day 7. Consequently, edema extent measured by T2-weighted short-tau triple inversion-recovery (CMR-MaR) varied with the timing of the CMR examination. These findings were confirmed in the experimental model by showing that only CMR-MaR values for day 4 and day 7 postreperfusion, coinciding with the deferred edema wave, were similar to values measured by reference contrast-multidetector computed tomography.

CONCLUSIONS: Post-MI edema in patients follows a bimodal pattern that affects CMR estimates of MaR. Dynamic changes in post–ST-segment–elevation MI edema highlight the need for standardization of CMR timing to retrospectively delineate MaR and quantify myocardial salvage. According to the present clinical and experimental data, a time window between days 4 and 7 post-MI seems a good compromise solution for standardization. Further studies are needed to study the effect of other factors on these variables.

Rodrigo Fernández-Jiménez, MD*
Manuel Barreiro-Pérez, MD, PhD*
Ana Martin-García, MD, PhD*
Javier Sánchez-González, PhD
Jaume Agüero, MD, PhD
Carlos Galán-Arriola, DVM
Jaime García-Prieto, BSc
Elena Díaz-Pelaez, MD
Pedro Vara, DCS
Irene Martinez, DCS
Ivan Zamarro, DCS
Beatriz Garde, BPharm
Javier Sanz, MD
Valentin Fuster, MD PhD
Pedro L. Sánchez, MD, PhD
Borja Ibanez, MD, PhD

*Drs Fernández-Jiménez, Barreiro-Pérez, and Martin-García contributed equally.

Correspondence to: Borja Ibanez, MD, PhD, Translational Laboratory for Cardiovascular Imaging and Therapy, Centro Nacional de Investigaciones Cardiovasculares Carlos III (CNIC) & Cardiology Department, IIS-Fundación Jiménez Díaz. Melchor Fernández Almagro, 3. 28029, Madrid, Spain, or Pedro L. Sánchez, MD, PhD, Cardiology Department. Hospital Universitario Salamanca-IBSAL, Paseo de San Vicente 58-182, 37007, Salamanca, Spain. E-mail bibanez@cnic.es or pedrolsanchez@secardiologia.es

Sources of Funding, see page 1298

Key Words: edema ■ magnetic resonance imaging ■ myocardial infarction ■ translational medical research

Clinical Perspective

What Is New?

- This work shows for the first time that myocardial edema in the week after ST-segment–elevation myocardial infarction in humans is a bimodal phenomenon.
- An initial wave of edema appears abruptly at reperfusion, but it is significantly attenuated by 24 hours.
- The initial wave of edema is followed by a second (deferred) healing-related wave of edema several days after reperfusion reaching a plateau ≈4 to 7 days after myocardial infarction.
- This bimodal edematous response has a major impact on retrospective myocardial area at risk and salvage quantification by cardiac magnetic resonance given that measures of edema are greatly influenced by the timing of imaging.

What Are the Clinical Implications?

- Both cardiac magnetic resonance imaging techniques and timing of postinfarction imaging for assessing myocardial area at risk and myocardial salvage should be standardized to take account of the pathophysiology of the bimodal edematous phenomenon.
- The time frame between day 4 and 7 postinfarction seems a good compromise solution according to clinical and experimental data here presented.
- Our results have important implications for the design and interpretation of clinical trials using edema-sensitive cardiac magnetic resonance protocols to quantify myocardium at risk and myocardial salvage as an end point.

Noninvasive tissue characterization by cardiac magnetic resonance (CMR) after myocardial infarction (MI) offers the possibility to evaluate the impact of interventions designed to preserve cardiac function and predict long-term remodeling.[1] It has been postulated that an intense edematous reaction confined to the postischemic region appears early after MI and persists in stable form for at least 1 week.[2,3] On the basis of this assumption, the use of edema-sensitive T2-CMR sequences to delineate the spatial extent of post-MI edema was rapidly incorporated as an index of the original occluded coronary artery perfusion territory (myocardium at risk, MaR).[4,5] Quantification of late gadolinium enhancement (LGE) and edema extent (assumed to delineate MaR) in the same imaging session has been extensively used to quantify the amount of salvaged myocardium, a theoretical surrogate of the effect of cardioprotective therapies,[6,7] thus reducing the required sample size in trials.[8] Consequently, CMR-based myocardial salvage has been and continues to be used as an end point in multiple clinical and experimental studies.[9]

On the basis of the assumed stable unimodal edematous reaction during the first week after MI, the timing of the end point imaging session in these studies varies considerably. However, recent work in the pig model showed that the post-MI edematous reaction is not stable, and instead follows a bimodal pattern.[10] An initial reperfusion-related wave of edema appears abruptly on reperfusion and dissipates at 24 hours. This is followed by a healing-related deferred wave of edema appearing several days after MI, peaking around postreperfusion day 7.[11] This coordinated bimodal edema pattern suggests that CMR-quantified MaR may vary according to the day of imaging, but to date this has not been tested in a controlled manner. Some recent studies evaluated MaR extent in patients according to the timing of post-MI imaging, but these were either retrospective analyses[12] or did not systematically scan patients at the same time points.[13] Consequently, whether this phenomenon occurs in MI patients is unclear.

This study was designed to address these specific 2 questions: (1) is post-MI edematous reaction bimodal in humans, and (2) does the bimodal edematous reaction affect the CMR-based quantification of MaR and myocardial salvage? We designed a longitudinal clinical study in which patients with ST-segment–elevation MI (STEMI) successfully treated by primary angioplasty were prospectively recruited and CMR performed within the first 3 hours postreperfusion and at 24 hours, 4 days, 7 days, and 40 days. The impact of the dynamic edematous response on post-MI CMR measures of MaR, infarct size (IS), and salvaged myocardium was evaluated in the pig model of reperfused MI by performing reference measures of MaR and a comprehensive serial CMR imaging study.

METHODS

Clinical Study

Design

Hemodynamically stable consecutive patients with a first anterior STEMI and undergoing primary percutaneous coronary intervention were prospectively recruited between February 2015 and November 2015 ad hoc for this study. Patients eligible for enrollment were aged ≥18 years, and showed symptoms consistent with STEMI for >90 minutes and ST-segment elevation ≥2 mm in ≥2 contiguous leads in V_1 through V_5, with an anticipated time from symptom onset to reperfusion of ≤8 hours. Additional mandatory inclusion criteria were evidence of complete occlusion in the proximal or mid portion of the left anterior descending coronary artery (TIMI 0–1 initial flow) and successful primary angioplasty evidenced by appropriate reestablishment of coronary flow in the culprit artery (TIMI-3 flow after angioplasty). Exclusion criteria were Killip class III to IV, persistent systolic blood pressure <100 mm Hg, persistent heart rate <50 bpm or >110 bpm, presence of bifascicular or trifascicular block, evidence of second- or third-degree atrioventricular block, atrial fibrillation, known history of previous MI, pregnancy, active breastfeeding, and the presence

of metallic objects or devices incompatible with MRI. Patients were managed according to current clinical guidelines.[14,15]

CMR examinations were performed within 3 hours of reperfusion (hyperacute reperfusion) and at 24 hours, 4 days, 7 days, and 40 days after reperfusion (Figure 1A). Normal T2 relaxation times (baseline) were obtained in 16 healthy age- and sex-matched volunteers. The study was approved by the hospital Ethics Committee, and all patients and volunteers gave written informed consent.

CMR Protocol

CMR examinations were conducted with a Philips 1.5-Tesla Achieva whole-body scanner (Philips Healthcare) equipped with a 16-element phased-array cardiac coil. At all time points, the imaging protocol included a standard segmented cine steady-state free-precession sequence to provide high-quality anatomic references; a T2-weighted short-tau triple inversion-recovery (T2W-STIR) sequence to assess the extent of edema and intramyocardial hemorrhage (IMH); and a T2-gradient-spin-echo mapping sequence to provide precise myocardial T2 relaxation time properties.[16] On day 7 and day 40 CMR, LGE imaging was performed to assess infarct size and microvascular obstruction (MVO), using a T1-weighted inversion recovery turbo field echo sequence acquired 10 to 15 minutes after intravenous administration of 0.20 mmol gadobutrol contrast agent per kg body weight.

CMR Analysis

CMR images were analyzed using dedicated software (MR Extended Work Space 2.6, Philips Healthcare; and QMassMR 7.6, Medis) by 2 observers experienced in CMR analysis and blinded to time-point allocation and patient identification. T2 maps were analyzed by placing the region of interest at the transmural ischemic, infarcted (with or without including areas suggestive of IMH), salvage, and transmural remote areas in a midapical ventricular short-axis slice corresponding to the same anatomic level in all acquisitions to track T2 relaxation time changes over time.[16,17] The extent of edema, expressed as a percentage of left ventricular (LV) mass (CMR-MaR), was initially identified by using the full width at half-maximum with subsequent manual correction and visual border delineation after tracing the endocardial and epicardial contours of T2W-STIR short-axis images.[18] Hypointense areas within the edematous zone, corresponding to IMH, were included within the edematous region.[19,20] In addition, IMH area was calculated by manual delineation of the hypointense areas on T2W images[19] and expressed as a percentage of LV mass.

IS, expressed as a percentage of LV mass, was defined according to the extent of LGE after manually tracing the endocardial and epicardial contours on T1-weighted inversion recovery turbo field echo short-axis images. Abnormal areas were defined using the full width at half-maximum, with manual correction if needed. Hypointense black areas within the necrotic zone, corresponding to MVO, were included within the necrotic area.[19,20] In addition, the size of the MVO area was calculated by manual delineation of

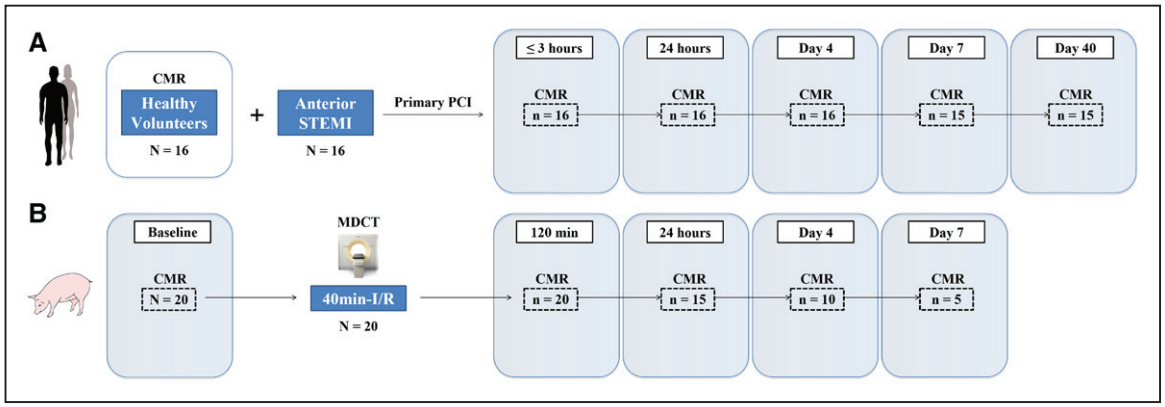

Figure 1. Study design.

A, Clinical study design. Twenty-two consecutive anterior patients with STEMI fulfilling the inclusion criteria were assessed for eligibility: 3 patients refused to participate; 1 patient experienced anxiety and a claustrophobic reaction requiring premature termination of the first CMR; 1 patient felt sick with vomiting before the first CMR, which could not be performed; and 1 patient had a failed CMR study because of frequent episodes of premature ventricular contraction and nonsustained ventricular tachycardia during the scan. The clinical study population thus included 16 consecutive hemodynamically stable patients with anterior STEMI reperfused by primary percutaneous coronary intervention. CMR examinations including T2-weighted short-tau triple inversion-recovery and T2-gradient-spin-echo mapping sequences were per protocol scheduled at the following times after reperfusion: within the first 3 hours and at 24 hours, 4 days, 7 days, and 40 days. To take account of baseline values, myocardial T2 relaxation time was measured in 16 healthy age- and sex-matched volunteers. **B,** Experimental study design. The study population comprised 20 pigs weighing 30 to 40 kg that underwent closed-chest 40 minutes reperfused acute anterior myocardial infarction. These pigs were euthanized at 120 minutes (n=5), 24 hours (n=5), 4 days (n=5), and 7 days (n=5) after myocardial infarction. Arterial enhanced multidetector computed tomography was performed during coronary occlusion in all pigs as a reference standard for measuring the myocardial area at risk. CMR scans, including T2-weighted short-tau triple inversion-recovery, T2 mapping, and late gadolinium enhancement imaging, were performed at every follow-up stage until euthanization. CMR indicates cardiac magnetic resonance; I/R, ischemia/reperfusion; MDCT, multidetector computed tomography; PCI, percutaneous coronary intervention; and STEMI, ST-segment–elevation myocardial infarction.

Circulation. 2017;136:1288–1300. DOI: 10.1161/CIRCULATIONAHA.116.025582

the hypointense areas on LGE images[19] and expressed as a percentage of LV mass.

Detailed information about CMR imaging protocol and parameters, and imaging analysis is presented in the online-only Data Supplement Methods.

Experimental Study

Design and MI Procedure

The study was approved by Institutional and Regional Animal Research Committees.

To study the impact of the dynamic edematous response on post-MI CMR time profile measures of MaR, IS, and salvaged myocardium, a group of 20 pigs underwent closed-chest reperfused MI by the percutaneous catheter–based technique, with 40-minute angioplasty-balloon occlusion of the mid left anterior descending coronary artery, followed by balloon deflation and reestablishment of blood flow[10] (Figure 1B). These pigs were euthanized at 120 minutes (n=5), 24 hours (n=5), 4 days (n=5), or 7 days (n=5) after ischemia/reperfusion (I/R). In all pigs, arterial enhanced multidetector computed tomography (MDCT) was performed during the index coronary occlusion, between minute 10 and minute 20 of ischemia, to delineate the reference MaR (hypoperfused region during coronary occlusion).[21] Comprehensive CMR scans were performed at every follow-up stage until euthanization (ie, animals euthanized on day 7 underwent baseline, 120 minutes, 24 hours, day4, and day7 CMR examinations).

Full methods can be found in the online-only Data Supplement Appendix.

Arterial Enhanced MDCT Protocol and Analysis

All MDCT studies were performed on a 64-slice CT scanner (Brilliance CT 64, Philips Healthcare) after intravenous administration of 60 mL of 400 mgI/mL iomeprol (Iomeron 400, Bracco Imaging).[21] MDCT images were analyzed using dedicated software (MR Extended Work Space 2.6, Philips Healthcare). MaR and remote areas were visually identified based on contrast enhancement differences, manually delineated, and expressed as a percentage of LV area.

CMR Protocol and Analysis

CMR examinations were conducted with a Philips 3-Tesla Achieva Tx whole body scanner (Philips Healthcare) equipped with a 32-element phased-array cardiac coil. The imaging protocol included an steady-state free-precession sequence to provide high-quality anatomic references, and assessment of LV mass and wall thickness; a T2W-STIR sequence to assess the extent of edema and IMH; a T2-gradient-spin-echo mapping sequence[10,16]; and a T1-weighted inversion recovery turbo field echo sequence to assess IS and MVO. CMR images were similarly analyzed using dedicated software (MR Extended Work Space 2.6, Philips Healthcare; and QMassMR 7.6, Medis) by 2 observers experienced in CMR analysis and blinded to group allocation.

Detailed information about MDCT and CMR imaging protocol and parameters, and imaging analysis, can be found in the online-only Data Supplement Methods.

Statistical Analysis

In the clinical study, the sample size calculation to detect a difference in T2 relaxation time in the ischemic myocardium between examination time points after STEMI was prespecified by using the user-written command *nsize* (Stata 12.0). A sample size of 16 patients was determined on the basis of our previous experimental results,[10] a 95% confidence level, a statistical power of 80%, a conservative significant mean difference to detect of 15 ms in T2, a SD of 12, and multiple pairwise comparisons between time points.

Normal distribution of each data subset was checked by using graphical methods and a Shapiro-Wilk test. The Leven test was performed to check the homogeneity of variances. For quantitative variables, data are expressed as mean±SD. For categorical variables, data are expressed as frequencies and percentages. To take account of repeated measures, generalized linear mixed models were conducted to analyze the time course of T2 relaxation time, CMR-MaR, IMH, MVO, IS, and salvaged myocardium. Models evaluating the time course of T2 or CMR-MaR were further adjusted by extent of hemorrhage, including the amount of IMH expressed as a percentage of the LV as a covariate, given that this parameter is known to affect T2. Given the hypothesis-driven nature of the study, comparisons among different time points were planned in advance. Nonetheless, *P* value was adjusted for multiple comparisons by using the Hochberg method.

All statistical analyses were performed with Stata v12.0 (StataCorp).

RESULTS

Clinical Study

General Characteristics of the Population

Clinical characteristics of the study population are summarized in Table 1. Serial CMR was performed with informed consent in 16 consecutive patients with anterior STEMI fulfilling the inclusion criteria (mean age 58.8±14.5 years, 14 [87.5%] male) and successfully treated by primary percutaneous coronary intervention. A total of 94 CMR examinations were performed: the 16 healthy volunteers were scanned once, and the 16 patients with STEMI were scanned at 2.2±0.5 hours, 24.8±1.8 hours, 3.8±0.4 days, 6.8±0.6 days, and 41.7±4.3 days after reperfusion. In all patients, the first CMR scan was performed within the first 3 hours (90–180 minutes) after primary percutaneous coronary intervention. The timing for the initial CMR scan (around the peak of reperfusion-related wave of edema) was identified before in a dedicated separate group of 5 pigs undergoing serial CMR scans every 20 minutes during the 6 hours following reperfusion (see online-only Data Supplement Methods and Results, and online-only Data Supplement Figures I and II). Evaluable T2-mapping and T2W-STIR data were available in 100% of CMR scans performed. Information on vital status was available for all participants.

Table 1. Baseline Patient Characteristics

Characteristic	All Patients (n=16)
Age, y	58.8±14.5
Male sex	14 (87.5)
Body mass index, kg/m^2	27.1±2.9
Hypertension	9 (56.3)
Smoking	
Current smoker	9 (56.3)
Ex-smoker (0–10 y before)	4 (25.0)
Dyslipidemia	10 (62.5)
Diabetes mellitus	3 (18.8)
Ischemia duration, min*	185±115
Killip class at recruitment	
I	11 (68.7)
II	5 (31.3)
Infarct artery lesion location	
Proximal left anterior descending coronary artery	16 (100.0)
Mid left anterior descending coronary artery	0 (0.0)
Treatment at the time of primary percutaneous intervention	
Heparin	16 (100.0)
Oral antiplatelet	
Aspirin	14 (87.5)
Clopidogrel	8 (50.0)
Prasugrel	5 (31.3)
Ticagrelor	4 (25.0)
Thrombus aspiration	9 (56.3)
Glycoprotein IIb/IIIa during primary percutaneous intervention	9 (56.3)

Data are presented as mean±SD or n (%).
*Mean time from symptom onset to reperfusion.

Edema Time Course in Patients With STEMI

T2 Relaxation Time

Mean myocardial T2 relaxation times in the 16 healthy volunteers (mean age 59.3±17.7 years, 12 [75%] male) were 53.1±4.1 ms and 51.1±4.5 ms for the midapical anteroseptal and posterolateral LV walls, respectively. In comparison with these values, hyperacute reperfusion in patients with STEMI (≤3 hours) was associated with significantly longer T2 relaxation times in the ischemic area (Figure 2A and 2B). T2 relaxation time in patients with STEMI showed a systematic and significant decrease at 24 hours post-MI. This was followed by a rebound increase, with T2 relaxation times on day 4 postreperfusion reaching values similar to those observed during early reperfusion. Thereafter, T2 relaxation time progressively decreased, with values on day 40 similar to those observed at 24 hours. Similar results were obtained after adjusting T2 for the amount of IMH (online-only Data Supplement Table I). During the first week after MI, T2 relaxation time in the remote myocardium showed a linear trend toward a progressive increase, albeit slight. T2 relaxation times in the ischemic and remote myocardium at different postreperfusion time points are summarized in Table 2. T2 relaxation time was longer in the transmural ischemic myocardium than in the remote myocardium at all time points evaluated. However, the differences observed at 24 hours and 40 days, albeit statistically significant, were of small magnitude and resulted in a wide overlapping of myocardial T2 values within ischemic and remote areas (Figure 2C). Individual trajectories for T2 relaxation time in the ischemic myocardium of STEMI patients are shown in online-only Data Supplement Figure III.

Extent of Edema (CMR-MaR)

The edematous area delineated by T2W-STIR sequences was similar in CMR scans performed at hyperacute reperfusion (≤3 hours) and on day 4 and day 7 (Figure 3). Conversely, the area of edema was significantly smaller at 24 hours postreperfusion. On day 40 post-MI, the area of edema was comparable to that seen at 24 hours. This time-course pattern for edema resembles that observed for T2 relaxation time, and similar results were obtained after adjusting the area of edema for the amount of IMH evaluated by T2W-STIR (online-only Data Supplement Table II). Edematous area at different postreperfusion time points is summarized in Table 2. Individual patient trajectories for area of edema measurements are shown in online-only Data Supplement Figure IV.

Experimental Study

Dynamics of CMR-MaR After Reperfused MI in Comparison With the Reference Standard

CMR-measured MaR values at different times after reperfusion in pigs are summarized in Table 3 and online-only Data Supplement Table III. Mean MaR as assessed by the MDCT reference method was 30.5±5.0% of the LV. Because of the initial swelling of the ischemic myocardium (online-only Data Supplement Table IV), CMR-measured MaR as delineated by T2W-STIR sequence was significantly higher than MaR measured by MDCT at early reperfusion (Figure 4A and 4B). Coinciding with the dissipation of the first edema wave,[10] MaR was strikingly underestimated by CMR at 24 hours postreperfusion. Conversely, CMR-estimated MaR values for day 4 and day 7 postreperfusion, coinciding with the deferred edema wave,[10] were similar to values measured by MDCT (ie, no overestimation or underestimation). The dynamics of CMR-measured MaR resembled the time course for myocardial T2 relaxation time and water content in the ischemic area.[10]

Circulation. 2017;136:1288–1300. DOI: 10.1161/CIRCULATIONAHA.116.025582

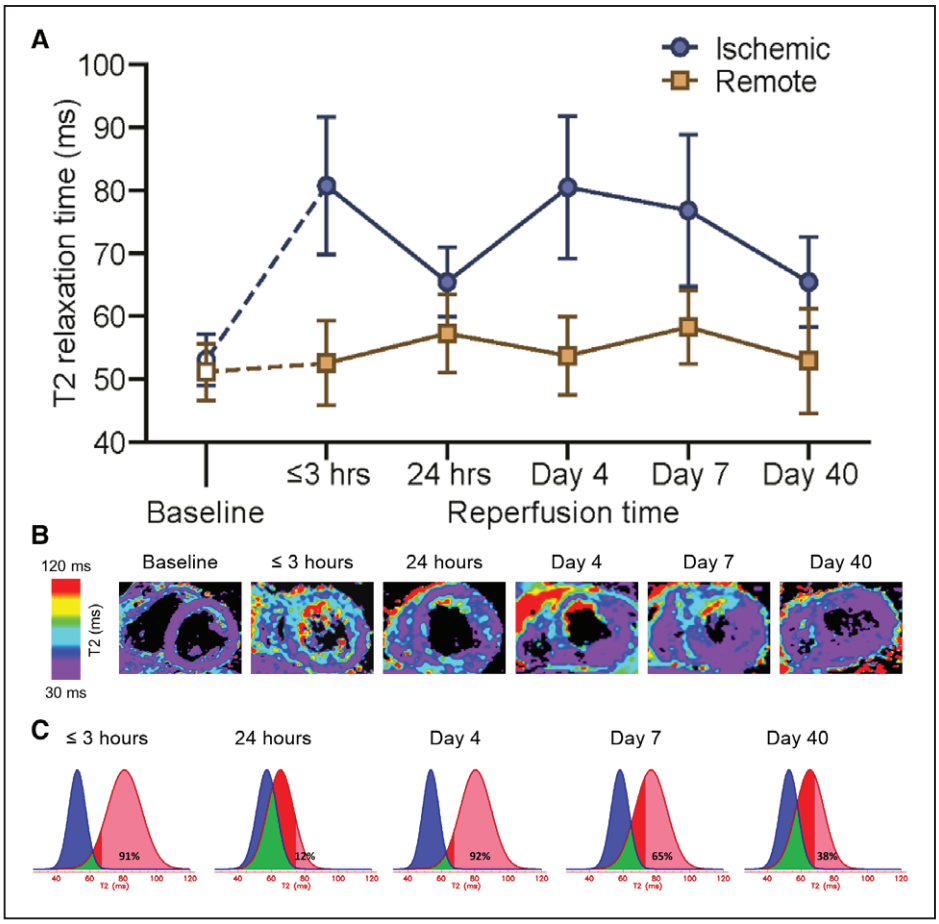

Figure 2. Temporal evolution of myocardial T2 relaxation time in patients with ST-segment–elevation myocardial infarction.

A, Time course of absolute T2 relaxation time (ms) in the ischemic and remote myocardium in patients with ST-segment–elevation myocardial infarction. Data are means and SD. For baseline values, myocardial T2 relaxation time was measured in 16 healthy age- and sex-matched volunteers. Dashed lines represent hypothetical mean trajectories for T2 from baseline to the hyperacute postreperfusion phase (≤3 hours). At all time points after reperfusion, T2 relaxation time in the ischemic myocardium of patients differed significantly from baseline values in heathy volunteers. It is noteworthy that cardiac magnetic resonance T2 mapping revealed similar T2 values at ≤3 hours and on day 4 and day 7 postreperfusion; in contrast, T2 relaxation time was significantly lower at 24 hours and on day 40 post-MI. **B,** Representative images from a patient with anterior ST-segment–elevation myocardial infarction who underwent serial cardiac magnetic resonance T2-mapping examinations at 150 minutes, 26 hours, 4 days, 7 days, and 44 days after reperfusion. For baseline cardiac magnetic resonance T2 mapping, an image from a healthy volunteer is shown. All T2 maps were scaled between 30 and 120 ms. **C,** T2 values distribution in the ischemic and remote myocardium in patients with ST-segment–elevation myocardial infarction at different time points. Mean and SD from all individual regions of interest placed in these areas at all time points were analyzed. Blue and red colors represent distribution of T2 values in the remote and ischemic myocardium, respectively. Green color represents the overlapping of T2 values, ie, pixels from both areas having the same T2. The percentages shown in each panel represent the percent of the ischemic myocardium region of interest with T2 >2 SDs from the mean T2 in the remote myocardium (pink). Despite that the mean T2 relaxation time in ischemic myocardium at all time points was longer than mean T2 in the remote, overlapping was patent and widest at the 24-hour time point.

Dynamics of CMR-Measured IS, Myocardial Salvage, IMH, and MVO After Reperfused MI

CMR-measured IS and myocardial salvage in pigs are summarized in Table 3 and online-only Data Supplement Table III. A progressive reduction of IS was observed during the first week after I/R (Figure 4C and 4D). Matching the temporal variations in CMR-MaR, CMR-estimated myocardial salvage quantification [(MaR-IS)/MaR, %] also changed dynamically during the first week after I/R (online-only Data Supplement Figure V).

CMR-estimated IMH and MVO are summarized in online-only Data Supplement Table V. IMH was apparent at 24 hours and peaked on day 4 post-I/R; in contrast, MVO was apparent at 120 minutes after reperfusion, peaking on day 1 post-I/R and progressively decreasing thereafter. The dynamics of CMR-estimated

IMH are consistent with histologically evaluated IMH in the same model previously reported.[11]

DISCUSSION

First Demonstration of the Postinfarction Bimodal Edema Reaction in the Human Heart

This is the first comprehensive evaluation of patients with STEMI by serial CMR to include the hyperacute postreperfusion period (the first 3 hours). CMR scans timing was designed as per the protocol of our previous experimental studies, in which we demonstrated the existence of bimodal post-MI edema in pigs.[10,11]

The main finding of the present clinical study is that, contrary to the accepted view, myocardial edema in the ischemic area after MI in humans is not stable, but rather follows a systematic bimodal pattern. An initial wave of edema appears abruptly very early after reperfusion, but it is significantly attenuated by 24 hours. This is followed by a second (deferred) wave of edema several days after reperfusion reaching a plateau ≈4 to 7 days after MI.

The Initial Wave of Edema

To select the optimal timing for the first CMR scan in STEMI patients, we first analyzed the dynamics of the initial wave of edema in a series of 5 pigs; serial CMR scans were performed every 20 minutes until the reperfusion-related edema wave faded. It is interesting to note that this initial wave of edema peaked very early, being significantly attenuated within a few hours after MI: at 180 minutes after reperfusion, the edema had declined by ≈50% from its maximum. In agreement with CMR data, quantification of myocardial water content and histological analysis at 6 hours after MI revealed partial resolution of the massive interstitial edema seen earlier after reperfusion (see online-only Data Supplement Results).[11] On the basis of these results in pigs, we decided to perform the first CMR scan in patients within a narrow 3-hour time window after primary percutaneous coronary intervention to be able to detect the noon of the initial wave of edema.

Controversy on the Bimodal Postinfarction Edema Occurrence in Humans

The recent demonstration of bimodal edema in the postischemic myocardium in pigs[10,11] has generated intense discussion in the cardiac imaging field.[6,22–28] Whether this phenomenon occurs in humans has been explored in 2 recent studies. Carrick and colleagues[13] performed a longitudinal assessment of IMH and edema in 30 patients with STEMI, concluding that "myocardial edema has a unimodal time course." This population was more heterogeneous than the population examined here: 20% had an open artery on angiography (TIMI coronary flow grade 2–3) and only 30% had an anterior MI, whereas all patients in our study had an anterior infarction with an occluded artery on angiography. These factors might affect edema dynamics and visualization.[11,18] In addition, patients in the Carrick et al study underwent 3 CMR examinations within the first 10 days after MI, at 8.6±3.1 hours, 2.9±1.5 days, and 9.6±2.3 days.[13] It is important to note that the first of these examinations was performed between 4 and 12 hours after reperfusion, which, according to the experimental data we present here, is after the dissipation of the first edema wave. Indeed, the T2 values in the infarcted zone reported for the first CMR examination in Carrick et al are similar to those observed in the second scan in our clinical study, performed 24 hours after MI.

In the second report, Nordlund et al[12] retrospectively analyzed pooled data from 3 studies assessing the MaR by qualitative CMR, concluding that no bimodal edema pattern was apparent. However, most patients in the evaluated studies underwent a single CMR scan at disparate times to from each other, and there were no systematic serial examinations. It is important to note that no CMR scans were performed on day 0, and very few were performed on day 1 after MI. Moreover, no quantitative parametric T2 mapping was performed, despite this technique being demonstrated to improve detection and quantification of myocardial edema.[29] Unlike these recent reports, our study was specifically designed to provide insight into the existence of bimodal edema in patients with MI by mimicking time points and CMR sequences performed in the previous experimental studies.[10,11]

Implications of the Bimodal Edema Phenomenon for Quantifying MaR and Salvage

On the basis of an assumed stable edematous reaction lasting for several days after MI and despite recent controversy,[30,31] T2-CMR sequences have been widely used to retrospectively quantify the MaR.[6,29] In the present clinical study, we show that T2 relaxation time in the ischemic region changes systematically with the post-MI timing of the examination. In parallel, we confirmed significant variation in the extent of the MaR as measured by T2W-STIR. Consistent with the drop in T2 relaxation time at 1 day post-MI, T2W-estimated MaR at this time point was significantly lower than values obtained before and subsequently.

We experimentally confirmed clinical findings by accomplishing a comprehensive CMR serial imaging study in 20 pigs subjected to reperfused MI. Remarkably, we included prereperfusion MDCT imaging as a reference for the assessment of MaR,[21] which otherwise we con-

Circulation. 2017;136:1288–1300. DOI: 10.1161/CIRCULATIONAHA.116.025582

Table 2. CMR Data of Patients

	Reperfusion Time				
	≤3 h	24 h	4 days	7 days	40 days
T2 transmural ischemic, ms	80.8 (10.9)	65.4 (5.5)	80.5 (11.3)	76.8 (12.1)	65.4 (7.2)
T2 transmural remote, ms	52.5 (6.7)	57.2 (6.2)	53.7 (6.2)	58.3 (5.9)	52.9 (8.3)
T2 infarct incl. hypointense core, ms	80.5 (16.4)	63.0 (9.0)	81.5 (15.3)	76.3 (16.6)	65.2 (8.4)
T2 infarct excl. hypointense core, ms	87.2 (15.1)	65.2 (8.8)	86.0 (16.6)	81.3 (16.9)	66.4 (7.0)
T2 salvaged, ms	70.2 (9.7)	64.4 (8.3)	78.5 (14.9)	68.9 (9.5)	62.3 (8.2)
Myocardial area at risk, % of left ventricle	39.9 (13.0)	21.8 (12.2)	42.8 (11.5)	42.9 (13.0)	20.1 (11.5)
Intramyocardial hemorrhage, % of left ventricle	0.6 (0.5)	1.1 (0.6)	1.7 (1.4)	1.7 (1.8)	0.7 (0.6)
Infarct size, % of left ventricle	–	–	–	30.3 (14.6)	21.9 (11.9)
Microvascular obstruction, % of left ventricle	–	–	–	2.7 (2.4)	0.9 (0.8)

Data are presented as mean (SD). T2 maps were analyzed by placing regions of interests at the transmural ischemic, infarcted (with or without including areas suggestive of intramyocardial hemorrhage), salvage, and transmural remote areas in a midapical ventricular short-axis slice corresponding to the same anatomic level in all acquisitions to track T2 relaxation time changes over time. The different myocardial states were initially defined by the localization relative to late gadolinium enhancement.[17] One patient died between day 4 and day 7 cardiac magnetic resonance, and 1 patient was unable to undergo late gadolinium enhancement imaging because of severe renal impairment; therefore, T2 information from the different myocardial states within the ischemic region was obtained from 14 of 16 patients.

T2 relaxation time was longer in the transmural ischemic myocardium than in the remote myocardium at all time points evaluated (≤3 hour, day 1, day 4, day 7, and day 40 after reperfusion). At the 24-hour time point, T2 values were 65.4±5.5 ms and 57.2±6.2 ms in the ischemic and remote myocardium, respectively ($P<0.01$). Similar results (even of greater magnitude) were shown when comparing T2 in the ischemic and remote myocardium at day 40 (65.4±7.2 ms versus 52.9±8.3 ms, $P<0.01$). However, T2 relaxation time in the ischemic myocardium showed significant variations across time: T2 at 24 hours was statistically shorter than at ≤3 hours (65.4±5.5 ms versus 80.8±10.9 ms, $P<0.01$), than at day 4 (65.4±5.5 ms versus 80.5±11.3 ms, $P<0.01$), and than at day 7 (65.4±5.5 ms versus 76.8±12.1 ms, $P<0.01$). In contrast, T2 in the ischemic myocardium at 24 hours did not differ from T2 at day 40 (65.4±5.5 ms versus 65.4±7.2 ms, $P=0.99$).

CMR indicates cardiac magnetic resonance.

sidered unethical to perform in patients with STEMI. In the experimental study, our results show that, because of the bimodal pattern of post-I/R edema formation, the extent of MaR delineated by T2-CMR varies during the first week after I/R. Specifically, the edema-sensitive T2W-STIR CMR sequence overestimates MaR in comparison with MDCT at early time points (120 minutes) after reperfusion, which is in agreement with previous reports.[21] This overestimate is mainly driven by swelling of the reperfused myocardium. By 24 hours, the scenario is completely altered, with a substantial resorption of edema and normalization of T2 relaxation time,[10] resulting in systematic underestimation of MaR by CMR. This underestimation resulted in biologically implausible negative myocardial salvage data at 24 hours. This finding reinforces the idea that MaR (and consequently salvaged myocardium) cannot reliably be quantified by CMR around this time point. Conversely, on days 4 and 7, CMR-measured MaR was similar to MaR measured by MDCT.

More pronounced dynamic tissue changes were shown in the experimental model. This is a common phenomenon seen in the experimental setting in which many variables are controlled, as opposed to clinical studies. In addition, the more severe ischemic process in the porcine myocardium in the presence of poor collateral circulation, among other reasons, could influence the magnification of this phenomenon. However, the parallel courses of T2 and CMR-MaR fluctuations observed in the clinical and experimental settings strengthen the message of the present study. Thus, our data suggest that between day 4 and day 7 would be a good compromise solution for the delineation of theoretical MaR.

Nevertheless, our results highlight the need for caution in interpreting CMR of the post-MI heart. In the clinical study, 3 of the 16 patients with STEMI showed more limited changes in T2 and extent of edema (see online-only Data Supplement Figures III and IV). Remarkably, these 3 patients were older and showed significantly smaller infarcts and less extent of IMH and MVO, and greater myocardial salvage areas despite having longer intervals between symptom onset to reperfusion (data not shown). We speculate that there might be several factors affecting the dynamics of the bimodal edematous reaction such as the existence of preformed collateral circulation, episodes of spontaneous reperfusion/reocclusion during ischemia duration, or the presence of specific comorbidities. The impossibility of controlling these aspects in the clinical scenario

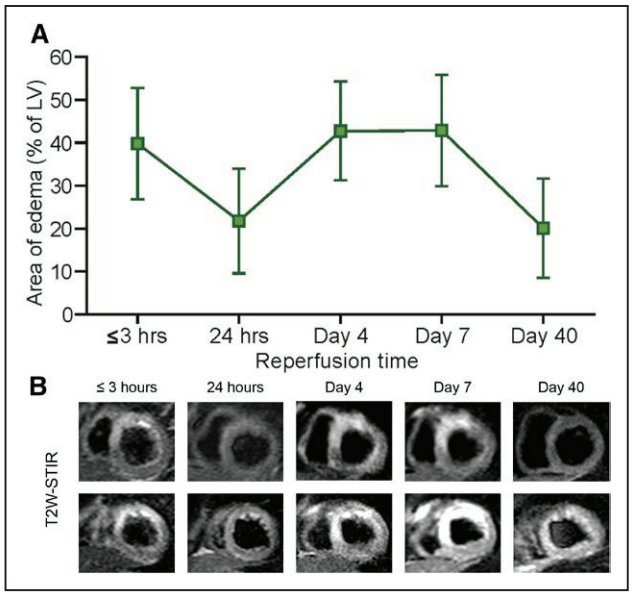

Figure 3. Time profile of edematous area in patients with ST-segment–elevation myocardial infarction. **A,** Time profile of edematous area in patients with ST-segment–elevation myocardial infarction, evaluated by T2W-STIR imaging. Data are means and SD. Cardiac magnetic resonance T2W-STIR scans at ≤3 hours and on day 4 and day 7 revealed a similar edematous area (% left ventricle); in contrast, the edematous area was significantly smaller at 24 hours and on day 40 post-MI. Note the parallel courses of T2 relaxation time fluctuations and the extent of edema by cardiac magnetic resonance. **B,** Representative contiguous short-axis images from a patient with anterior ST-segment–elevation myocardial infarction who underwent serial cardiac magnetic resonance T2W-STIR examinations at 150 minutes, 26 hours, 4 days, 7 days, and 44 days after reperfusion. LV indicates left ventricle; and T2W-STIR, T2-weighted short-tau inversion recovery.

and the limited sample size preclude any definitive conclusion in this regard, but further studies are warranted.

In comparison with T2W-STIR, parametric T2 mapping might improve the detection and quantification of myocardial edema[16]; however, it is unlikely to alter the dynamic pattern of post-MI edema that is attributable to pathophysiological phenomena. The deferred edema wave is related to the post-MI healing process,[11,32] and therefore interventions that protect the myocardium could affect the dynamics of edema, and thus bias MaR estimation. This idea is supported by recent suggestions that the extent of edema can be affected by the degree of damage[9] or exposure to infarct-limiting interventions.[33–35] However, patients in these studies received 1 CMR examination at a single time point, which was not the same for all. Therefore, a dedicated study would be needed to provide evidence to support this hypothesis.

IMH Is Not the Main Mechanism Underlying Bimodal Post-MI Edema

In the clinical study, IMH, assessed by T2W-CMR, peaked around day 4 after reperfusion. This finding is in agreement with the present experimental CMR data and histologically validated data from our previous pig study.[11] Given that T2 can be affected by hemorrhage, some authors have argued that the bimodal post-MI T2-CMR pattern could be explained entirely by the destructive paramagnetic effects of deoxyhemoglobin, rather than by a real fluctuation of tissue water content.[13,36] However, if hemorrhage was the sole explanation for the bimodal T2 pattern, it would be difficult to understand why T2 (both in the pig model[10] and in the present clinical study) and water content (in the pig model)[10] increased to day 4, coinciding with the maximum extent of hemorrhage.[11,23] In fact, in the clinical study, we observed no significant influence of IMH on T2 relaxation time or area of edema delineation. The finding that infarcted (either with or without IMH areas) and salvaged myocardium displayed the same bimodal pattern strengthen our results. In line with our data, Carrick et al[13] found small differences in T2 (<5 ms) between patients with and without hemorrhage, whereas

Table 3. Time Profile of CMR-Assessed Myocardium at Risk, Infarct Size, and Myocardial Salvage During the First Week After Reperfused Myocardial Infarction in Pigs

CMR	Follow-Up			
	120 min After Reperfusion (n=20)	24 h After Reperfusion (n=15)	Day 4 After Reperfusion(n=10)	Day 7 After Reperfusion(n=5)
MaR, % of left ventricle	48.1 (6.0)	3.6 (2.8)	30.2 (6.2)	30.1 (2.3)
Infarct size, % of left ventricle	45.1 (5.3)	35.3 (5.2)	30.2 (4.3)	25.4 (4.0)
Myocardial salvage, %	4.7 (4.7)	–1285 (858)	–2.5 (20.3)	15.7 (13.3)

Data are presented as mean (SD). CMR data for each time point correspond to pooled data from all animals undergoing 40 minutes ischemia/reperfusion. n values decrease over time because 5 pigs were euthanized after each CMR examination for histological measurement of water content.[10] The extent of myocardium at risk was assessed by MDCT reference during coronary occlusion in all animals (MDCT-MaR). MDCT-MaR as assessed during the index coronary occlusion was 30.5±5.0%, 29.6±4.7%, 29.1±3.9%, and 28.3±4.3% of left ventricle; for pigs followed up to 120 minutes (n=20), 24 hours (n=15), 4 days (n=10), and 7 days (n=5) after reperfusion. Myocardial salvage as assessed by MDCT/CMR [(MDCT MaR – CMR Infarct Size) / MDCT MaR, %] in each of these groups was –50.6±24.4% at 120 minutes, –20.4±16.9% at 24 hours, –4.8±17.1% at 4 days, and 9.1±19.9% at 7 days after reperfusion, respectively. Note that MDCT was performed in all pigs only once (during the index ischemic event). Online-only Data Supplement Table III shows all individual data from animals euthanized at each time point.

CMR indicates cardiac magnetic resonance; MaR, myocardium at risk; and MDCT, multidetector computed tomography.

Circulation. 2017;136:1288–1300. DOI: 10.1161/CIRCULATIONAHA.116.025582

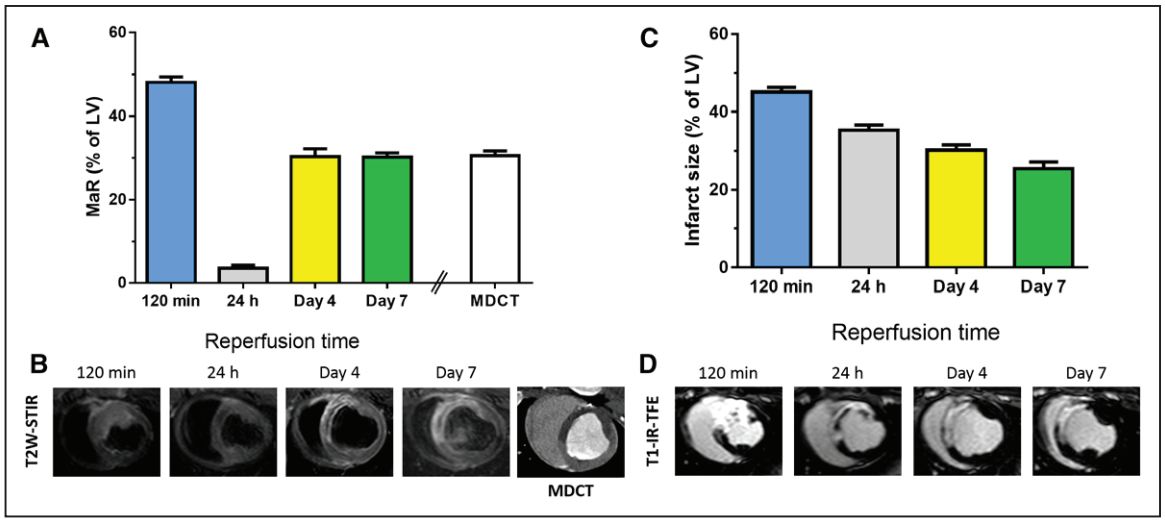

Figure 4. Temporal evolution of cardiac magnetic resonance-myocardium at risk and infarct size after reperfused myocardial infarction in the pig model.
Time profile of myocardium at risk evaluated by T2-weighted short-tau inversion recovery imaging (**A**) and infarct size evaluated by T1-weighted inversion recovery turbo-field echo in pigs subjected to 40 minutes inversion-recovery (**C**). Arterial enhanced multidetector computed tomography was performed during coronary occlusion in all pigs as a reference standard measure of myocardium at risk. Data are shown as mean±standard error of the mean. **B** and **D,** Representative images from a pig that underwent multidetector computed tomography during coronary occlusion followed by serial T2-weighted short-tau inversion recovery (**B**) and late gadolinium enhancement (**D**) examinations at 120 minutes, 24 hours, 4 days, and 7 days after reperfusion. LV indicates left ventricle; MaR, myocardium at risk; MDCT, multidetector computed tomography; T1-IR-TFE, T1-weighted inversion recovery turbo-field echo; and T2W-STIR, T2-weighted short-tau inversion recovery.

Hammer-Hansen et al[17] found that T2 relaxation time differed in the infarcted and salvaged myocardium, and both were significantly longer than remote in the postreperfused dog heart. It is interesting to note that the later study followed animals at 4 and 48 hours after MI with results indicating a partial resolution of edema in the first 48 hours after reperfusion.[17,26] Nevertheless, hemorrhage might exert some influence on T2 relaxation time, as we previously conceded.[10,11,16,23,24]

Dynamics of Infarct Size Over the First Week After MI

Consistent with previous observations,[3,37,38] our experimental data show a progressive decrease of CMR-based IS. The substantial swelling of the early postreperfused myocardium might explain the large IS detected in our experimental study 120 minutes after reperfusion. The early period after reperfusion is associated with significant transient expansion of extracellular volume[11,38]; gadolinium gets trapped in this expanded extracellular volume, but when extracellular volume recedes, gadolinium no longer stays in this area. In this interpretation, acutely detected LGE does not necessarily equate to irreversible injury and may severely distort estimates of salvaged myocardium. These data highlight the importance of performing CMR infarct imaging within a consistently defined and narrow time frame, preferably at the end of the first week, when using IS as an end point in clinical trials during the acute post-MI period.

Chronotherapeutic Approaches

New treatments demonstrating significant promise in preclinical experiments frequently produce no benefits in clinical trials,[1,39] and the present results hint that timing of intervention might be a key determinant of this mismatch.[40–43] We believe the discovery of the bimodal nature of post-MI edema will help in the design and new therapies for reducing infarct size and post-MI LV dysfunction.

In summary, we present the first demonstration that myocardial edema after MI is not stable in patients but instead follows a bimodal pattern, confirming recent experimental findings in pigs. The identification of such a pattern has important biological, diagnostic, prognostic, and therapeutic implications, and opens a route to further exploration of factors influencing this phenomenon. Remarkably, this bimodal edematous response after MI has a major impact on CMR-MaR, and consequently, myocardial salvage quantification given that measures of edema are greatly influenced by the timing of post-MI imaging.

LIMITATIONS

Only patients with anterior STEMI were recruited to the clinical study. The reasons for this choice include the

avoidance of possible magnetic-field nonhomogeneity related to the inferolateral wall.[4,29] These eligibility criteria closely resemble recommendations for patient selection in clinical trials of cardioprotective interventions.[39,44] The bimodal edema pattern may occur regardless of MI location; however, caution should be exercised when extrapolating results to other MI locations, especially regarding adequate visualization of the phenomenon by T2W-CMR in lateral MI where signal loss attributable to through-plane cardiac motion might occur.[18] Given that patients were serially scanned, including 1 examination very early after reperfusion, we planned the shortest CMR protocol possible. For this reason we did not include T2* CMR as a diagnostic method for quantifying IMH in vivo.[29] Instead, we assessed both edema and hemorrhage by T2W-STIR imaging, a sequence validated and used for these purposes by many authors.[19]

Extrapolation of the experimental results to the clinic should be done with caution. Nonetheless, the pig is one of the most clinically translatable large-animal models for the study of reperfused MI.[45] The similar edema and hemorrhage time courses in the pig and the patient cohort highlight the great translational value of the pig model, especially considering the difficulty of performing a comprehensive CMR study that includes serial examinations within the first hours after reperfusion and reference techniques for the assessment of the MaR. The fact that myocardial edema and LGE follow a disparate dynamic pattern after ischemia/reperfusion highlights the complexity of measuring myocardial salvage in real practice. Thus, acutely detected LGE does not necessarily equate to irreversible injury and may contribute to severely distorted estimates of salvaged myocardium when comparing against a prereperfusion standard to assess MaR.[38] Other reasons might contribute to inaccurate estimations. Among them, it has been previously demonstrated that damage after ischemia/reperfusion may extend beyond the boundaries of the hypoperfused region during coronary occlusion[21]; that MaR might slightly shrink in MDCT performed during coronary occlusion because of a lack of perfusion in animal models with poor collateral circulation; and that residual edema in salvaged myocardium might contribute to the overestimation of infarct size early after reperfusion.[38]

Last, it is fair to acknowledge that although previous studies have validated the use of MDCT to measure MaR,[21,46] there is probably no perfect method for such purpose, because there is no consensus on a standardized method for the identification of MaR on T2W-CMR imaging.[47] Underestimation of the maximum intensity at time points exhibiting shorter myocardial T2, ie, 24 hours and day 40, could potentially bias results in the case of the full width at half-maximum method. However, we believe the region of interest selection as initial thresholding for the full width at half-maximum method did not have a significant impact on our results for several reasons. First, the blinded analysis included manual correction and visual border delineation after initial thresholding. Second, the hemorrhagic area was larger at day 4 and day 7 coinciding with the largest edematous area delineated. Third, the demonstration of a similar bimodal edema pattern by the use of a quantitative and more objective method, ie, T2 mapping, both in the human and pig myocardium strongly supports our findings here reported.

CONCLUSIONS

Contrary to the accepted view, the post-MI edematous reaction in patients is not stable, but follows a bimodal pattern. The initial edema wave appears early on reperfusion and dissipates by 24 hours. The deferred edema wave emerges thereafter and reaches a plateau lasting from approximately day 4 to day 7 postreperfusion. Consequently, the MaR as measured by T2W-CMR changes dynamically according to timing of the CMR examination. Timing of CMR after MI for assessing MaR and salvaged myocardium needs to be standardized. According to the data presented, a time frame between day 4 and day 7 after reperfusion seems a good compromise solution although some other factors might affect these variables.

ACKNOWLEDGMENTS

The authors are greatly indebted to G. J. Lopez-Martin and Mª J. García-Sánchez for image acquisition in pigs and patient recruitment, respectively, and to the Cardiology Department at Hospital Universitario de Salamanca for patient recruitment and care. The authors thank T. Córdoba, O. Sanz, E. Fernández, and other members of the CNIC animal facility and farm for outstanding animal care and support. S. Bartlett (CNIC) provided English editing.

SOURCES OF FUNDING

This study was partially supported by a competitive grant from the Spanish Society of Cardiology (Proyectos de Investigación Traslacional en Cardiología de la Sociedad Española de Cardiología 2015, for the project Caracterización tiSUlar miocáRdica con resonancia magnética en pacientes tras inFarto agudo de mioCardio con elevacióN de ST sometidos a angIoplastia Coronaria primaria. Estudio SURF-CNIC), by a competitive grant from the Carlos III Institute of Health-Fondo de Investigacion Sanitaria- and the European Regional Development Fund (ERDF/FEDER) (PI10/02268 and PI13/01979), the Spanish Ministry of economy, industry, and competitiveness (MEIC) and ERDF/FEDER SAF2013-49663-EXP. Dr Fernández-Jiménez holds a FICNIC fellowship from the Fundació Jesús Serra, the Fundación Interhospitalaria de Investigación Cardiovascular, and the Centro Nacional de Investigaciones Cardiovasculares Carlos III (CNIC), and Dr Agüero is a FP7-PEOPLE-2013-ITN-

Cardionext fellow. This study forms part of a Master Research Agreement between the CNIC and Philips Healthcare, and is part of a bilateral research program between Hospital de Salamanca Cardiology Department and the CNIC. This research program is part of an institutional agreement between FIIS-Fundación Jiménez Díaz and CNIC. The CNIC is supported by the MEIC and the Pro CNIC Foundation, and is a Severo Ochoa Center of Excellence (MEIC award SEV-2015-0505).

DISCLOSURES

Dr Sánchez-González is a Philips Healthcare employee. The other authors declare no conflict of interest.

AFFILIATIONS

From Centro Nacional de Investigaciones Cardiovasculares Carlos III (CNIC), Madrid, Spain (R.F.-J., J.A., C.G.-A., J.G.-P., J.S., V.F., B.I.); CIBER de Enfermedades Cardiovasculares (CIBERCV), Madrid, Spain (R.F.-J., M.B.-P., A.M.-G., J.A., C.G.-A., J.G.-P., B.G., P.L.S., B.I.); The Zena and Michael A. Wiener CVI, Icahn School of Medicine at Mount Sinai, New York (R.F.-J., J.S., V.F.); Hospital Universitario de Salamanca, Spain (M.B.-P., A.M.-G., E.D.-P., P.V., I.M., I.Z., B.G., P.L.S.); Philips Healthcare, Madrid, Spain (J.S.-G.); Cardiology Department, Hospital Universitari i Politecnic La Fe, Valencia, Spain (J.A.); and IIS-Fundación Jiménez Díaz Hospital, Madrid, Spain (B.I.).

FOOTNOTES

Received September 30, 2016; accepted June 26, 2017.

The online-only Data Supplement is available with this article at http://circ.ahajournals.org/lookup/suppl/doi:10.1161/CIRCULATIONAHA.116.025582/-/DC1.

Circulation is available at http://circ.ahajournals.org.

REFERENCES

1. Ibáñez B, Heusch G, Ovize M, Van de Werf F. Evolving therapies for myocardial ischemia/reperfusion injury. *J Am Coll Cardiol*. 2015;65:1454–1471. doi: 10.1016/j.jacc.2015.02.032.
2. Carlsson M, Ubachs JF, Hedström E, Heiberg E, Jovinge S, Arheden H. Myocardium at risk after acute infarction in humans on cardiac magnetic resonance: quantitative assessment during follow-up and validation with single-photon emission computed tomography. *JACC Cardiovasc Imaging*. 2009;2:569–576. doi: 10.1016/j.jcmg.2008.11.018.
3. Dall'Armellina E, Karia N, Lindsay AC, Karamitsos TD, Ferreira V, Robson MD, Kellman P, Francis JM, Forfar C, Prendergast BD, Banning AP, Channon KM, Kharbanda RK, Neubauer S, Choudhury RP. Dynamic changes of edema and late gadolinium enhancement after acute myocardial infarction and their relationship to functional recovery and salvage index. *Circ Cardiovasc Imaging*. 2011;4:228–236. doi: 10.1161/CIRCIMAGING.111.963421.
4. Friedrich MG, Kim HW, Kim RJ. T2-weighted imaging to assess post-infarct myocardium at risk. *JACC Cardiovasc Imaging*. 2011;4:1014–1021. doi: 10.1016/j.jcmg.2011.07.005.
5. Aletras AH, Tilak GS, Natanzon A, Hsu LY, Gonzalez FM, Hoyt RF Jr, Arai AE. Retrospective determination of the area at risk for reperfused acute myocardial infarction with T2-weighted cardiac magnetic resonance imaging: histopathological and displacement encoding with stimulated echoes (DENSE) functional validations. *Circulation*. 2006;113:1865–1870. doi: 10.1161/CIRCULATIONAHA.105.576025.
6. Heusch P, Nensa F, Heusch G. Is MRI really the gold standard for the quantification of salvage from myocardial infarction? *Circ Res*. 2015;117:222–224. doi: 10.1161/CIRCRESAHA.117.306929.
7. Friedrich MG, Abdel-Aty H, Taylor A, Schulz-Menger J, Messroghli D, Dietz R. The salvaged area at risk in reperfused acute myocardial infarction as visualized by cardiovascular magnetic resonance. *J Am Coll Cardiol*. 2008;51:1581–1587. doi: 10.1016/j.jacc.2008.01.019.
8. Engblom H, Heiberg E, Erlinge D, Jensen SE, Nordrehaug JE, Dubois-Randé JL, Halvorsen S, Hoffmann P, Koul S, Carlsson M, Atar D, Arheden H. Sample size in clinical cardioprotection trials using myocardial salvage index, infarct size, or biochemical markers as endpoint. *J Am Heart Assoc*. 2016;5:e002708. doi: 10.1161/JAHA.115.002708.
9. Kim HW, Van Assche L, Jennings RB, Wince WB, Jensen CJ, Rehwald WG, Wendell DC, Bhatti L, Spatz DM, Parker MA, Jenista ER, Klem I, Crowley AL, Chen EL, Judd RM, Kim RJ. Relationship of T2-weighted MRI myocardial hyperintensity and the ischemic area-at-risk. *Circ Res*. 2015;117:254–265. doi: 10.1161/CIRCRESAHA.117.305771.
10. Fernández-Jiménez R, Sánchez-González J, Agüero J, García-Prieto J, López-Martín GJ, García-Ruiz JM, Molina-Iracheta A, Rosselló X, Fernández-Friera L, Pizarro G, García-Álvarez A, Dall'Armellina E, Macaya C, Choudhury RP, Fuster V, Ibáñez B. Myocardial edema after ischemia/reperfusion is not stable and follows a bimodal pattern: imaging and histological tissue characterization. *J Am Coll Cardiol*. 2015;65:315–323. doi: 10.1016/j.jacc.2014.11.004.
11. Fernández-Jiménez R, García-Prieto J, Sánchez-González J, Agüero J, López-Martín GJ, Galán-Arriola C, Molina-Iracheta A, Doohan R, Fuster V, Ibáñez B. Pathophysiology underlying the bimodal edema phenomenon after myocardial ischemia/reperfusion. *J Am Coll Cardiol*. 2015;66:816–828. doi: 10.1016/j.jacc.2015.06.023.
12. Nordlund D, Klug G, Heiberg E, Koul S, Larsen TH, Hoffmann P, Metzler B, Erlinge D, Atar D, Aletras AH, Carlsson M, Engblom H, Arheden H. Multi-vendor, multicentre comparison of contrast-enhanced SSFP and T2-STIR CMR for determining myocardium at risk in ST-elevation myocardial infarction. *Eur Heart J Cardiovasc Imaging*. 2016;17:744–753. doi: 10.1093/ehjci/jew027.
13. Carrick D, Haig C, Ahmed N, Rauhalammi S, Clerfond G, Carberry J, Mordi I, McEntegart M, Petrie MC, Eteiba H, Hood S, Watkins S, Lindsay MM, Mahrous A, Welsh P, Sattar N, Ford I, Oldroyd KG, Radjenovic A, Berry C. Temporal evolution of myocardial hemorrhage and edema in patients after acute ST-segment elevation myocardial infarction: pathophysiological insights and clinical implications. *J Am Heart Assoc*. 2016;5:e002834.
14. O'Gara PT, Kushner FG, Ascheim DD, Casey Jr DE, Chung MK, de Lemos JA, Ettinger SM, Fang JC, Fesmire FM, Franklin BA, Granger CB, Krumholz HM, Linderbaum JA, Morrow DA, Newby LK, Ornato JP, Ou N, Radford MJ, Tamis-Holland JE, Tommaso CL, Tracy CM, Woo YJ, Zhao DX. 2013 ACCF/AHA guideline for the management of ST-elevation myocardial infarction: a report of the American College of Cardiology Foundation/American Heart Association Task Force on Practice Guidelines. *Circulation*. 2013;127:e362–e425. doi: 10.1161/CIR.0b013e3182742cf6.
15. Steg PG, James SK, Atar D, Badano LP, Lundqvist CB, Borger MA, Di Mario C, Dickstein K, Ducrocq G, Fernandez-Aviles F, Gershlick AH, Giannuzzi P, Halvorsen S, Huber K, Juni P, Kastrati A, Knuuti J, Lenzen MJ, Mahaffey KW, Valgimigli M, van't Hof A, Widimsky P, Zahger D, Bax JJ, Baumgartner H, Ceconi C, Dean V, Deaton C, Fagard R, Funck-Brentano C, Hasdai D, Hoes A, Kirchhof P, Knuuti J, Kolh P, McDonagh T, Moulin C, Popescu BA, Reiner Ž, Sechtem U, Sirnes PA, Tendera M, Torbicki A, Vahanian A, Windecker S, Hasdai D, Astin F, Åström-Olsson K, Budaj A, Clemmensen P, Collet J-P, Fox KA, Fuat A, Gustiene O, Hamm CW, Kala P, Lancellotti P, Maggioni AP, Merkely B, Neumann F-J, Piepoli MF, Van de Werf F, Verheugt F, Wallentin L. ESC Guidelines for the management of acute myocardial infarction in patients presenting with ST-segment elevation. *Eur Heart J*. 2012;33:2569–2619.
16. Fernández-Jiménez R, Sánchez-González J, Aguero J, Del Trigo M, Galán-Arriola C, Fuster V, Ibáñez B. Fast T2 gradient-spin-echo (T2-GraSE) mapping for myocardial edema quantification: first *in vivo* validation in a porcine model of ischemia/reperfusion. *J Cardiovasc Magn Reson*. 2015;17:92. doi: 10.1186/s12968-015-0199-9.
17. Hammer-Hansen S, Ugander M, Hsu LY, Taylor J, Thune JJ, Køber L, Kellman P, Arai AE. Distinction of salvaged and infarcted myocardium within the ischaemic area-at-risk with T2 mapping. *Eur Heart J Cardiovasc Imaging*. 2014;15:1048–1053. doi: 10.1093/ehjci/jeu073.
18. Fernández-Friera L, García-Ruiz JM, García-Álvarez A, Fernández-Jiménez R, Sánchez-González J, Rossello X, Gómez-Talavera S, López-Martín GJ, Pizarro G, Fuster V, Ibáñez B. Accuracy of area at risk quantification by

cardiac magnetic resonance according to the myocardial infarction territory. *Rev Esp Cardiol (Engl Ed)*. 2017;70:323–330. doi: 10.1016/j.rec.2016.07.004.
19. Robbers LF, Eerenberg ES, Teunissen PF, Jansen MF, Hollander MR, Horrevoets AJ, Knaapen P, Nijveldt R, Heymans MW, Levi MM, van Rossum AC, Niessen HW, Marcu CB, Beek AM, van Royen N. Magnetic resonance imaging-defined areas of microvascular obstruction after acute myocardial infarction represent microvascular destruction and haemorrhage. *Eur Heart J*. 2013;34:2346–2353. doi: 10.1093/eurheartj/eht100.
20. Valle-Caballero MJ, Fernández-Jiménez R, Díaz-Munoz R, Mateos A, Rodríguez-Álvarez M, Iglesias-Vázquez JA, Saborido C, Navarro C, Dominguez ML, Gorjón L, Fontoira JC, Fuster V, García-Rubira JC, Ibanez B. QRS distortion in pre-reperfusion electrocardiogram is a bedside predictor of large myocardium at risk and infarct size (a METOCARD-CNIC trial substudy). *Int J Cardiol*. 2016;202:666–673. doi: 10.1016/j.ijcard.2015.09.117.
21. Mewton N, Rapacchi S, Augeul L, Ferrera R, Loufouat J, Boussel L, Micolich A, Rioufol G, Revel D, Ovize M, Croisille P. Determination of the myocardial area at risk with pre- versus post-reperfusion imaging techniques in the pig model. *Basic Res Cardiol*. 2011;106:1247–1257. doi: 10.1007/s00395-011-0214-8.
22. Fernández-Jiménez R, Fuster V, Ibáñez B. Reply: myocardial salvage, area at risk by T2w CMR: the resolution of the retrospective radio wave paradigm? *J Am Coll Cardiol*. 2015;65:2358–2359. doi: 10.1016/j.jacc.2015.02.071.
23. Fernández-Jiménez R, Fuster V, Ibanez B. Reply: "waves of edema" seem implausible. *J Am Coll Cardiol*. 2016;67:1869–1870. doi: 10.1016/j.jacc.2016.01.052.
24. Fernández-Jiménez R, Fuster V, Ibáñez B. Reply: myocardial edema should be stratified according to the state of cardiomyocytes within the ischemic region. *J Am Coll Cardiol*. 2015;65:2356–2357. doi: 10.1016/j.jacc.2015.02.070.
25. Arai AE. Healing after myocardial infarction: a loosely defined process. *JACC Cardiovasc Imaging*. 2015;8:680–683. doi: 10.1016/j.jcmg.2015.02.012.
26. Arai AE. Area at risk in acute myocardial infarction: oedema imaging and species-specific findings. *Eur Heart J Cardiovasc Imaging*. 2016;17:754–755. doi: 10.1093/ehjci/jew074.
27. Dharmakumar R. Building a unified mechanistic insight into the bimodal pattern of edema in reperfused acute myocardial infarctions: observations, interpretations, and outlook. *J Am Coll Cardiol*. 2015;66:829–831. doi: 10.1016/j.jacc.2015.05.074.
28. Kloner RA. New observations regarding post-ischemia/reperfusion myocardial swelling. *J Am Coll Cardiol*. 2015;65:324–326. doi: 10.1016/j.jacc.2014.11.006.
29. Salerno M, Kramer CM. Advances in parametric mapping with CMR imaging. *JACC Cardiovasc Imaging*. 2013;6:806–822. doi: 10.1016/j.jcmg.2013.05.005.
30. Arai AE, Leung S, Kellman P. Controversies in cardiovascular MR imaging: reasons why imaging myocardial T2 has clinical and pathophysiologic value in acute myocardial infarction. *Radiology*. 2012;265:23–32. doi: 10.1148/radiol.12112491.
31. Croisille P, Kim HW, Kim RJ. Controversies in cardiovascular MR imaging: T2-weighted imaging should not be used to delineate the area at risk in ischemic myocardial injury. *Radiology*. 2012;265:12–22. doi: 10.1148/radiol.12111769.
32. Samouillan V, Revuelta-López E, Soler-Botija C, Dandurand J, Benitez-Amaro A, Nasarre L, de Gonzalo-Calvo D, Bayes-Genis A, Lacabanne C, Llorente-Cortés V. Conformational and thermal characterization of left ventricle remodeling post-myocardial infarction. *Biochim Biophys Acta*. 2017;1863:1500–1509. doi: 10.1016/j.bbadis.2017.02.025.
33. Crimi G, Pica S, Raineri C, Bramucci E, De Ferrari GM, Klersy C, Ferlini M, Marinoni B, Repetto A, Romeo M, Rosti V, Massa M, Raisaro A, Leonardi S, Rubartelli P, Oltrona Visconti L, Ferrario M. Remote ischemic post-conditioning of the lower limb during primary percutaneous coronary intervention safely reduces enzymatic infarct size in anterior myocardial infarction: a randomized controlled trial. *JACC Cardiovasc Interv*. 2013;6:1055–1063. doi: 10.1016/j.jcin.2013.05.011.
34. Thuny F, Lairez O, Roubille F, Mewton N, Rioufol G, Sportouch C, Sanchez I, Bergerot C, Thibault H, Cung TT, Finet G, Argaud L, Revel D, Derumeaux G, Bonnefoy-Cudraz E, Elbaz M, Piot C, Ovize M, Croisille P. Post-conditioning reduces infarct size and edema in patients with ST-segment elevation myocardial infarction. *J Am Coll Cardiol*. 2012;59:2175–2181. doi: 10.1016/j.jacc.2012.03.026.
35. White SK, Frohlich GM, Sado DM, Maestrini V, Fontana M, Treibel TA, Tehrani S, Flett AS, Meier P, Ariti C, Davies JR, Moon JC, Yellon DM, Hausenloy DJ. Remote ischemic conditioning reduces myocardial infarct size and edema in patients with ST-segment elevation myocardial infarction. *JACC Cardiovasc Interv*. 2015;8(1 pt B):178–188. doi: 10.1016/j.jcin.2014.05.015.
36. Berry C, Carrick D, Haig C, Oldroyd KG. "Waves of edema" seem implausible. *J Am Coll Cardiol*. 2016;67:1868–1869. doi: 10.1016/j.jacc.2015.11.073.
37. Ibrahim T, Hackl T, Nekolla SG, Breuer M, Feldmair M, Schömig A, Schwaiger M. Acute myocardial infarction: serial cardiac MR imaging shows a decrease in delayed enhancement of the myocardium during the 1st week after reperfusion. *Radiology*. 2010;254:88–97. doi: 10.1148/radiol.09090660.
38. Jablonowski R, Engblom H, Kanski M, Nordlund D, Koul S, van der Pals J, Englund E, Heiberg E, Erlinge D, Carlsson M, Arheden H. Contrast-Enhanced CMR overestimates early myocardial infarct size: mechanistic insights using ECV measurements on day 1 and day 7. *JACC Cardiovasc Imaging*. 2015;8:1379–1389. doi: 10.1016/j.jcmg.2015.08.015.
39. Hausenloy DJ, Botker HE, Engstrom T, Erlinge D, Heusch G, Ibanez B, Kloner RA, Ovize M, Yellon DM, Garcia-Dorado D. Targeting reperfusion injury in patients with ST-segment elevation myocardial infarction: trials and tribulations. *Eur Heart J*. 2017;38:935–941. doi: 10.1093/eurheartj/ehw145.
40. García-Ruiz JM, Fernández-Jiménez R, García-Alvarez A, Pizarro G, Galán-Arriola C, Fernández-Friera L, Mateos A, Nuno-Ayala M, Aguero J, Sánchez-González J, García-Prieto J, López-Melgar B, Martínez-Tenorio P, López-Martín GJ, Macías A, Pérez-Asenjo B, Cabrera JA, Fernández-Ortiz A, Fuster V, Ibáñez B. Impact of the timing of metoprolol administration during STEMI on infarct size and ventricular function. *J Am Coll Cardiol*. 2016;67:2093–2104. doi: 10.1016/j.jacc.2016.02.050.
41. Pryds K, Terkelsen CJ, Sloth AD, Munk K, Nielsen SS, Schmidt MR, Bøtker HE; CONDI Investigators. Remote ischaemic conditioning and healthcare system delay in patients with ST-segment elevation myocardial infarction. *Heart*. 2016;102:1023–1028. doi: 10.1136/heartjnl-2015-308980.
42. Roubille F, Mewton N, Elbaz M, Roth O, Prunier F, Cung TT, Piot C, Roncalli J, Rioufol G, Bonnefoy-Cudraz E, Wiedemann JY, Furber A, Jacquemin L, Willoteaux S, Abi-Khallil W, Sanchez I, Finet G, Sibellas F, Ranc S, Boussaha I, Croisille P, Ovize M. No post-conditioning in the human heart with thrombolysis in myocardial infarction flow 2-3 on admission. *Eur Heart J*. 2014;35:1675–1682. doi: 10.1093/eurheartj/ehu054.
43. Liu B, Duan CY, Luo CF, Ou CW, Wu ZY, Zhang JW, Ni XB, Chen PY, Chen MS. Impact of timing following acute myocardial infarction on efficacy and safety of bone marrow stem cells therapy: a network meta-analysis. *Stem Cells Int*. 2016;2016:1031794. doi: 10.1155/2016/1031794.
44. Bell RM, Bøtker HE, Carr RD, Davidson SM, Downey JM, Dutka DP, Heusch G, Ibanez B, Macallister R, Stoppe C, Ovize M, Redington A, Walker JM, Yellon DM. 9th Hatter Biannual Meeting: position document on ischaemia/reperfusion injury, conditioning and the ten commandments of cardioprotection. *Basic Res Cardiol*. 2016;111:41. doi: 10.1007/s00395-016-0558-1.
45. Fernández-Jiménez R, Fernández-Friera L, Sánchez-González J, Ibáñez B. Animal models of tissue characterization of area at risk, edema and fibrosis. *Curr Cardiovasc Imaging Rep*. 2014;7:1–10.
46. van der Pals J, Hammer-Hansen S, Nielles-Vallespin S, Kellman P, Taylor J, Kozlov S, Hsu LY, Chen MY, Arai AE. Temporal and spatial characteristics of the area at risk investigated using computed tomography and T1-weighted magnetic resonance imaging. *Eur Heart J Cardiovasc Imaging*. 2015;16:1232–1240. doi: 10.1093/ehjci/jev072.
47. McAlindon E, Pufulete M, Lawton C, Angelini GD, Bucciarelli-Ducci C. Quantification of infarct size and myocardium at risk: evaluation of different techniques and its implications. *Eur Heart J Cardiovasc Imaging*. 2015;16:738–746. doi: 10.1093/ehjci/jev001.

SUPPLEMENTAL MATERIAL

SUPPLEMENTAL METHODS

Clinical study

Design

Hemodynamically stable consecutive patients with a first anterior ST-segment-elevation acute myocardial infarction (STEMI) and undergoing primary percutaneous coronary intervention (PCI) were prospectively recruited between February 2015 and November 2015. Patients eligible for enrollment were aged 18 years or older, and showed symptoms consistent with STEMI for >90 minutes and ST-segment elevation ≥2 mm in ≥2 contiguous leads in V1 through V5, with an anticipated time of symptom onset to reperfusion of ≤8 hours. Additional compulsory inclusion criteria were evidence of complete occlusion in the proximal or mid portion of the LAD coronary artery (TIMI 0-1 initial flow) and successful primary angioplasty evidenced by appropriate reestablishment of coronary flow in the culprit artery (TIMI-3 flow after angioplasty). Exclusion criteria were Killip class III to IV, persistent systolic blood pressure <100 mmHg, persistent heart rate <50 bpm or >110 bpm, presence of bifascicular or trifascicular block, evidence of second- or third-degree atrioventricular block, atrial fibrillation, known history of previous MI, pregnancy, active breastfeeding, and the presence of metallic objects or devices incompatible with MR imaging. Patients were managed according to current clinical guidelines.[1, 2]

CMR exams were performed within 3 hours of reperfusion (hyperacute reperfusion) and at 24 hours, 4 days, 7 days, and 40 days after reperfusion. Baseline myocardial T2 relaxation time was measured in 16 healthy age- and sex-matched volunteers. The study was approved by the hospital Ethics Committee, and patients and volunteers gave written informed consent.

CMR protocol

CMR examinations were conducted with a Philips 1.5-Tesla Achieva whole-body scanner (Philips Healthcare, Best, the Netherlands) equipped with a 16-element phased-array cardiac coil. At all time-points, the imaging protocol included a standard segmented cine steady-state free-precession (SSFP) sequence to provide high-quality anatomical references; a T2-weighted short-tau triple inversion-recovery (T2W-STIR) sequence to assess the extent of edema and intramyocardial hemorrhage (IMH); and a T2-gradient-spin-echo mapping (T2-GraSE map) sequence to provide precise myocardial T2 relaxation time properties.[3] On day-7 and day-40 CMR, late gadolinium enhancement (LGE) imaging was performed to assess infarct size (IS) and microvascular obstruction (MVO), using a T1-weighted inversion recovery turbo field echo (T1-IR-TFE) sequence acquired 10 to 15 minutes after intravenous administration of 0.20 mmol gadobutrol contrast agent per kg body weight (Gadovist, Bayer HealthCare Pharmaceuticals). All sequences were acquired during expiration breath-hold mode.

The imaging parameters for the SSFP sequence were a FOV of 342 x 342 mm, a slice thickness of 8 mm with no gap, TR 3.0 ms, TE 1.5 ms, flip angle 60°, cardiac phases 30, voxel size 2.0 x 2.0 mm^2, and 1 NEX. The imaging parameters for the T2W-STIR sequence were FOV 320 x 320, slice thickness 10 mm, TR 2 heartbeats, TE 85 ms, voxel size 1.9 x 2.4 mm^2, delay 160 ms, end-diastolic acquisition, echo-train length 28, and 2 NEX. The imaging parameters for the T2-GraSE mapping were FOV 320 x 320 with an acquisition voxel size of 2.0 x 2.5 mm^2 and slice thickness 8 mm, TR 2 heartbeats, and eight echo times ranging from 23 to 194 ms, EPI factor 7. No registration algorithm was used before T2 maps estimation; however the presence of motion artifacts between different TE for every analyzed T2 map was specifically checked. To minimize motion artefact, the breath-hold per slice in the T2-GraSE sequence was less than 10 seconds to enable proper patient breath-hold during the acquisition at every time point, including the within 3 hours post-reperfusion exam. The imaging parameters for T1-IR-TFE were as follows: FOV 265 x 265, slice thickness 10 mm with no gap, TR 8.1 ms, TE 4.0 ms, flip angle 20°, voxel size 1.8 x 2.1 mm^2, inversion time 250 to 350 (optimized to null normal myocardium), TFE factor 18, averages 1.

SSFP, T2W-STIR and T1-IR-TFE sequences were performed to acquire 8-11 contiguous short axis slices covering the heart from the base to the apex, whereas T2-maps were analyzed in a mid-apical ventricular short axis slice corresponding to the same anatomical level in all acquisitions, in order to track T2 relaxation time changes over time.

CMR analysis

CMR images were analyzed using dedicated softwares (MR Extended Work Space 2.6, Philips Healthcare, The Netherlands; and QMassMR 7.6, Medis, Leiden, The Netherlands) by two observers experienced in CMR analysis and blinded to time-point allocation and patient identification.

T2-maps were automatically generated on the acquisition scanner by fitting the signal intensity of all echo times to a monoexponential decay curve at each pixel with a maximum likelihood expectation maximization algorithm. The different myocardial states were initially defined by the localization relative to LGE defined infarction.[4] Regions of interest (ROI) were manually drawn at the transmural ischemic, infarcted (with or without including areas suggestive of IMH), salvage and transmural remote areas; and then copied to the corresponding areas of the individual T2 maps. Care was taken to include the entire wall thickness and were individually adjusted by hand to avoid the ventricular cavities or image artefacts.

The extent of edema, expressed as a percentage of LV mass (CMR-MaR), was defined after manually tracing the endocardial and epicardial contours of T2W-STIR short-axis images. Abnormal areas were initially identified using the full-width at half-maximum (FWHM) method.[5, 6] Given that the solely use of FWHM may be prompt to patchy inaccurate estimations,[7, 8] extensive manual correction and visual border delineation were performed. Extreme care was taken to avoid including any artificially high signal intensity due to inadequately suppressed slow flow within the cavity space. Hypointense areas within the edematous zone, corresponding to IMH, were included within the edematous region.[9, 10] Additionally, the size of IMH area was calculated by manual delineation of the hypointense areas on T2W-images[9] and expressed as a percentage of

LV mass. Manual delineation of clear hypointense areas was permitted in the absence of discernible hyperintense myocardium.

IS, expressed as a percentage of LV mass, was defined according the extent of late gadolinium enhancement after manually tracing the endocardial and epicardial contours on T1-IR-TFE short axis images. Abnormal areas were defined using the FWHM, with manual correction if needed. Hypointense black areas within the necrotic zone, corresponding to MVO, were included within the necrotic area.[9, 10] Additionally, the size of the MVO area was calculated by manual delineation of the hypointense areas on LGE images[9] and expressed as a percentage of LV mass.

Experimental study

Design

The study was approved by Institutional and Regional Animal Research Committees. Myocardial infarction was induced in 5 castrated male Large-White pigs weighing 30 to 40 kg to identify the optimal time-window for the first post-reperfusion CMR scan in the clinical study. Reperfused MI was generated by the percutaneous catheter-based technique, with 40min angioplasty-balloon occlusion of the mid-LAD coronary followed by balloon deflation and reestablishment of blood flow.[11] CMR exams including CINE, T2W-STIR and T2-mapping were performed immediately before MI induction and at 20 minute intervals post-reperfusion to 6 hours, when LGE sequence was performed. Immediately after, animals were sacrificed and myocardial tissue samples from ischemic and remote areas were rapidly collected for histology and evaluation of water content.

In a second set of experiments, a total of 20 pigs underwent reperfused acute myocardial infarction induced experimentally by closed-chest 40-minute left anterior descending coronary artery ischemia/reperfusion (I/R). These pigs were sacrificed at 120 minutes (n=5), 24 hours (n=5), 4 days (n=5), and 7 days (n=5) after reperfusion. CMR scans including CINE, T2W-STIR, T2-mapping, and LGE sequences were performed at every follow-up stage until sacrifice. Thus, animals sacrificed on day 7 underwent baseline, 120 min, 24 hours, day 4, and day 7 CMR exams. In all pigs, arterial enhanced multidetector computed tomography (MDCT) was performed during

the index coronary occlusion, between minute 10 and minute 20 of ischemia, to delineate the reference MaR (hypoperfused region during coronary occlusion).[12]

Myocardial infarction procedure

The MI protocol has been detailed elsewhere.[11] Anesthesia was induced by intramuscular injection of ketamine (20 mg/kg), xylazine (2 mg/kg), and midazolam (0.5 mg/kg), and maintained by continuous intravenous infusion of ketamine (2 mg/kg/h), xylazine (0.2 mg/kg/h) and midazolam (0.2 mg/kg/h). Animals were intubated and mechanically ventilated with oxygen (fraction of inspired O_2: 28%). Central venous and arterial lines were inserted and a single bolus of unfractioned heparin (300 IU/kg) was administered at the onset of instrumentation. The LAD coronary artery, immediately distal to the origin of the first diagonal branch, was occluded for 40 minutes with an angioplasty balloon introduced via the percutaneous femoral route using the Seldinger technique. Balloon location and maintenance of inflation were monitored angiographically. After balloon deflation, a coronary angiogram was recorded to confirm patency of the coronary artery. Continuous infusion of amiodarone (300 mg/h) was maintained during the procedure in all pigs to prevent malignant ventricular arrhythmias. In cases of ventricular fibrillation, a biphasic defibrillator was used to deliver non-synchronized shocks.

Arterial enhanced MDCT protocol

Arterial enhanced multidetector computed tomography (MDCT) was performed during coronary occlusion in all pigs, between minute 10 and minute 20 of ischemia, to delineate the reference MaR (hypoperfused region during coronary occlusion).[12] All MDCT studies were performed on a 64-slice CT-scanner (Brilliance CT 64, Philips Healthcare, Cleveland, Ohio). The pigs were positioned supine, and all scans were performed in the cranio-caudal direction during free-breathing. Arterial phase MDCT was performed after intravenous administration of 60 ml iomeprol 400 mgI/ml (Iomeron 400, Bracco Imaging, Milano, Italy) at a flow rate of 3 ml/s followed by a 20-ml saline chaser bolus at the same flow rate. The scan delay was determined

using a bolus tracking technique. Data acquisition started 15 seconds after a threshold of 180 Hounsfield Units was reached in a region of interest placed in the descending aorta.[12]

MDCT examinations were acquired using retrospective cardiac triggered at the 75% of the cardiac cycle with 64 x 0.625 mm collimation and a pitch of 0.2, 120 kV tube voltage, 800 mA tube current and tube rotation time of 400 ms. Image reconstruction was performed with a 512x512 matrix size over a 273x273mm^2 FOV and 0.45mm slice thickness by using high resolution filter (Xres Sharp).

Arterial enhanced MDCT analysis

MDCT images were analyzed using dedicated software (MR Extended Work Space 2.6, Philips Healthcare, Best, The Netherlands). Short axes orientation were obtained from volumetric CT images by multi-planar reconstruction using equivalent anatomical coordinates used for T2W-STIR planning acquisition. In order to have equivalent LV sections, MDCT studies had to be reconstructed in slices equivalent in thickness and level to the CMR ones. Thus, T2W-STIR and multi-planar reconstructed (MPR) short axis CT images were co-registered in 13 to 15 short-axis LV slices by one observer. To ensure CT as independent reference for MaR, endocardial and epicardial borders from MPR CT short-axis images were manually traced by a different observer blinded to the co-registration information; and MaR and remote areas were visually identified based on contrast enhancement differences, manually delineated, and expressed as a percentage of LV area.

CMR protocol

Baseline CMR scans were performed immediately before myocardial infarction and scans were subsequently repeated at all post-infarction follow-up times until sacrifice. CMR examinations were conducted with a Philips 3-Tesla Achieva Tx whole body scanner (Philips Healthcare, Best, the Netherlands) equipped with a 32-element phased-array cardiac coil. The imaging protocol included a standard segmented cine SSFP sequence to provide high quality anatomical references,

and assessment of LV mass and wall thickness; a T2W-STIR sequence to assess the extent of edema and IMH; a T2-GraSE mapping sequence to provide precise myocardial T2 relaxation time properties;[3] and a LGE sequence to assess IS and MVO. To avoid interference with T2 measures at immediate reperfusion, gadolinium contrast was not administered at baseline CMR scans.

All sequences were acquired in free-breathing mode. The imaging parameters for the SSFP sequence were FOV 280 x 280 mm, slice thickness 6 mm with no gap, TR 2.8 ms, TE 1.4 ms, flip angle 45°, cardiac phases 30, voxel size 1.8 x 1.8 mm, and 3 NEX. The imaging parameters for the T2W-STIR sequence were FOV 300 x 300, slice thickness 6 mm, TR 2 heartbeats, TE 80 ms, voxel size 1.4 x 1.9 mm^2, delay 210 ms, end-diastolic acquisition, echo-train length 18, and 2 NEX. The imaging parameters for the T2-GraSE mapping were FOV 300 x 300 with an acquisition voxel size of 1.8 x 2.0 mm^2 and a slice thickness 8 mm, TR 2 heartbeats, and eight echo times ranging from 6.7 to 53.6ms, EPI factor 3. LGE imaging was performed 10 to 15 min after intravenous administration of 0.20 mmol of gadopentetate dimeglumine contrast agent per kg of body weight using a T1-IR-TFE sequence with the following parameters: FOV 280 × 280 mm, voxel size 1.6 × 1.6 mm, end-diastolic acquisition, thickness 6 mm with no gap, TR 5.6 ms, TE 2.8 ms, inversion delay time optimized to null normal myocardium, and 2 NEX.

SSFP, T2W-STIR, and T1-IR-TFE sequences were performed to acquire 13 to 15 contiguous short-axis slices covering the heart from the base to the apex, whereas T2-maps were analyzed in a mid-apical ventricular short axis slice corresponding to the same anatomical level in all acquisitions in order to track T2 relaxation time changes over time. In the experiments to identify the optimal time-window for the first post-reperfusion CMR scan in the clinical study, SSFP and T2W-STIR sequences were performed to acquire only 3 short axis slices (mid-basal, mid, and mid-apical) given that shorter time acquisitions were needed to image at 20 minute intervals.

CMR analysis

CMR images were analyzed using dedicated softwares (MR Extended Work Space 2.6, Philips Healthcare, The Netherlands; and QMassMR 7.6, Medis, Leiden, The Netherlands) by two

observers experienced in CMR analysis. LV mass, myocardial T2 relaxation time, and extent of edema, necrosis, IMH and MVO were determined.

LV endocardial borders were automatically traced with manual adjustment in each cine image. In the tracing convention used, the papillary muscles were included as part of the LV cavity volume. LV epicardial borders were also traced on the end-diastolic images to measure end-diastolic wall thickness, with LV mass computed as the end-diastolic myocardial volume (ie, the difference between the epicardial and endocardial volumes) multiplied by myocardial density (1.05 g/mL). Values of LV mass normalized to body surface area were calculated with the modified Brody's formula.[13]

T2-maps were automatically generated on the acquisition scanner by fitting the signal intensity of all echo times to a monoexponential decay curve at each pixel with a maximum likelihood expectation maximization algorithm. T2 relaxation maps were quantitatively analyzed by placing a wide transmural ROI at the ischemic and remote areas of the corresponding slice in all studies. Hypointense areas suggestive of IMH or MVO were included in the ROI for T2 quantification purposes.[3, 11, 14]

The extent of edema, expressed as a percentage of LV mass (CMR-MaR), was defined after manually tracing the endocardial and epicardial contours of T2W-STIR short-axis images. Abnormal areas were initially identified using the FWHM method.[5, 6] Given that the solely use of FWHM may be prompt to inaccurate patchy estimations,[7, 8] extensive manual correction and visual border delineation were performed. Areas corresponding to slow-flow artifacts were carefully excluded from edematous area. Hypointense areas within the edematous zone, corresponding to IMH, were included within the edematous region.[9, 10] Additionally, the size of the area of IMH was calculated by manual delineation of the hypointense areas on T2W-images,[9] and expressed as a percentage of LV mass. Manual delineation of clear hypointense areas was permitted in the absence of discernible hyperintense myocardium.

IS, expressed as a percentage of LV mass, was defined according the extent of late gadolinium enhancement after manually tracing the endocardial and epicardial contours on T1-IR-TFE short

axis images. Abnormal areas were defined using the FWHM, with manual correction if needed. Hypointense black areas within the necrotic zone, corresponding to MVO, were included within the necrotic area.[9, 10] Additionally, the size of the area MVO was calculated by manual delineation of the hypointense areas on LGE images,[9] and expressed as a percentage of LV mass.

Quantification of myocardial water content

Paired myocardial samples were collected within minutes of euthanasia from the ischemic myocardium of all pigs. Tissue samples were immediately blotted to remove surface moisture and introduced into laboratory crystal containers previously weighed on a high-precision scale. The containers were weighed before and after drying for 48 hours at 100°C in a desiccating oven. Tissue water content was calculated as follows: water content (%) = [(wet weight−dry weight)/wet weight] ×100. An empty container was weighed before and after desiccation as an additional calibration control.

Histological and immunnohistochemical analysis

Myocardial samples were collected within minutes of euthanasia from the ischemic (anteroseptal) and remote (posterolateral) mid-apical ventricular wall. Tissue samples were fixed in 10% neutral buffered formalin for 48 hours and processed by dehydrating the tissue in increasing concentrations of ethanol. Samples were then cleared in xylene, embedded in paraffin wax and cut into 4 micron sections.

For histopathological analysis, sections were stained with hematoxylin and eosin (H&E) and Masson's Trichrome. Necrotic tissue was identified by the presence of typical signs of coagulative necrosis, including marginal contraction bands, fading, and eventually loss of nuclei and striation in cardiomyocytes.

For immunohistochemical analysis, sections were deparaffinized and antigens were unmasked using heat induced epitope retrieval (HIER) with citrate buffer at pH6. Before incubation with

primary antibodies, endogenous peroxidase was blocked by incubation with H_2O_2 for 5 minutes, and endogenous antigens were blocked with fetal bovine serum (FBS) for 20 minutes.

Neutrophils were detected with mouse monoclonal anti-PM1 primary antibody (BMA biomedicals; T-3503) as previously described.[14] The secondary antibody was HRP-conjugated goat anti-mouse (Dako; P0447). Bound antibody was revealed by staining with diaminobenzidine, and nuclei were counterstained with hematoxylin. All immunohistochemical procedures were performed using an automated autostainer (Autostainer Plus®, Dako). For analysis, images were digitalized with a scanner (Nanozoomer-RS C110730®, Hamamatsu) and examined with image analysis software (Tissuemorph®, Visiopharm) by an experienced veterinary pathologist blinded to experimental procedure.

SUPPLEMENTAL RESULTS

Dynamics of the initial wave of edema

Five male pigs (mean body weight 36.4±2.9 kg) underwent CMR exam before MI induction (baseline) and at 20 min intervals after reperfusion for 6 hours (19 CMR exams per pig). Mean myocardial T2 relaxation time before MI induction was 44.3±1.6 ms and 43.0±1.3 ms for the mid-apical anteroseptal and posterolateral left ventricular walls, respectively. In the ischemic area, reperfusion was associated with an immediate sharp increase in T2 relaxation time above baseline values, reaching a peak at 40 minutes after reperfusion (**Supplemental Figure 1**). Thereafter, a progressive decrease in T2 was observed, with T2 relaxation time at 6 hours closer to the values obtained in baseline CMR scans. In the remote myocardium, T2 relaxation time showed no significant trend or differences at different times post reperfusion. Tissue water content in the formerly ischemic myocardium at 6 hours after reperfusion was 82.7 ± 1.0%. Histological analysis of such myocardial tissue at 6 hours after reperfusion revealed typical features of early acute transmural necrosis (**Supplemental Figure 2**).

SUPPLEMENTAL TABLES

Supplemental Table 1. Point estimates and differences in T2 relaxation time in the transmural ischemic myocardium relative to the value obtained in the hyperacute CMR exam (≤3 hour reperfusion), with adjustment for the extent of intramyocardial hemorrhage.

	Reperfusion time				
	≤ 3 hours	**24 hours**	**4 days**	**7 days**	**40 days**
T2 transmural ischemic, ms	80.8 (76.1, 85.4)	65.4 (60.8, 70.0)	80.5 (75.9, 85.1)	76.8 (72.1, 81.6)	65.4 (60.7, 70.2)
Δ T2 transmural ischemic, ms	-	-15.3 (-21.3, -9.4)	-0.3 (-6.2, 5.7)	-3.9 (-10.0, 2.2)	-15.3 (-21.3, -9.2)
Δ T2 transmural ischemic (*), ms	-	-14.7 (-20.7, -8.7)	1.0 (-5.3, 7.3)	-2.7 (-9.1, 3.7)	-15.1 (-21.1, -9.1)

To take account of repeated measures, a generalized linear mixed model was conducted to analyze the time course of T2 relaxation time. The model was further adjusted by extent of hemorrhage, including the amount of intramyocardial hemorrhage (IMH) expressed as a percentage of the left ventricle as a covariate.

Data are presented as point estimates (95% confidence interval), or mean difference (95% confidence interval) in T2 relaxation time (Δ T2) in the transmural ischemic myocardium relative to the first CMR examination, performed within 3 hours after reperfusion. The table shows nonadjusted differences and (*) differences adjusted for the amount of IMH (% of left ventricle). Globally, T2 relaxation time in the transmural ischemic area decreased 1.1 ms (95% CI, -3.1 to 1.0, p = 0.297) for every 1% absolute increase in IMH (expresses as a percentage of the left ventricle).

Supplemental Table 2. Point estimates and differences in edematous area relative to the value obtained in the hyperacute CMR exam (≤3 hour reperfusion), with adjustment for the extent intramyocardial hemorrhage.

	Reperfusion time				
	≤ 3 hours	**24 hours**	**4 days**	**7 days**	**40 days**
Area of edema, % of LV	39.9 (34.1, 45.7)	21.8 (16.1, 27.6)	42.8 (37.0, 48.6)	43.0 (37.1, 48.9)	20.3 (14.3, 26.2)
Δ Area of edema, % of LV	-	-18.0 (-24.2, -11.9)	2.9 (-3.2, 9.1)	3.1 (-3.2, 9.4)	-19.6 (-25.9, -13.3)
Δ Area of edema (*), % of LV	-	-19.0 (-25.3, -12.7)	1.0 (-5.7, 7.7)	1.2 (-5.6, 8.0)	-19.9 (-26.1, -13.6)

To take account of repeated measures, a generalized linear mixed model was conducted to analyze the time course of edematous area as measured by T2W-STIR. The model was further adjusted by extent of hemorrhage, including the amount of intramyocardial hemorrhage (IMH) expressed as a percentage of the left ventricle as a covariate.

Data are presented as point estimates (95% confidence interval), or mean difference (95% confidence interval) in edematous area (Δ Area of edema) relative to the first CMR examination, performed within 3 hours after reperfusion. The table shows nonadjusted differences and (*) differences adjusted for the amount of IMH (% of left ventricle). Globally, the area of edema increased 1.7% of the left ventricle (95% CI, -0.6 to 4.0, p = 0.154) for every 1% absolute increase in IMH (expresses as a percentage of the left ventricle).

Supplemental Table 3. Time course of myocardium at risk, infarct size, and myocardial salvage as assessed by cardiac magnetic resonance during the first week after reperfused myocardial infarction in pigs.

Endpoint	CMR measure	Follow up			
		R-120min	**R-24hours**	**R-Day4**	**R-Day7**
Sacrificed at 120 min	MaR, % of LV	51.6 (6.2)			
	Infarct size, % of LV	47.2 (2.9)			
	Myocardial salvage, %	3.7 (3.4)			
Sacrificed at 24 hours	MaR, % of LV	47.7 (5.7)	4.7 (3.7)		
	Infarct size, % of LV	46.8 (5.6)	40.0 (3.4)		
	Myocardial salvage, %	1.9 (1.7)	-1339 (1077)		
Sacrificed at 4 days	MaR, % of LV	50.0 (3.5)	3.8 (2.8)	33.4 (7.0)	
	Infarct size, % of LV	47.6 (3.6)	35.7 (3.7)	32.1 (3.3)	
	Myocardial salvage, %	4.6 (4.6)	-1209 (690)	-0.6 (26.7)	
Sacrificed at 7 days	MaR, % of LV	42.9 (5.7)	2.2 (1.7)	27.1 (3.4)	30.1 (2.3)
	Infarct size, % of LV	39.2 (3.8)	30.2 (3.1)	28.2 (4.6)	25.4 (4.0)
	Myocardial salvage, %	8.3 (6.4)	-1310 (996)	-4.4 (14.2)	15.7 (13.3)

Values are mean (standard deviation). Mean myocardium at risk assessed by MDCT reference standard for pigs was 33.7±5.8 % of the LV for those sacrificed at 120 minutes, 30.7±6.2 % for 24 hours, 29.8±3.9 % for day 4, and 28.3±4.3 % for day 7.

CMR: cardiac magnetic resonance; MaR: myocardium at risk; LV: left ventricle; I/R: ischemia/reperfusion; R: reperfusion.

Supplemental Table 4 Time profile of left ventricular mass and wall thickness ratio as assessed by cardiac magnetic resonance during the first week after reperfused myocardial infarction in pigs.

Endpoint	CMR measure	Follow up				
		Baseline	**R-120min**	**R-24hours**	**R-Day4**	**R-Day7**
Sacrificed at 120 min	LV mass, g/m^2	75.8 (7.9)	105.5 (11.1)			
	Wall thickness ratio, ischemic/remote	1.07 (0.04)	1.91 (0.23)			
Sacrificed at 24 hours	LV mass, g/m^2	79.6 (9.3)	103.8 (16.1)	81.5 (10.0)		
	Wall thickness ratio, ischemic/remote	1.08 (0.07)	2.43 (0.53)	1.25 (0.06)		
Sacrificed at 4 days	LV mass, g/m^2	72.5 (3.1)	108.6 (14.9)	81.3 (7.0)	81.7 (8.3)	
	Wall thickness ratio, ischemic/remote	1.07 (0.04)	1.88 (0.33)	1.16 (0.11)	1.15 (0.20)	
Sacrificed at 7 days	LV mass, g/m^2	64.0 (7.4)	92.6 (6.0)	71.1 (4.7)	73.6 (5.2)	74.3 (4.7)
	Wall thickness ratio, ischemic/remote	1.06 (0.18)	2.08 (0.36)	1.23 (0.13)	1.17 (0.15)	1.08 (0.06)
Pooled	**LV mass, g/m^2**	**73.0 (9.0)**	**102.6 (13.2)**	**78.0 (8.6)**	**77.6 (7.8)**	**74.3 (4.7)**
	Wall thickness ratio, ischemic/remote	**1.07 (0.09)**	**2.07 (0.41)**	**1.21 (0.11)**	**1.16 (0.17)**	**1.08 (0.06)**

Values are mean (standard deviation). No significant statistical differences were found between time-points except for R-120 min CMR, when LV mass and end-diastolic wall thickness ratio (MaR/remote) were significantly higher than at the other time-points due to the intense swelling of the ischemic myocardium at early reperfusion.

CMR: cardiac magnetic resonance; R: reperfusion; LV: left ventricle.

Supplementary Table 5. Time course of intramyocardial hemorrhage (IMH) and microvascular obstruction (MVO) assessed by cardiac magnetic resonance during the first week after reperfused myocardial infarction in pigs.

Endpoint	CMR measure	Follow up			
		R-120min	**R-24hours**	**R-Day4**	**R-Day7**
Sacrificed at 120 min	IMH, % of LV	0.0 (0.0)			
	MVO, % of LV	4.7 (4.8)			
Sacrificed at 24 hours	IMH, % of LV	0.5 (0.9)	2.2 (1.8)		
	MVO, % of LV	3.8 (3.6)	9.9 (5.4)		
Sacrificed at 4 days	IMH, % of LV	0.2 (0.5)	4.1 (1.3)	5.7 (2.5)	
	MVO, % of LV	1.5 (1.3)	7.5 (4.9)	4.7 (4.8)	
Sacrificed at 7 days	IMH, % of LV	0.2 (0.5)	4.3 (1.8)	4.4 (1.9)	1.4 (1.4)
	MVO, % of LV	5.1 (4.5)	6.5 (2.1)	2.3 (2.8)	1.8 (2.9)
Pooled	**IMH, % of LV**	**0.2 (0.5)**	**3.5 (1.8)**	**5.0 (2.2)**	**1.4 (1.4)**
	MVO, % of LV	**3.7 (3.7)**	**8.0 (4.3)**	**3.5 (3.9)**	**1.8 (2.9)**

Values are mean (standard deviation).

CMR: cardiac magnetic resonance; I/R: ischemia/reperfusion; IMH: intramyocardial hemorrhage; MVO: microvascular obstruction; LV: left ventricle.

SUPPLEMENTAL FIGURES AND FIGURE LEGENDS

Supplemental Figure 1. Dynamics of the initial wave of edema

(A) Time course of T2 relaxation time (ms) in the ischemic and remote myocardium during the first 6 hours after ischemia/reperfusion in the pig model. Data are means and standard deviation. Cardiac magnetic resonance (CMR) scans were performed immediately before induction of myocardial infarction and at 20 minute intervals after reperfusion up to 6 hours, when pigs were sacrificed.

(B) Representative images from an animal that underwent 40min-I/R and serial CMR T2W-STIR and T2-mapping exams to study the precise dynamics of the first edema wave. Due to space restrictions, the representative images shown were taken at 40 minute intervals. All T2 maps were scaled between 30 and 120 ms.

CMR: cardiac magnetic resonance; R: reperfusion; STIR: Short-tau inversion recovery; ms: milliseconds.

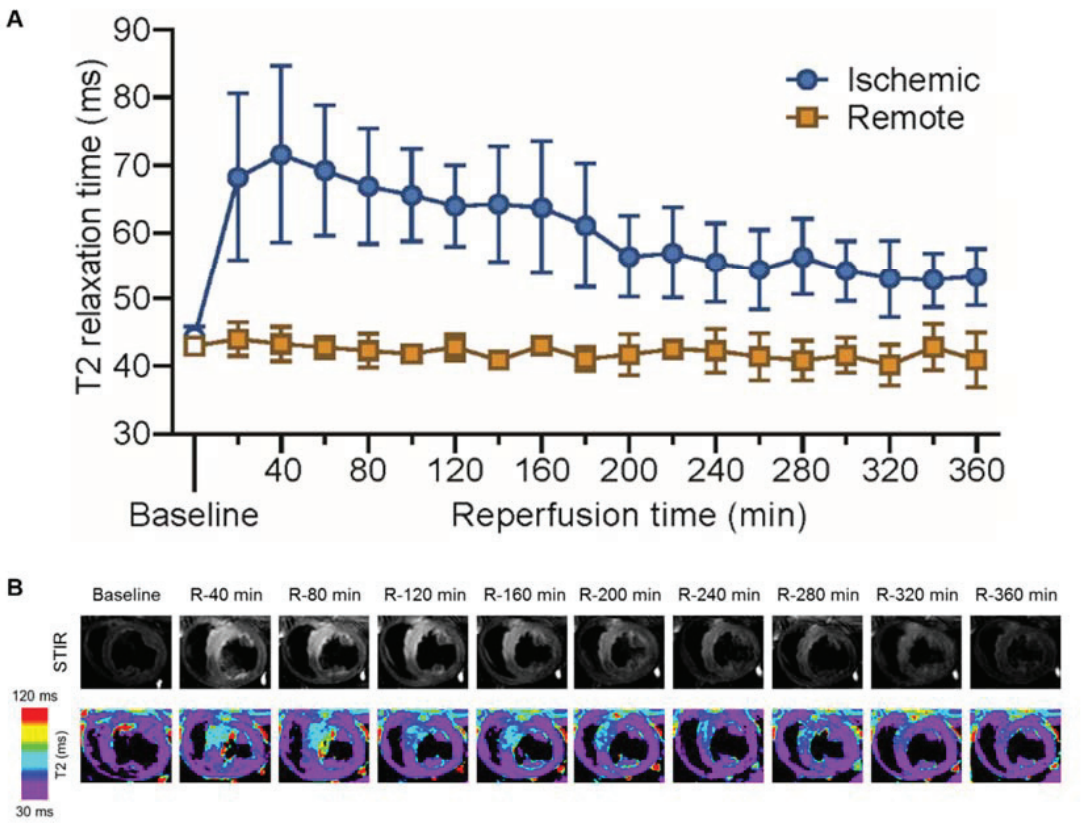

Supplemental Figure 2. Histological analysis of porcine myocardium 6 hours after ischemia/reperfusion

Representative histological images of ischemic myocardium (top) and remote myocardium (bottom) 6 hours after 40-minute ischemia and reperfusion (I/R) in the pig model. Images show staining with hematoxylin and eosin (H/E), anti-PM1 antibody (PMN), and Masson's trichrome. Neutrophils were quantified and interstitial hemorrhage was graded from 0 (absence) to 5 (very severe). The remote area showed no relevant pathological findings at this time-point. In contrast, ischemic myocardium exhibited typical features of acute transmural myocardial infarction, with extensive coagulative necrosis, contraction bands, loss of nuclei and striation in cardiomyocytes, wavy fibers, and cell edema. Interstitial edema in the ischemic area at 6 hours post-I/R was significantly lower than at 120 min after ischemia onset,[14] consistent with partial resolution of the initial wave of edema. Massive tissue infiltration by neutrophils (473±190 cells per mm^2 in the lesion area) was observed at 6 hours post-I/R, which was at least as high as that observed at 24 hours post-I/R.[14] Mild interstitial hemorrhage was detected (median score of 1; interquartile range, 0-1). Scale bars, 100μM.

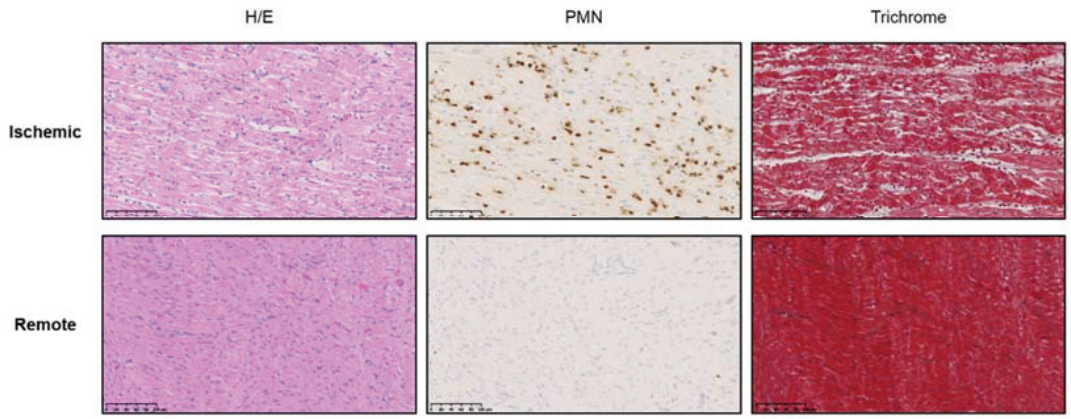

Supplemental Figure 3. Individual patient T2 relaxation time trajectories in the ischemic myocardium

Line-plots showing changes in individual T2 relaxation times in the ischemic myocardium of anterior STEMI patients after reperfusion by primary PCI. Cardiac magnetic resonance was scheduled within the first 3 hours and at 24 hours, 4 days, 7 days, and 40 days after reperfusion. T2 values at all time-points were obtained from T2-GraSE mapping sequences.[3]

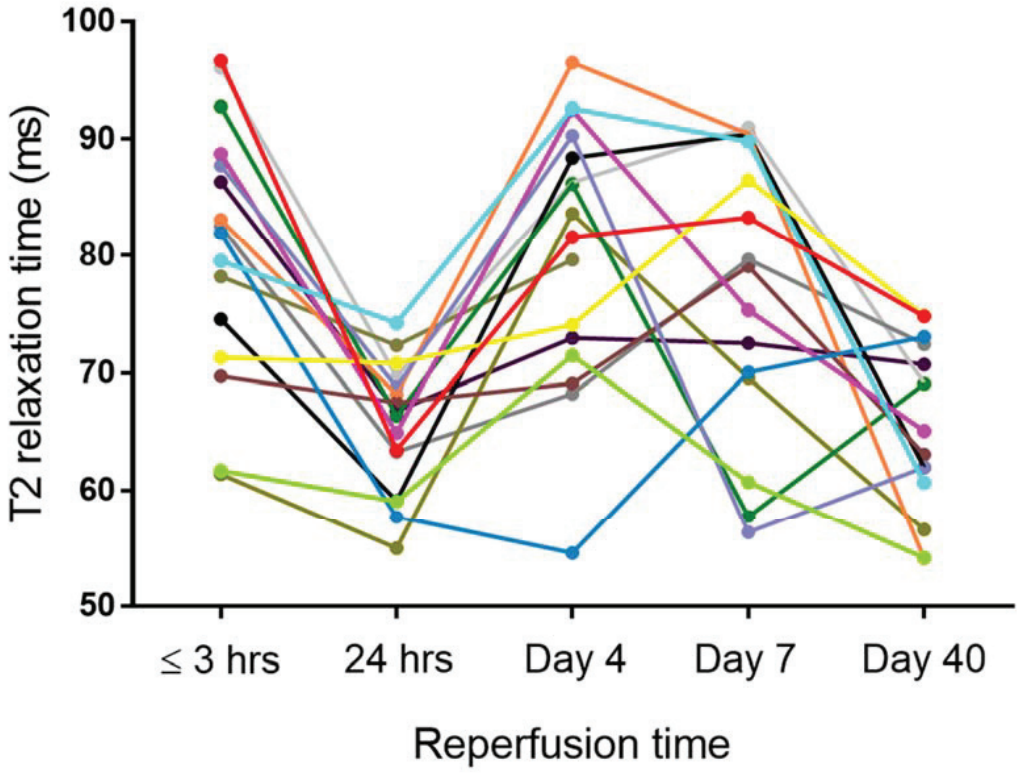

Supplemental Figure 4. Individual patient trajectories for area of edema

Line-plots showing changes in individual area of edema measurements of anterior STEMI patients after reperfusion by primary PCI. Colors identify the same individuals as in Supplemental Figure 3. Cardiac magnetic resonance was scheduled within the first 3 hours and at 24 hours, 4 days, 7 days, and 40 days after reperfusion. Edematous area at all time points was determined from T2W-STIR sequences.

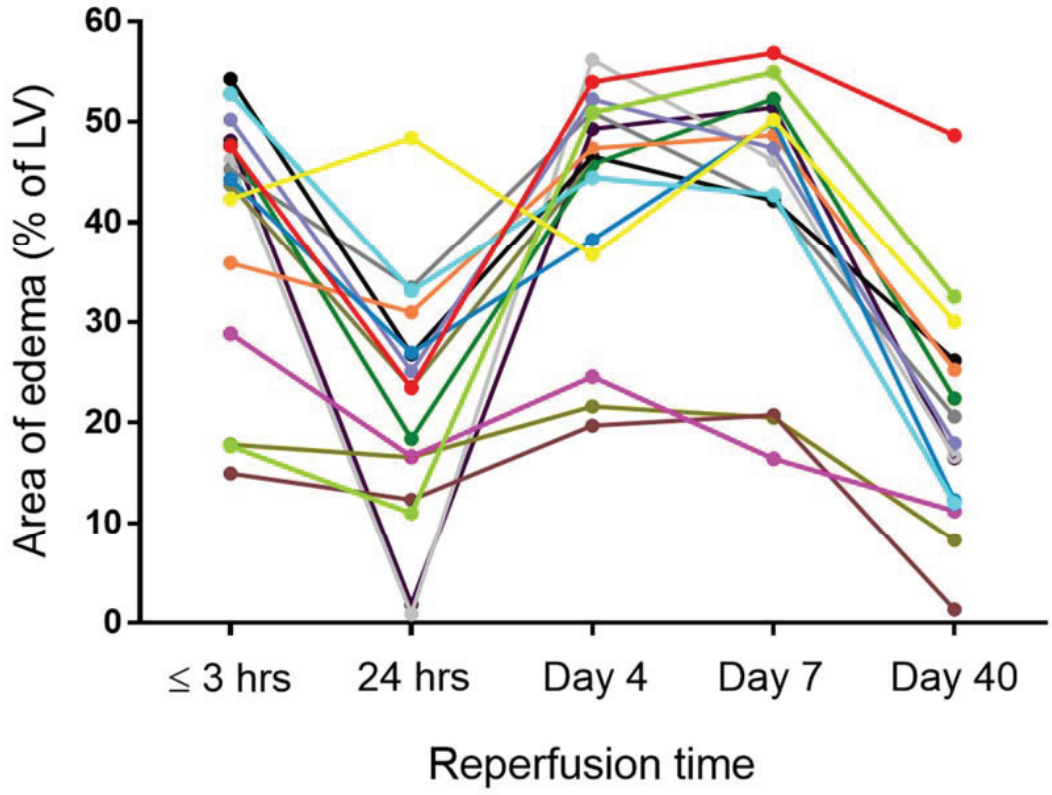

Supplemental Figure 5. Temporal evolution of myocardial salvage assessed by cardiac magnetic resonance after reperfused myocardial infarction in pigs.

Data are means ±standard error of the mean.

MaR: myocardium at risk.

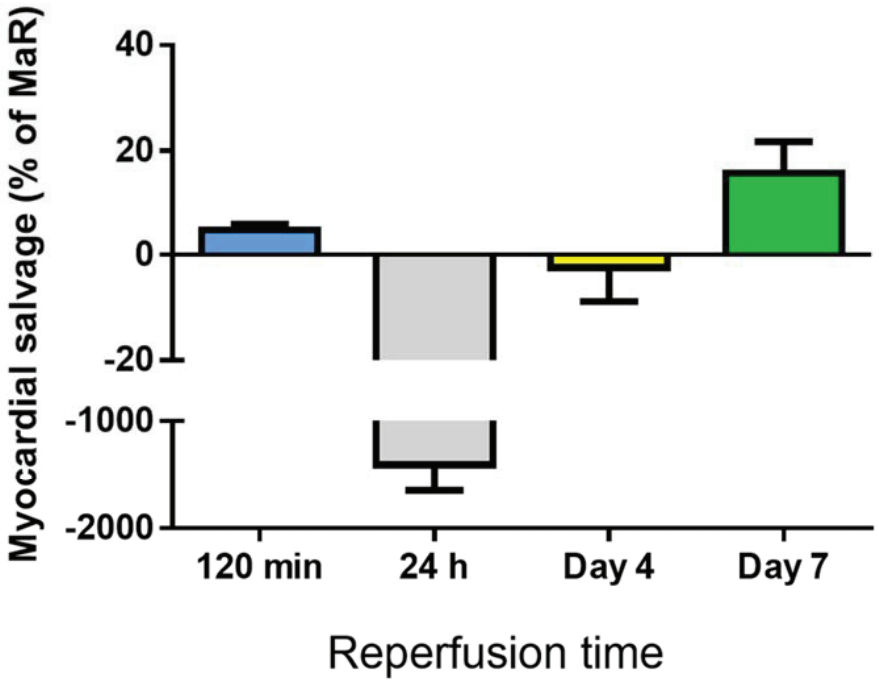

SUPPLEMENTAL REFERENCES

1. O'Gara PT, Kushner FG, Ascheim DD, Casey DE, Chung MK, de Lemos JA, Ettinger SM, Fang JC, Fesmire FM, Franklin BA, Granger CB, Krumholz HM, Linderbaum JA, Morrow DA, Newby LK, Ornato JP, Ou N, Radford MJ, Tamis-Holland JE, Tommaso CL, Tracy CM, Woo YJ and Zhao DX. 2013 ACCF/AHA Guideline for the Management of ST-Elevation Myocardial Infarction: Executive SummaryA Report of the American College of Cardiology Foundation/American Heart Association Task Force on Practice Guidelines. *J Am Coll Cardiol*. 2013;61:485-510.

2. Steg PG, James SK, Atar D, Badano LP, Lundqvist CB, Borger MA, Di Mario C, Dickstein K, Ducrocq G, Fernandez-Aviles F, Gershlick AH, Giannuzzi P, Halvorsen S, Huber K, Juni P, Kastrati A, Knuuti J, Lenzen MJ, Mahaffey KW, Valgimigli M, van't Hof A, Widimsky P, Zahger D, Bax JJ, Baumgartner H, Ceconi C, Dean V, Deaton C, Fagard R, Funck-Brentano C, Hasdai D, Hoes A, Kirchhof P, Knuuti J, Kolh P, McDonagh T, Moulin C, Popescu BA, Reiner Ž, Sechtem U, Sirnes PA, Tendera M, Torbicki A, Vahanian A, Windecker S, Hasdai D, Astin F, Åström-Olsson K, Budaj A, Clemmensen P, Collet J-P, Fox KA, Fuat A, Gustiene O, Hamm CW, Kala P, Lancellotti P, Maggioni AP, Merkely B, Neumann F-J, Piepoli MF, Van de Werf F, Verheugt F and Wallentin L. ESC Guidelines for the management of acute myocardial infarction in patients presenting with ST-segment elevation. *The Task Force on the management of ST-segment elevation acute myocardial infarction of the European Society of Cardiology (ESC)*. 2012;33:2569-2619.

3. Fernandez-Jimenez R, Sanchez-Gonzalez J, Aguero J, Del Trigo M, Galan-Arriola C, Fuster V and Ibanez B. Fast T2 gradient-spin-echo (T2-GraSE) mapping for myocardial edema quantification: first in vivo validation in a porcine model of ischemia/reperfusion. *J Cardiovasc Magn Reson*. 2015;17:92.

4. Hammer-Hansen S, Ugander M, Hsu LY, Taylor J, Thune JJ, Kober L, Kellman P and Arai AE. Distinction of salvaged and infarcted myocardium within the ischaemic area-at-risk with T2 mapping. *European heart journal cardiovascular Imaging*. 2014;15:1048-53.

5. Aletras AH, Tilak GS, Natanzon A, Hsu LY, Gonzalez FM, Hoyt RF, Jr. and Arai AE. Retrospective determination of the area at risk for reperfused acute myocardial infarction with T2-weighted cardiac magnetic resonance imaging: histopathological and displacement encoding with stimulated echoes (DENSE) functional validations. *Circulation*. 2006;113:1865-70.

6. Fernandez-Friera L, Garcia-Ruiz JM, Garcia-Alvarez A, Fernandez-Jimenez R, Sanchez-Gonzalez J, Rossello X, Gomez-Talavera S, Lopez-Martin GJ, Pizarro G, Fuster V and Ibanez B. Accuracy of Area at Risk Quantification by Cardiac Magnetic Resonance According to the Myocardial Infarction Territory. *Revista espanola de cardiologia*. 2017;70:323-330.

7. McAlindon E, Pufulete M, Lawton C, Angelini GD and Bucciarelli-Ducci C. Quantification of infarct size and myocardium at risk: evaluation of different techniques and its implications. *European heart journal cardiovascular Imaging*. 2015;16:738-46.

8. Sjogren J, Ubachs JF, Engblom H, Carlsson M, Arheden H and Heiberg E. Semi-automatic segmentation of myocardium at risk in T2-weighted cardiovascular magnetic resonance. *J Cardiovasc Magn Reson*. 2012;14:10.

9. Robbers LF, Eerenberg ES, Teunissen PF, Jansen MF, Hollander MR, Horrevoets AJ, Knaapen P, Nijveldt R, Heymans MW, Levi MM, van Rossum AC, Niessen HW, Marcu CB, Beek AM and van Royen N. Magnetic resonance imaging-defined areas of microvascular obstruction after acute myocardial infarction represent microvascular destruction and haemorrhage. *Eur Heart J*. 2013;34:2346-53.

10. Valle-Caballero MJ, Fernandez-Jimenez R, Diaz-Munoz R, Mateos A, Rodriguez-Alvarez M, Iglesias-Vazquez JA, Saborido C, Navarro C, Dominguez ML, Gorjon L, Fontoira JC, Fuster V, Garcia-Rubira JC and Ibanez B. QRS distortion in pre-reperfusion electrocardiogram is a bedside predictor of large myocardium at risk and infarct size (a METOCARD-CNIC trial substudy). *Int J Cardiol*. 2016;202:666-73.

11. Fernandez-Jimenez R, Sanchez-Gonzalez J, Aguero J, Garcia-Prieto J, Lopez-Martin GJ, Garcia-Ruiz JM, Molina-Iracheta A, Rossello X, Fernandez-Friera L, Pizarro G, Garcia-Alvarez A, Dall'Armellina E, Macaya C, Choudhury RP, Fuster V and Ibanez B. Myocardial

edema after ischemia/reperfusion is not stable and follows a bimodal pattern: imaging and histological tissue characterization. *J Am Coll Cardiol*. 2015;65:315-23.

12. Mewton N, Rapacchi S, Augeul L, Ferrera R, Loufouat J, Boussel L, Micolich A, Rioufol G, Revel D, Ovize M and Croisille P. Determination of the myocardial area at risk with pre- versus post-reperfusion imaging techniques in the pig model. *Basic Res Cardiol*. 2011;106:1247-57.

13. Kelley KW, Curtis SE, Marzan GT, Karara HM and Anderson CR. Body surface area of female swine. *Journal of animal science*. 1973;36:927-30.

14. Fernandez-Jimenez R, Garcia-Prieto J, Sanchez-Gonzalez J, Aguero J, Lopez-Martin GJ, Galan-Arriola C, Molina-Iracheta A, Doohan R, Fuster V and Ibanez B. Pathophysiology Underlying the Bimodal Edema Phenomenon After Myocardial Ischemia/Reperfusion. *J Am Coll Cardiol*. 2015;66:816-28.

Letter to the Editor #1. “*Reply: myocardial edema should be stratified according to the state of cardiomyocytes within the ischemic region*”.[75]

associated with SCD were detected by an ECG and would have been missed by only a screening history and physical examination.

This analysis exhibits the rather vague nature and low yield of screening questionnaires. More than one-third of athletes reported at least 1 positive cardiac symptom or family history response. The American Heart Association recently expanded their primary recommendations for screening from a 12-point to a 14-point assessment (2). However, simply asking more questions is unlikely to improve detection of athletes at risk when the sensitivity and specificity of the tool itself have considerable limitations.

SCD in NCAA athletes is more frequent than initial estimates, with an overall incidence of 1:43,000, with male basketball players having the highest risk of SCD at 1:7,000 athletes per year (1). Strong consideration must be given to implementing improved models of prevention.

Accurate interpretation of an athlete's ECG requires proper training and experience. The false-positive rate in this study was only 2.2%, and approximately 1 in 4 athletes with abnormal ECG findings were found to have a cardiac disorder associated with SCD. Physician expertise, cardiology, and institutional resources vary among NCAA institutions, which will affect both the capacity and ability to implement ECG screening. Thus, the findings of this study may not be applicable to institutions with less experience. If an ECG is included in the cardiovascular screening of athletes, it must be interpreted with modern standards that distinguish physiological cardiac remodeling from findings suggestive of underlying cardiac pathology and be conducted with adequate cardiology oversight and resources to assist with the secondary investigation of ECG abnormalities.

Screening history questionnaires have a high response rate, and their value in the detection of athletes at risk when used as the sole screening tool is uncertain. ECG screening increases the ability to identify athletes with disorders associated with SCD and thus meet the primary objective of pre-participation screening. An integrated cardiovascular screening that includes an ECG should be considered best practice for the pre-participation evaluation of college athletes.

*Jonathan A. Drezner, MD
Jordan M. Prutkin, MD, MHS
Kimberly G. Harmon, MD
John W. O'Kane, MD
Hank F. Pelto, MD
Ashwin L. Rao, MD
Jeffrey D. Hassebrock, BS
Bradley J. Petek, BS
Colin Teteak, BA
Miranda Timonen, BA
Monica Zigman, MPH
David S. Owens, MD, MS
*Department of Family Medicine
Sports Medicine Section
University of Washington
3800 Montlake Boulevard NE
P.O. Box 354060
Seattle, Washington 98195-4060
E-mail: jdrezner@uw.edu

http://dx.doi.org/10.1016/j.jacc.2015.02.072

Please note: The authors have reported that they have no relationships relevant to the contents of this paper to disclose.

REFERENCES

1. Harmon KG, Asif IM, Klossner D, Drezner JA. Incidence of sudden cardiac death in national collegiate athletic association athletes. Circulation 2011;123:1594–600.

2. Maron BJ, Friedman RA, Kligfield P, et al. Assessment of the 12-lead electrocardiogram as a screening test for detection of cardiovascular disease in healthy general populations of young people (12-25 years of age): a scientific statement from the American Heart Association and the American College of Cardiology. J Am Coll Cardiol 2014;64:1479–514.

Myocardial Edema Should Be Stratified According to the State of Cardiomyocytes Within the Ischemic Region

We read the article by Fernández-Jiménez et al. (1) published in the *Journal* with great interest. The investigators conclude that the evolution of myocardial edema within a week after ischemia/reperfusion (I/R) follows a bimodal pattern: T_2 relaxation times and water content reach the highest level at 2 h of reperfusion in the ischemia area, decrease to the lowest at 24 h, and rise to a peak again on day 7.

Myocardial edema, namely a bright signal intensity zone on T_2-weighted short tau inversion recovery cardiac magnetic resonance, is referred to as an area at risk that consists of irreversible and reversible injured tissue. The cardiomyocytes located in the irreversible region are necrotic and unsalvageable. Irreversible region is surrounded by a reversible region encompassing cells that are integrated without membrane disruption and can recover structure and function after reperfusion. A severe degree of edema will overwhelm the necrotic cells when reperfusion is

performed for their defective sarcolemmal membrane, which fails to control the volume of fluids and electrolytes (2). Combined with contrast delayed-enhancement cardiac magnetic resonance to locate and quantify infarct zone, it is feasible to identify the salvageable myocardium as the area at risk minus infarct size (3). As the state of cardiomyocytes is different in salvageable and infarct regions, the edema might follow disparate evolution patterns, so it is of great necessity to stratify them to obtain curves exhibiting specific regions.

As Fernández-Jiménez et al. (1) put it, "the first wave appears abruptly upon reperfusion and dissipates at 24 h." We quite agree with this phenomenon, which is also observed in our research (4). We notice that diastolic wall thickness significantly increased at early reperfusion, dropped sharply to nearly normal at 24 h and remained constant until day 7 as is shown in Figure 3 of Fernández-Jiménez et al. (1). It is obvious that an abrupt elevation and absorption of overloaded fluids after ischemia/reperfusion forms such a wave of diastolic wall thickness that is consistent with the first wave of T_2 relaxation times. However, we do not think it is appropriate to draw the conclusion that the second wave is also developed by edematous reaction.

Although edema might be generated by the subsequent inflammatory response and myocardial water content accumulates gradually, it is not the predominant factor that elevates T_2 relaxation times of the ischemic tissue during the period from 24 h to day 7. Foltz et al. (5) consider that T_2 relaxation fluctuates with edema and hemoglobin oxidative denaturation to methemoglobin in acute reperfused hemorrhagic infarction, which is similar to the bimodal pattern reported by Fernández-Jiménez et al. (1). Compartmentalized deoxyhemoglobin and methemoglobin are paramagnetic and would greatly reduce T_2 relaxation, whereas decompartmentalized methemoglobin due to erythrocyte rupture is characteristic of diamagnetism and would extend T_2 relaxation time. Despite the different occlusion times in these 2 articles (1,5), both of them occur with intramyocardial hemorrhage, as is shown in Figure 3A of Fernández-Jiménez et al. (1): hypointensity within edematous tissue. In terms of amplitude of variation in a different time, T_2 relaxation time is more significant than water content in the myocardium.

Taking the edematous region as a whole without differentiating the components within it, we find that T_2 relaxation fluctuations follow a bimodal pattern. However, this curve does not exactly show evolution of myocardial edema. To acquire more accurate change curves reflecting the specific state of cardiomyocytes, we should stratify the edema region into salvageable and infarcted zones, or simply edematous and hemorrhagic zones.

Bing Zhang, MD
Wei Chen, MD, PhD
Yushu Chen, MD
***Fabao Gao, MD, PhD**
*Molecular Imaging Laboratory
Department of Radiology
West China Hospital
Sichuan University
No. 37, Guoxue Alley
Chengdu 610041
China
E-mail: gaofabao@yahoo.com

http://dx.doi.org/10.1016/j.jacc.2015.01.065

Please note: The authors have reported that they have no relationships relevant to the contents of this paper to disclose. Derek Yellon, MD, served as Guest Editor for this paper.

REFERENCES

1. Fernández-Jiménez R, Sánchez-González J, Agüero J, et al. Myocardial edema after ischemia/reperfusion is not stable and follows a bimodal pattern: advanced imaging and histological tissue characterization. J Am Coll Cardiol 2015;65:315–23.

2. Kloner RA. New observations regarding post-ischemia/reperfusion myocardial swelling. J Am Coll Cardiol 2015;65:324–6.

3. Carlsson M, Ubachs JF, Hedström E, Heiberg E, Jovinge S, Arheden H. Myocardium at risk after acute infarction in humans on cardiac magnetic resonance: quantitative assessment during follow-up and validation with single-photon emission computed tomography. J Am Coll Cardiol Img 2009;2:569–76.

4. Xia R, Lu X, Zhang B, et al. Early reperfusion can reduce infarction size but not salvaged myocardial size in acute myocardial infarction rats. J Am Coll Cardiol Img 2015;8:616–7.

5. Foltz WD, Yang Y, Graham JJ, Detsky JS, Wright GA, Dick AJ. MRI relaxation fluctuations in acute reperfused hemorrhagic infarction. Magn Reson Med 2006;56:1311–9.

REPLY: Myocardial Edema Should Be Stratified According to the State of Cardiomyocytes Within the Ischemic Region

We read with great interest the letter from Dr. Zhang and colleagues commenting on our recently published work (1). Noninvasive evaluation of myocardial edema has become possible with the development of T_2-weighted and lately T_2-mapping cardiac magnetic resonance sequences able to detect changes in tissue water content (2,3). Interestingly, although edema is defined as an abnormal water accumulation within a tissue, it is well known that T_2 relaxation properties of myocardium are affected by other factors besides water content such as hemorrhage or microvascular obstruction, among others (4). Evaluation of tissue water content by a reference standard is therefore necessary for detecting, quantifying, and tracking the

real post-myocardial infarction edema reaction. We respectfully disagree with Dr. Zhang and colleagues on their comment regarding the inappropriateness to draw the conclusion from our work that the second wave is also developed by edematous reaction. Indeed, we demonstrated that T_2 abnormalities and, more importantly, increased water content in the ischemic region, as measured by the gold standard desiccation technique, were ultimately as high at day 7 as that documented at early reperfusion. Definitely, the quantification of the myocardial water content by reference standards was crucial for demonstrating a consistent appearance of 2 consecutive waves of real edema during the first week after ischemia/reperfusion in our experimental study.

Dr. Zhang and colleagues point out that salvageable and infarct regions might follow disparate edema evolution patterns. From the cardiac magnetic resonance point of view, we agree that placing a region of interest in the full thickness of the left ventricular wall is troublesome as it will contain different myocardial states. However, the identification of "clean" regions clearly outside hemorrhage/microvascular obstruction areas may be extremely difficult and, more importantly, may be subjected to a big source of bias. The quantification of water content by reference standard in such small regions would be even more difficult to perform as this procedure needs to be done in a rapid and careful manner, avoiding tissue manipulation as much as possible. We tend to disagree with the idea that edematous and infarcted zones are equivalent to salvageable and hemorrhagic areas, respectively, as suggested by Dr. Zhang and colleagues. In any case, we believe that the possibility of including different myocardial states had little effect on the results reported in our work given that transmural extent of infarction was >80% in all evaluated segments containing the regions of interest, and the observed parallel course of T_2 relaxation times and water content.

Rodrigo Fernández-Jiménez, MD
Valentin Fuster, MD, PhD
***Borja Ibáñez, MD, PhD**

*Myocardial Pathophysiology Program
Centro Nacional de Investigaciones Cardiovasculares Carlos III (CNIC)
Melchor Fernández Almagro, 3.
Madrid 28029
Spain
E-mail: bibanez@cnic.es

http://dx.doi.org/10.1016/j.jacc.2015.02.070

Please note: The authors have reported that they have no relationships relevant to the contents of this paper to disclose. Derek Yellon, MD, served as Guest Editor for this paper.

REFERENCES

1. Fernández-Jiménez R, Sánchez-González J, Agüero J, et al. Myocardial edema after ischemia/reperfusion is not stable and follows a bimodal pattern: imaging and histological tissue characterization. J Am Coll Cardiol 2015;65:315–23.

2. Verhaert D, Thavendiranathan P, Giri S, et al. Direct T2 quantification of myocardial edema in acute ischemic injury. J Am Coll Cardiol Img 2011;4:269–78.

3. Kloner RA. New observations regarding post-ischemia/reperfusion myocardial swelling. J Am Coll Cardiol 2015;65:324–6.

4. Croisille P, Kim HW, Kim RJ. Controversies in cardiovascular MR imaging: T2-weighted imaging should not be used to delineate the area at risk in ischemic myocardial injury. Radiology 2012;265:12–22.

Myocardial Salvage, Area at Risk by T2w CMR

The Resolution of the Retrospective Radio Wave Paradigm?

In 2006, in an editorial published in a fellow journal by Pennell (1) T_2-weighted (T2w) cardiac magnetic resonance (CMR) imaging was presented as a promising method to retrospectively assess the myocardial area at risk. The area at risk could be reliably measured by contouring the myocardial edema using T2w sequences. The combination with late gadolinium-enhanced myocardial volume assessed during the same examination allowed the final infarct size measurement, and from there the simple and powerful concept of myocardial salvage was issued (2). Since then, numerous trials assessing new reperfusion strategies have used the salvage index as a clinical endpoint (3).

With this in mind, we read with great interest in the *Journal*, the paper by Fernández-Jiménez et al. (4). These investigators, relying on very solid and consistent work, unveil very new findings. They show with striking results that myocardial edema after ischemia reperfusion is highly variable and follows a bimodal pattern. These findings are novel and challenge the accepted view on the development of edema after an ischemic insult. In our opinion, these findings also significantly question the accepted view of T2w CMR as a reliable tool to assess the area at risk, and thus the myocardial salvage index, which we had already challenged recently (5).

Although the investigators are very cautious about this topic in their paper, we would value their opinion on this debated issue of CMR retrospective accuracy to assess the area at risk. Also, considering that these investigators have used the myocardial salvage index as an endpoint in a previous trial (3), we would

Letter to the Editor #2. “*Reply: myocardial salvage, area at risk by T2W CMR: the resolution of the retrospective radio wave paradigm?*”.[76]

real post-myocardial infarction edema reaction. We respectfully disagree with Dr. Zhang and colleagues on their comment regarding the inappropriateness to draw the conclusion from our work that the second wave is also developed by edematous reaction. Indeed, we demonstrated that T_2 abnormalities and, more importantly, increased water content in the ischemic region, as measured by the gold standard desiccation technique, were ultimately as high at day 7 as that documented at early reperfusion. Definitely, the quantification of the myocardial water content by reference standards was crucial for demonstrating a consistent appearance of 2 consecutive waves of real edema during the first week after ischemia/reperfusion in our experimental study.

Dr. Zhang and colleagues point out that salvageable and infarct regions might follow disparate edema evolution patterns. From the cardiac magnetic resonance point of view, we agree that placing a region of interest in the full thickness of the left ventricular wall is troublesome as it will contain different myocardial states. However, the identification of "clean" regions clearly outside hemorrhage/microvascular obstruction areas may be extremely difficult and, more importantly, may be subjected to a big source of bias. The quantification of water content by reference standard in such small regions would be even more difficult to perform as this procedure needs to be done in a rapid and careful manner, avoiding tissue manipulation as much as possible. We tend to disagree with the idea that edematous and infarcted zones are equivalent to salvageable and hemorrhagic areas, respectively, as suggested by Dr. Zhang and colleagues. In any case, we believe that the possibility of including different myocardial states had little effect on the results reported in our work given that transmural extent of infarction was >80% in all evaluated segments containing the regions of interest, and the observed parallel course of T_2 relaxation times and water content.

Rodrigo Fernández-Jiménez, MD
Valentin Fuster, MD, PhD
***Borja Ibáñez, MD, PhD**

*Myocardial Pathophysiology Program
Centro Nacional de Investigaciones Cardiovasculares Carlos III (CNIC)
Melchor Fernández Almagro, 3.
Madrid 28029
Spain
E-mail: bibanez@cnic.es

http://dx.doi.org/10.1016/j.jacc.2015.02.070

Please note: The authors have reported that they have no relationships relevant to the contents of this paper to disclose. Derek Yellon, MD, served as Guest Editor for this paper.

REFERENCES

1. Fernández-Jiménez R, Sánchez-González J, Agüero J, et al. Myocardial edema after ischemia/reperfusion is not stable and follows a bimodal pattern: imaging and histological tissue characterization. J Am Coll Cardiol 2015;65:315–23.

2. Verhaert D, Thavendiranathan P, Giri S, et al. Direct T2 quantification of myocardial edema in acute ischemic injury. J Am Coll Cardiol Img 2011;4:269–78.

3. Kloner RA. New observations regarding post-ischemia/reperfusion myocardial swelling. J Am Coll Cardiol 2015;65:324–6.

4. Croisille P, Kim HW, Kim RJ. Controversies in cardiovascular MR imaging: T2-weighted imaging should not be used to delineate the area at risk in ischemic myocardial injury. Radiology 2012;265:12–22.

Myocardial Salvage, Area at Risk by T2w CMR

The Resolution of the Retrospective Radio Wave Paradigm?

In 2006, in an editorial published in a fellow journal by Pennell (1) T_2-weighted (T2w) cardiac magnetic resonance (CMR) imaging was presented as a promising method to retrospectively assess the myocardial area at risk. The area at risk could be reliably measured by contouring the myocardial edema using T2w sequences. The combination with late gadolinium-enhanced myocardial volume assessed during the same examination allowed the final infarct size measurement, and from there the simple and powerful concept of myocardial salvage was issued (2). Since then, numerous trials assessing new reperfusion strategies have used the salvage index as a clinical endpoint (3).

With this in mind, we read with great interest in the *Journal*, the paper by Fernández-Jiménez et al. (4). These investigators, relying on very solid and consistent work, unveil very new findings. They show with striking results that myocardial edema after ischemia reperfusion is highly variable and follows a bimodal pattern. These findings are novel and challenge the accepted view on the development of edema after an ischemic insult. In our opinion, these findings also significantly question the accepted view of T2w CMR as a reliable tool to assess the area at risk, and thus the myocardial salvage index, which we had already challenged recently (5).

Although the investigators are very cautious about this topic in their paper, we would value their opinion on this debated issue of CMR retrospective accuracy to assess the area at risk. Also, considering that these investigators have used the myocardial salvage index as an endpoint in a previous trial (3), we would

appreciate their opinion on the use of such an index in the light shed by their paper.

*Nathan Mewton, MD, PhD
Pierre Croisille, MD, PhD
Michel Ovize, MD, PhD

*Hopital Cardiologique Louis Pradel
Centre d'Investigation Clinique, Institut National de la Santé et de la Recherche Médicale 1407
28 avenue du Doyen Lepine
Lyon, Rhone 69677
France
E-mail: nathan.mewton@chu-lyon.fr or nmewton@gmail.com

http://dx.doi.org/10.1016/j.jacc.2015.02.068

Please note: The authors have reported that they have no relationships relevant to the contents of this paper to disclose. Derek Yellon, MD, served as Guest Editor for this paper.

REFERENCES

1. Pennell D. Myocardial salvage: retrospection, resolution, and radio waves. Circulation 2006;113:1821–3.

2. Friedrich MG, Abdel-Aty H, Taylor A, Schulz-Menger J, Messroghli D, Dietz R. The salvaged area at risk in reperfused acute myocardial infarction as visualized by cardiovascular magnetic resonance. J Am Coll Cardiol 2008;51:1581–7.

3. Ibanez B, Macaya C, Sánchez-Brunete V, et al. Effect of early metoprolol on infarct size in ST-segment-elevation myocardial infarction patients undergoing primary percutaneous coronary intervention: the Effect of Metoprolol in Cardioprotection During an Acute Myocardial Infarction (METOCARD-CNIC) trial. Circulation 2013;128:1495–503.

4. Fernández-Jiménez R, Sánchez-González J, Agüero J, et al. Myocardial edema after ischemia/reperfusion is not stable and follows a bimodal pattern: advanced imaging and histological tissue characterization. J Am Coll Cardiol 2015;65:315–23.

5. Mewton N, Rapacchi S, Augeul L, et al. Determination of the myocardial area at risk with pre- versus post-reperfusion imaging techniques in the pig model. Basic Res Cardiol 2011;106:1247–57.

REPLY: Myocardial Salvage, Area at Risk by T2w CMR

The Resolution of the Retrospective Radio Wave Paradigm?

We appreciate the interest and comments from Dr. Mewton and colleagues about our recently published work (1). In the context of myocardial infarction (MI), tissue edema appears initially in the form of cardiomyocyte swelling during the early stages of ischemia and is then significantly exacerbated on restoration of blood flow to the ischemic region (2). The relationship between MI and disturbed cardiac magnetic resonance (CMR) T_2 was initially reported 3 decades ago. However, the potential correlation between the extent of post-MI altered T_2-weighted CMR imaging and the actual area at risk (AAR) was not proposed until 2006 (3). After this initial in vivo report, the extent of post-MI T_2 CMR alteration has been exponentially used to quantify the extent of AAR, assuming its accuracy in this regard. For many years, the post-MI edematous reaction was assumed to appear early after ischemia/reperfusion and to persist in stable form for at least 1 week. Our recent report on the post-ischemia/-reperfusion bimodal edema phenomenon (1) disrupts this classical view and calls for revisiting the assumptions described here.

Dr. Mewton and colleagues raise a highly relevant issue: What are the implications of our findings for the retrospective AAR (and myocardial salvage) quantification? Given that myocardial edema fluctuates during the first week after MI, it seems intuitive to argue that CMR-based AAR quantification will vary during the initial days after reperfusion, yet this is to be formally proven. Our data suggest that the use of CMR-based surrogate markers of infarct size (i.e., normalized to AAR) in clinical trials evaluating the effect of cardioprotective therapies, while interesting to reduce sample size, is a risky business. This call of warning is not new, and has been previously proposed by other investigators (including Dr. Mewton and colleagues), and our work supports this precaution. Please note, given the controversy in the field, in our recently published METOCARD-CNIC (Effect of Metoprolol in Cardioprotection During an Acute Myocardial Infarction) trial, we intentionally chose total infarct size as the primary endpoint, having salvage index as a secondary analysis (4,5).

Rodrigo Fernández-Jiménez, MD
Valentin Fuster, MD, PhD
*Borja Ibáñez, MD, PhD

*Myocardial Pathophysiology Program
Centro Nacional de Investigaciones Cardiovasculares Carlos III (CNIC)
Melchor Fernández Almagro, 3
Madrid 28029
Spain
E-mail: bibanez@cnic.es

http://dx.doi.org/10.1016/j.jacc.2015.02.071

Please note: The authors have reported that they have no relationships relevant to the contents of this paper to disclose. Derek Yellon, MD, served as Guest Editor for this paper.

REFERENCES

1. Fernández-Jiménez R, Sánchez-González J, Agüero J, et al. Myocardial edema after ischemia/reperfusion is not stable and follows a bimodal pattern: imaging and histological tissue characterization. J Am Coll Cardiol 2015;65:315–23.

2. Kloner RA. New observations regarding post-ischemia/reperfusion myocardial swelling. J Am Coll Cardiol 2015;65:324–6.

3. Aletras AH, Tilak GS, Natanzon A, et al. Retrospective determination of the area at risk for reperfused acute myocardial infarction with T2-weighted cardiac magnetic resonance imaging: histopathological and displacement encoding with stimulated echoes (DENSE) functional validations. Circulation 2006;113:1865–70.

4. Ibanez B, Macaya C, Sánchez-Brunete V, et al. Effect of early metoprolol on infarct size in ST-segment-elevation myocardial infarction patients undergoing primary percutaneous coronary intervention: the Effect of Metoprolol in Cardioprotection During an Acute Myocardial Infarction (METOCARD-CNIC) trial. Circulation 2013;128:1495–503.

5. Pizarro G, Fernández-Friera L, Fuster V, et al. Long-term benefit of early pre-reperfusion metoprolol administration in patients with acute myocardial infarction: results from the METOCARD-CNIC trial (Effect of Metoprolol in Cardioprotection During an Acute Myocardial Infarction). J Am Coll Cardiol 2014;63:2356–62.

Noninferiority of 6 Versus 12 Months of Dual Antiplatelet Therapy

With great interest, I read the article by Colombo et al. (1) that examined the noninferiority of 6 versus 12 months of dual antiplatelet therapy (DAPT) in patients undergoing percutaneous coronary intervention with second-generation drug-eluting stents. The investigators described in the Results section (p. 2091) that "There was at least 1 occurrence of the primary composite endpoint by 12 months in 31 patients in the 6-month DAPT group (4.5%; 95% CI: 2.9 to 6.1) and 27 patients in the 12-month DAPT group (3.7%; 95% CI: 2.3 to 5.1; $p = 0.469$) (Table 5). There was a 0.8% (95% CI: -2.4 to 1.7) difference in occurrence of the primary endpoint between the 6-month and 12-month groups. The upper limit of the 95% CI was lower than the pre-set margin of 2%, confirming the noninferiority hypothesis ($p < 0.05$)." However, on the basis of the result (31 of 682 vs. 27 of 717) in Table 5, the 95% confidence interval (CI) for the difference between 2 sample proportions is -1.3% to 2.9% (90% CI: -1.0 to 2.5). Therefore, the upper limit of the 95% CI appears more than the pre-set margin of 2%, rejecting the noninferiority hypothesis of 6 months versus 12 months of DAPT. It would be of great help if the investigators could provide the method they used to calculate 95% CI.

*Hideaki Kaneda, MD, PhD
*Okinaka Memorial Institute for Medical Research
2-2-2 Toranomon
Tokyo 105-8470
Japan
E-mail: hdkaneda@gmail.com

http://dx.doi.org/10.1016/j.jacc.2015.02.069

Please note: Dr. Kaneda has reported that he has no relationships relevant to the contents of this paper to disclose.

REFERENCE

1. Colombo A, Chieffo A, Frasheri A, et al. Second-generation drug-eluting stent implantation followed by 6- versus 12-month dual antiplatelet therapy: the SECURITY randomized clinical trial. J Am Coll Cardiol 2014;64:2086–97.

SECURITY Did Not Establish Noninferiority

In presenting the results of the SECURITY (Second-Generation Drug-Eluting Stent Implantation Followed by 6- Versus 12-Month Dual Antiplatelet Therapy) trial, Colombo et al. (1) concluded that "6 months of DAPT appeared noninferior to a 12-month regimen with respect to the primary composite endpoint." However, this conclusion, repeated several times in the paper, is not supported by the data.

The composite event was observed in 31 of 682 patients in the 6-month treatment arm, and in 27 of 717 patients in the 12-month arm. The risks were correctly reported as 4.5% versus 3.7%, and the risk difference as 0.8%. The 95% confidence interval was given as -2.4% to 1.7%, such that "the upper limit of the 95% CI was lower than the pre-set margin of 2%, confirming the noninferiority hypothesis." Unfortunately, the confidence bounds are incorrect. The tell-tale sign of a problem is the asymmetry; the confidence interval should be approximately symmetric about the point estimate of 0.8%. Reanalysis shows an asymptotic 95% confidence interval of -1.3% to 2.9%, which exceeds the noninferiority margin. If an exact confidence interval is preferred, which may be a good idea given the low numbers of events, the bounds are -1.7% to 3.9%. This means that the data are compatible with an absolute excess risk of a composite event of up to 2.9% (or 3.9%) in a patient treated for 6 months, compared with a patient treated for 12 months. Noninferiority up to an excess risk of 2% does not hold.

The problem remains if a 1-sided 95% confidence interval is obtained, as it should according to the Methods section. A 1-sided upper limit on the risk difference of 0.8% is 2.5% (asymptotic method) or 3.4% (exact method). In all instances, the upper limit exceeds the noninferiority margin.

Another issue that argues against noninferiority is the rather high proportion of patients (34%) in the 6-month treatment group who continued their medications beyond the scheduled stopping time. Non-compliance with the assigned treatment dilutes the contrast between the groups. This favors the null hypothesis and causes a conservative bias in superiority trials: indeed, if a significant difference is observed between the treatment arms despite noncompliance, the true difference must be even greater. In contrast, in a noninferiority trial, the bias caused by noncompliance runs against the tested

Letter to the Editor #3. “*Reply: waves of edema seem implausible*”.[77]

morphological features of coronary plaque in culprit lesions.

Various pathological types of vulnerable plaques (e.g., plaque rupture, plaque erosion, and calcified nodules) can cause thrombosis with or without luminal obstruction and could lead to acute coronary syndromes, including myocardial infarction and unstable angina (2). Plaque rupture is the most common cause of coronary thrombosis, accounting for approximately 70% of fatal coronary thrombi (3). Thin-capped fibroatheroma is the characteristic morphology of rupture-prone plaques, in which a thin and inflamed fibrous cap covers a large and soft lipid-rich necrotic core, frequently with positive remodeling mitigating luminal obstruction (mild stenosis by angiography) (2). In intravascular ultrasound studies, intravascular ultrasound-virtual histology-derived thin-capped fibroatheroma lesions are independently associated with adverse cardiovascular events (4). However, little is known about the natural history of thin-capped fibroatheroma and the detailed process of vulnerable plaque rupture, because most published studies have thus far been cross-sectional analyses, and none have presented changes on serial intravascular images.

What is the mechanism responsible for rupture of vulnerable plaques? Although it is still uncertain that coronary spasm could cause plaque rupture, Wang et al. (5) provided evidence for the important role of coronary spasm in triggering vulnerable plaque rupture. Accordingly, we believe that by combining the acetylcholine provocation test for the evaluation of vasomotor abnormalities and intravascular imaging for defining plaque morphology, we can identify patients at high risk for future adverse cardiovascular events.

Masanobu Ishii, MD
***Koichi Kaikita, MD, PhD**
Hisao Ogawa, MD, PhD
*Department of Cardiovascular Medicine
Graduate School of Medical Sciences
Kumamoto University
1-1-1, Honjo
Chuo-ku, Kumamoto, 860-8556
Japan
E-mail: kaikitak@kumamoto-u.ac.jp

http://dx.doi.org/10.1016/j.jacc.2016.01.051

Please note: The authors have reported that they have no relationships relevant to the contents of this paper to disclose.

REFERENCES

1. Ishii M, Kaikita K, Sato K, et al. Acetylcholine-provoked coronary spasm at site of significant organic stenosis predicts poor prognosis in patients with coronary vasospastic angina. J Am Coll Cardiol 2015;66:1105–15.

2. Falk E, Nakano M, Bentzon JF, Finn AV, Virmani R. Update on acute coronary syndromes: the pathologists' view. Eur heart J 2013;34:719–28.

3. Naghavi M, Libby P, Falk E, et al. From vulnerable plaque to vulnerable patient: a call for new definitions and risk assessment strategies: part I. Circulation 2003;108:1664–72.

4. Yun KH, Mintz GS, Farhat N, et al. Relation between angiographic lesion severity, vulnerable plaque morphology and future adverse cardiac events (from the Providing Regional Observations to Study Predictors of Events in the Coronary Tree study). Am J Cardiol 2012;110:471–7.

5. Wang LX, Lu SZ, Zhang WJ, Song XT, Chen H, Zhang LJ. Coronary spasm, a pathogenic trigger of vulnerable plaque rupture. Chin Med J 2011;124:4071–8.

"Waves of Edema" Seem Implausible

Fernández-Jiménez et al. (1) described a bimodal time course of myocardial edema in a pig model of ST-segment elevation myocardial infarction. We concur with their observations regarding a dynamic pattern in infarct zone T2, but "waves of edema" seem implausible.

We have studied myocardial hemorrhage in 245 patients with ST-segment elevation myocardial infarction (NCT02072850). In a serial imaging substudy (n = 30, 100% compliance), we observed a progressive increase in infarct zone T2 relaxation time in patients without myocardial hemorrhage, whereas in those with hemorrhage we observed a "bimodal" pattern for T2 (milliseconds) but not for edema (area-at-risk) (2). We conclude that the subacute reduction in T2 can be explained by the destructive paramagnetic effects of deoxyhemoglobin.

Myocardial hemorrhage is very common in reperfused pigs post-myocardial infarction (3). However, Fernández-Jiménez et al. (1) concluded that other myocardial states (i.e., myocardial hemorrhage) "had little effect on the results," despite finding that infarct-zone hemorrhage increased progressively to day 4 ($p = 0.02$).

They describe tissue water content on the basis of desiccation (1). This method provides no information on water distribution, and baking will also desiccate gelatinous blood clot.

Dark-blood T2 short-tau inversion recovery cardiac magnetic resonance imaging has suboptimal accuracy for imaging edema (4). Because the investigators' model involved anterior ST-segment elevation myocardial infarction (1), surface coil intensity issues may have rendered the inferoposterior ventricular wall dark and the anterior wall relatively bright.

Because of euthanasia, the initial population (n = 25) was reduced successively by 25% to 75% (1), and inevitably, results based on 5 animals are statistically

fragile. Conclusions that are based on nonrandomized, open-label drug assignment, partial blinding, and loss to follow-up of the majority should be viewed cautiously, especially when alternative explanations may be valid (2,3).

*Colin Berry, PhD
David Carrick, PhD
Caroline Haig, PhD
Keith G. Oldroyd, MD(Hons)

*BHF Glasgow Cardiovascular Research Centre
Institute of Cardiovascular and Medical Sciences
University of Glasgow
126 University Place
Glasgow, G12 8TA
United Kingdom
E-mail: colin.berry@glasgow.ac.uk

http://dx.doi.org/10.1016/j.jacc.2015.11.073

Please note: The authors are coinvestigators on the British Heart Foundation Project Grant (PG/11/2/28474; ClinicalTrials.gov identifier NCT02072850). Their research involves work-in-progress methods provided by Siemens Healthcare. The authors have reported that they have no relationships relevant to the contents of this paper to disclose. Joao Lima, MD, served as Guest Editor for this letter.

REFERENCES

1. Fernández-Jiménez R, García-Prieto J, Sánchez-González J, et al. Pathophysiology underlying the bimodal edema phenomenon after myocardial ischemia/reperfusion. J Am Coll Cardiol 2015;66:816–28.

2. Carrick D, Haig C, Ahmed N, et al. Temporal evolution of myocardial hemorrhage and edema in patients after acute ST-segment elevation myocardial infarction: pathophysiological insights and clinical implications. J Am Heart Assoc 2016;5:e002834.

3. Payne AR, Berry C, Kellman P, et al. Bright-blood T_2-weighted MRI has high diagnostic accuracy for myocardial hemorrhage in myocardial infarction: a preclinical validation study in swine. Circ Cardiovasc Imaging 2011;4:738–45.

4. Payne AR, Casey M, McClure J, et al. Bright-blood T2-weighted MRI has higher diagnostic accuracy than dark-blood short tau inversion recovery MRI for detection of acute myocardial infarction and for assessment of the ischemic area-at-risk and myocardial salvage. Circ Cardiovasc Imaging 2011;4:210–9.

REPLY: "Waves of Edema" Seem Implausible

We read the comments of Dr. Berry and colleagues on our recent study with great interest (1). On the basis of an imaging substudy of 30 patients with myocardial infarctions, they propose that the bimodal post-infarction T2 cardiac magnetic resonance imaging (CMR) pattern can be explained entirely by the effects of myocardial hemorrhage rather than by the existence of 2 distinct waves of edema. Interestingly, they state that patients with hemorrhages displayed a "bimodal" pattern for T2 but not for edema, an intriguing finding given that the identification of edema by CMR is based on T2.

We admire the important imaging work done by Berry's group. However, clinical studies by themselves are limited when it comes to mechanistic interpretation; despite the obvious differences from humans, pre-clinical animal models are the basis of progress in the understanding of pathophysiological mechanisms. It is also the case that desiccation remains a reference technique for water content quantification, although it is true that it does not differentiate between intra- and extracellular water components, as we have acknowledged (1,2). Using this technique, we were able to clearly demonstrate a bimodal post-infarction edematous reaction (1,3), and the dynamics of edema correlated with the observed CMR changes. We agree with Berry et al. that qualitative T2 CMR sequences have suboptimal accuracy for imaging edema, and for this reason, we included in all cases 2 quantitative T2-mapping methods, in addition to T2 short-tau inversion recovery (4). The evidence from these independent approaches, conducted in a human-like animal model, provide robust evidence that myocardial ischemia and reperfusion is followed by a genuinely bimodal edematous reaction.

We were challenged by the suggestion that "baking will also desiccate gelatinous blood clot," and we have performed new experiments to address this. Subjection of pig blood clots to the same desiccation protocol resulted in a mean water content of about 75%. If Berry et al. were correct and the edema at reperfusion (measured water content ~84% to 85%) were stable throughout reperfusion, hemorrhage could account for the measured water content values (~81% at 24 h) (1,3) only if it affects more than 40% of the infarcted region. However, hemorrhage affected "only" ~10% of the injury area at 24 h (unpublished data). In addition, if hemorrhage were the sole explanation for the bimodal T2 pattern, it would be difficult to understand why T2 and water content increased to day 4, coinciding with the peak of hemorrhage (1). These 2 lines of evidence (the extent of hemorrhage in the model and the coincidence of increased water content and T2 with peak hemorrhage) refute the interesting hypothesis proposed by Berry and colleagues.

Complex biological events seldom have single explanations, and we have consistently acknowledged (1–4) that T2 can be affected by other factors, including hemorrhage, in addition to myocardial water content. It is plausible that the observed bimodal post-infarction T2 pattern is due to at least 2 components: mainly the dynamic changes in myocardial water content and a lesser contribution from the classically described paramagnetic effect of hemoglobin denaturation (1,3).

Rodrigo Fernández-Jiménez, MD
Valentin Fuster, MD PhD
***Borja Ibanez, MD PhD**
*Myocardial Pathophysiology Program
Centro Nacional de Investigaciones
Cardiovasculares Carlos III
Melchor Fernández Almagro, 3
28029 Madrid
Spain
E-mail: bibanez@cnic.es

http://dx.doi.org/10.1016/j.jacc.2016.01.052

Please note: The authors thank Simon Bartlett (from Centro Nacional de Investigaciones Cardiovasculares Carlos III), who provided English editing. The authors have reported that they have no relationships relevant to the contents of this paper to disclose. Joao Lima, MD, served as Guest Editor for this letter.

REFERENCES

1. Fernandez-Jimenez R, Garcia-Prieto J, Sanchez-Gonzalez J, et al. Pathophysiology underlying the bimodal edema phenomenon after myocardial ischemia/reperfusion. J Am Coll Cardiol 2015;66:816–28.

2. Fernandez-Jimenez R, Fuster V, Ibanez B. Reply: myocardial edema should be stratified according to the state of cardiomyocytes within the ischemic region. J Am Coll Cardiol 2015;65:2356–7.

3. Fernandez-Jimenez R, Sanchez-Gonzalez J, Aguero J, et al. Myocardial edema after ischemia/reperfusion is not stable and follows a bimodal pattern: imaging and histological tissue characterization. J Am Coll Cardiol 2015;65:315–23.

4. Fernandez-Jimenez R, Sanchez-Gonzalez J, Aguero J, et al. Fast T2 gradient-spin-echo (T2-GraSE) mapping for myocardial edema quantification: first in vivo validation in a porcine model of ischemia/reperfusion. J Cardiovasc Magn Reson 2015;17:92.

Letter to the Editor #4. "*Letter by Fernandez-Jimenez et al regarding article, Protective effects of ticagrelor on myocardial injury after infarction*".[78]

Letter by Fernandez-Jimenez et al Regarding Article, "Protective Effects of Ticagrelor on Myocardial Injury After Infarction"

Rodrigo Fernandez-Jimenez, MD
Javier Sanchez-Gonzalez, PhD
Borja Ibanez, MD, PhD

To the Editor:

We read with interest the article by Vilahur and colleagues.[1] The authors should be congratulated for using the human-like pig model of ischemia/reperfusion to provide evidence that ticagrelor may limit myocardial injury (necrosis and edema formation), as measured by cardiac magnetic resonance (CMR).

Given that CMR can accurately identify myocardial areas with high water content, it has been widely used in the past years to retrospectively delineate the myocardium at risk (MaR). It is interesting to note that it has been assumed that the postischemia/reperfusion edematous reaction is stable for several days after myocardial infarction. On this basis, experimental and clinical studies performed CMR examinations at a variable time after myocardial infarction. Our group recently demonstrated in a pig model of transmural myocardial infarction that myocardial edema after ischemia/reperfusion is not stable but rather follows a bimodal pattern.[2] In this model, an initial hyperacute edema reaction on reperfusion largely resolves within 24 hours, and is followed by a deferred healing-related edema wave occurring a few days after reperfusion.[3] This coordinated bimodal edema pattern suggests that CMR-quantified MaR may vary according to the day of imaging and degree of injury (and subsequent healing), but to date this has not been tested in a controlled manner.

In the present article,[1] intriguing data about histological (blue-dye injection) versus CMR (edema) measurements of the MaR are presented. Although the median of histological reference MaR was similar in all experimental groups (≈50% of the left ventricle), an important underestimation of MaR by T2-weighted short-tau inversion recovery CMR was reported at 24 hours in all study groups. Although individual comparison is not possible with the data presented, it is remarkable that even in placebo animals, a ≈25% underestimation of MaR by CMR was observed (47.5% of left ventricle by histology versus 36.2% by 24-hour CMR). Thus, it seems plausible that the physiological resorption of the initial wave of edema contributed to these histology-CMR discrepancies. In fact, according to the data presented, salvage index quantification [1 – (infarct size/MaR), %] in placebo animals using dye histology or 24-hour CMR would be as disparate as 14% or 35%, respectively.

Consequently, although the infarct-limiting effect of ticagrelor in this article is robust, its effect on edema is less. The authors used T2-weighted short-tau inversion recovery CMR sequence, which suffers from technical limitations. Conversely, quantitative T2 mapping has been shown to strongly correlate with actual myocardial water content measurements.[4] It might be that the use of T2 mapping and, especially, a serial imaging protocol, including a hyperacute and later time points, would have helped in the interpretation of the mechanisms leading to injury sparing by ticagrelor.

Overall, we believe that the work by Vilahur et al adds incremental evidence of the risks of using nonstandardized CMR protocols and timings to measure MaR.

Circulation is available at http://circ.ahajournals.org.

Circulation. 2017;135:e1002–e1003. DOI: 10.1161/CIRCULATIONAHA.116.026578

DISCLOSURES

Dr Sánchez-González is an employee of Philips Healthcare. The other authors have no conflicts to disclose.

AFFILIATIONS

From Centro Nacional de Investigaciones Cardiovasculares Carlos III (CNIC), Madrid, Spain (R.F.-J., B.I.); CIBER de enfermedades CardioVasculares (CIBERCV), Madrid, Spain (R.F.-J., B.I.); Philips Healthcare, Madrid, Spain (J.S.-G.); and IIS-Fundación Jiménez Díaz University Hospital, Madrid, Spain (B.I.).

REFERENCES

1. Vilahur G, Gutiérrez M, Casani L, Varela L, Capdevila A, Pons-Lladó G, Carreras F, Carlsson L, Hidalgo A, Badimon L. Protective effects of ticagrelor on myocardial injury after infarction. *Circulation*. 2016;134:1708–1719. doi: 10.1161/CIRCULATIONAHA.116.024014.
2. Fernández-Jiménez R, Sánchez-González J, Agüero J, García-Prieto J, López-Martín GJ, García-Ruiz JM, Molina-Iracheta A, Rosselló X, Fernández-Friera L, Pizarro G, García-Álvarez A, Dall'Armellina E, Macaya C, Choudhury RP, Fuster V, Ibáñez B. Myocardial edema after ischemia/reperfusion is not stable and follows a bimodal pattern: imaging and histological tissue characterization. *J Am Coll Cardiol*. 2015;65:315–323. doi: 10.1016/j.jacc.2014.11.004.
3. Fernández-Jiménez R, García-Prieto J, Sánchez-González J, Agüero J, López-Martín GJ, Galán-Arriola C, Molina-Iracheta A, Doohan R, Fuster V, Ibáñez B. Pathophysiology underlying the bimodal edema phenomenon after myocardial ischemia/reperfusion. *J Am Coll Cardiol*. 2015;66:816–828. doi: 10.1016/j.jacc.2015.06.023.
4. Fernández-Jiménez R, Sánchez-González J, Aguero J, Del Trigo M, Galán-Arriola C, Fuster V, Ibáñez B. Fast T2 gradient-spin-echo (T2-GraSE) mapping for myocardial edema quantification: first *in vivo* validation in a porcine model of ischemia/reperfusion. *J Cardiovasc Magn Reson*. 2015;17:92. doi: 10.1186/s12968-015-0199-9.

4 DISCUSSION

The results presented in this thesis work have been discussed in detail in the manuscripts published as a part of this dissertation. Nevertheless, a critical discussion of such results in the context of previous literature and evolving studies in the field can be found in this section.

4.1 First demonstration of the post-infarction bimodal edema reaction

Because edema has been perceived as both stable and persistent during at least 1 week after myocardial I/R, numerous experimental and clinical studies have used T2W CMR imaging to retrospectively evaluate the edematous reaction associated with MI as a marker of “ischemic memory”. However, T2W imaging is subject to several technical limitations and does not offer quantitative T2 relaxation time tissue measurements that would allow for comparisons between different studies. Recently developed quantitative T2 mapping methods have been proposed to overcome at least some of the limitations for the detection and quantification of myocardial edema.[53, 79] However, most of proposed T2 mapping sequences are time-consuming, and are thus mostly used as a research tool. As a part of this thesis work, we initially performed an in vivo validation of a T2 GraSE mapping method that could be easily integrated in routine protocols, and used in our subsequent experimental and clinical work for a fast and accurate quantification and tracking of myocardial edema.[69]

The results presented in this thesis work challenge the accepted view of the development of post-I/R myocardial edema. We first showed, through state-of-the-art CMR analysis and histological validation in a pig model of I/R, that the edematous reaction during the first week after reperfusion is not stable, instead following a bimodal pattern.[70] A first wave appears abruptly upon reperfusion and dissipates at

24 hours. Conversely, a second wave of edema appears progressively days after I/R and increases to a maximum on postreperfusion day 7. To the best of our knowledge, this was the first study to comprehensively characterize the time course of myocardial edema during the first week after I/R, covering from very early to late reperfusion stages. In a previous study, Foltz et al. suggested a similar myocardial T2 relaxation time course in a pig model of I/R, with CMR scans at days 0, 2, and 7 after reperfusion.[80, 81] However, this study lacked histological validation of myocardial water content, and the observed T2 relaxation time fluctuations were interpreted as reflecting the oxidative denaturation of hemoglobin to methemoglobin rather than fluctuations in actual myocardial water content. The histological validation performed in the experiments presented in this dissertation demonstrates the consistent appearance of two consecutive waves of edema during the first week after I/R, a groundbreaking concept in the field.

Remarkably, we were able to replicate these results in the clinical setting.[74] Thus, we demonstrated for the first time that myocardial edema in the ischemic area after MI in humans is not stable, but rather follows a systematic bimodal pattern. In the same way as shown in the preclinical setting, an initial wave of edema appears abruptly very early after reperfusion but it is significantly attenuated by 24 hours. This is followed by a second (deferred) wave of edema several days after reperfusion reaching a plateau around days 4 to 7 after MI. CMR scans timing was designed as per the protocol of our previous experimental studies, in which we demonstrated the existence of bimodal post-MI edema in pigs,[69, 70, 72, 73] including the hyperacute post-reperfusion period (the first 3 hours after primary PCI). Noteworthy, to select the optimal timing for the first CMR scan in ST-segment elevation MI patients, we first analyzed the dynamics of the initial wave of edema in a series of 5 pigs; serial CMR scans were performed every 20 minutes until the reperfusion-related edema wave faded.[74] Interestingly, this initial wave of edema peaked very early, being significantly attenuated within a few hours after MI: at 180 minutes after reperfusion the edema had declined by approximately 50% from its maximum. In agreement with CMR data, quantification of myocardial water content and histological analysis at 6 hours after MI revealed partial resolution of the massive interstitial edema seen earlier after reperfusion.[72] On the basis of these results in pigs, we decided to perform the first CMR scan in patients within a narrow

3-hour time-window after primary PCI to be able to detect the noon of the initial wave of edema.

4.2 Pathophysiology underlying the post-infarction edema reaction

Under the hypothesis that the initial wave of edema is a direct consequence of reperfusion while the deferred wave is caused by healing processes, we then manipulated each wave independently through the use of reperfused and nonreperfused MI models, and exposure to high-dose steroid therapy, interventions that are known to alter healing processes.[72] The absence of reperfusion almost completely abolishes the initial wave, indicating that it is a direct consequence of the reperfusion process. The deferred wave is substantially altered by interventions that impair healing in the post-infarcted myocardium (absence of reperfusion and high-dose steroid therapy), thus implicating tissue healing processes in this second phase of edema. Moreover, these processes can be visualized and quantified by state-of-the-art contemporaneous T2 CMR sequences, a finding of special translational relevance.

We later studied the impact of cardioprotective strategies (preconditioning and post-conditioning) and ischemia duration on the temporal evolution and extent of myocardial edema and other tissue composition changes (necrosis, IMH and MVO) by CMR.[73] Our results showed that preconditioning (a potent cardioprotective strategy) and short ischemia duration have a major impact on the intensity and dynamics of post-MI edema. Preconditioning reduced the initial edema wave and also the deferred wave, which peaked early, on day 4, contrasting with the peak on day 7 in control animals. Shortening the duration of coronary occlusion to 20 minutes (20min-I/R) also blunted initial edema wave, and in this case the second edema wave was absent. These CMR results are consistent with histologically determined water content at day 7 after MI, which was reduced in pigs undergoing preconditioning and within the normal range in pigs undergoing short-duration ischemia. The cardioprotection (reduced infarct size) afforded by preconditioning or short-duration ischemia was demonstrated by CMR and histology. In pigs undergoing short-duration ischemia necrosis was barely detectable, and so was

edema from day 1 on, supporting the notion that the deferred edema wave is related to post-MI healing.

We finally characterized the dynamic changes that take place in both the ischemic and remote myocardium during the first week after infarction in a clinically relevant animal model at the molecular level. This was undertaken by high-throughput multiplexed quantitative proteomics and histological analyses of pig myocardium at different times during the first week after I/R.[71] In a first screening approach, we provided a detailed pattern of the time-course behavior of more than 5,000 proteins in both the ischemic and remote areas. This was followed by a further validation step in which we focused on most relevant protein changes. Our results reveal a highly coordinated, multimodal pattern of functional protein alterations in both myocardium regions in the early post-MI stages. Most notably, the remote myocardium undergoes transitory alterations in the contractile machinery that result in a stunned myocardium within the first 24 hours.

Elucidation of the pathophysiology and molecular mechanisms underlying bimodal post-I/R edema has potential translational implications in diagnosis, prognosis, and therapy. Pharmacological or other interventions targeting the pathways implicated in the initial or deferred waves of post-I/R edema could contribute to better cardiac recovery and remodeling, and thus improve prognosis in patients experiencing an acute MI.

4.3 Implications for quantifying myocardium at risk and salvage

The disparate time points examined in different experimental and clinical studies are an important source of confusion in CMR evaluation of post-I/R edema. In parallel with T2 relaxation changes, we confirmed significant variation in the extent of the MaR as measured by T2W-STIR CMR both in the experimental and clinical setting.[73, 74] Consistent with the drop in T2 relaxation time at 1 day post-MI, T2W-estimated MaR at this time point was significantly lower than values obtained before and subsequently. Remarkably, we included pre-reperfusion contrast computed tomography imaging as a reference for the assessment of MaR in the preclinical work,[82, 83] which otherwise we considered unethical to perform in acute MI patients. More pronounced dynamic tissue changes were shown in the experimental model. This is a common phenomenon seen in the preclinical setting in which many

variables are controlled, as opposed to clinical studies. In addition, the more severe ischemic process in the porcine myocardium in the presence of poor collateral circulation, among other reasons, could influence the magnification of this phenomenon. However, the parallel courses of T2 and CMR-MaR fluctuations observed in the clinical and experimental settings strengthen the existence of a real bimodal edematous reaction after MI.

Thus, our data suggest that between day 4 and day 7 would be a good compromise solution for the delineation of theoretical MaR. Nevertheless, our results highlight the need for caution in interpreting CMR of the post-MI heart. In the clinical study, several patients showed more limited changes in T2 and extent of edema. Remarkably, these patients were older and showed significantly smaller infarcts and less extent of IMH and MVO, and greater myocardial salvage areas despite having longer intervals between symptom onset to reperfusion. We speculate that there might be several factors affecting the dynamics of the bimodal edematous reaction such as the existence of preformed collateral circulation, episodes of spontaneous reperfusion/re-occlusion during ischemia duration, or the presence of specific comorbidities. The impossibility of controlling these aspects in the clinical scenario, and the limited sample size preclude any definitive conclusion in this regard, but warrants further clinical studies.

As compared to T2W-STIR, parametric T2-mapping might improve the detection and quantification of myocardial edema; however, it is unlikely to alter the dynamic pattern of post-MI edema that is due to pathophysiological phenomena. The deferred edema wave is related to the post-MI healing process, and therefore interventions that protect the myocardium could affect the dynamics of edema, and thus bias MaR estimation. This idea was supported by recent suggestions that the extent of edema can be affected by the degree of damage[28] or exposure to infarct-limiting interventions.[54-56] However, patients in these studies received one CMR examination at a single time point, which was not the same for all. Therefore a dedicated study was needed to provide evidence to support this hypothesis, which was tested in a subsequent set of experiments.

By performing ad hoc experiments, we demonstrated that the dynamics of post-ischemia edema are altered by cardioprotective strategies and ischemia duration, with further implications for CMR measured MaR and salvage.[73] Thus, the smaller

extent of edema at reperfusion in pigs that underwent preconditioning or short-duration ischemia was associated with less prolonged T2 relaxation time and lower degree of myocardial swelling. Interestingly, these 2 groups of cardioprotected animals had significantly smaller infarcts on day 7. This would imply that interventions that protect the myocardium could affect edema dynamics, therefore having an impact on CMR estimations of MaR and salvage, as suggested by indirect preclinical[84, 85] and clinical[54-56] data before. However, whether any intervention that reduces infarct size diminishes myocardial edema remains to be demonstrated.

4.4 Evolving controversy

The recent demonstration of a bimodal edema in the post-ischemic myocardium in pigs[70, 72] and humans[74] has generated intense discussion in the cardiac imaging field.[14, 18, 75-78, 86-93] Given that T2 can be affected by hemorrhage, some authors have argued that the bimodal post-MI T2 pattern could be explained entirely by the destructive paramagnetic effects of deoxyhemoglobin, rather than by a real fluctuation of tissue water content.[89, 94] However, if hemorrhage was the sole explanation for the bimodal T2 pattern, it would be difficult to understand why T2 (both in the pig model[70] and in the clinical study[74]) and water content (in the pig model) increased to day 4, coinciding with the maximum extent of hemorrhage.[72, 73] In fact, in the clinical study we observed no significant influence of IMH on T2 relaxation time or area of edema delineation. The finding that infarcted (either with or without IMH areas) and salvaged myocardium displayed the same bimodal pattern strengthen our results. In line with our data, Carrick, et al., found small differences in T2 (< 5 ms) between patients with and without hemorrhage;[94] while Hammer-Hansen, et al., found that T2 relaxation time differed in the infarcted and salvaged myocardium, and both were significantly longer than remote in the post-reperfused dog heart.[95] Interestingly, the later study followed animals at 4 and 48 hours after MI with results indicating a partial resolution of edema in the first 48 hours after reperfusion.[88, 95] Nevertheless, hemorrhage might exert some influence on T2 relaxation time, as we previously conceded.[69, 70, 72, 77]

Whether this phenomenon occurs in humans has been explored in 3 recent studies. Carrick and colleagues performed a longitudinal assessment of IMH and edema in 30 ST-segment elevation MI patients, concluding that “myocardial edema has a

unimodal time course".[94] This population was more heterogeneous than the population examined in our work: 20% had an open artery on angiography (TIMI coronary flow grade 2-3) and only 30% had an anterior MI, whereas all patients in our study had an anterior infarction with an occluded artery on angiography. These factors might affect edema dynamics and visualization.[38, 72] In addition, patients in the Carrick, et al., study underwent 3 CMR exams within the first 10 days after MI, at 8.6±3.1 hours, 2.9±1.5 days, and 9.6±2.3 days.[94] Importantly, the first of these examinations was performed between 4 and 12 hours after reperfusion, which according to the experimental data we present here is during the dissipation of the first wave of edema. In fact, the T2 relaxation times in the infarcted zone reported for the first CMR examination in the work by Carrick, et al., are similar to those observed in the second scan in our clinical study, performed 24 hours after MI.

In a second report, Nordlund, et al., retrospectively analyzed pooled data from 3 studies assessing the MaR by qualitative CMR, concluding that no bimodal edema pattern was apparent.[96] However, most patients in the evaluated studies underwent a single CMR scan at disparate times to from each other, and there were no systematic serial examinations. Importantly, no CMR scans were performed on day 0, and very few were performed on day 1 after MI. Moreover, no quantitative parametric T2-mapping was performed, despite this technique being demonstrated to improve detection and quantification of myocardial edema.

Finally, Stiermaier and colleagues retrospectively compared MaR, infarct size and salvage according to the time between infarction and CMR imaging in a large multicenter ST-segment elevation MI cohort.[97] Their results did not provide sound evidence for a dynamic edematous reaction. Otherwise, they observed a slight rise and fall of MaR that was congruent with the amount of infarct size over the course of the first week after MI which is likely to be explained by the non-longitudinal retrospective nature of their data. Even more importantly, few CMR scans were performed within first 24 hours after reperfusion, and no CMR exams covered the first 12 hours after reperfusion when the first peak of edema was observed in our studies. Unlike these recent reports, our clinical study was specifically designed to provide insight into the existence of bimodal edema in MI patients by mimicking time-points and CMR sequences performed in the previous experimental studies.[70, 72, 73]

4.5 Limitations

Extrapolation of the experimental results to the clinic should be done with caution. Nonetheless, the pig is one of the most clinically translatable large animal models for the study of reperfused MI as discussed before. The similar edema and hemorrhage time courses in the pig and the patient cohort[74] highlight the great translational value of the pig model, especially considering the difficulty of performing a comprehensive CMR study that includes serial examinations within the first hours after reperfusion and reference methods for assessing the actual MaR. Nevertheless, the fact that myocardial edema and positive gadolinium enhanced areas follow a disparate dynamic pattern after I/R highlights the complexity of measuring myocardial salvage in real practice.

The nature of the experimental study, that is, longitudinal follow-up, precluded individual histological reference standard measurements of area at risk (i.e., Evans Blue by coronary re-occlusion), infarct size (i.e., triphenyl tetrazolium chloride), or MVO (thioflavin-S) at each time point. In addition, the heart was harvested at sacrifice to perform reference standard myocardial water content measurements and histological quantification of different tissue components, which otherwise might be altered by such procedures. It is fair to acknowledge that although previous studies have used histological standards to validate the use of CMR to measure infarct size and MVO,[98-100] and multi-detector computed tomography to measure MaR,[82, 83] there is probably no perfect noninvasive method for such purposes.

Similarly to the experimental study, only anterior ST-segment elevation MI patients were recruited to the clinical study. The reasons for this choice include the avoidance of possible magnetic-field non-homogeneity related to the inferolateral wall.[44] These eligibility criteria closely resemble recommendations for patient selection in clinical trials of cardioprotective interventions.[35, 36] The bimodal edema pattern may occur regardless of MI location; however, caution should be exercised when extrapolating results to other MI locations, especially regarding adequate visualization of the phenomenon by T2W CMR in lateral MI where signal loss due to through-plane cardiac motion might occur.[38] Given that patients were serially scanned, including one examination very early after reperfusion, we planned the shortest CMR protocol possible. For this reason we did not include T2* CMR as a diagnostic method for quantifying IMH in vivo.[44] Instead, we assessed both edema

and hemorrhage by T2W-STIR imaging, a sequence validated and used for these purposes by many authors.[32]

There is no consensus on a standardized method for the identification of MaR on T2W CMR imaging.[101] Underestimation of the maximum intensity at time points exhibiting shorter myocardial T2, i.e. 24 hour and day 40, could potentially bias results in the case of the full-width at half-maximum method. However, we believe the region of interest (ROI) selection as initial threshold for the full-width at half-maximum method did not have a significant impact in our results for several reasons. First, the blinded analysis included manual correction and visual border delineation after initial thresholding. Second, the hemorrhagic area was larger at day 4 and day 7 coinciding with the largest edematous area delineated. Third, the demonstration of a similar bimodal edema pattern by the use of a quantitative and more objective method, i.e. T2-mapping, both in the human and pig myocardium strongly supports our findings.

In the experimental studies, the ROI for quantification of T2 relaxation time were placed in the entire wall thickness, then were carefully and individually adjusted by hand to avoid the right and left ventricular cavities. Therefore, ROI might include different myocardial states (i.e., IMH and/or MVO). We took this approach to mimic the histological water content evaluation, which was performed in the entire wall thickness, and because the differentiation of such small areas might be challenging. This might have contributed to the differences in absolute T2 relaxation time between our study and others taking a different approach to ROI selection.[91, 95] In contrast, in the clinical study T2 maps were analyzed by placing different ROI at the transmural ischemic, infarcted (with or without including areas suggestive of IMH), salvage, and transmural remote areas in order to stratify myocardial edema according to the state of cardiomyocytes within the ischemic region. The different myocardial states were initially defined by the localization relative to late gadolinium enhanced defined infarction, as previously described by others.[95]

Finally, it is fair to acknowledge that the limited sample of MI patients included in our clinical study and the fact that this is a first time ever-described phenomenon both in the preclinical and clinical setting warrants further confirmation in other experimental settings and larger clinical cohorts, ideally performed by external independent groups.

5 CONCLUSIONS

1. Post-myocardial infarction tissue composition is highly dynamic and can be characterized by cardiac magnetic resonance, which has been used to assess surrogate outcomes and efficacy endpoints in many experimental and clinical studies.

2. Accounting for the temporal dynamics, pathophysiology and factors affecting post-myocardial infarction tissue composition might be crucial for a precise assessment of related imaging endpoints. However, to date this has not been studied in a comprehensive manner.

3. Given its shorter acquisition time, high accuracy in quantifying T2 relaxation time and good correlation with actual myocardial water content, and no requirement for specific software for data acquisition or post-processing, fast T2 gradient-spin-echo mapping of the heart is an attractive alternative to current cardiac magnetic resonance methods for T2 and edema quantification.

4. Contrary to the accepted view, it is shown for the first time that myocardial edema in the week after ischemia/reperfusion is a bimodal phenomenon.

5. The initial wave of edema, appearing abruptly on reperfusion and dissipating at 24 hours, is directly secondary to the reperfusion process itself. The deferred wave of edema, appearing progressively days after ischemia/reperfusion and reaching a plateau between days 4 to 7, is mainly caused by tissue healing processes.

6. The temporal dynamics and extent of post-myocardial infarction tissue composition changes seem to be greatly influenced by the timing of imaging, the application of cardioprotective interventions, the duration of the index ischemia, and the interplay between them.

7. Consequently, the bimodal edematous response after myocardial infarction has a major impact on the retrospective delineation of myocardial area at risk and salvage quantification by cardiac magnetic resonance.

8. These findings highlight the need for protocol standardization when using post-infarction imaging methods to measure relevant efficacy and prognostic endpoints in experimental and clinical studies.

9. The timeframe between day 4 and 7 post-infarction seems a good compromise solution according to the translational data here presented. However, further studies and expert consensus are needed to stablish more precise recommendations.

CONCLUSIONES

1. La evolución de la composición del tejido miocárdico post-infarto es un proceso muy dinámico que se puede caracterizar mediante resonancia magnética cardíaca. Ello se ha utilizado para evaluar parámetros de eficacia terapéutica y pronósticos en multitud de estudios experimentales y clínicos.

2. El conocimiento de la evolución temporal, fisiopatología y factores que influyen en la composición del tejido miocárdico post-infarto es clave para una evaluación precisa de dichos parámetros de eficacia y pronósticos. Sin embargo, esto no se ha estudiado previamente de una forma detallada.

3. La secuencia de mapeo cardíaco T2 basada en el método spin eco de gradiente es una buena alternativa a las secuencias actuales de resonancia

magnética cardíaca para la determinación del tiempo de relajación T2 y la cuantificación del edema miocárdico, dado que ofrecen una alta precisión en la cuantificación del tiempo de T2 y buena correlación con la cantidad de agua presente en el tejido al mismo tiempo que un menor tiempo de adquisición, y la ausencia de requerimientos técnicos específicos para la adquisición y post-procesado de las imágenes.

4. Contrariamente a la visión establecida, se demuestra por primera vez que el edema miocárdico en la semana posterior al proceso de isquemia/reperfusión es un fenómeno bimodal.

5. La onda de edema inicial, que aparece abruptamente tras la reperfusión y que se disipa alrededor de las 24 horas, está directamente relacionada con el propio proceso de reperfusión. La onda de edema posterior, que aparece progresivamente días después del proceso de isquemia/reperfusión y alcanza una meseta entre el día 4 al 7, está originada fundamentalmente por los procesos de cicatrización del tejido.

6. La evolución temporal y la magnitud de los cambios en la composición tisular del miocardio post-infarto están muy influenciados por el momento temporal en que se evalúa al individuo, la duración de la isquemia, la utilización de estrategias cardioprotectoras, y la interacción entre estos factores.

7. Como consecuencia, la evaluación retrospectiva del miocardio en riesgo y la cuantificación del área salvada mediante resonancia magnética cardíaca están muy afectadas por la respuesta edematosa bimodal post-infarto.

8. Estos hallazgos ponen de relieve la necesidad de estandarizar los protocolos de imagen cardíaca cuyo objeto sea evaluar parámetros de eficacia terapéutica y pronósticos en estudios experimentales y clínicos.

9. En base a los resultados translacionales que aquí se presentan, el período de tiempo comprendido entre el día 4 y el 7 después del infarto pudiera ser

un buen momento para este fin. Sin embargo, se necesitan estudios adicionales y un consenso de expertos para establecer recomendaciones más precisas.

6 REFERENCES

1. Reed GW, Rossi JE and Cannon CP. Acute myocardial infarction. *Lancet*. 2017;389:197-210.

2. Menees DS, Peterson ED, Wang Y, Curtis JP, Messenger JC, Rumsfeld JS and Gurm HS. Door-to-balloon time and mortality among patients undergoing primary PCI. *The New England journal of medicine*. 2013;369:901-9.

3. Nallamothu BK, Normand SL, Wang Y, Hofer TP, Brush JE, Jr., Messenger JC, Bradley EH, Rumsfeld JS and Krumholz HM. Relation between door-to-balloon times and mortality after primary percutaneous coronary intervention over time: a retrospective study. *Lancet*. 2015;385:1114-22.

4. Benjamin EJ, Blaha MJ, Chiuve SE, Cushman M, Das SR, Deo R, de Ferranti SD, Floyd J, Fornage M, Gillespie C, Isasi CR, Jimenez MC, Jordan LC, Judd SE, Lackland D, Lichtman JH, Lisabeth L, Liu S, Longenecker CT, Mackey RH, Matsushita K, Mozaffarian D, Mussolino ME, Nasir K, Neumar RW, Palaniappan L, Pandey DK, Thiagarajan RR, Reeves MJ, Ritchey M, Rodriguez CJ, Roth GA, Rosamond WD, Sasson C, Towfighi A, Tsao CW, Turner MB, Virani SS, Voeks JH, Willey JZ, Wilkins JT, Wu JH, Alger HM, Wong SS, Muntner P, American Heart Association Statistics C and Stroke Statistics S. Heart Disease and Stroke Statistics-2017 Update: A Report From the American Heart Association. *Circulation*. 2017;135:e146-e603.

5. Eapen ZJ, Tang WH, Felker GM, Hernandez AF, Mahaffey KW, Lincoff AM and Roe MT. Defining heart failure end points in ST-segment elevation myocardial infarction trials: integrating past experiences to chart a path forward. *Circulation Cardiovascular quality and outcomes*. 2012;5:594-600.

6. Ambrosy AP, Fonarow GC, Butler J, Chioncel O, Greene SJ, Vaduganathan M, Nodari S, Lam CS, Sato N, Shah AN and Gheorghiade M. The global health and economic burden of hospitalizations for heart failure: lessons learned from hospitalized heart failure registries. *J Am Coll Cardiol*. 2014;63:1123-33.

7. Ponikowski P, Voors AA, Anker SD, Bueno H, Cleland JG, Coats AJ, Falk V, Gonzalez-Juanatey JR, Harjola VP, Jankowska EA, Jessup M, Linde C, Nihoyannopoulos P, Parissis JT, Pieske B, Riley JP, Rosano GM, Ruilope LM, Ruschitzka F, Rutten FH, van der Meer P and Authors/Task Force M. 2016 ESC Guidelines for the diagnosis and treatment of acute and chronic heart failure: The Task Force for the diagnosis and treatment of acute and chronic heart failure of the European Society of Cardiology (ESC)Developed with the special contribution of the Heart Failure Association (HFA) of the ESC. *Eur Heart J*. 2016;37:2129-200.

8. LaPointe NM, Al-Khatib SM, Piccini JP, Atwater BD, Honeycutt E, Thomas K, Shah BR, Zimmer LO, Sanders G and Peterson ED. Extent of and reasons for nonuse of implantable cardioverter defibrillator devices in clinical practice among eligible patients with left ventricular systolic dysfunction. *Circulation Cardiovascular quality and outcomes*. 2011;4:146-51.

9. Heusch G and Gersh BJ. The pathophysiology of acute myocardial infarction and strategies of protection beyond reperfusion: a continual challenge. *Eur Heart J*. 2017;38:774-784.

10. Ibanez B, Heusch G, Ovize M and Van de Werf F. Evolving therapies for myocardial ischemia/reperfusion injury. *J Am Coll Cardiol*. 2015;65:1454-71.

11. Ibanez B, Fuster V, Jimenez-Borreguero J and Badimon JJ. Lethal myocardial reperfusion injury: a necessary evil? *Int J Cardiol*. 2011;151:3-11.

12. Romero ME, Fernandez-Jimenez R, Ladich E, Fuster V, Ibanez B and Virmani R. Pathology of myocardial infarction and sudden death. In: V. Fuster, R. A. Harrington, J. Narula and Z. J. Eapen, eds. *Hurst's The Heart, 14e* New York, NY: McGraw-Hill Education; 2017.

13. Heusch G. The Coronary Circulation as a Target of Cardioprotection. *Circulation research*. 2016;118:1643-58.

14. Kloner RA. New observations regarding post-ischemia/reperfusion myocardial swelling. *J Am Coll Cardiol*. 2015;65:324-6.

15. Usman AA, Taimen K, Wasielewski M, McDonald J, Shah S, Giri S, Cotts W, McGee E, Gordon R, Collins JD, Markl M and Carr JC. Cardiac magnetic resonance T2 mapping in the monitoring and follow-up of acute cardiac transplant rejection: a pilot study. *Circ Cardiovasc Imaging*. 2012;5:782-90.

16. von Knobelsdorff-Brenkenhoff F, Schuler J, Doganguzel S, Dieringer MA, Rudolph A, Greiser A, Kellman P and Schulz-Menger J. Detection and Monitoring of Acute Myocarditis Applying Quantitative Cardiovascular Magnetic Resonance. *Circ Cardiovasc Imaging*. 2017;10. doi: 10.1161/CIRCIMAGING.116.005242.

17. Salerno M, Sharif B, Arheden H, Kumar A, Axel L, Li D and Neubauer S. Recent Advances in Cardiovascular Magnetic Resonance: Techniques and Applications. *Circ Cardiovasc Imaging*. 2017;10. doi: 10.1161/CIRCIMAGING.116.003951.

18. Heusch P, Nensa F and Heusch G. Is MRI Really the Gold Standard for the Quantification of Salvage From Myocardial Infarction? *Circulation research*. 2015;117:222-4.

19. Friedrich MG, Abdel-Aty H, Taylor A, Schulz-Menger J, Messroghli D and Dietz R. The salvaged area at risk in reperfused acute myocardial infarction as visualized by cardiovascular magnetic resonance. *J Am Coll Cardiol*. 2008;51:1581-7.

20. Engblom H, Heiberg E, Erlinge D, Jensen SE, Nordrehaug JE, Dubois-Rande JL, Halvorsen S, Hoffmann P, Koul S, Carlsson M, Atar D and Arheden H. Sample Size in Clinical Cardioprotection Trials Using Myocardial Salvage Index, Infarct Size, or Biochemical Markers as Endpoint. *J Am Heart Assoc*. 2016;5:e002708.

21. Carlsson M, Ubachs JF, Hedstrom E, Heiberg E, Jovinge S and Arheden H. Myocardium at risk after acute infarction in humans on cardiac magnetic resonance: quantitative assessment during follow-up and validation with single-photon emission computed tomography. *JACC Cardiovasc Imaging*. 2009;2:569-76.

22. Dall'Armellina E, Karia N, Lindsay AC, Karamitsos TD, Ferreira V, Robson MD, Kellman P, Francis JM, Forfar C, Prendergast BD, Banning AP, Channon KM, Kharbanda RK, Neubauer S and Choudhury RP. Dynamic changes of edema and late gadolinium enhancement after acute myocardial infarction and their relationship to functional recovery and salvage index. *Circ Cardiovasc Imaging*. 2011;4:228-36.

23. Arai AE, Leung S and Kellman P. Controversies in cardiovascular MR imaging: reasons why imaging myocardial T2 has clinical and pathophysiologic value in acute myocardial infarction. *Radiology*. 2012;265:23-32.

24. Friedrich MG, Kim HW and Kim RJ. T2-weighted imaging to assess post-infarct myocardium at risk. *JACC Cardiovasc Imaging*. 2011;4:1014-21.

25. Aletras AH, Tilak GS, Natanzon A, Hsu LY, Gonzalez FM, Hoyt RF, Jr. and Arai AE. Retrospective determination of the area at risk for reperfused acute myocardial infarction with T2-weighted cardiac magnetic resonance imaging: histopathological and displacement encoding with stimulated echoes (DENSE) functional validations. *Circulation*. 2006;113:1865-70.
26. Larose E, Rodes-Cabau J, Pibarot P, Rinfret S, Proulx G, Nguyen CM, Dery JP, Gleeton O, Roy L, Noel B, Barbeau G, Rouleau J, Boudreault JR, Amyot M, De Larochelliere R and Bertrand OF. Predicting late myocardial recovery and outcomes in the early hours of ST-segment elevation myocardial infarction traditional measures compared with microvascular obstruction, salvaged myocardium, and necrosis characteristics by cardiovascular magnetic resonance. *J Am Coll Cardiol*. 2010;55:2459-69.
27. Kim RJ, Albert TS, Wible JH, Elliott MD, Allen JC, Lee JC, Parker M, Napoli A, Judd RM and Gadoversetamide Myocardial Infarction Imaging I. Performance of delayed-enhancement magnetic resonance imaging with gadoversetamide contrast for the detection and assessment of myocardial infarction: an international, multicenter, double-blinded, randomized trial. *Circulation*. 2008;117:629-37.
28. Kim HW, Van Assche L, Jennings RB, Wince WB, Jensen CJ, Rehwald WG, Wendell DC, Bhatti L, Spatz DM, Parker MA, Jenista ER, Klem I, Crowley AL, Chen EL, Judd RM and Kim RJ. Relationship of T2-Weighted MRI Myocardial Hyperintensity and the Ischemic Area-At-Risk. *Circulation research*. 2015;117:254-65.
29. Hamirani YS, Wong A, Kramer CM and Salerno M. Effect of microvascular obstruction and intramyocardial hemorrhage by CMR on LV remodeling and outcomes after myocardial infarction: a systematic review and meta-analysis. *JACC Cardiovasc Imaging*. 2014;7:940-52.
30. Carrick D, Haig C, Ahmed N, McEntegart M, Petrie MC, Eteiba H, Hood S, Watkins S, Lindsay MM, Davie A, Mahrous A, Mordi I, Rauhalammi S, Sattar N, Welsh P, Radjenovic A, Ford I, Oldroyd KG and Berry C. Myocardial Hemorrhage After Acute Reperfused ST-Segment-Elevation Myocardial Infarction: Relation to Microvascular Obstruction and Prognostic Significance. *Circ Cardiovasc Imaging*. 2016;9:e004148.

31. Bodi V, Monmeneu JV, Ortiz-Perez JT, Lopez-Lereu MP, Bonanad C, Husser O, Minana G, Gomez C, Nunez J, Forteza MJ, Hervas A, de Dios E, Moratal D, Bosch X and Chorro FJ. Prediction of Reverse Remodeling at Cardiac MR Imaging Soon after First ST-Segment-Elevation Myocardial Infarction: Results of a Large Prospective Registry. *Radiology*. 2016;278:54-63.

32. Robbers LF, Eerenberg ES, Teunissen PF, Jansen MF, Hollander MR, Horrevoets AJ, Knaapen P, Nijveldt R, Heymans MW, Levi MM, van Rossum AC, Niessen HW, Marcu CB, Beek AM and van Royen N. Magnetic resonance imaging-defined areas of microvascular obstruction after acute myocardial infarction represent microvascular destruction and haemorrhage. *Eur Heart J*. 2013;34:2346-53.

33. Rossello X and Yellon DM. A critical review on the translational journey of cardioprotective therapies! *Int J Cardiol*. 2016;220:176-84.

34. Jones SP, Tang XL, Guo Y, Steenbergen C, Lefer DJ, Kukreja RC, Kong M, Li Q, Bhushan S, Zhu X, Du J, Nong Y, Stowers HL, Kondo K, Hunt GN, Goodchild TT, Orr A, Chang CC, Ockaili R, Salloum FN and Bolli R. The NHLBI-sponsored Consortium for preclinicAl assESsment of cARdioprotective therapies (CAESAR): a new paradigm for rigorous, accurate, and reproducible evaluation of putative infarct-sparing interventions in mice, rabbits, and pigs. *Circulation research*. 2015;116:572-86.

35. Bell RM, Botker HE, Carr RD, Davidson SM, Downey JM, Dutka DP, Heusch G, Ibanez B, Macallister R, Stoppe C, Ovize M, Redington A, Walker JM and Yellon DM. 9th Hatter Biannual Meeting: position document on ischaemia/reperfusion injury, conditioning and the ten commandments of cardioprotection. *Basic Res Cardiol*. 2016;111:41.

36. Hausenloy DJ, Botker HE, Engstrom T, Erlinge D, Heusch G, Ibanez B, Kloner RA, Ovize M, Yellon DM and Garcia-Dorado D. Targeting reperfusion injury in patients with ST-segment elevation myocardial infarction: trials and tribulations. *Eur Heart J*. 2017;38:935-941.

37. Hedstrom E, Engblom H, Frogner F, Astrom-Olsson K, Ohlin H, Jovinge S and Arheden H. Infarct evolution in man studied in patients with first-time coronary occlusion in comparison to different species - implications for assessment of myocardial salvage. *J Cardiovasc Magn Reson*. 2009;11:38.

38. Fernandez-Friera L, Garcia-Ruiz JM, Garcia-Alvarez A, Fernandez-Jimenez R, Sanchez-Gonzalez J, Rossello X, Gomez-Talavera S, Lopez-Martin GJ, Pizarro G, Fuster V and Ibanez B. Accuracy of Area at Risk Quantification by Cardiac Magnetic Resonance According to the Myocardial Infarction Territory. *Revista espanola de cardiologia*. 2017;70:323-330.

39. Garcia-Prieto J, Garcia-Ruiz JM, Sanz-Rosa D, Pun A, Garcia-Alvarez A, Davidson SM, Fernandez-Friera L, Nuno-Ayala M, Fernandez-Jimenez R, Bernal JA, Izquierdo-Garcia JL, Jimenez-Borreguero J, Pizarro G, Ruiz-Cabello J, Macaya C, Fuster V, Yellon DM and Ibanez B. beta3 adrenergic receptor selective stimulation during ischemia/reperfusion improves cardiac function in translational models through inhibition of mPTP opening in cardiomyocytes. *Basic Res Cardiol*. 2014;109:422.

40. Garcia-Ruiz JM, Fernandez-Jimenez R, Garcia-Alvarez A, Pizarro G, Galan-Arriola C, Fernandez-Friera L, Mateos A, Nuno-Ayala M, Aguero J, Sanchez-Gonzalez J, Garcia-Prieto J, Lopez-Melgar B, Martinez-Tenorio P, Lopez-Martin GJ, Macias A, Perez-Asenjo B, Cabrera JA, Fernandez-Ortiz A, Fuster V and Ibanez B. Impact of the Timing of Metoprolol Administration During STEMI on Infarct Size and Ventricular Function. *J Am Coll Cardiol*. 2016;67:2093-2104.

41. Garcia-Ruiz JM, Galan-Arriola C, Fernandez-Jimenez R, Aguero J, Sanchez-Gonzalez J, Garcia-Alvarez A, Nuno-Ayala M, Dube GP, Zafirelis Z, Lopez-Martin GJ, Bernal JA, Lara-Pezzi E, Fuster V and Ibanez B. Bloodless reperfusion with the oxygen carrier HBOC-201 in acute myocardial infarction: a novel platform for cardioprotective probes delivery. *Basic Res Cardiol*. 2017;112:17.

42. Payne AR, Casey M, McClure J, McGeoch R, Murphy A, Woodward R, Saul A, Bi X, Zuehlsdorff S, Oldroyd KG, Tzemos N and Berry C. Bright-blood T2-weighted MRI has higher diagnostic accuracy than dark-blood short tau inversion recovery MRI for detection of acute myocardial infarction and for assessment of the ischemic area at risk and myocardial salvage. *Circ Cardiovasc Imaging*. 2011;4:210-9.

43. Stiermaier T, Thiele H and Eitel I. T2-weighted Cardiovascular Magnetic Resonance Imaging to Delineate Ischemic Myocardium at Risk: Fact or Fiction? *Revista espanola de cardiologia*. 2017;70:316-317.

44. Salerno M and Kramer CM. Advances in parametric mapping with CMR imaging. *JACC Cardiovasc Imaging*. 2013;6:806-22.
45. Boxt LM, Hsu D, Katz J, Detweiler P, McLaughlin S, Kolb TJ and Spotnitz HM. Estimation of myocardial water content using transverse relaxation time from dual spin-echo magnetic resonance imaging. *Magnetic resonance imaging*. 1993;11:375-83.
46. Garcia-Dorado D, Oliveras J, Gili J, Sanz E, Perez-Villa F, Barrabes J, Carreras MJ, Solares J and Soler-Soler J. Analysis of myocardial oedema by magnetic resonance imaging early after coronary artery occlusion with or without reperfusion. *Cardiovasc Res*. 1993;27:1462-9.
47. Higgins CB, Herfkens R, Lipton MJ, Sievers R, Sheldon P, Kaufman L and Crooks LE. Nuclear magnetic resonance imaging of acute myocardial infarction in dogs: alterations in magnetic relaxation times. *The American journal of cardiology*. 1983;52:184-8.
48. Scholz TD, Martins JB and Skorton DJ. NMR relaxation times in acute myocardial infarction: relative influence of changes in tissue water and fat content. *Magn Reson Med*. 1992;23:89-95.
49. Wisenberg G, Prato FS, Carroll SE, Turner KL and Marshall T. Serial nuclear magnetic resonance imaging of acute myocardial infarction with and without reperfusion. *Am Heart J*. 1988;115:510-8.
50. Liu P, Johnston DL, Brady TJ, Lutrario DM and Okada RD. The alterations of magnetic resonance relaxation parameters in excised myocardial tissue during NMR spectroscopy: the effects of time, environmental exposure and TTC staining. *Magnetic resonance imaging*. 1989;7:109-13.
51. Ibanez B, Macaya C, Sanchez-Brunete V, Pizarro G, Fernandez-Friera L, Mateos A, Fernandez-Ortiz A, Garcia-Ruiz JM, Garcia-Alvarez A, Iniguez A, Jimenez-Borreguero J, Lopez-Romero P, Fernandez-Jimenez R, Goicolea J, Ruiz-Mateos B, Bastante T, Arias M, Iglesias-Vazquez JA, Rodriguez MD, Escalera N, Acebal C, Cabrera JA, Valenciano J, Perez de Prado A, Fernandez-Campos MJ, Casado I, Garcia-Rubira JC, Garcia-Prieto J, Sanz-Rosa D, Cuellas C, Hernandez-Antolin R, Albarran A, Fernandez-Vazquez F, de la Torre-Hernandez JM, Pocock S, Sanz G and Fuster V. Effect of early metoprolol on infarct size in ST-segment-elevation myocardial infarction patients undergoing primary percutaneous coronary

intervention: the Effect of Metoprolol in Cardioprotection During an Acute Myocardial Infarction (METOCARD-CNIC) trial. *Circulation*. 2013;128:1495-503.

52. Wright J, Adriaenssens T, Dymarkowski S, Desmet W and Bogaert J. Quantification of myocardial area at risk with T2-weighted CMR: comparison with contrast-enhanced CMR and coronary angiography. *JACC Cardiovasc Imaging*. 2009;2:825-31.

53. Verhaert D, Thavendiranathan P, Giri S, Mihai G, Rajagopalan S, Simonetti OP and Raman SV. Direct T2 quantification of myocardial edema in acute ischemic injury. *JACC Cardiovasc Imaging*. 2011;4:269-78.

54. Thuny F, Lairez O, Roubille F, Mewton N, Rioufol G, Sportouch C, Sanchez I, Bergerot C, Thibault H, Cung TT, Finet G, Argaud L, Revel D, Derumeaux G, Bonnefoy-Cudraz E, Elbaz M, Piot C, Ovize M and Croisille P. Post-conditioning reduces infarct size and edema in patients with ST-segment elevation myocardial infarction. *J Am Coll Cardiol*. 2012;59:2175-81.

55. White SK, Frohlich GM, Sado DM, Maestrini V, Fontana M, Treibel TA, Tehrani S, Flett AS, Meier P, Ariti C, Davies JR, Moon JC, Yellon DM and Hausenloy DJ. Remote ischemic conditioning reduces myocardial infarct size and edema in patients with ST-segment elevation myocardial infarction. *JACC Cardiovasc Interv*. 2015;8:178-188.

56. Crimi G, Pica S, Raineri C, Bramucci E, De Ferrari GM, Klersy C, Ferlini M, Marinoni B, Repetto A, Romeo M, Rosti V, Massa M, Raisaro A, Leonardi S, Rubartelli P, Oltrona Visconti L and Ferrario M. Remote ischemic post-conditioning of the lower limb during primary percutaneous coronary intervention safely reduces enzymatic infarct size in anterior myocardial infarction: a randomized controlled trial. *JACC Cardiovasc Interv*. 2013;6:1055-63.

57. Croisille P, Kim HW and Kim RJ. Controversies in cardiovascular MR imaging: T2-weighted imaging should not be used to delineate the area at risk in ischemic myocardial injury. *Radiology*. 2012;265:12-22.

58. Fernandez-Jimenez R and Ibanez B. Health and cost benefits associated with the use of metoprolol in heart attack patients. *Expert Rev Clin Pharmacol*. 2014;7:687-9.

59. Mateos A, Garcia-Lunar I, Garcia-Ruiz JM, Pizarro G, Fernandez-Jimenez R, Huertas P, Garcia-Alvarez A, Fernandez-Friera L, Bravo J, Flores-Arias J, Barreiro

MV, Chayan-Zas L, Corral E, Fuster V, Sanchez-Brunete V, Ibanez B and Investigators M-C. Efficacy and safety of out-of-hospital intravenous metoprolol administration in anterior ST-segment elevation acute myocardial infarction: insights from the METOCARD-CNIC trial. *Annals of emergency medicine*. 2015;65:318-24.

60. Pizarro G, Fernandez-Friera L, Fuster V, Fernandez-Jimenez R, Garcia-Ruiz JM, Garcia-Alvarez A, Mateos A, Barreiro MV, Escalera N, Rodriguez MD, de Miguel A, Garcia-Lunar I, Parra-Fuertes JJ, Sanchez-Gonzalez J, Pardillos L, Nieto B, Jimenez A, Abejon R, Bastante T, Martinez de Vega V, Cabrera JA, Lopez-Melgar B, Guzman G, Garcia-Prieto J, Mirelis JG, Zamorano JL, Albarran A, Goicolea J, Escaned J, Pocock S, Iniguez A, Fernandez-Ortiz A, Sanchez-Brunete V, Macaya C and Ibanez B. Long-term benefit of early pre-reperfusion metoprolol administration in patients with acute myocardial infarction: results from the METOCARD-CNIC trial (Effect of Metoprolol in Cardioprotection During an Acute Myocardial Infarction). *J Am Coll Cardiol*. 2014;63:2356-62.

61. Ibanez B, Prat-Gonzalez S, Speidl WS, Vilahur G, Pinero A, Cimmino G, Garcia MJ, Fuster V, Sanz J and Badimon JJ. Early metoprolol administration before coronary reperfusion results in increased myocardial salvage: analysis of ischemic myocardium at risk using cardiac magnetic resonance. *Circulation*. 2007;115:2909-16.

62. Garcia-Prieto J, Villena-Gutierrez R, Gomez M, Bernardo E, Pun-Garcia A, Garcia-Lunar I, Crainiciuc G, Fernandez-Jimenez R, Sreeramkumar V, Bourio-Martinez R, Garcia-Ruiz JM, Del Valle AS, Sanz-Rosa D, Pizarro G, Fernandez-Ortiz A, Hidalgo A, Fuster V and Ibanez B. Neutrophil stunning by metoprolol reduces infarct size. *Nat Commun*. 2017;8:14780.

63. Fernández-Jiménez R, Fernández-Friera L, Sánchez-González J and Ibáñez B. Animal Models of Tissue Characterization of Area at Risk, Edema and Fibrosis. *Curr Cardiovasc Imaging Rep*. 2014;7:1-10.

64. Fernandez-Jimenez R and Ibanez B. CAESAR: one step beyond in the construction of a translational bridge for cardioprotection. *Circulation research*. 2015;116:554-6.

65. Hausenloy DJ, Garcia-Dorado D, Botker HE, Davidson SM, Downey J, Engel FB, Jennings R, Lecour S, Leor J, Madonna R, Ovize M, Perrino C, Prunier F, Schulz R, Sluijter JPG, Van Laake LW, Vinten-Johansen J, Yellon DM, Ytrehus K, Heusch

G and Ferdinandy P. Novel targets and future strategies for acute cardioprotection: Position Paper of the European Society of Cardiology Working Group on Cellular Biology of the Heart. *Cardiovasc Res*. 2017;113:564-585.

66. Fernandez-Jimenez R, Lopez-Romero P, Suarez-Barrientos A, Garcia-Rubira JC, Fernandez-Ortiz A, Fuster V, Macaya C and Ibanez B. Troponin release overestimates infarct size in presence of left ventricular hypertrophy. *J Am Coll Cardiol*. 2012;60:640-1.

67. Fernandez-Jimenez R, Silva J, Martinez-Martinez S, Lopez-Maderuelo MD, Nuno-Ayala M, Garcia-Ruiz JM, Garcia-Alvarez A, Fernandez-Friera L, Pizarro TG, Garcia-Prieto J, Sanz-Rosa D, Lopez-Martin G, Fernandez-Ortiz A, Macaya C, Fuster V, Redondo JM and Ibanez B. Impact of left ventricular hypertrophy on troponin release during acute myocardial infarction: new insights from a comprehensive translational study. *J Am Heart Assoc*. 2015;4:e001218.

68. Sala-Vila A, Fernandez-Jimenez R, Pizarro G, Calvo C, Garcia-Ruiz JM, Fernandez-Friera L, Rodriguez MD, Escalera N, Palazuelos J, Macias A, Perez-Asenjo B, Fernandez-Ortiz A, Ros E, Fuster V and Ibanez B. Nutritional preconditioning by marine omega-3 fatty acids in patients with ST-segment elevation myocardial infarction: A METOCARD-CNIC trial substudy. *Int J Cardiol*. 2017;228:828-833.

69. Fernandez-Jimenez R, Sanchez-Gonzalez J, Aguero J, Del Trigo M, Galan-Arriola C, Fuster V and Ibanez B. Fast T2 gradient-spin-echo (T2-GraSE) mapping for myocardial edema quantification: first in vivo validation in a porcine model of ischemia/reperfusion. *J Cardiovasc Magn Reson*. 2015;17:92.

70. Fernandez-Jimenez R, Sanchez-Gonzalez J, Aguero J, Garcia-Prieto J, Lopez-Martin GJ, Garcia-Ruiz JM, Molina-Iracheta A, Rossello X, Fernandez-Friera L, Pizarro G, Garcia-Alvarez A, Dall'Armellina E, Macaya C, Choudhury RP, Fuster V and Ibanez B. Myocardial edema after ischemia/reperfusion is not stable and follows a bimodal pattern: imaging and histological tissue characterization. *J Am Coll Cardiol*. 2015;65:315-23.

71. Binek A, Fernández-Jiménez R, Jorge I, Camafeita E, López JA, Bagwan N, Galán-Arriola C, Pun A, Agüero J, Fuster V, Ibanez B and Vázquez J. Proteomic footprint of myocardial ischemia/reperfusion injury: Longitudinal study of the at-risk and remote regions in the pig model. *Scientific Reports*. 2017;7:12343.

72. Fernandez-Jimenez R, Garcia-Prieto J, Sanchez-Gonzalez J, Aguero J, Lopez-Martin GJ, Galan-Arriola C, Molina-Iracheta A, Doohan R, Fuster V and Ibanez B. Pathophysiology Underlying the Bimodal Edema Phenomenon After Myocardial Ischemia/Reperfusion. *J Am Coll Cardiol*. 2015;66:816-828.

73. Fernandez-Jimenez R, Galan-Arriola C, Sanchez-Gonzalez J, Aguero J, Lopez-Martin GJ, Gomez-Talavera S, Garcia-Prieto J, Benn A, Molina-Iracheta A, Barreiro-Perez M, Martin-Garcia A, Garcia-Lunar I, Pizarro G, Sanz J, Sanchez PL, Fuster V and Ibanez B. Effect of Ischemia Duration and Protective Interventions on the Temporal Dynamics of Tissue Composition After Myocardial Infarction. *Circulation research*. 2017;121:439-450.

74. Fernandez-Jimenez R, Barreiro-Perez M, Martin-Garcia A, Sanchez-Gonzalez J, Aguero J, Galan-Arriola C, Garcia-Prieto J, Diaz-Pelaez E, Vara P, Martinez I, Zamarro I, Garde B, Sanz J, Fuster V, Sanchez PL and Ibanez B. Dynamic Edematous Response of the Human Heart to Myocardial Infarction: Implications for Assessing Myocardial Area at Risk and Salvage. *Circulation*. 2017;136:1288-1300.

75. Fernandez-Jimenez R, Fuster V and Ibanez B. Reply: myocardial edema should be stratified according to the state of cardiomyocytes within the ischemic region. *J Am Coll Cardiol*. 2015;65:2356-7.

76. Fernandez-Jimenez R, Fuster V and Ibanez B. Reply: Myocardial Salvage, Area at Risk by T2w CMR: The Resolution of the Retrospective Radio Wave Paradigm? *J Am Coll Cardiol*. 2015;65:2358-9.

77. Fernandez-Jimenez R, Fuster V and Ibanez B. Reply: "Waves of Edema" Seem Implausible. *J Am Coll Cardiol*. 2016;67:1869-1870.

78. Fernandez-Jimenez R, Sanchez-Gonzalez J and Ibanez B. Letter by Fernandez-Jimenez et al Regarding Article, "Protective Effects of Ticagrelor on Myocardial Injury After Infarction". *Circulation*. 2017;135:e1002-e1003.

79. Ugander M, Bagi PS, Oki AJ, Chen B, Hsu LY, Aletras AH, Shah S, Greiser A, Kellman P and Arai AE. Myocardial edema as detected by pre-contrast T1 and T2 CMR delineates area at risk associated with acute myocardial infarction. *JACC Cardiovasc Imaging*. 2012;5:596-603.

80. Foltz WD, Yang Y, Graham JJ, Detsky JS, Dick AJ and Wright GA. T2 fluctuations in ischemic and post-ischemic viable porcine myocardium in vivo. *J Cardiovasc Magn Reson*. 2006;8:469-74.
81. Foltz WD, Yang Y, Graham JJ, Detsky JS, Wright GA and Dick AJ. MRI relaxation fluctuations in acute reperfused hemorrhagic infarction. *Magn Reson Med*. 2006;56:1311-9.
82. Mewton N, Rapacchi S, Augeul L, Ferrera R, Loufouat J, Boussel L, Micolich A, Rioufol G, Revel D, Ovize M and Croisille P. Determination of the myocardial area at risk with pre- versus post-reperfusion imaging techniques in the pig model. *Basic Res Cardiol*. 2011;106:1247-57.
83. van der Pals J, Hammer-Hansen S, Nielles-Vallespin S, Kellman P, Taylor J, Kozlov S, Hsu LY, Chen MY and Arai AE. Temporal and spatial characteristics of the area at risk investigated using computed tomography and T1-weighted magnetic resonance imaging. *European heart journal cardiovascular Imaging*. 2015;16:1232-40.
84. Vilahur G, Gutierrez M, Casani L, Varela L, Capdevila A, Pons-Llado G, Carreras F, Carlsson L, Hidalgo A and Badimon L. Protective Effects of Ticagrelor on Myocardial Injury After Infarction. *Circulation*. 2016;134:1708-1719.
85. Baranyai T, Giricz Z, Varga ZV, Koncsos G, Lukovic D, Makkos A, Sarkozy M, Pavo N, Jakab A, Czimbalmos C, Vago H, Ruzsa Z, Toth L, Garamvolgyi R, Merkely B, Schulz R, Gyongyosi M and Ferdinandy P. In vivo MRI and ex vivo histological assessment of the cardioprotection induced by ischemic preconditioning, postconditioning and remote conditioning in a closed-chest porcine model of reperfused acute myocardial infarction: importance of microvasculature. *J Transl Med*. 2017;15:67.
86. Dharmakumar R. Building a Unified Mechanistic Insight Into the Bimodal Pattern of Edema in Reperfused Acute Myocardial Infarctions: Observations, Interpretations, and Outlook. *J Am Coll Cardiol*. 2015;66:829-831.
87. Arai AE. Healing After Myocardial Infarction: A Loosely Defined Process. *JACC Cardiovasc Imaging*. 2015;8:680-3.
88. Arai AE. Area at risk in acute myocardial infarction: oedema imaging and species-specific findings. *European heart journal cardiovascular Imaging*. 2016;17:754-5.

89. Berry C, Carrick D, Haig C and Oldroyd KG. "Waves of Edema" Seem Implausible. *J Am Coll Cardiol*. 2016;67:1868-1869.
90. Mewton N, Croisille P and Ovize M. Myocardial Salvage, Area at Risk by T2w CMR: The Resolution of the Retrospective Radio Wave Paradigm? *J Am Coll Cardiol*. 2015;65:2357-8.
91. Zhang B, Chen W, Chen Y and Gao F. Myocardial edema should be stratified according to the state of cardiomyocytes within the ischemic region. *J Am Coll Cardiol*. 2015;65:2355-6.
92. Tada Y and Yang PC. Myocardial Edema on T2-Weighted MRI: New Marker of Ischemia Reperfusion Injury and Adverse Myocardial Remodeling. *Circulation research*. 2017;121:326-328.
93. Arai AE. Time-Varying Edema Requires Cautious Interpretation of Myocardium at Risk and Infarct Size by All Imaging Methods. *Circulation*. 2017;136:1301.
94. Carrick D, Haig C, Ahmed N, Rauhalammi S, Clerfond G, Carberry J, Mordi I, McEntegart M, Petrie MC, Eteiba H, Hood S, Watkins S, Lindsay MM, Mahrous A, Welsh P, Sattar N, Ford I, Oldroyd KG, Radjenovic A and Berry C. Temporal Evolution of Myocardial Hemorrhage and Edema in Patients After Acute ST-Segment Elevation Myocardial Infarction: Pathophysiological Insights and Clinical Implications. *J Am Heart Assoc*. 2016;5:e002834.
95. Hammer-Hansen S, Ugander M, Hsu LY, Taylor J, Thune JJ, Kober L, Kellman P and Arai AE. Distinction of salvaged and infarcted myocardium within the ischaemic area-at-risk with T2 mapping. *European heart journal cardiovascular Imaging*. 2014;15:1048-53.
96. Nordlund D, Klug G, Heiberg E, Koul S, Larsen TH, Hoffmann P, Metzler B, Erlinge D, Atar D, Aletras AH, Carlsson M, Engblom H and Arheden H. Multi-vendor, multicentre comparison of contrast-enhanced SSFP and T2-STIR CMR for determining myocardium at risk in ST-elevation myocardial infarction. *European heart journal cardiovascular Imaging*. 2016;17:744-53.
97. Stiermaier T, Thiele H and Eitel I. Early myocardial edema after acute myocardial infarction is stable and not bimodal in humans - Evidence from a large CMR multicenter study. *Int J Cardiol*. 2017;246:87-89.

98. Bodi V, Ruiz-Nodar JM, Feliu E, Minana G, Nunez J, Husser O, Martinez-Elvira J, Ruiz A, Bonanad C, Monmeneu JV, Lopez-Lereu MP, Forteza MJ, de Dios E, Hervas A, Moratal D, Gomez C, Mainar L, Sanchis J, Mainar V, Valencia J, Diaz A, Noguera I, Chaustre F and Chorro FJ. Effect of ischemic postconditioning on microvascular obstruction in reperfused myocardial infarction. Results of a randomized study in patients and of an experimental model in swine. *Int J Cardiol*. 2014;175:138-46.

99. Jablonowski R, Engblom H, Kanski M, Nordlund D, Koul S, van der Pals J, Englund E, Heiberg E, Erlinge D, Carlsson M and Arheden H. Contrast-Enhanced CMR Overestimates Early Myocardial Infarct Size: Mechanistic Insights Using ECV Measurements on Day 1 and Day 7. *JACC Cardiovasc Imaging*. 2015;8:1379-1389.

100. Wu KC. CMR of microvascular obstruction and hemorrhage in myocardial infarction. *J Cardiovasc Magn Reson*. 2012;14:68.

101. McAlindon E, Pufulete M, Lawton C, Angelini GD and Bucciarelli-Ducci C. Quantification of infarct size and myocardium at risk: evaluation of different techniques and its implications. *European heart journal cardiovascular Imaging*. 2015;16:738-46.